



UNIVERSIDADE ESTADUAL DE CAMPINAS
FACULDADE DE ENGENHARIA MECÂNICA
E INSTITUTO DE GEOCIÊNCIAS

CHARLIE VAN DER GEEST

**STUDY OF FLOW ASSURANCE PROBLEMS
RELATED TO WAXY CRUDE OILS: RHEOLOGICAL
BEHAVIOUR, FLOW START-UP AND DEPOSITION**

**ESTUDO DE PROBLEMAS DE GARANTIA DE
ESCOAMENTO ENVOLVENDO ÓLEOS
PARAFÍNICOS: REOLOGIA, REPARTIDA E
DEPOSIÇÃO**

CAMPINAS

2018

CHARLIE VAN DER GEEST

**STUDY OF FLOW ASSURANCE PROBLEMS RELATED TO
WAXY CRUDE OILS: RHEOLOGICAL BEHAVIOUR, FLOW
START-UP AND DEPOSITION**

**ESTUDO DE PROBLEMAS DE GARANTIA DE
ESCOAMENTO ENVOLVENDO ÓLEOS PARAFÍNICOS:
REOLOGIA, REPARTIDA E DEPOSIÇÃO**

Thesis presented to the Mechanical Engineering Faculty and Geosciences Institute of the University of Campinas in partial fulfillment of the requirements for the degree of Doctor in Petroleum Sciences and Engineering in the area of Exploitation.

Tese apresentada à Faculdade de Engenharia Mecânica e Instituto de Geociências da Universidade Estadual de Campinas como parte dos requisitos exigidos para a obtenção do título de Doutor em Ciências e Engenharia de Petróleo na área de Exploração.

Orientador: Prof. Dr. Antonio Carlos Bannwart

Coorientador: Dra. Vanessa Cristina Bizotto Guersoni

Este exemplar corresponde à versão final da Tese defendida pelo aluno Charlie Van Der Geest e orientada pelo Prof. Dr. Antonio Carlos Bannwart.

Assinatura do Orientador

CAMPINAS

2018

Agência(s) de fomento e nº(s) de processo(s): CAPES, 33003017
ORCID: <https://orcid.org/0000-0003-3469-2140>

Ficha catalográfica
Universidade Estadual de Campinas
Biblioteca da Área de Engenharia e Arquitetura
Rose Meire da Silva - CRB 8/5974

G271s Geest, Charlie Van Der, 1988-
Study of flow assurance problems related to waxy crude oils : rheological behaviour, flow start-up and deposition / Charlie Van Der Geest. – Campinas, SP : [s.n.], 2018.

Orientador: Antonio Carlos Bannwart.
Coorientador: Vanessa Cristina Bizotto Guersoni.
Tese (doutorado) – Universidade Estadual de Campinas, Faculdade de Engenharia Mecânica.

1. Reologia. 2. Parafinas. 3. Escoamento. I. Bannwart, Antonio Carlos, 1955-. II. Guersoni, Vanessa Cristina Bizotto, 1979-. III. Universidade Estadual de Campinas. Faculdade de Engenharia Mecânica. IV. Título.

Informações para Biblioteca Digital

Título em outro idioma: Estudo de problemas de garantia de escoamento envolvendo óleos parafínicos : reologia, repartida e deposição

Palavras-chave em inglês:

Rheology

Paraffins

Flow

Área de concentração: Exploração

Titulação: Doutor em Ciências e Engenharia de Petróleo

Banca examinadora:

Antonio Carlos Bannwart [Orientador]

Jorge Luis Baliño

Roney Leon Thompson

Erick de Moraes Franklin

Jorge Luiz Biazussi

Data de defesa: 24-10-2018

Programa de Pós-Graduação: Ciências e Engenharia de Petróleo

UNIVERSIDADE ESTADUAL DE CAMPINAS
FACULDADE DE ENGENHARIA MECÂNICA
E INSTITUTO DE GEOCIÊNCIAS

TESE DE DOUTORADO

**STUDY OF FLOW ASSURANCE PROBLEMS RELATED TO
WAXY CRUDE OILS: RHEOLOGICAL BEHAVIOUR, FLOW
START-UP AND DEPOSITION**

**ESTUDO DE PROBLEMAS DE GARANTIA DE
ESCOAMENTO ENVOLVENDO ÓLEOS PARAFÍNICOS:
REOLOGIA, REPARTIDA E DEPOSIÇÃO**

Autor: Charlie Van Der Geest

Orientador: Prof. Dr. Antonio Carlos Bannwart

Coorientador: Dra. Vanessa Cristina Bizotto Guersoni

A Banca Examinadora composta pelos membros abaixo aprovou esta Tese:

Prof. Dr. Antonio Carlos Bannwart
DE / FEM / UNICAMP

Prof. Dr. Erick de Moraes Franklin
DE / FEM / UNICAMP

Prof. Dr. Roney Leon Thompson
PEM / COPPE / UFRJ

Prof. Dr. Jorge Luis Baliño
PME / USP

Dr. Jorge Luiz Biazussi
CEPETRO/UNICAMP

A Ata de Defesa com as respectivas assinaturas dos membros encontra-se no SIGA/Sistema de Fluxo de Dissertação/Tese e na Secretaria do Programa da Unidade.

Campinas, [24] de [Outubro] de [2018].

DEDICATION

I apologize for the readers but both dedications and acknowledgments will be written in Portuguese, my native language.

Eu gostaria de dedicar essa tese de doutorado à minha mulher, Nathalia. Também a minha família, Lucia, Simão, Janete, Mirian, Stefany, André, Teresa e Paulinho.

ACKNOWLEDGEMENTS

Primeiramente à minha companheira durante esses anos namorada, Nathalia.

À minha família, Simão, Lucia, Janete, André, Mirian, Stefany, Teresa e Paulo Cesar.

Ao Prof. Dr. Antonio Carlos Bannwart pela orientação e todo o suporte.

À Dra. Vanessa C. Bizzoto Guersoni pela orientação e ajuda.

Aos professores e pesquisadores do CEPETRO pelo auxílio direto e indireto na realização deste trabalho, especialmente ao Jorge, Caio, William, Natan, Carlos e Marta pela ajuda diária.

Aos técnicos do CEPETRO, Cláudio e Luiz, pela ajuda diária em todos os experimentos.

À empresa Repsol-Sinopec, especialmente ao Dr. Daniel Merino-Garcia, pelo investimento e apoio técnico fornecido nos anos de pesquisa.

O presente trabalho foi realizado com apoio da Coordenação de Aperfeiçoamento de Pessoal de Nível Superior - Brasil (CAPES) - Código de Financiamento 001.

Aos meus amigos de Campinas que sempre estiveram presentes, especialmente os que moraram comigo durante esses anos: Adriano, Mario e Natacha.

.

RESUMO

Nesta tese de doutorado, apresentamos um estudo de problemas de garantia de escoamento relacionados a óleos parafínicos. Os dois principais problemas encontrados pela indústria do petróleo ao produzir óleos parafínicos são: o reinício do escoamento de óleos gelificados e a deposição de parafina durante a produção. Para entender melhor esses dois fenômenos, estudamos a reologia desses óleos, também estudamos experimentalmente a repartida de escoamento e a deposição de parafina de óleos altamente parafínicos.

Quando um óleo parafínico permanece estático no fundo do mar por qualquer motivo, ele irá esfriar abaixo do ponto de fluidez e formar uma estrutura cristalina, levando a um comportamento não-newtoniano. O comportamento reológico de óleos parafínicos gelificados é fundamental para projetar arquitetura submarina para campos petrolíferos. Esta tese apresenta um estudo reológico de seis óleos parafínicos a uma temperatura de 5 °C. A validação dos modelos existentes com dados experimentais de uma ampla gama de óleos parafínicos é essencial para a compreensão do comportamento reológico. Os principais desafios são prever o pico de tensão em um experimento de taxa de cisalhamento constante e prever o comportamento da taxa de cisalhamento em experimentos de tensão cisalhamento constante. Uma vez que podemos prever todo o comportamento transiente dos óleos gelificados, estamos um passo mais perto de prever o comportamento de todo o sistema, melhorando assim o projeto de estruturas submarinas em campos petrolíferos.

Criamos um aparato experimental composto por uma tubulação de uma polegada que é submersa em um banho de água (5 ° C), e um sistema de nitrogênio com válvulas controladas para pressurizar a entrada da tubulação. Nós realizamos experimentos com óleo contendo uma alta porcentagem de parafina que formam uma forte estrutura cristalina. Para poder fornecer à indústria uma previsão confiável da pressão de reinício de óleos gelificados, são necessários muitos experimentos e melhorias nos modelos. Comparamos os dados experimentais com a previsão de um modelo que compreende um fluido fracamente compressível com um comportamento tixotrópico elasto-viscoplástico para poder melhorar o conhecimento e se aproximar dos resultados esperados da indústria.

A deposição de parafina foi investigada usando a mesma instalação projetada para estudar problemas de garantia de fluxo relacionados a óleos parafínicos. Além disso, as experiências de deposição mostram um fenômeno que não é comumente relatado na literatura. Uma vez que a temperatura do óleo estava abaixo da temperatura da aparência de cristais e a

temperatura da água a 5°C, o depósito não começou a se acumular imediatamente, só começou após um período. Em algumas condições, a queda de pressão só começou a aumentar após um dia. Esses resultados mostram que, pelo menos para os óleos altamente parafínicos, os modelos baseados em difusão molecular por si só não podem prever quando e onde o depósito se formará. Devem ser considerados outros mecanismos como dispersão por cisalhamento, difusão browniana e comportamento não-newtoniano.

Key Word: Óleos Parafínicos, Repartida, Deposição

ABSTRACT

In this PhD dissertation, we presented a study of flow assurance problems related to waxy crude oils. The main two problems encountered by the petroleum industry when producing waxy crudes are: start-up of flow of gelled waxy crudes and the wax deposition during production. To better understand these two phenomena, we studied the rheology of gelled waxy crudes, we also studied experimentally the start-up of flow of gelled crudes and the wax deposition of highly paraffinic crude oils.

When a waxy crude stays static in the seabed for any reason, it will cool down below the pour point and form a crystalline structure, leading to a non-Newtonian behavior. Rheological behavior of gelled waxy crude oils is critical to designing subsea architecture for petroleum fields. This dissertation presents a rheological study of six commercial gelled waxy crude oils at a temperature of 5 °C. Validation of the existing models with experimental data from a wide range of gelled waxy crudes is an essential step towards understanding the rheological behavior. The main challenges are to predict the overshoot of the stress in constant shear rate experiments and to predict the shear rate behavior in constant shear stress experiments. Once we can predict all the transient behavior of the gelled crudes, we are one step closer to predicting the behavior of the whole system, thus better designing subsea structures in petroleum fields.

We build an experimental apparatus composed of a one-inch pipeline that is submerged in a water bath (5°C) and a nitrogen system with controlled valves to pressurize the inlet of the pipeline. We did experiments with oil containing a high percentage of wax that build up a strong crystalline structure. To be able to provide to the industry a reliable prediction of the gelled waxy restart pressure, a lot of experiments and improvement in the models are necessary. We compared the experimental data with the prediction of a model comprising a weakly compressible fluid with an elasto-viscoplastic thixotropic behavior to be able to improve the knowledge and the get closer to the results expected from the industry.

Wax deposition was investigated using the same facility designed to study flow assurance problems related to waxy crude oils. Additionally, deposition experiments show a phenomenon that is not commonly reported in the literature. Once the oil's temperature was below the Wax Appearance Temperature and the water temperature at 5°C, the deposit did not start to build up immediately, it only began after a period. Under some conditions the pressure drop only began increasing after one day. These results show that, at least for highly paraffinic

crudes, models based on molecular diffusion alone cannot predict when and where the deposit will form. Other mechanisms like shear dispersion, Brownian diffusion and the non-Newtonian behavior of waxy crudes at low temperatures should be considered.

Key Word: Waxy Crude Oil, Deposition, Flow Start-Up

TABLE OF CONTENTS

INTRODUCTION	13
1.1. Brief Review on Gelation	13
1.1.1. Rheological Behavior of Gelled Waxy Cruder	14
1.1.2. Restart of the flow in a pipeline	15
1.2. Brief Review on Wax Deposition	15
1.3. Motivation	16
1.4. Objectives.....	16
1.5. Dissertation Overview.....	17
1.5.1. PAPER 1: Rheological study under simple shear of six gelled waxy crude oils ..	17
1.5.2. PAPER 2: Experimental study of the necessary pressure to start-up the flow of a gelled waxy crude oil.....	18
1.5.3. PAPER 3: Wax Deposition Experiment with Highly Paraffinic Crude Oil in Laminar Single-Phase Flow Unpredictable by Molecular Diffusion Mechanism	18
1.5.4. PAPER 4: A modified elasto-viscoplastic thixotropic model for two commercial gelled waxy crude oils	19
1.5.5. PAPER 5: Influence of Aging in Equilibrium Time of Gelled Waxy Crude Oil in Rheometer and Pipeline.....	19
1. PAPER 1: Rheological study under simple shear of six gelled waxy crude oils.....	21
2. PAPER 2: Experimental study of the necessary pressure to start-up the flow of a gelled waxy crude oil	42
3. PAPER 3: Wax Deposition Experiment with Highly Paraffinic Crude Oil in Laminar Single-Phase Flow Unpredictable by Molecular Diffusion Mechanism	54
4. PAPER 4: A modified elasto-viscoplastic thixotropic model for two commercial gelled waxy crude oils.....	69

5. PAPER 5: INFLUENCE OF AGING IN EQUILIBRIUM TIME OF GELLED WAXY CRUDE OIL IN RHEOMETER AND PIPELINE	87
6. CONCLUSIONS.....	115
7. FUTURE WORK.....	118
Rheology	118
Flow Restart.....	118
Wax Deposition	118
8. BIBLIOGRAPHY.....	120
APPENDIX A: COPYRIGHT LICENSE AGREEMENTS	126
Paper 1	126
Paper 2	128
Paper 3	129
Paper 4	130

INTRODUCTION

A considerable number of petroleum reservoirs are in deep water offshore fields. Because of environmental conditions at the bottom of the sea, there are several problems that occur when crude oil/gas flows from the reservoir to the production unit. To address all those issues and guarantee a smooth operation, the petroleum industry developed a technical discipline called Flow Assurance. The most common Flow Assurance concerns are wax deposition, restart of gelled waxy crudes, emulsion/foam formation, hydrate blockages, asphaltene precipitation and inorganic scaling.

Crude oil is a complex mixture of non-polar and polar organic compounds, they are called waxy crudes any time the weight fraction of alkanes and iso-alkanes with carbon numbers ranging from C_{18} to C_{60} . are higher than 1% (Ajienka & Ikoku, 1991). where high molecular weight non-polar molecules lead to solid deposits upon temperature reduction. This phenomenon is critical in areas with low ambient temperatures, such as the seabed in deep waters. The precipitated solid molecules cause the two main problems when waxy crude oil is being produced. The restart of gelled crudes and wax deposition, both have been addressed in this PhD dissertation.

1.1. Brief Review on Gelation

When production is interrupted is when the restart problems arise. During interruptions of deep sea operations, for example, a pipeline may become blocked, filled with gelled waxy crudes. At the bottom of the sea, at 4 °C, the heat loss leads to the precipitation of wax crystals in the oil. When the temperature of the crude drops below the gelation temperature, the rheological behaviour changes abruptly, potentially leading to pipeline blockages (Wardhaugh, & Boger, 1987; Thomason, 2000; Venkatesan, *et al.*, 2003; Fung *et al.*, 2006). The literature regarding the rheological behavior of gelled waxy crude oils is extensive. The reason is that the industry has been dealing with this problem for at least five decades (Davenport & Conti, 1971).

When Paraffin crystals precipitate all over the pipeline, they form a crystalline matrix distributed across the oil, leading to a rheological behaviour modification, the oils behaves as a gel (Davidson *et al.*, 2004), thus gelation problem. The characteristics of this crystalline structure are among the most published and discussed issues in the flow assurance field. Every boundary condition the oil is subjected during its formation seem to influence its structure. Initial temperature (Andrade 2014), final temperature (Davenport & Conti, 1971; Lee

et al., 2008; Rønningsen, 2012), cooling rate (Singh et al., 1999; Rønningsen et al., 1991), shear rate during cooling down (Rønningsen et al., 1991; Venkatesan et al., 2005; Lin et al., 2011), aging time (Wardhaugh and Boger, 1991b; Chang et al., 2000), among others.

There are a few ways of characterizing the molecular crystalline structure formed during a gelation process. There are works that study the macroscopic behaviour of the gelled crude by measuring the rheological properties, such as storage modulus (G') and loss modulus (G'') under the linear viscoelastic region (Rønningsen 2012; Andrade 2014); there are studies that use the overshoot of stress caused when the material is subjected to a small shear rate (Chang et al., 1998); there are studies that use the critical shear stress that can start a flow before some pre-defined time (Tarcha et al., 2015), among others methods. There are also the studies that study the microscopic scale, how linear molecules interact with iso molecules and how the nucleation process is influenced by all the boundary conditions (Kurniawan et al., 2018; Marinho et al., 2018).

1.1.1. Rheological Behavior of Gelled Waxy Crude

As has been discussed, one of the ways of determining the characteristics of the crystalline structure is by studying the rheological behavior of the gelled waxy crude. That is usually done in a rheometer, the literature is vast, waxy crudes can show elastic, plastic and, depending on the definition, thixotropic like behavior.

Waxy crude oils, when gelled, present one of the most debatable rheological property, the yield stress. That property is an open scientific debate for many reasons. There are different ways to measure it, it is time sensitive and there are arguments that it does not exist when time goes to infinity. Another problem is that the sensitivity of the measurement is in some cases proportional to the property itself. The yield stress can be briefly defined as a threshold stress below which there is zero flow.

In this research, an engineering approach was used by defining an appropriate experimental time and then calling the property apparent yield stress. Thus, if the gelled crude oil flowed within the experimental time the apparent yield stress was reached, otherwise the experiment was done below the threshold. Even though there is an extensive debate on the best way to measure this property, the scientific community seems to be converging on the methodology of applying a constant shear stress and waiting a predefined time, if the oil flows the stress is reduced until it does not flow within that time at which point the stress is considered the threshold.

There are other rheological properties that crude oils present that are also open debates, but they are not relevant for the restart of flow of gelled waxy crude oils, thus they shall not be discussed here. And because we have extensively discussed the models in the chapters ahead, we will not discuss the modelling we used at this point.

1.1.2. Restart of the flow in a pipeline

Besides all the important discussion on how the crystalline structure is form and how the boundary conditions influence it, when the subject is the restart of the pipeline, the scale changes and volumetric phenomena becomes relevant, the thermodynamics of the oil, how it shrinks and expands with temperature and pressure. Also, how the radial heat transfer causes a variation on the rheological behavior.

The oil shrinks as it cools down, thus compressibility starts to play a role, the pressure wave propagation is a critical issue when pressure is applied at one side of the pipeline. The shrinking process generates voids that are not filled due to the elastic response of the crystalline structure, thus when submitted to pressure the elastic behavior also influence the pressure wave propagation. In order to model this complex phenomenon of restart, it is necessary to consider a complex rheological behavior, the conservation of mass and momentum considering compressibility, the heat transfer that the oil is subjected during the cooling process.

1.2. Brief Review on Wax Deposition

Wax deposition is a problem that has been known for decades, and there is vast literature regarding this phenomenon. The oldest references deal with onshore problems (Reistle, 1928; Bilderback & McDougall, 1969) and, as operations expanded in the industry, offshore ones had to be dealt with (Asperger *et al.*, 1981; Singh *et al.*, 2000; Paso & Fogler, 2003). In the literature there are also a few reviews on this issue, discussing the mechanisms which cause deposition, the influence of other phases (gas and water), technologies for inhibiting wax growth and methods for measuring the performance of said technologies (Aiyejina *et al.*, 2011; Sarica & Panacharoensawad, 2012; Azevedo & Teixeira, 2003; Merino-Garcia & Correria, 2008).

The solubility of wax molecules decreases with temperature, because of the radial temperature gradient, as you get closer to the wall, at some point the oil reaches the wax appearance temperature (WAT) and wax molecules starts to precipitate. At that time a mass gradient starts to exist and diffusion starts to work. The process continues to happen as you get closer and closer to the wall, more paraffin crystal precipitate and diffusion tends to keeps

playing a role. The diffusion mechanism is without a doubt the strongest mechanism in wax deposition, it is however insufficient to explain the whole phenomenon, there has been a few studies showing that this is a complex multi mechanism phenomenon.

One thing that most studies agree is that the deposit is a porous medium that store both liquid and precipitated molecules. Because of this nature, diffusion also occurs in the deposit, which means that the deposit ages with time, the light hydrocarbons molecules suffer a counter-diffusion outside the deposit as heavier molecules suffer diffusion inwards. This is normally called aging of the deposit and has been shown in innumerable studies.

There are other mechanisms that need to be added to molecular diffusion to explain the deposition process and its behavior. The influence of non-newtonian behavior near the wall, the influence of non-isoviscous flow radially, the influence of super-saturation in diffusion, the influence of precipitated wax molecules within the bulk among others. All this discussion is in a single phase flow, while in reality, there a tri-phase flow, studies with two-phase flow are common in the literature, the influence of emulsions, of flow patterns, increasing the complexity of the problem.

1.3. Motivation

There are a few highly costly problems in the petroleum industry related to waxy crude oils. A better understanding of these problems would allow the industry to avoid or to mitigate the loss of tens of millions of dollars a year, the two phenomena discussed in this PhD dissertation are the cause of the industry's major concerns when discussing waxy crudes. This study has special importance for the industry extracting crude oil from reservoirs at Brazilian's offshore pre-salt layer, because some reservoirs are at low temperature and have a high percentage of wax, both increase the probability of problems occurring.

1.4. Objectives

The main objective of this research is to help the scientific community and the industry to better understand the two main problems of flow assurance related to waxy crude oils, the start-up of gelled waxy crudes and wax deposition during flow. Through both experimental investigation and mathematical models, the goal is to investigate the physical phenomena involved in both problems and develop some tools to help the industry dealing with them.

1.5. Dissertation Overview

This dissertation is divided in five main chapter, each chapter is a manuscript, at the end there is a chapter of conclusions. The first four manuscripts have been peer-reviewed and the fifth is under review and they can be read independently. Due to this format, the introduction and general affirmations at the beginning of each chapter might be redundant. The overview of each chapter, abstract of the manuscript, is given below.

It is important to point out that the chapters are not in chronological order of publication. There are two papers discussing the rheological behavior of gelled waxy crudes (chapter 1 and 4), two discussing the restart of the flow, one published and one under review (chapter 2 and 5) and one discussing the wax deposition (chapter 3). The reason why the paper 4 is not at the beginning is because paper 1 is a considerable improvement of the results presented in paper 4. For paper 1 there are improvements in the mathematical model and experimental methodology. Another reason is that we have studied two gelled crudes in paper 4 and studied 6 (including the ones in paper 4) in paper 1.

1.5.1. PAPER 1: Rheological study under simple shear of six gelled waxy crude oils

Van Der Geest, C., Guersoni, V. C. B., Merino-Garcia, D., & Bannwart, A. C. (2017). Rheological study under simple shear of six gelled waxy crude oils. *Journal of Non-Newtonian Fluid Mechanics*, 247, 188-206.

Rheological behavior of gelled waxy crude oils is critical to designing subsea architecture for petroleum fields. The ability to generate dimensionless models to predict the rheological behavior of any gelled waxy crudes would be a powerful tool. Validation of the model with experimental data from a wide range of gelled waxy crudes is an essential step to reach that goal. This study presents a rheological study of six commercial gelled waxy crude oils at a temperature of 5 °C. Four experimental procedures were performed in a controlled-stress rheometer MARS III from HAAKE GmbH with a cone and plate geometry. The rheological curves are steady state, stress sweep curve, constant shear rate and constant shear stress. We also did a study of the aging time with two of those oils. The strength of the crystalline structure of the six gelled waxy crudes have considerable difference, where the apparent yield stress ranges from 1 to 1000 Pa. The main challenges are to predict the overshoot of the stress in constant shear rate experiments and to predict the shear rate behavior in constant shear stress experiments. Good accuracy was obtained from comparison of the model with the experimental data.

1.5.2. PAPER 2: Experimental study of the necessary pressure to start-up the flow of a gelled waxy crude oil

Van Der Geest, C., Guersoni, V. C. B., Junior, L. A. S. S., & Bannwart, A. C. (2017, June). Experimental Study of the Necessary Pressure to Start-Up the Flow of a Gelled Waxy Crude Oil. In ASME 2017 36th International Conference on Ocean, Offshore and Arctic Engineering. American Society of Mechanical Engineers.

The current study concerns a recurrent problem in the oil industry when dealing with waxy crude oils in offshore fields. When a waxy crude stays static in the seabed for any reason and cools down below the pour point of the oil, wax crystals form a crystalline structure that modifies the behavior of the oil. We build an experimental apparatus that allows us to represent the condition of the temperature close to bottom of the sea, and a pressurization system that allows us to precisely control the inlet pressure. The apparatus is composed of a one-inch pipeline that is submerged in a water bath (5°C) and a nitrogen system with controlled valves to pressurize the inlet of the pipeline. The current study contributes to the literature by demonstrating that the behavior of a gelled waxy crude oil having a high percentage of wax that builds up a strong crystalline structure is impacted by rheological behavior, time, and aging time. To be able to provide the industry a reliable prediction of the gelled waxy restart pressure, it is necessary for engineers to carry out a great deal of experimentation and improvement in the models. In this paper, we compare the experimental data with the prediction of a model consisting of a weakly compressible fluid with an elasto-viscoplastic thixotropic behavior. The comparison advances our knowledge in the phenomena involved in restart of gelled crudes and, in fact, shows the model capable of approaching the results expected by the industry.

1.5.3. PAPER 3: Wax Deposition Experiment with Highly Paraffinic Crude Oil in Laminar Single-Phase Flow Unpredictable by Molecular Diffusion Mechanism

Van Der Geest, C., Guersoni, V. C. B., Merino-Garcia, D., & Bannwart, A. C. (2018). Wax Deposition Experiment with Highly Paraffinic Crude Oil in Laminar Single-Phase Flow Unpredictable by Molecular Diffusion Mechanism. *Energy & Fuels*

Wax deposition data for a Brazilian crude oil was investigated using a facility designed to study flow assurance problems related to waxy crude oils. This work reports the preliminary efforts behind validating the pressure drop methods in place for identifying deposition, i.e., isothermal and nonisothermal flows were evaluated, to confirm whether it was possible to differentiate between temperature gradient effects, and wax deposition. Additionally, deposition experiments show a phenomenon that is not commonly reported in the literature. Once the oil's temperature was below the wax appearance temperature and the water

temperature at 5 °C, the deposit did not start to build up immediately; it only began after a period of time. Under some conditions the pressure drop only began increasing after 1 day. These results show that, at least for highly paraffinic crudes, models based on molecular diffusion alone cannot predict when and where the deposit will form, which is a major concern in the industry. We believe that other mechanisms such as shear dispersion, Brownian diffusion, and the non Newtonian behavior of waxy crudes at low temperatures should be considered. In this experimental setup two different ways were used to measure deposit thickness: (1) pressure drop and (2) weight of the deposit.

1.5.4. PAPER 4: A modified elasto-viscoplastic thixotropic model for two commercial gelled waxy crude oils

Van Der Geest, C., Guersoni, V. C. B., Merino-Garcia, D., & Bannwart, A. C. (2015). A modified elasto-viscoplastic thixotropic model for two commercial gelled waxy crude oils. *Rheologica Acta*, 54(6), 545-561.

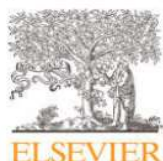
A severe problem to flow assurance occurs when subsea flowlines become blocked with gelled waxy crudes. To design proper surface pump facilities, it is essential to know the minimum pressure required to restart the flow. Simulating and predicting this minimum pressure require the understanding of several physical phenomena, including compressibility, shrinkage, and rheological behavior. This study aims to characterize and simulate the rheological behavior of two commercial waxy crude oils. Based on its survey of the literature, we select the de Souza Mendes and Thompson (2013) model to fit the oil's behavior and then conduct, using a rheometer, a considerable number of experiments with the selected oils. To verify the solution of our algorithm, we compared our theoretical solutions with some results of the literature. When comparing the simulation with experiments, the model was unable to predict the data perfectly; hence, we propose a modified version without changing the physical meaning of the equations, to improve its predictions. Once any of the empirical parameters were able to influence the elastic behavior in such a way that the shear stress decreased with time, the structural elastic modulus function was modified, which means that the relation of the structure parameter and the storage modulus was modified. One of the interesting results of the analysis is when relating the storage modulus and a new parameter added in the modification, a value was found to be, regardless of the aging time or the oil used, constant.

1.5.5. PAPER 5: Influence of Aging in Equilibrium Time of Gelled Waxy Crude Oil in Rheometer and Pipeline

Paper under Review.

For this study, an experimental apparatus was built to investigate the phenomenon of flow start-up of gelled waxy crudes. The apparatus is composed of a cold-water bath and a pipeline inside it connected to two tanks. These tanks can be pressurized, which enabled us to study the pressure start-up and the transient flow during start-up. In this paper, we study the influence of aging on the flow start-up, both in a rheometer and in the experimental apparatus; we model the rheological behaviour with an elasto-viscoplastic thixotropic model and the restart of the pipeline with a weakly compressible fluid. Our experimental procedure diverges from those of most experiments in the literature. In these, the inlet pressure increases continuously until the flow starts, at which point, so the argument goes, the apparent yield stress has been reached. With that type of procedure, however, it is impossible to distinguish whether there was an overshoot due to the elastic response of the material. Thus, we propose a different type of procedure wherein a constant pressure is applied and the time until the flow restart is measured. The idea of the study is to isolate the influence of aging on the equilibrium time, an important variable that has yet to receive in the literature the attention it warrants. The comparison between model and experimental data sheds light on the phenomena involved in the restart of gelled waxy crudes.

1. PAPER 1: Rheological study under simple shear of six gelled waxy crude oils



Contents lists available at ScienceDirect

Journal of Non-Newtonian Fluid Mechanics

journal homepage: www.elsevier.com/locate/jnnfm

Rheological study under simple shear of six gelled waxy crude oils



Charlie Van Der Geest^{a,*}, Vanessa C. Bizotto Guersoni^b, Daniel Merino-Garcia^c,
Antonio Carlos Bannwart^a

^a Department of Mechanical Engineering, University of Campinas, Campinas, São Paulo, Brazil

^b Center for Petroleum Studies, University of Campinas, Campinas, São Paulo, Brazil

^c Repsol Sinopec Brazil, Rio de Janeiro, 22250-040, Brazil

ARTICLE INFO

Article history:

Received 18 April 2017

Revised 19 July 2017

Accepted 31 July 2017

Available online 1 August 2017

ABSTRACT

Rheological behaviour of gelled waxy crude oils is critical to designing subsea architecture for petroleum fields. The ability to generate dimensionless models to predict the rheological behaviour of any gelled waxy crudes would be a powerful tool. Validation of the model with experimental data from a wide range of gelled waxy crudes is an essential step to reach that goal. This study presents a rheological study of six commercial gelled waxy crude oils at a temperature of 5 °C. Four experimental procedures were performed in a controlled-stress rheometer MARS III from HAAKE GmbH with a cone and plate geometry. The rheological curves are steady state, stress sweep curve, constant shear rate and constant shear stress. We also did a study of the aging time with two of those oils. The strength of the crystalline structure of the six gelled waxy crudes have considerable difference, where the apparent yield stress ranges from 1 to 1000 Pa. The main challenges are to predict the overshoot of the stress in constant shear rate experiments and to predict the shear rate behaviour in constant shear stress experiments. Good accuracy was obtained from comparison of the model with the experimental data.

© 2017 Elsevier B.V. All rights reserved.

1. Introduction

There are two main reasons to study the behaviour of different gelled waxy crude oils; to improve academic knowledge regarding rheology, and to provide solutions for the petroleum industry. On the academic side, the goal is to study the rheological behaviour itself, trying to improve the rheological characterization and the methods of obtaining the experimental data, while generalizing models in a way that would allow the ultimate goal of predicting the behaviour of any material. For the petroleum industry, the idea is to provide a final answer regarding the necessary pressure to restart the flow in a pipeline filled with gelled waxy crude. This means an approximate amount of pressure for overcoming the apparent yield stress and the time necessary for that to happen.

The literature regarding the rheological behaviour of gelled waxy crude oils is extensive. The reason is that the industry has been dealing with this problem for at least five decades [1]. There are characteristics regarding their behaviour that are well established in the literature, we briefly describe some of them in the next two paragraphs.

First well established concepts are two characteristic temperatures. The first is the WAT (Wax Appearance Temperature), which is when crystals of wax start to appear in the oil. The second is the gelation temperature, which is when the elastic behaviour overcomes the viscous behaviour. This can be observed with a small amplitude oscillatory shear (SAOS) test during the cooling down of the crude, the gelation temperature is where occurs the crossover of the storage modulus with the loss modulus [2]. When the viscous behaviour is dominant, the loss modulus is higher, when the elastic behaviour becomes dominant, the storage modulus becomes higher [3–10].

Another known behaviour is that at temperatures below the gelation point, as temperature decreases under static condition, the storage modulus, loss modulus, viscosity and apparent yield stress increase. This is because the crystalline structure builds up, hence the strength of the structure increases [5,6,8,11–16].

When discussing transient phenomenon however, the data in the literature regarding gelled waxy crude oil behaviour offers some discrepancies. There are two important discussions still going on in the scientific community where the behaviour of gelled waxy crudes fits perfectly. The definition and modelling of thixotropy [17–21] and the definition and modelling of yield stress [22–28].

Gelled waxy crude oils have been classified as thixotropic for a great number of studies [14,29–34]. A recent article from [21], however, has shown that the way the constitutive equations for

* Corresponding author.

E-mail address: charlievander@gmail.com (C. Van Der Geest).

Table 1
General properties of the 6 oils.

Parameters	Oil 1	Oil 2	Oil 3	Oil 4	Oil 5	Oil 6	Units
ρ @ 20 °C	877	888	811	865	805	852	kg/m ³
°API	29.2	27.2	42.1	30.9	43.3	33.9	—
H ₂ O	0.62	0.017 ± 0.008	0.60 ± 0.2	0.13	0	1.24 ± 0.04	%
Saturates	73.75	84.12	88.87	81.35	98.44	97.35	%
Aromatics	3.73	0.30	4.02	2.09	0.96	1.94	%
Resins	21.18	3.07	6.32	14.83	0.48	0.37	%
Asphaltenes	1.34	2.51	0.80	1.73	0.12	0.34	%

some of those studies are proposed cannot be differentiated from nonlinear viscoelasticity models. As Larson [21] argues, time dependence does not define a material as thixotropic, rather the “ideal thixotropy” would be “a time dependent viscous response to the history of the strain rate, with fading memory of that history”. Even though that discussion is necessary for the development of the concept of thixotropy, hence, for the better understanding of the behaviour of gelled waxy crudes, we do not go further into that discussion because the experimental results shown here do not represent the thixotropy in any way.

We used the model proposed by de Souza Mendes and Thompson [38] in this manuscript. De Souza Mendes and Thompson [38] classified the model as elasto-viscoplastic thixotropic, in this manuscript we only explore the elasto-viscoplastic behaviour, which involves the breakdown of the structure. Therefore the elastic, plastic and viscous behaviours, the prediction of the history of the strain rate or the reversible behaviour that are related to thixotropy, are not discussed.

When dealing with the yield stress discussion, we focus on the solution for the industry, and therefore an engineering viewpoint [35]; which considers that when the gelled crude is submitted to stresses smaller than a threshold named apparent yield stress, it behaves as a viscous fluid, with massive but finite viscosity [36].

In this manuscript, we present an experimental study of the rheological behaviour and the attempt on model the data for six commercial gelled waxy crudes. There is an extensive rheological characterization of the oils, which are based on four experiments performed in a controlled-stress rheometer MARS III from HAAKE GmbH with a cone and plate geometry. The rheological curves are steady state, stress sweep curve, constant shear rate and constant shear stress, which are a few of the possible procedures to verify the rheological behaviour [37].

2. Experimental procedure

2.1. Properties of the oils

Six crude oils of different compositions and API degrees have been studied. The density was measured using an Anton Paar DMA 4500 Density Meter at temperatures 15.55 °C and 20 °C. The water content was measured by the Karl-Fischer method, using a Mettler Toledo T50 Titrator. The wax appearance temperature (WAT) was obtained by Differential Scanning Calorimetry (DSC) with a Q2000 TA Instruments calorimeter. For this, a sample of crude oil was first heated to 80 °C for 10 min to be sure that all paraffins were dissolved. Then, the sample was cooled at 3 °C/min until −30 °C. In this case, there was the appearance of an exothermic peak corresponding to the wax appearance temperature (WAT), which is when the first wax crystal begins to crystallize. The composition in saturates, aromatics, resins and asphaltenes (SARA analysis, ASTM 2007) was obtained. The quantification of wax was made by centrifugation of crude oil, using a Rotanta 460R centrifuge, at 4000 rpm (3756 G) below the pour point (5 °C for Oils 1, 2, 3, 4 and

6 and −5 °C for Oil 5). The properties of the different crude oils are summarized in Table 1.

2.2. Rheological tests

We performed all experiments using a controlled-stress rheometer MARS III from HAAKE GmbH with a cone and plate geometry. We used two different sizes of cone and plate because for one of the oils, the experiment reached the upper stress limit of the rheometer. For Oils 1, 2, 3, 5 and 6, the diameter of 60 mm and a cone angle of 1 degree with a truncation of 0.054 mm were used. For Oil 4, the diameter of 35 mm and a 2 degrees of angle with a truncation of 0.105 mm were used.

The cone and plane geometry was used because it provides a more homogenous shear stress and shear rate. A study with real gelled waxy crudes comparing different geometries was done by Tarcha et al. [36] and shown that this geometry could measure accurately the behaviour of gelled waxy crudes. In both cases, the crystal size was more than 10 times smaller than the truncation size, which guarantees that the measurements were not erroneous due to crystal's influence.

The rheometer controls temperature and cooling rate using a Peltier plate and control the gap with the thermo-gap option. The gap option is necessary to prevent the oil from losing contact with the cone once it shrinks, guaranteeing no mistakes due to slippage on the surface.

Pre-experimental procedure was to homogenize the sample by preheating it to 70 °C and maintaining it for 2 h. Once the samples were in the rheometer, the Peltier plate controlled the temperature at 70 °C and the rheometer applied a shear rate of 10 s^{−1} for 10 min to erase thermal history effects. Following, we cooled down to 5 °C at the rate of 1 °C/min without shear rate and finally, the aging time of 1, 5 and 24 h.

We did most experiments in triplicate. The data from different samples of the same oil have a difference up to 20% in the results. When the experiments were done in triplicate, the results shown are not the mean value, rather the one where the important values, like apparent yield stress, were in the middle.

It is important to comment that the rheometer MARS III from HAAKE GmbH is a stress controlled rheometer, thus, when it does shear deformation rate controlled experiments, it actually uses the measured stress to try to control the shear deformation rate. The ideal would be to do such experiments in a deformation controlled rheometer. When we measure non-monotonic flow curves, as is presented below, they are an approximation of the true non-monotonic flow curves.

3. Rheological model

The model proposed by de Souza Mendes and Thompson [38] was used to predict the behaviour of the six oils studied. This section presents and briefly discusses the model. Further information can be found in the literature.

3.1. Steady state equation

The model proposed by de Souza Mendes and Thompson [38] use the Eq. (1) as the steady state viscosity function. In this equation, there are two yield stresses, the apparent (σ_y) and dynamic (σ_{yd}), the shear rate of transition between them ($\dot{\gamma}_{yd}$), there are the Herschel Bulkley parameters (K, n) and two viscosities, the viscosity of the fully structured fluid (η_0) and the viscosity when the crystalline structure is completely destroyed (η_∞).

There are plenty of equilibrium viscosity functions in the literature, and we could have used any of them. Eq. (1) predicted the data with good accuracy.

Eq. (1) has the capacity to predict two yield stresses. The transition from the apparent to the dynamic provokes an apparent discontinuity at small shear rates in the steady state. This behaviour is called shear banding and has been observed in a number of materials, with rheological characterization and modelling studies in the literature [39,40].

Chang et al. [29] consider that the value of the dynamic yield stress is just an extrapolation of the purely viscous behaviour. Applying that definition in Eq. (1) we could not predict the data. Once we apply the definition where the dynamic yield stress is related to the phenomenon of shear banding the model predicted the experimental data.

$$\eta_{eq}(\dot{\gamma}) = \left(1 - e^{-\frac{\eta_0 \dot{\gamma}}{\sigma_y}}\right) \left(\frac{\sigma_y - \sigma_{yd}}{\dot{\gamma}} e^{-\frac{\dot{\gamma}}{\dot{\gamma}_{yd}}} + \frac{\sigma_{yd}}{\dot{\gamma}} + K \dot{\gamma}^{n-1} \right) + \eta_\infty \quad (1)$$

Once we have the value of the viscosity in the equilibrium (η_{eq}), it is possible to calculate the value of the shear stress (σ_{eq}) in the equilibrium by multiplying the viscosity with the shear rate as shown in Eq. (2).

$$\sigma_{eq}(\dot{\gamma}) = \eta_{eq} \dot{\gamma} \quad (2)$$

The last equation of the steady state is about a commonly used structural parameter. Briefly, the idea is for the structure to be represented by a dimensionless number. When it is destroyed the parameter is zero and when it is completely formed is equal to the highest value. This parameter changes related to the amount of stress or strain to which the material is subjected. The differential equation that rules this parameter is discussed in a next section.

As to steady state, the structure does not change with time, as has been discussed. The structural parameter reaches equilibrium when the build-up and breakdown rates equalize. Eq. (3) shows the formula proposed by de Souza Mendes and Thompson [38].

$$\lambda_{eq} = \ln \left(\frac{\eta_{eq}}{\eta_\infty} \right) \quad (3)$$

3.2. Completely structured condition

From the steady state we obtain the viscosity when the crystalline structure is completely formed (λ_0), as has been discussed. With this value it is possible to obtain the value of the structural parameter for the completely structured material, Eq. (4) shows the equation proposed.

$$\lambda_0 = \ln \left(\frac{\eta_0}{\eta_\infty} \right) \quad (4)$$

3.3. Constitutive equation

The constitutive equation is based on an analogue with one spring and two dashpots as shown in Fig. 1. Where $G_s(\lambda)$ is the structural elastic modulus function and $\eta_s(\lambda)$ is the structural viscosity function.

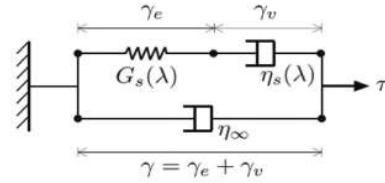


Fig. 1. Mechanical analog proposed by de Souza Mendes and Thompson [38].

The idea is to represent the elastic behaviour with a spring and the viscous behaviour with dampers, allowing the model to predict the nonlinear viscoelastic behaviour. For better understanding all the possible prediction of the model, the literature is available, but to explain briefly, if the structural elastic function goes to infinity, the behaviour is purely viscous ($\eta_v = \eta_s + \eta_\infty$) if the structural viscosity goes to infinity, the solution is the Kelvin-Voigt model.

Eq. (5) is the constitutive equation obtained from the mechanical analog proposed by de Souza Mendes and Thompson [38]. Eq. (5) is a differential equation that can be written with both relaxation (θ_1) and retardation (θ_2) times.

$$\frac{\theta_2}{\eta_\infty} \left(\frac{\sigma}{\theta_1} + \dot{\sigma} \right) = (\dot{\gamma} + \theta_2 \ddot{\gamma}) \quad (5)$$

De Souza Mendes and Thompson [38] have classified their model as an elasto-thixotropic viscoelastic model. Even though the constitutive equation is able to predict all of those behaviours, as Larson [21] has argued, this could be defined as an equation to predict nonlinear viscoelastic behaviour as well.

3.4. Characteristic times

Time dependence is related to how long the material responds to an applied stress or strain. Eq. (6) is the relaxation time, which represents the response time of a material after the stress is applied. Retardation time, Eq. (7), is related to the build-up time for the structure once the stress stops.

$$\theta_1 = \left(1 - \frac{\eta_\infty}{\eta_v(\lambda)} \right) \frac{\eta_v(\lambda)}{G_s(\lambda)} \quad (6)$$

$$\theta_2 = \left(1 - \frac{\eta_\infty}{\eta_v(\lambda)} \right) \frac{\eta_\infty}{G_s(\lambda)} \quad (7)$$

3.5. The structural elastic modulus function

Elastic response of the spring is shown in Eq. (8). This equation was proposed by de Souza Mendes and Thompson [38]. In our previous paper [41] we had proposed a modification to Eq. (8), where an empirical parameter was included dividing the storage modulus (G_0). We proposed this because without it the model could not predict the experimental data for gelled waxy crude oils. The problem is that there was a small inconsistency in the proposed equation. Therefore we used the equation proposed by de Souza Mendes and Thompson [38], where the difference is the method for measuring the storage modulus in the elastic region.

The only parameter that has not been described yet in Eq. (8) is m , which is an empirical parameter.

$$G_s = G_0 e^{m \left(\frac{1}{\lambda} - \frac{1}{\lambda_0} \right)} \quad (8)$$

Divoux et al. [42] showed a comparison of the storage modulus obtained from the oscillatory experimental test and from the dynamic constant shear rate test. As is discussed below, for our oils, those values present a considerable discrepancy.

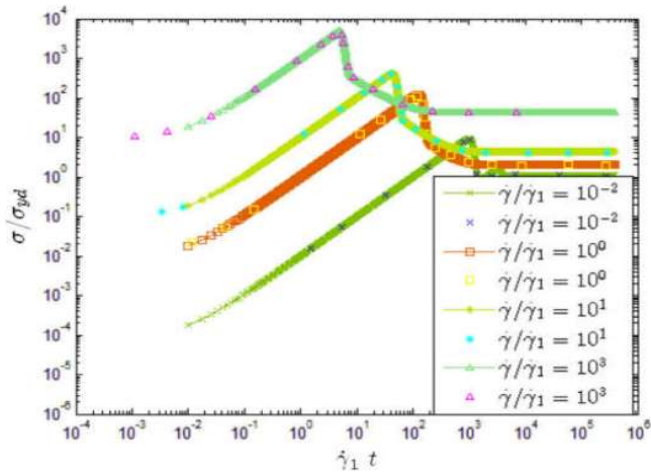


Fig. 2. Comparison of the stress evolution in time obtained with our algorithm and the results shown in [38] for a constant shear rate flow.

3.6. The structural viscosity function

In Eq. (9) there is the structural viscosity which is a function of the structure parameter λ and the purely viscous component η_∞ .

$$\eta_v(\lambda) = \eta_\infty e^\lambda \quad (9)$$

3.7. The Structure parameter

There are a number of models based on structural parameters like Eq. (10), which is basically made up of a term representing the build-up and a term represent the breakdown of the structure.

Larson [21] argues that when a constitutive equation like Eq. (5) is part of the same model as an equation for the structural parameter like Eq. (10), it is impossible to distinguish the thixotropy and the nonlinear viscoelasticity. The reason is that nonlinear viscoelasticity has the exact same behaviour in the exact same time scale. We do not intend to distinguish non ideal thixotropy from nonlinear viscoelasticity in this manuscript, instead, we want to verify whether the model is able to predict the breakdown of the crystalline structure.

In Eq. (10) there is the equilibrium time (t_{eq}) and the empirical parameters a and b , which are related to the build-up and break down, respectively, of the structure.

$$\frac{d\lambda}{dt} = \frac{1}{t_{eq}} \left[\left(\frac{1}{\lambda} - \frac{1}{\lambda_0} \right)^a - \left(\frac{\lambda}{\lambda_{eq}(\tau)} \right)^b \left(\frac{1}{\lambda_{eq}(\tau)} - \frac{1}{\lambda_0} \right)^a \right] \quad (10)$$

3.8. Algorithm validation

We build an algorithm using the Runge–Kutta method for solving the differential equations of the model. In order to validate our algorithm, the numerical solution is compared with the data published by de Souza Mendes and Thompson [38]. All the parameters were kept the same as the ones in that literature and the results can be seen in Figs. 2 and 3.

3.9. Dimensionless analysis

The variables of interest are now scaled based on what de Souza Mendes and Thompson [38] proposed. We choose the characteristic shear rate to be the point of transition between the ap-

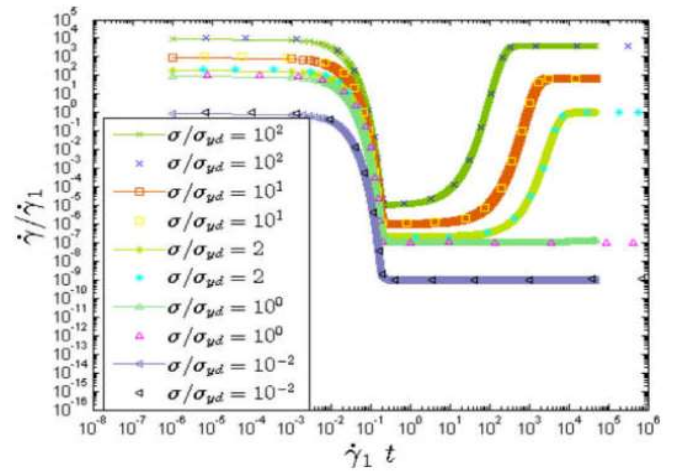


Fig. 3. Comparison of the shear rate evolution in time obtained with our algorithm and the results shown in [38] for a constant shear stress flow.

parent yield stress and the dynamic yield stress $\dot{\gamma}_{yd}$ and the characteristic shear stress to be the dynamic shear stress σ_{yd} .

Using those characteristic variables, we can obtain the following dimensionless parameter:

$$\eta_0^* = \frac{\eta_0 \dot{\gamma}_{yd}}{\sigma_{yd}}; \quad \eta_\infty^* = \frac{\eta_\infty \dot{\gamma}_{yd}}{\sigma_{yd}}; \quad \sigma_y^* = \frac{\sigma_y}{\sigma_{yd}}; \quad \dot{\gamma}_{eq}^* = \frac{\dot{\gamma}_{eq}}{\dot{\gamma}_{yd}}; \quad K^* = \frac{K \sigma_{yd}^{n-1}}{\eta_\infty^n}$$

In order to facilitate the understanding we first show the experimental data in dimensional form, and then we use the model to predict the data. Finally we compare the data in dimensionless form for all the oils and try to simulate the result of all the oils combined.

4. Results and discussion

4.1. Properties of the oils

All the data shown in Table 1 is to allow further studies to compare their rheological behaviour with the oils that we studied. This data is not directly of interest to anyone interested in studying the rheology itself, but is beneficial to those who might be interested in reproducing the experimental data, or may want to use the data for simulating the behaviour of similar oils.

4.2. Shear Stress as a Function of Shear Rate

When dealing with simple shear flow, like cone and plate geometry in a rheometer, the steady state flow theory is well known; you apply a shear rate, wait until the transient flow is over and when the shear stress is constant, the data is collected [37]. In the literature, however, different results are common when dealing with steady state flow of time-dependent materials. The capability of the experiment to predict the physical phenomena involved depends on whether it is based on controlled stress or controlled shear rate. The phenomenon of shear banding, for example, is better observed in a controlled shear rate experiment. The reason is the stress decay once it overcomes the apparent yield stress.

When dealing with materials with long characteristic times, the errors originated by neglecting the transient phenomena may be considerable, leading to wrong conclusions. This discussion is being offered because, as in the study shown by Tarcha et al. [36], we obtained some discrepancy depending on the duration of the

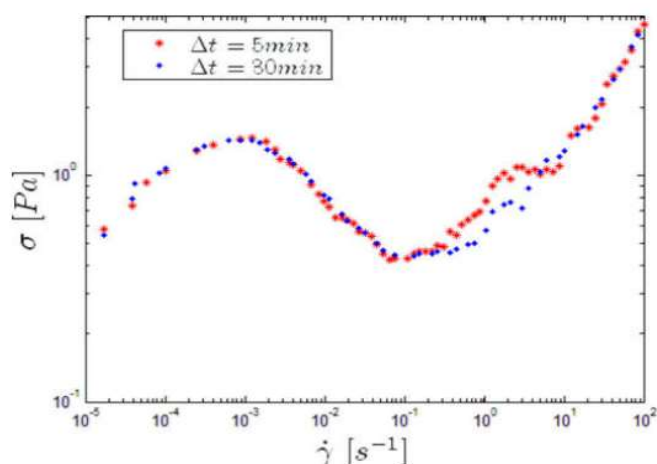


Fig. 4. Comparison of shear stress as a function of shear rate experiments with different time steps at each shear rate.

experiment. The amount of time between the applied shear rate and the measured shear stress is relevant.

When we did experiments with time steps of 5 min, we observed some transient phenomena around the dynamic yield stress. There was a second abrupt decrease in the shear stress as the shear deformation rate increased; the data showed something similar to what happens just as the shear stress rises above the apparent shear stress, which is the phenomenon called shear banding [43]. After we realized it was transient flow, we did a time step of 30 min and it disappeared.

We observed this oscillation for four of the six oils. Fig. 4 shows the result for Oil 3, notice that the gradient of the curve changes drastically twice. First is the expected breakdown of the structure after the apparent yield stress is reached. The second was a peculiar result that we could not find in the literature. Once we changed the time step, we obtained results similar to many other materials, and there are models perfectly capable of predicting them. The oscillation was probably due to the time necessary for homogenizing the oil.

Oil 3 builds-up the weakest structure among the oils we are studying. The second abrupt derivative decrease was even stronger with the other oils, exactly because they build-up stronger structures, therefore the time necessary to homogenization is greater, leading to a longer transient flow. Thirty minutes was enough to not see the oscillation for high shear rates for all oils.

In a previous study, published by this group [41], we show a rheological characterization for two of the six oils. The steady state experiments were done via stress-controlled method. In those results, some essential points were the same, like the apparent yield stress, but because of the abrupt increase in the shear rate with a tiny increase of the stress above the critical yield stress, there was a quantity of data that was not observed, as discussed before.

Before we discussed the data presented from Figs. 5–10 it is important to comment on steady state verification. In Figs. 5–10 there are lines showing the point where we verified that we reached steady state by doing the constant shear rate experiments, those results are shown in the sections below. For shear rates smaller than that line we could not show that the steady state was reached in 30 min, the values are reproducible though and they might be the same values of steady state.

The Datatips shown from Figs. 5–10 are the main values regarding the structure breakdown, and therefore the yielding of the material. Points of interest are the apparent yield stress, the dynamic

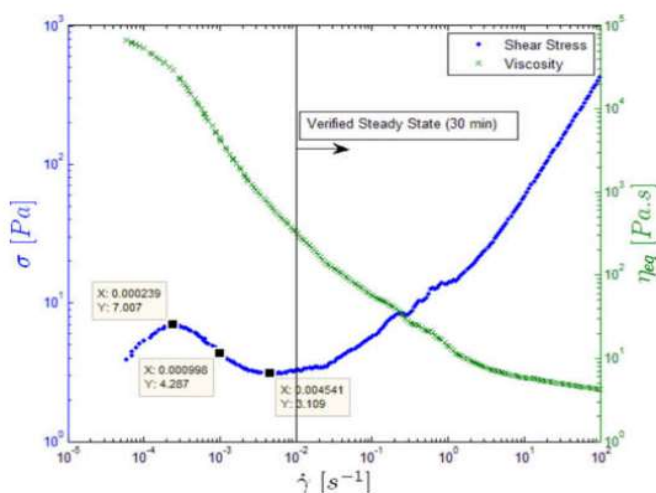


Fig. 5. Shear stress and viscosity as a function of shear rate curve for Oil 1 after 1 h of aging at 5 °C. Step duration for each measurement of 30 min.

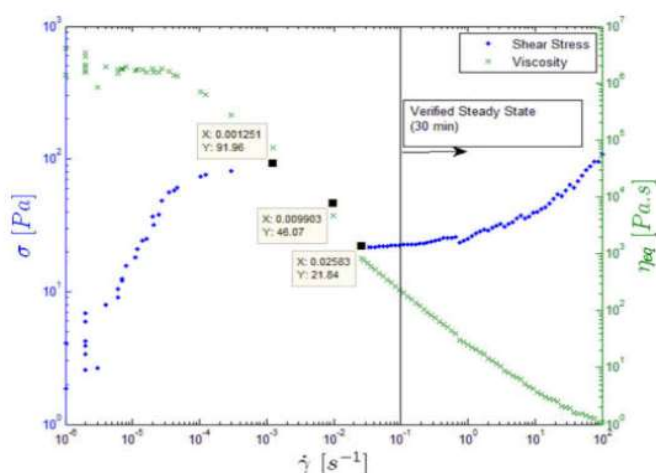


Fig. 6. Shear stress and viscosity as a function of shear rate curve for Oil 2 after 1 h of aging at 5 °C. Step duration for each measurement of 30 min.

yield stress and the shear rate of transition between them. As can be seen in Figs. 6, 8, 9 and 10, we did not manage to continuously measure the breakdown for the oils that build up strong structures. Tarcha et al. [36] show also some discontinuity in the experimental data depending on the experimental procedure.

Obtaining the continuous breakdown of a highly structured fluids is an arduous attempt. To fracture the structure we need to apply a large stress, hence, the flow occurs rapidly and the shear rate increases rapidly. In order to accomplish such results, a deformation controlled rheometer would probably be the solution.

One important physical value is the viscosity of the material under small shear rates. If the oils had a real yield stress, this viscosity would be infinite. However, as can be seen in Figs. 6 and 10, the rheometer was able to measure the viscosity under small shear rates for Oil 2 and Oil 6, the value is the plateau for small shear rates. Even though the rheometer could not measure the viscosity in such condition for the other oils with sufficient accuracy, we assumed that they exist, and we calculated their value by the minimum square method using the data we had.

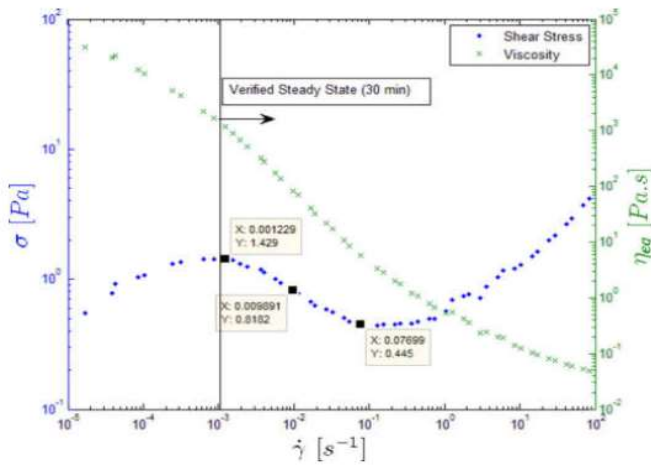


Fig. 7. Shear stress and viscosity as a function of shear rate curve for Oil 3 after 1 h of aging at 5 °C. Step duration for each measurement of 30 min.

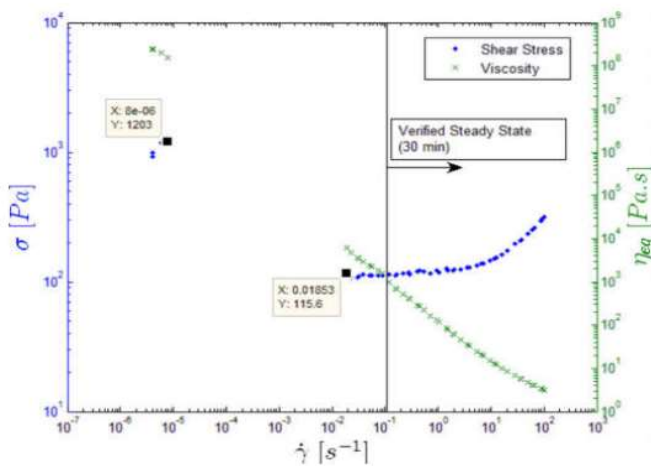


Fig. 8. Shear stress and viscosity as a function of shear rate curve for Oil 4 after 1 h of aging at 5 °C. Step duration for each measurement of 30 min.

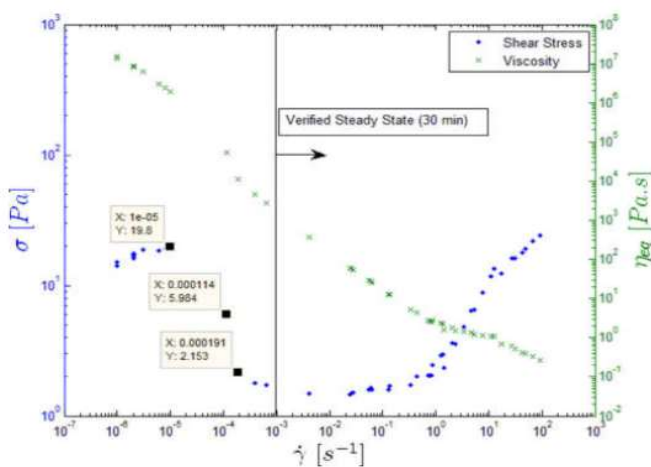


Fig. 9. Shear stress and viscosity as a function of shear rate curve for Oil 5 after 1 h of aging at 5 °C. Step duration for each measurement of 30 min.

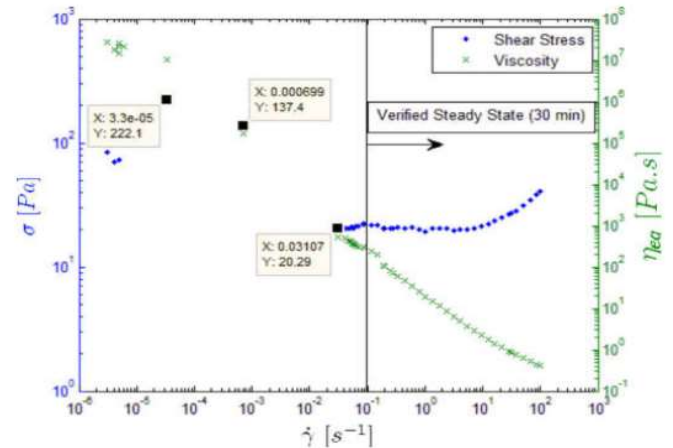


Fig. 10. Shear stress and viscosity as a function of shear rate curve for Oil 6 after 1 h of aging at 5 °C. Step duration for each measurement of 30 min.

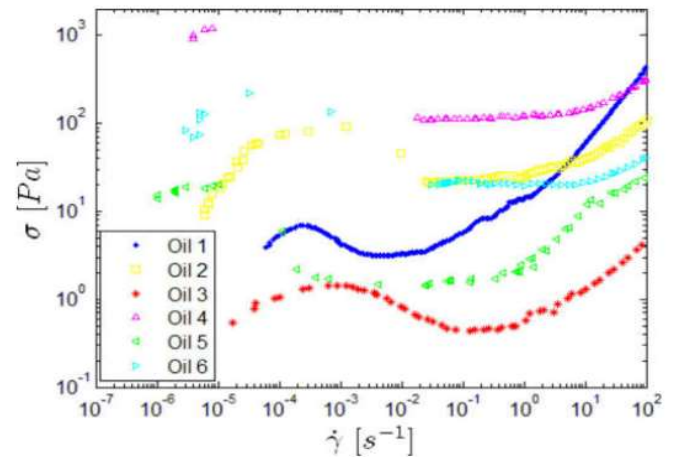


Fig. 11. Shear stress as a function of shear rate of the six oils after 1 h of aging at 5 °C.

The data obtained from the steady state results and used in the model are in Table 2. Besides the values shown in the datatips and the viscosity at low shear rates, discussed before, the table shows the viscosity at high shear rates and the parameters of the Herschel Bulkley model. Herschel Bulkley parameters (K , n) were proposed to model the stress after the yield stress was overcome.

The viscosity under large shear rates used in further simulations is shown in Table 2. When the fluid is under large shear rates, it reaches a constant viscosity, like the plateau in small shear rates. Note that we only nearly reached the plateau for Oil 1, in Fig. 5. For all the other oils, the value presented in Table 2 is the value obtained from the minimum square method.

Figs. 11 and 12 are the steady state of all the oils in one figure. The idea is to show the results in perspective. The stress tendency is clear for small shear rates, Oil 4 has the strongest structure, followed by Oil 6, Oil 2, Oil 5, Oil 1 and finally Oil 3, the weakest. When the breakdown occurs and the shear rate increases, the viscosity of Oil 1 decreases slower than the others, thus for high shear rates Oil 1 has the highest viscosity, as can be confirmed in Fig. 12. For small shear rates note that for Oils 1, 3 and 6 the plateau for the constant viscosity regions has been reached, while for the others it has not.

Table 2
Parameters obtained from the steady state.

Parameters	Oil 1	Oil 2	Oil 3	Oil 4	Oil 5	Oil 6	Units
K	5	3.5	0.1	6	1	0.5	Pa s ⁿ
n	0.5	0.45	0.7	0.7	0.5	0.5	—
η_0	10 ⁵	2 10 ⁶	4 10 ⁴	5 10 ⁸	2 10 ⁸	3 10 ⁷	Pa s
η_∞	4.25	0.2	0.02	1	0.2	0.2	Pa s
σ_y	7	91	1.43	1203	19.8	222.1	Pa
σ_{yd}	3.1	21.8	0.44	118.3	1.45	20.29	Pa
$\dot{\gamma}_{yd}$	10 ⁻³	9 10 ⁻³	9.9 10 ⁻³	3 10 ⁻³	1.1 10 ⁻⁴	7 10 ⁻⁴	s ⁻¹

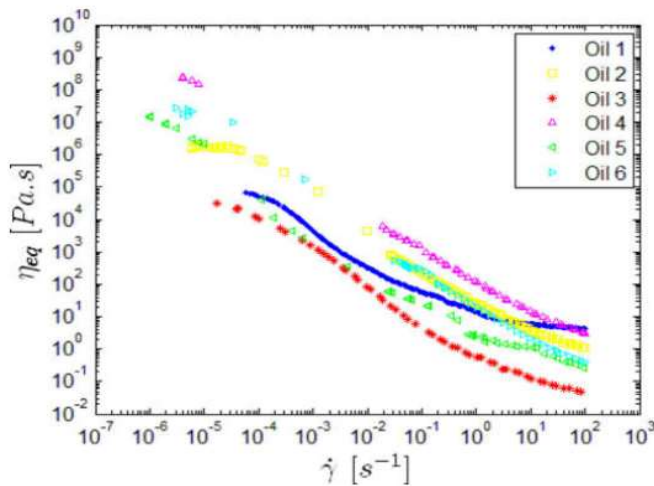


Fig. 12. Viscosity as a function of shear rate of the six oils after 1 h of aging at 5 °C.

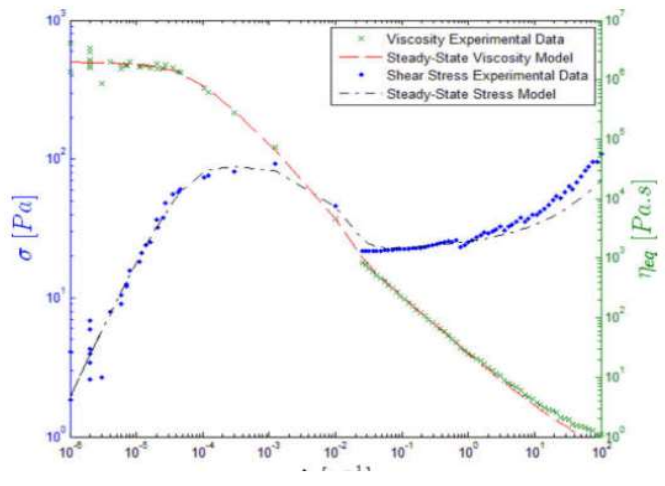


Fig. 14. Experimental data and model using Eq. (1) for Oil 2.

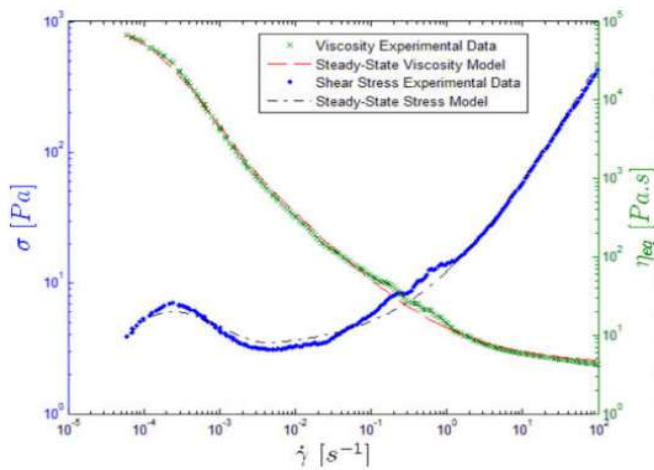


Fig. 13. Experimental data and model using Eq. (1) for Oil 1.

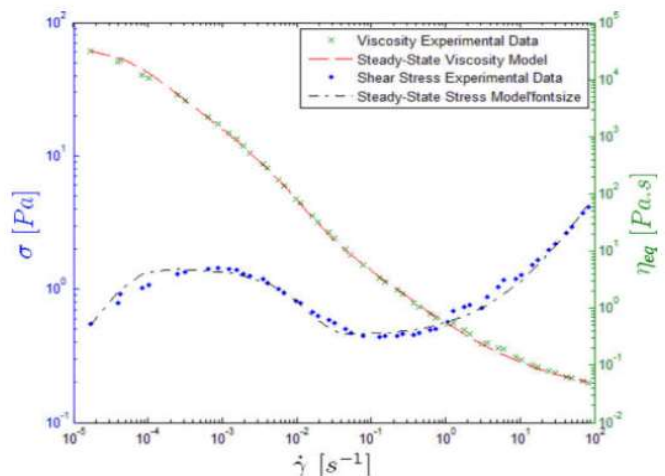


Fig. 15. Experimental data and model using Eq. (1) for Oil 3.

There are some interesting points to be noted when discussing the shear rate where the yielding occurs. Oil 5 has the smallest shear rate of transition from apparent to dynamic yield stress. This shows that there is no linear correlation between the value of the apparent yield stress and the transition shear rate. An increase can be seen following from Oil 3, Oil 1, Oil 6 and finally Oil 4, but the Oil 5 and Oil 2 do not follow.

In Figs. 13–18 we show the comparison of the experimental data of all the oils with the steady state equations. The results show good accuracy, the model is able to predict the be-

haviour well. Only when the breakdown is abrupt, for the oil with strong structure, the model predicts an abrupt behaviour. That may be reasonable but further studies are needed, in order to verify whether the breakdown occurs smoothly or if this abrupt breakdown really is a physical reality.

After discussing the dimensional data and the prediction of the dimensional model, we discuss the dimensionless results. Because we have a wide range of behaviours among the six oils we studied, if we could predict with a reasonable margin of error the steady

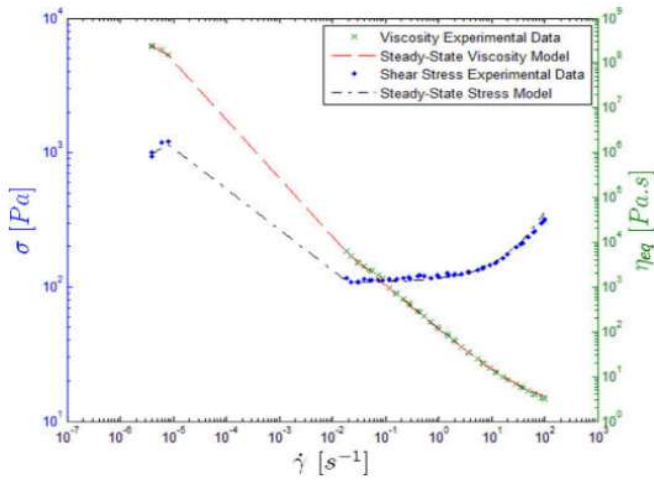


Fig. 16. Experimental data and model using Eq. (1) for Oil 4.

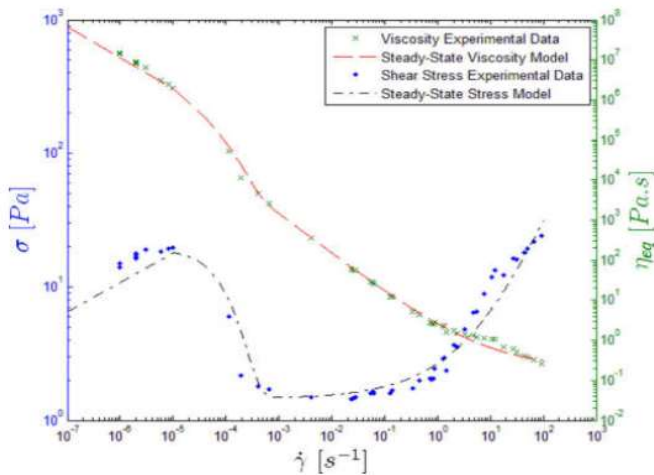


Fig. 17. Experimental data and model using Eq. (1) for Oil 5.

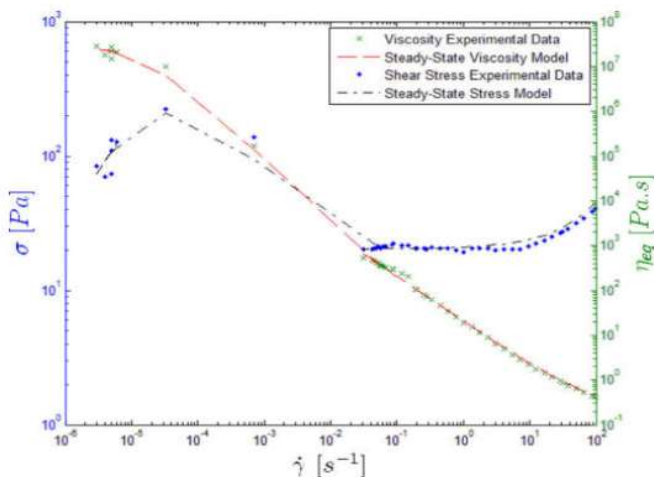


Fig. 18. Experimental data and model using Eq. (1) for Oil 6.

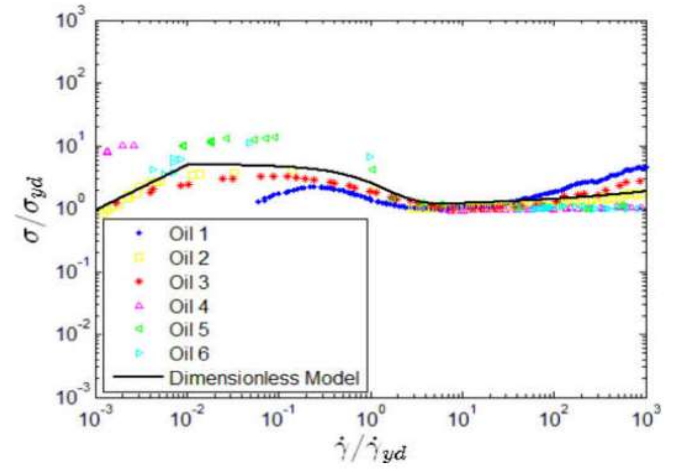


Fig. 19. Dimensionless shear stress as a function of shear rate for the six oils and a dimensionless model.

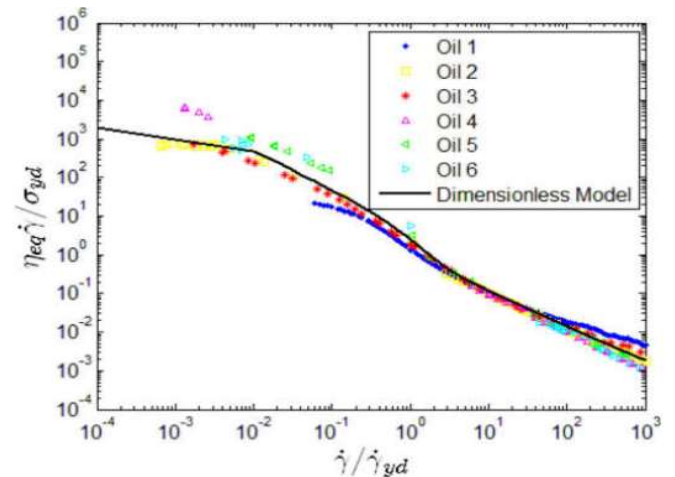


Fig. 20. Dimensionless viscosity as a function of shear rate for the six oils and a dimensionless model.

state for any of those with only one equation, this could become a powerful tool both for academia and industry.

Fig. 19 is the results of steady state stress divided by the dynamic yield stress, as has been discussed in the dimensionless section of the model, and Fig. 20 is the dimensionless viscosity increase with the dimensionless shear rate.

Note that the oils follow a tendency which is predicted by the dimensionless model. However, there are some discrepancies in the both extreme shear rates. Even with those discrepancies, we believe that these results are of interest. The highest error occurs for small shear rates.

4.3. Oscillatory test

Oscillatory test data are shown in Figs. 21–26. The viscoelastic region can be seen for all the oils, where the material has constant and stable storage and loss moduli. The measurement error increases as the stress amplitude decreases, leading eventually to an oscillation in the data. When the error rose above a particular threshold we stopped the measurement.

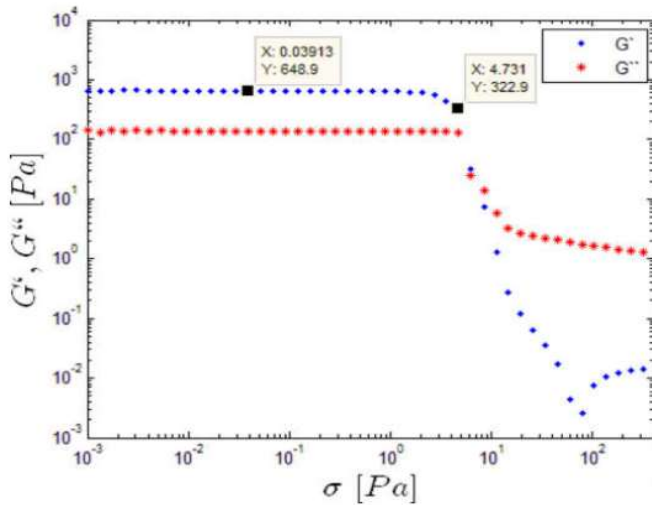


Fig. 21. Stress sweep curve for Oil 1 at 1 Hz 1 h of aging time.

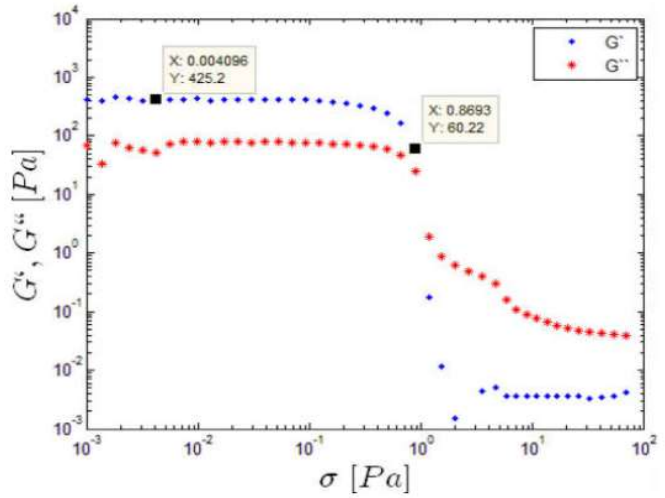


Fig. 23. Stress sweep curve for Oil 3 at 1 Hz 1 h of aging time.

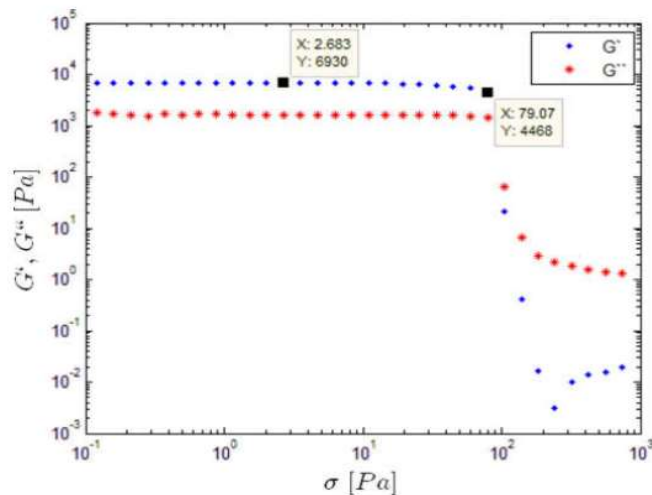


Fig. 22. Stress sweep curve for Oil 2 at 1 Hz 1 h of aging time.

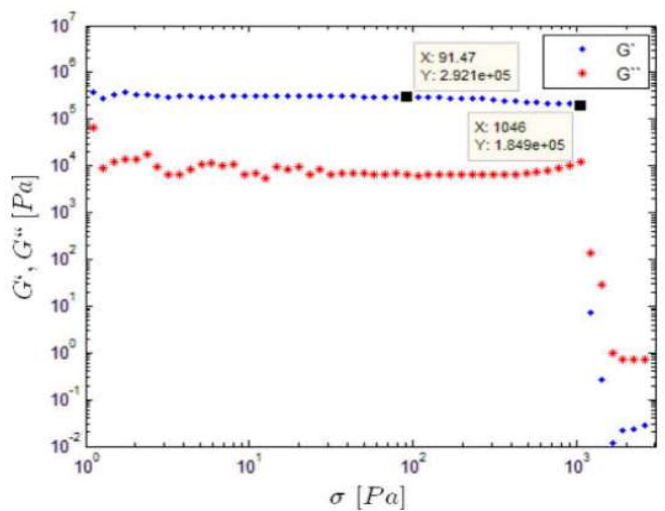


Fig. 24. Stress sweep curve for Oil 4 at 1 Hz 1 h of aging time.

The creep region can be seen for Oil 1, 3 and 5, where there is a continuum decrease in the derivative of the moduli. For those three oils, the creep region ends in the crossover of the storage with the loss moduli. Oils 2, 4 and 6 have more abrupt response in the limit of the solid-like behaviour, the breakdown occurs without the continuum decrease in the derivative of the storage modulus.

The physical meaning of the moduli under large amplitude oscillation is an open discussion in the scientific community with a few recent studies on the subject [44–46]. For all the oils, what looks like an inertial effect can be seen before the storage modulus reaches a constant value after the breakdown. After the crossover point, the storage modulus keeps decreasing, eventually reaching a lower limit. After this point, the modulus rises again approaching asymptotically to the final value. Only Oil 5, Fig. 25, does not show an abrupt variation in the derivative of the storage modulus.

Some studies argue that the value of the apparent yield stress is where the crossover of the storage modulus and the loss modulus occurs, [29] is one example. If the creep region ends at the crossover, it can be said that at that point the solid-like behaviour becomes dominant. However, that is not the definition of apparent

yield stress. In oscillatory tests it is hard to define where the plastic deformation ends and the viscous behaviour starts, therefore, it is possible to say that there is a range of stress amplitudes that might be the apparent yield stress.

When the oil shows a strong slope from the creep region and the crossover, like the results for Oils 4 and 6, the discussion is clearer, because the breakdown is definitely not in the crossover, rather in the end of the plateau. In the results shown in Figs. 24 and 26 it is possible to see that the oil does not present a soft gradient in the creep region, instead there is an abrupt break in the gel from the plateau to the dynamic behaviour. That might mean that the structure formed by these oils breaks down without much plastic deformation, and therefore, the point that defines the apparent yield stress is similar to the elastic yield stress, hence, in this special case, it is not the crossover of the storage and the loss moduli that define the apparent yield stress.

When dealing with the molecular level, the chain network drives the primary structure to undergo yielding and plastic flow in the cases of smooth breakdown. In the case of the abrupt break-

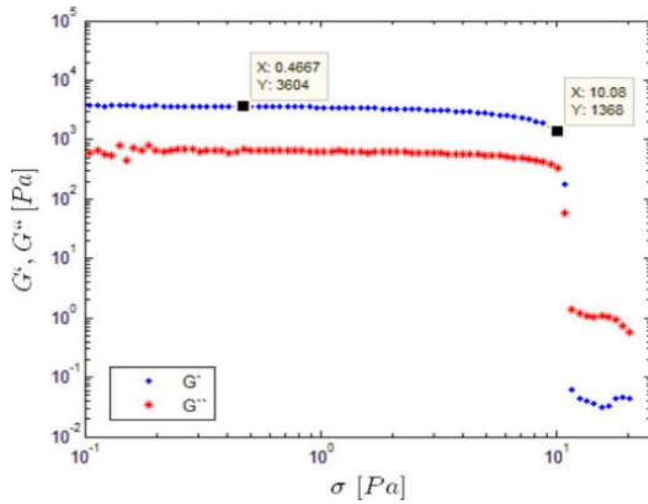


Fig. 25. Stress sweep curve for Oil 5 at 1 Hz 1 h of aging time.

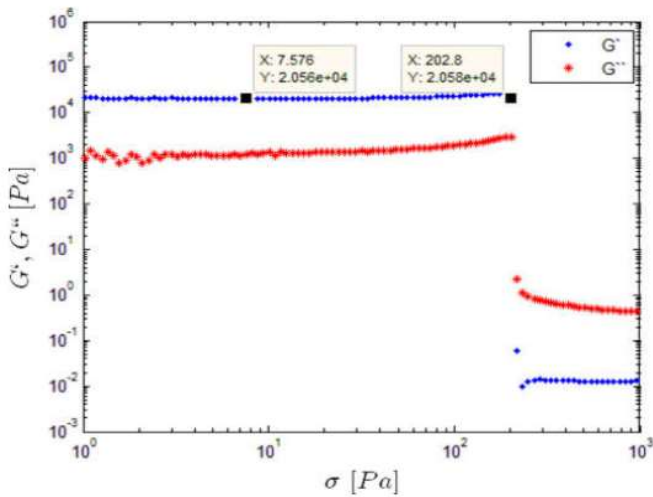


Fig. 26. Stress sweep curve for Oil 6 at 1 Hz 1 h of aging time.

Table 3
Parameters obtained from the oscillatory test.

Parameters	Oil 1	Oil 2	Oil 3	Oil 4	Oil 5	Oil 6	Units
G_0	649	6930	425	$2.9 \cdot 10^5$	3640	$2 \cdot 10^4$	Pa
σ_y	4.7	80	0.9	1046	10	203	Pa

down, it is probably a crack that breaks the crystalline structure at the apparent yield stress.

Because there is a possible range of stresses where the material yields, we used the last data point before the abrupt decrease of the storage modulus as values for the apparent yield stress. Those values are shown in the datatips from Figs. 21–26 and in Table 3.

In Figs. 27 and 28 it is possible to see that the values of apparent yield stress for the six oils are different and following the same tendency discussed in steady state, Oil 4 has the strongest and Oil 3 the weakest structure.

The apparent yield stresses obtained in the oscillatory test are smaller than in steady state for the six gelled waxy crudes, the results are close though. In [41] there is an error for one oil of

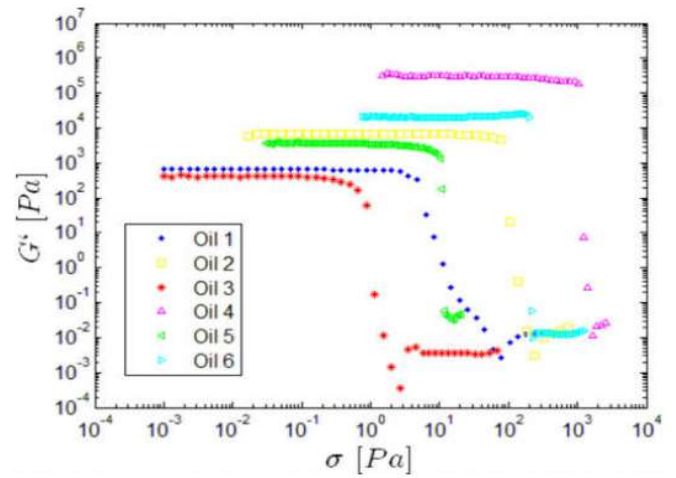


Fig. 27. Comparison of the storage modulus for the 6 oils.

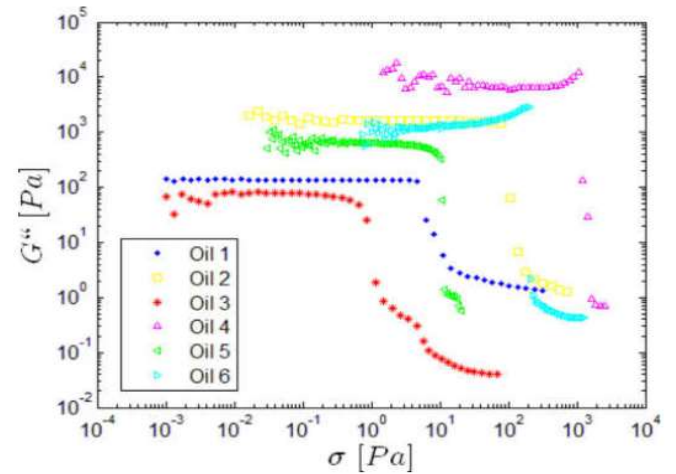


Fig. 28. Comparison of the loss modulus for the 6 oils.

Table 4
Comparison of the values obtained from the steady state and oscillatory tests.

Oils	σ_y [Pa]	
	Steady state	Oscillatory
Oil 1	7.0	4.7
Oil 2	91	80
Oil 3	1.43	0.9
Oil 4	1203	1046
Oil 5	19.8	10
Oil 6	222.1	2.3

one scale of magnitude from the steady state to the oscillatory. That result were obtained using a procedure that did not consider the time-dependent behaviour when doing the steady state procedure. Once that procedure was corrected, the results became similar. Table 4 shows a comparison between values obtained in oscillatory tests and in steady state.

Chang et al. [47] and Luthi [48] argue that the oscillatory test is more reliable for obtaining the apparent yield stress, once it is less sensitive to operational procedures. In further analysis and simu-

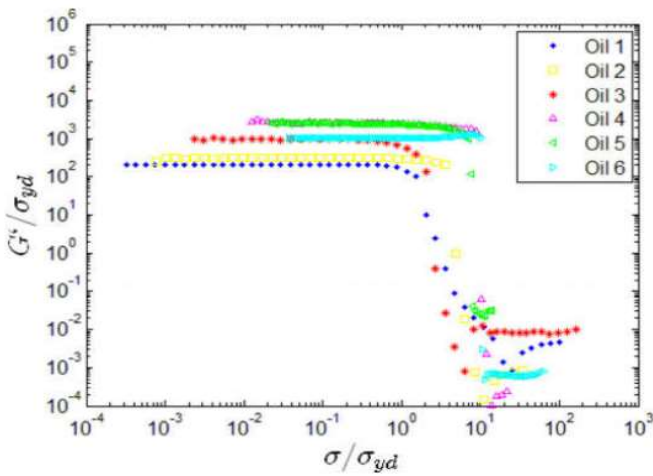


Fig. 29. Dimensionless storage modulus for the six gelled waxy crude oils.

lations, we used the value of apparent yield stress obtained in the oscillatory test.

The dimensionless oscillatory results are not as good as the steady state ones. Fig. 29 shows the different plateaus and different dimensionless apparent yield stress.

4.4. Constant shear rate flow

When dealing with complex rheological characterization, transient behaviour can enhance knowledge and understanding. As described previously we did two transient tests, applying constant shear rate, measuring the stress, applying constant shear stress, and measuring the shear rate.

When the rheometer applies a constant shear rate in a sample of the gelled waxy crude, three results can occur. First, the stress necessary to obtain the shear rate is so small that the structure is not destroyed, the gel responds elastically regardless of how long it is applied, hence the steady state is not reached in the experimental time. Second, the stress rises above the point necessary to destroy the structure, but it takes some time. The elastic behaviour is dominant for a while, an overshoot in the stress happens, and afterwards, the steady state is reached. Finally, an initial stress is high enough to destroy the structure and no elastic behaviour or overshoot is observed [36,41,49].

The results of constant shear rate tests are shown from Figs. 30–35 from Oils 1 to 6. We did the experiments controlling five different shear rates for each of the oils. The three previously described behaviours can be seen for the oils, Oils 1, 2, 5. This occurs because the structure formed by these oils breaks down in the range of the stress necessary to apply the shear rates from the experiments.

For Oil 3, however, an overshoot is not seen, which is related to the structure's weakness. Because Oil 3 does not have a strong structure and therefore has a smaller characteristic time, when the material's apparent yield stress is overcome, the oil flows instantly, without the increase of stress while the structure is still present, which leads to the overshoot.

Finally, the two strongest oils do not show the instantaneous breakdown in structure. For the small shear rates only the elastic behaviour can be seen and for big shear rates, it is possible to see the overshoot. What we can expect is that if we continue raising the shear rate, at some point we would reach an instantaneous breakdown in the gel.

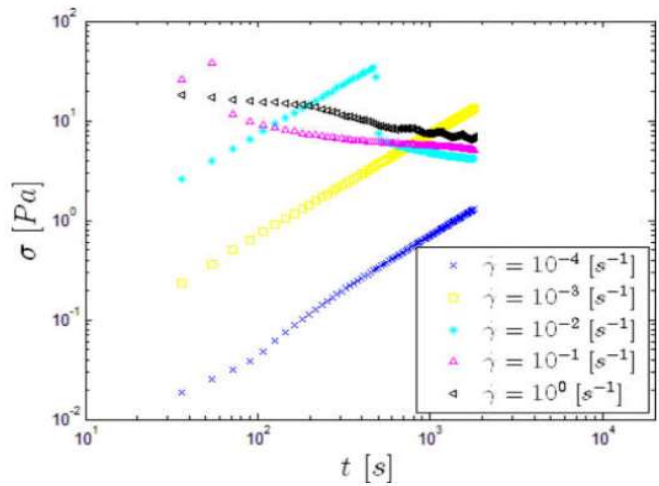


Fig. 30. Constant shear rate flow for Oil 1 and 1 h of aging time.

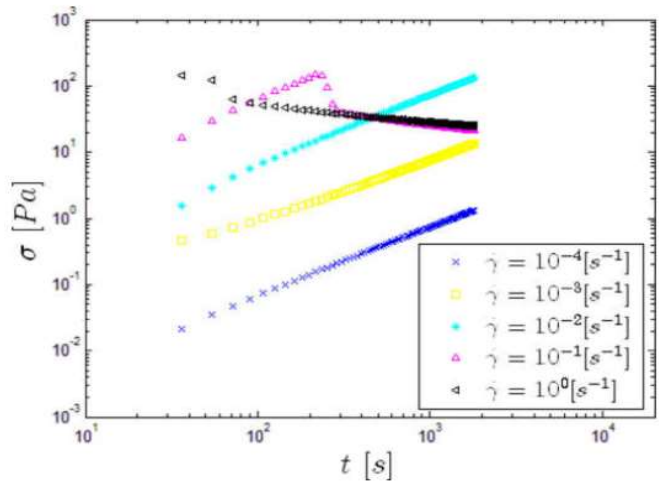


Fig. 31. Constant shear rate flow for Oil 2 and 1 h of aging time.

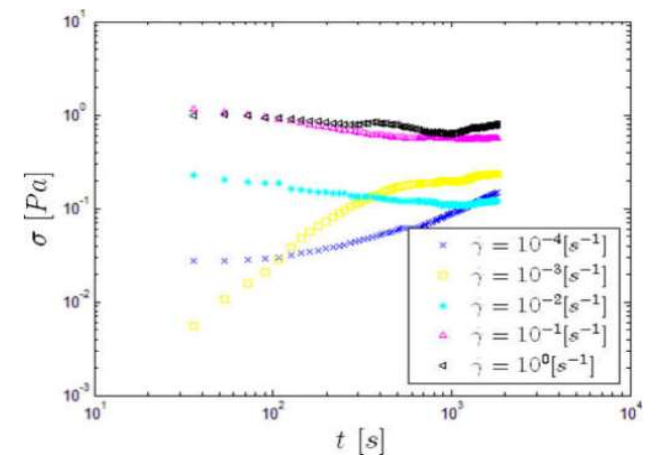


Fig. 32. Constant shear rate flow for Oil 3 and 1 h of aging time.

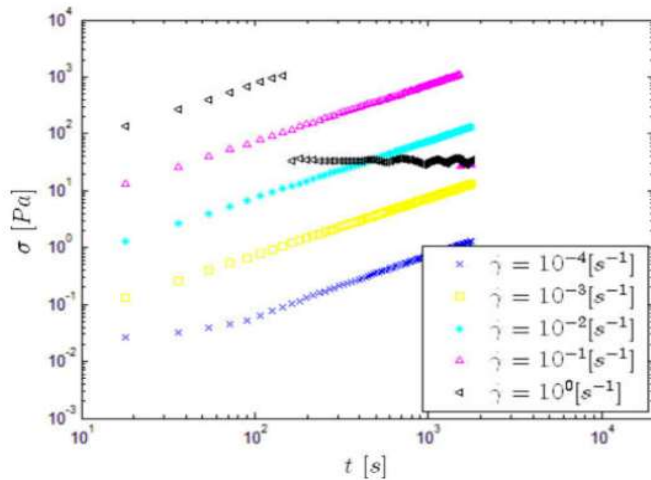


Fig. 33. Constant shear rate flow for Oil 4 and 1 h of aging time.

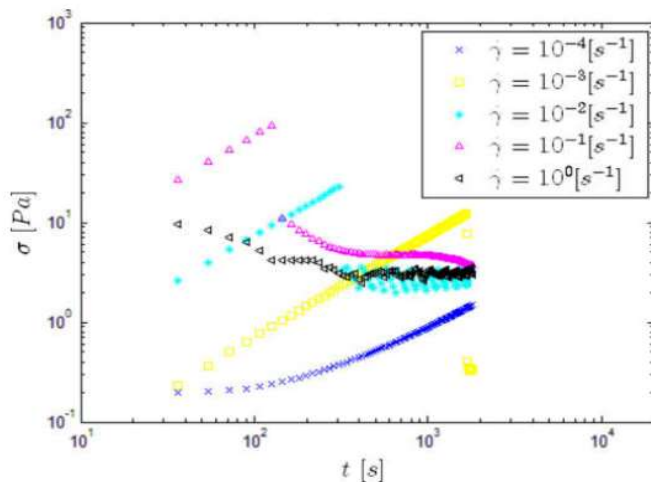


Fig. 34. Constant shear rate flow for Oil 5 and 1 h of aging time.

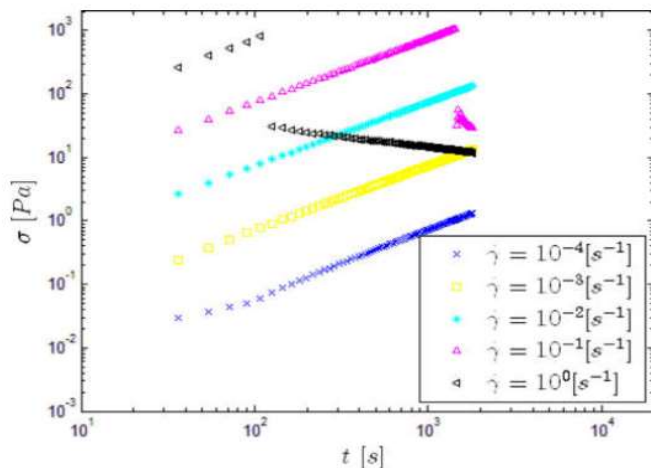


Fig. 35. Constant shear rate flow for Oil 6 and 1 h of aging time.

Table 5

Comparison of storage modulus measured with oscillatory and constant shear rate experiments.

Oils	G_0 [Pa]	
	Constant shear stress	Oscillatory
Oil 1	7.34	649
Oil 2	7.42	6930
Oil 3	0.75	425
Oil 4	7.44	2.910^5
Oil 5	7.53	3640
Oil 6	7.40	210^4

Another interesting discussion is related to the difference between the apparent yield stress and the value of the stress at the overshoot. For Oils 1 and 6, the overshoot is around 5 times higher than the apparent yield stress, for Oils 2, 4 and 5 the value is maximum two times higher. Considering exclusively the phenomenological theory of brittle and ductile, one explanation would be that Oils 1 and 6 are more ductile than Oils 2, 4 and 5. This means that Oils 2, 4 and 5 can support lower plastic deformation while Oils 1 and 6 can resist to a higher plastic deformation. What that means is, after the structure started to be destroyed it can still be deformed longer, the gel has a smaller variation of strength when suffering strain.

The storage modulus for the elastic region G_0 that has been shown in Table 3 obtained from the oscillatory test is measured differently in the constant shear rate experiment. As can be seen in Figs. 30–35, before the oil reaches the highest stress value, the overshoot, the stress grows linearly with time for constant shear rates, in this region, the elastic storage modulus can be calculated with Eq. (11).

$$\sigma = G_0 \dot{\gamma} t \quad (11)$$

Divoux et al. [42] have obtained similar values for both measurements of the storage modulus in the elastic region. For our oils, however, as can be seen in Table 5, the values are completely different. An interesting result is that for all the oils that build up a strong structure the storage modulus obtained in the constant shear rate experiments were nearly equal and around 7. These values were obtained by Van Der Geest et al. [41] for both Oils 1 and 2, now we have obtained the same values for another 3 gelled crudes, Oil 4, 5 and 6.

These measurements need to be further studied. The only reason for that would be the wax crystalline structure has the same strength regardless of the oil's composition, the problem is that we do not see that behaviour in other experiments, and the Oil 3, that builds the weakest structure has a different storage modulus.

The results comparing the experimental data with [38] model are shown from Figs. 36–41. The model can predict the three behaviours discussed before.

The comparison of the experimental data for the transient phenomena applying constant shear stress and the model is in a dimensionless form is order to be able to generalize the results.

The model has a few empirical parameters that allow for fitting transient curves such as constant shear rates. What we did was to use least square method for the data of the shear rate of $\dot{\gamma} = 1 \text{ s}^{-1}$ and then applied those values to simulate all the other experiments. It can be seen that for some shear rates, the overshoot value was not predicted with good accuracy, but in general, the model is able to predict the experimental data correctly.

4.5. Constant shear stress

When we apply a constant shear stress in the rheometer, three results can occur, which are related to the same phenomena as the three results in constant shear rate. First, the stress is not enough

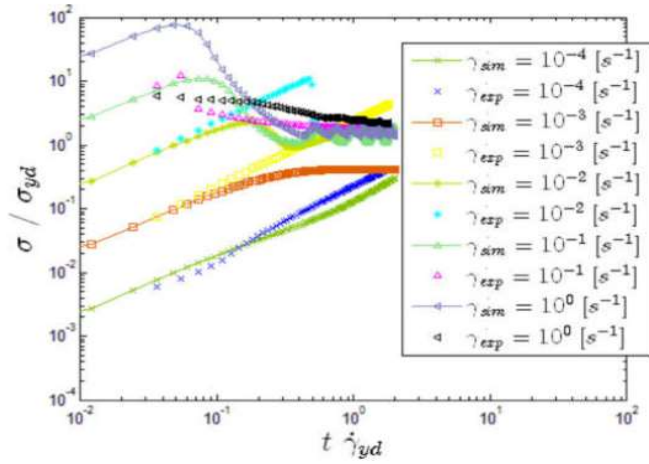


Fig. 36. Comparison of experimental data with the model for constant shear rate flow for Oil 1 and 1 h of aging time.

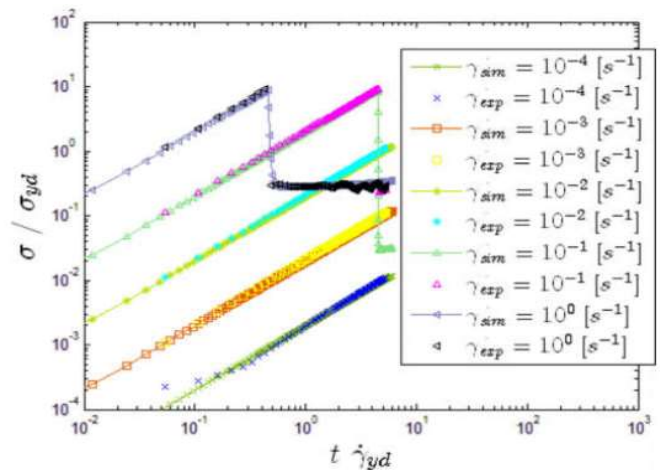


Fig. 39. Comparison of experimental data with the model for constant shear rate flow for Oil 4 and 1 h of aging time.

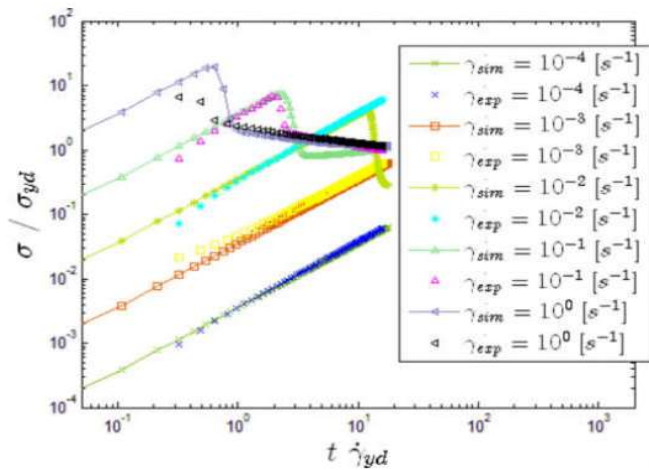


Fig. 37. Comparison of experimental data with the model for constant shear rate flow for Oil 2 and 1 h of aging time.

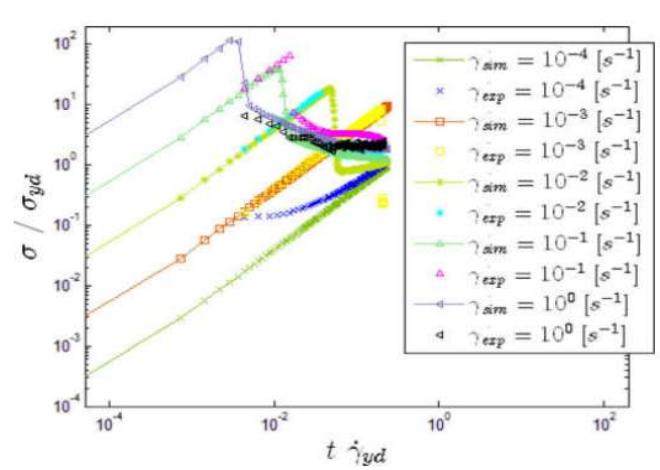


Fig. 40. Comparison of experimental data with the model for constant shear rate flow for Oil 5 and 1 h of aging time.

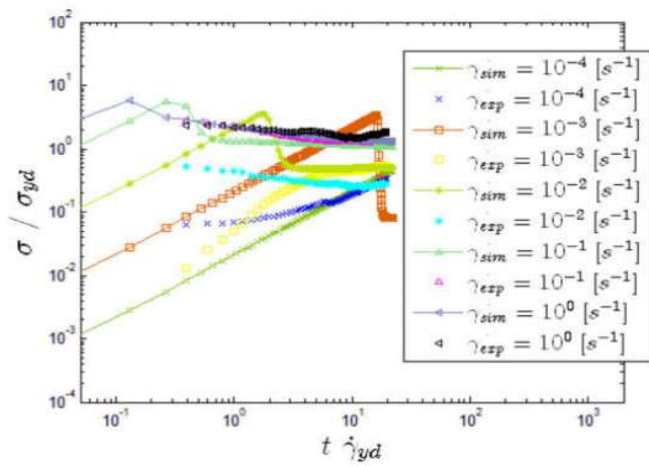


Fig. 38. Comparison of experimental data with the model for constant shear rate flow for Oil 3 and 1 h of aging time.

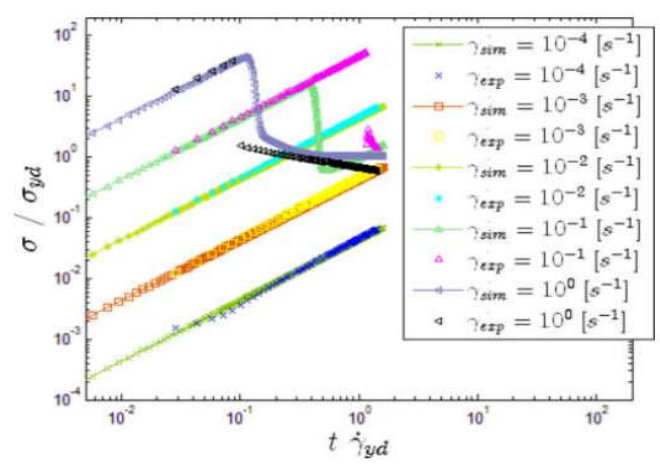


Fig. 41. Comparison of experimental data with the model for constant shear rate flow for Oil 6 and 1 h of aging time.

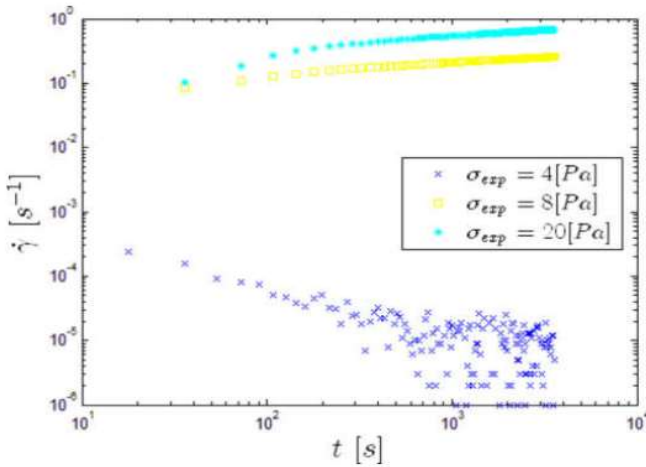


Fig. 42. Constant shear stress tests with Oil 1 for 1 h of aging time.

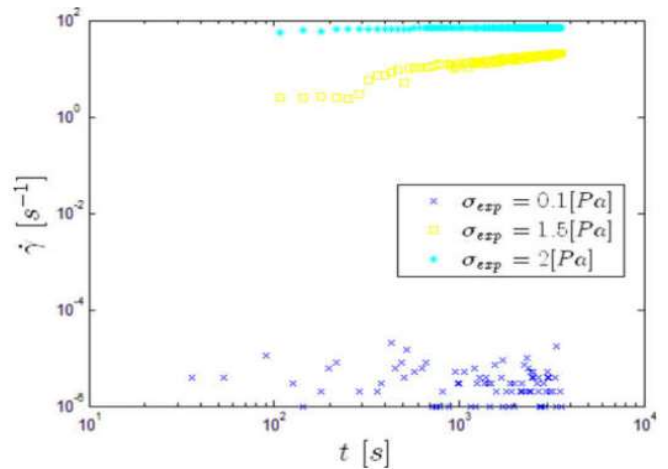


Fig. 44. Constant shear stress tests with Oil 3 for 1 h of aging time.

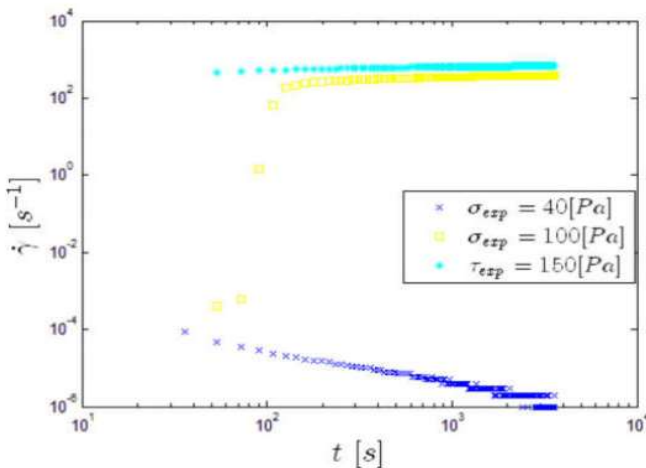


Fig. 43. Constant shear stress tests with Oil 2 for 1 h of aging time.

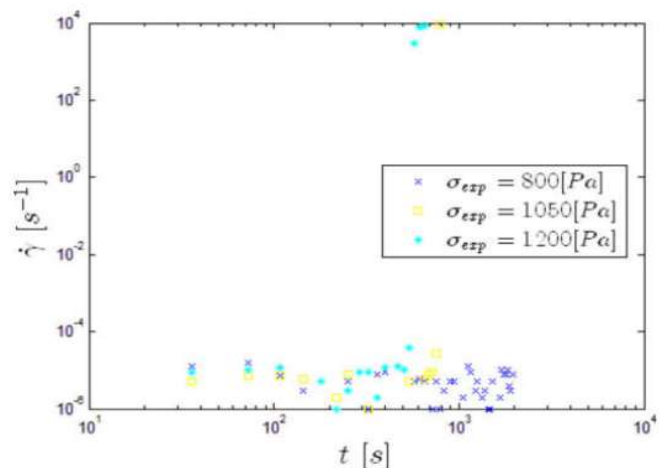


Fig. 45. Constant shear stress tests with Oil 4 for 1 h of aging time.

to generate any flow, hence there is no shear rate and no steady state. Second, the stress is enough to break down the structure, but it takes some time. Once the oil flows the structure breaks down really fast and the steady state is reached. Finally, the applied stress is high enough to destroy the structure and the steady state is reached without any significant variation in the shear rate [36].

The results are presented from Figs. 42–47. The transient phenomena can be seen for Oils 3, 4 and 6. For the others, the applied stress only shows the first and the third behaviour, which does not mean that these oils do not present the second behaviour, rather it implies that if we had chosen different stresses to do the experiment we might have seen it.

The results of the comparison of the model with the experimental data for constant shear stress are shown from Figs. 48–53. As we discussed before, we fitted all the empirical parameters using the constant shear rate results for the shear rate of $\dot{\gamma} = 1 \text{ s}^{-1}$, and used the values to do all the other shear rate simulation. We also used those values to do the simulations of constant shear stress.

It can be seen that for the transient phenomenon, the model either delayed or advanced the breakdown for all three oils. Another

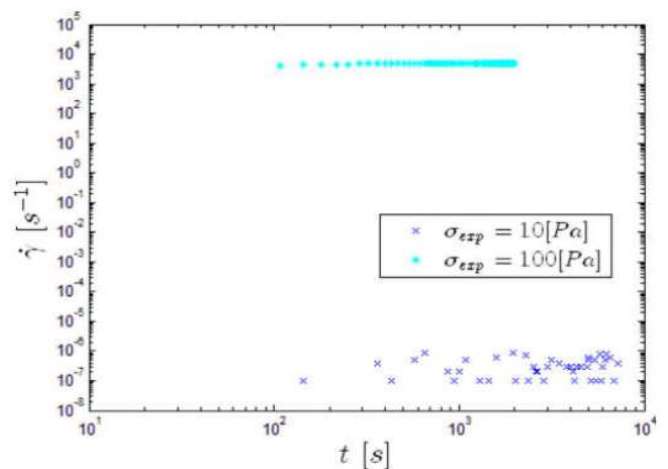


Fig. 46. Constant shear stress tests with Oil 5 for 1 h of aging time.

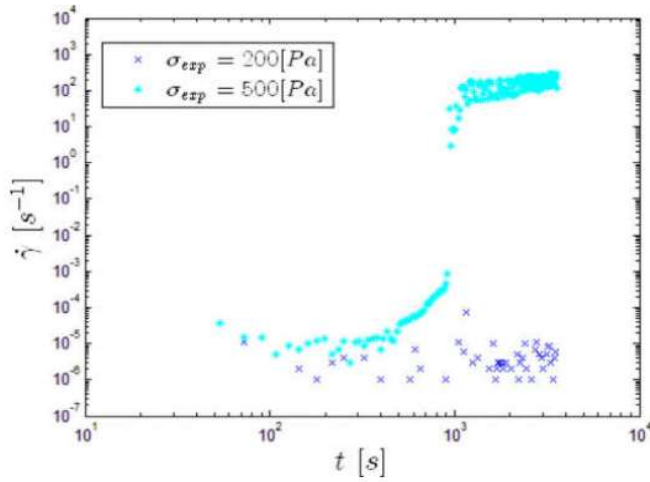


Fig. 47. Constant shear stress tests with Oil 6 for 1 h of aging time.

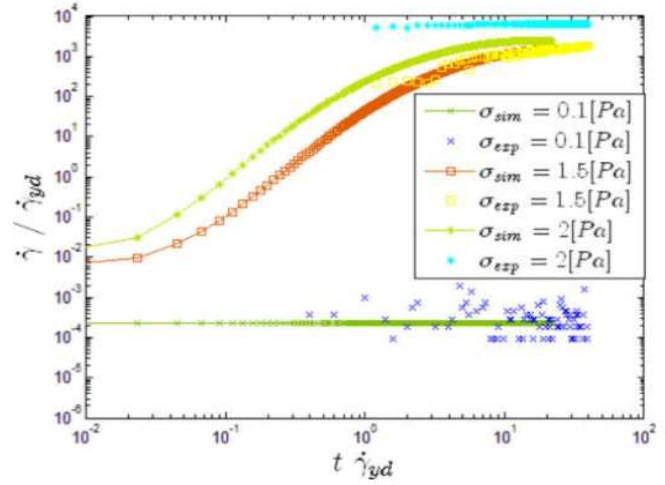


Fig. 50. Comparison of experimental data with the model for constant shear stress experiment for Oil 3 and 1 h of aging time.

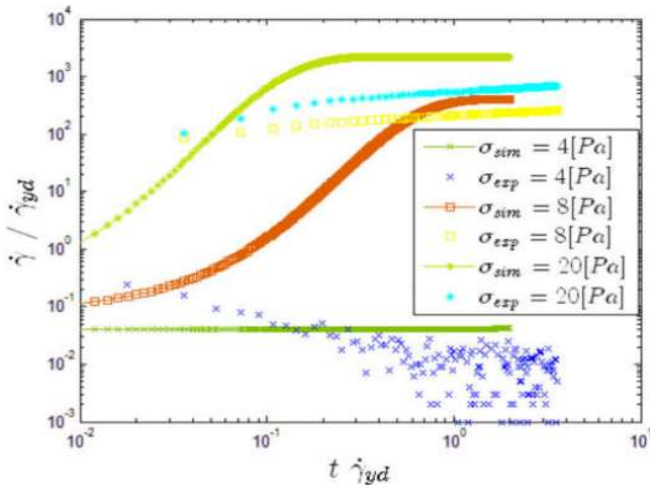


Fig. 48. Comparison of experimental data with the model for constant shear stress experiment for Oil 1 and 1 h of aging time.

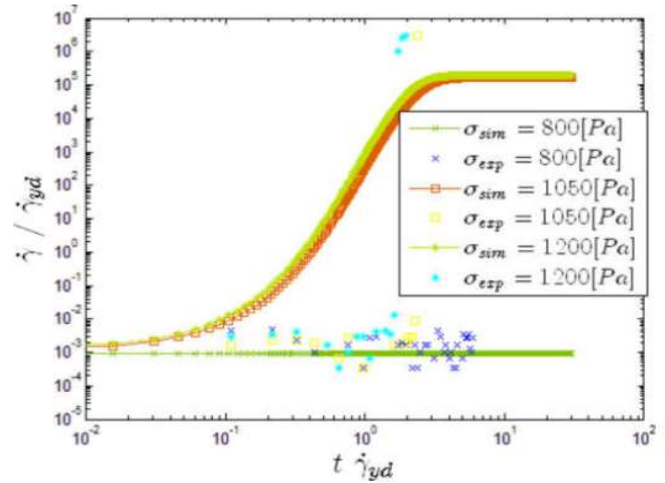


Fig. 51. Comparison of experimental data with the model for constant shear stress experiment for Oil 4 and 1 h of aging time.

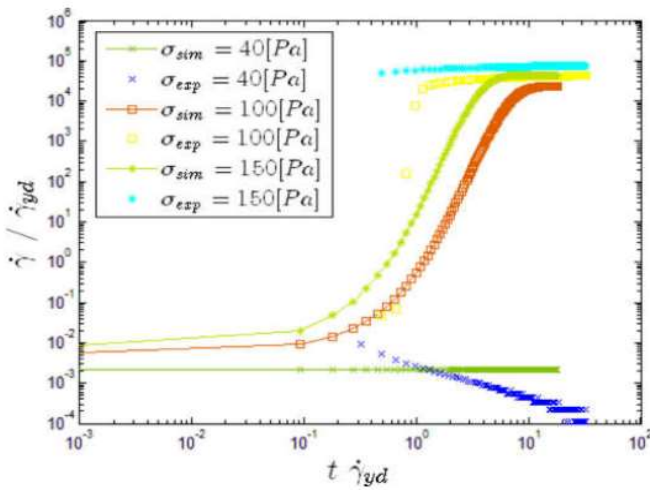


Fig. 49. Comparison of experimental data with the model for constant shear stress experiment for Oil 2 and 1 h of aging time.

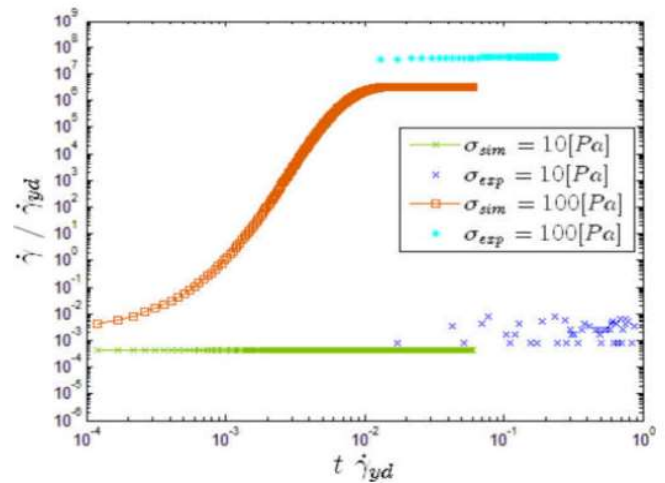


Fig. 52. Comparison of experimental data with the model for constant shear stress experiment for Oil 5 and 1 h of aging time.

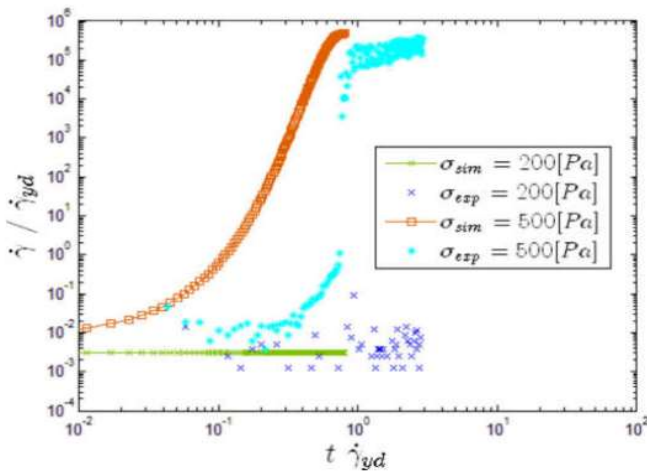


Fig. 53. Comparison of experimental data with the model for constant shear stress experiment for Oil 6 and 1 h of aging time.

result is the time necessary from the beginning of the breakdown until steady state is reached. For three of the oils the model predicted a much longer breakdown with the set of parameters used than the experimental data shows.

The model proposed by de Sousa Mendes and Thompson does not differentiate the second and the third behaviour. What it does is to suppose that if the experimental data does not show it, this is because the experiment was not accurate enough to get the data for small times [38]. Even if we cannot see the transient phenomena for the Oils 1, 3 and 5, we can compare the steady state value.

The steady state value is predicted with accuracy for some oils and with considerable errors for some others. There can be several explanations for this errors, from experimental uncertainty to the modification of the sample by aging.

4.6. Different aging times

To study the influence of aging time in gelled waxy crude rheological properties, we did three of the experiments discussed so far with different aging times. Oscillatory experiments, constant shear rate and constant shear stress with Oil 2 and Oil 4.

Figs. 54–56 show the results of the oscillatory tests for Oils 2 and 4. Beginning with an unexpected result it can be seen in Figs. 54–56 that the storage modulus in the linear region are independent of aging. There are studies that have seen no influence of aging time [34,50], while some studies have reported that aging has an influence when dealing with the storage modulus specifically [8,6,51,52].

It is important to comment that we are showing one result here, and we did tests in triplicate. The variation in the plateau value for different aging times are among the errors of the reproducibility for each of the aging times. The data of Oil 2 shows that for 5 h of aging the plateau was lower than for 1 h. For Oil 4, when the oil was left aging for 5 h, the plateau was the lowest. All the plateaus are within the range obtained in the triplicate results, which leads to the conclusion that for the crude oils studied, the storage modulus does not change with the studied aging time. Perhaps a longer aging time was necessary for the structure to get stronger.

With aging time, the value of apparent yield stress had a tendency to increase for Oils 2 and 4. The point where the oil structure breaks down is more visible for Oil 4. However, Oil 2 followed the same tendency. Therefore it can be said, that for these two oils,

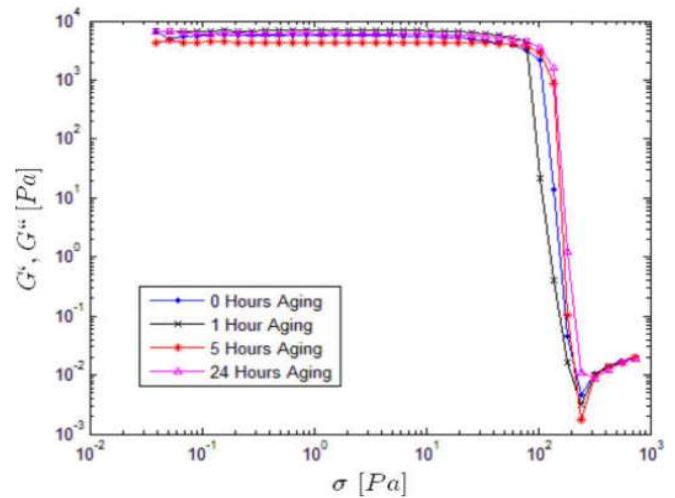


Fig. 54. Stress sweep curve for Oil 2 at 1 Hz for different aging times.

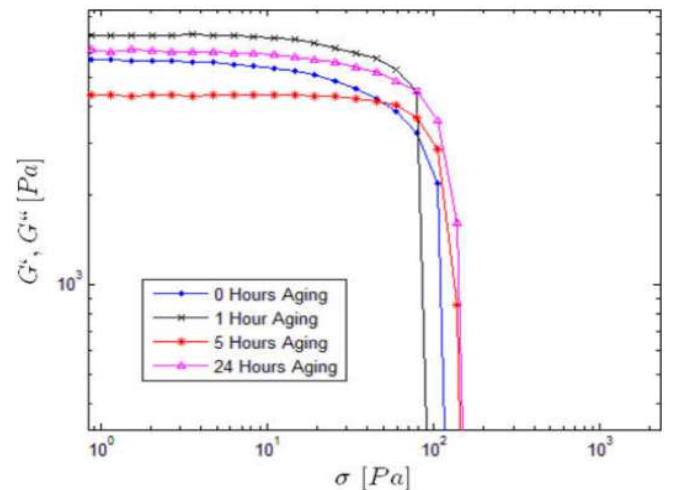


Fig. 55. Zoom of Fig. 54.

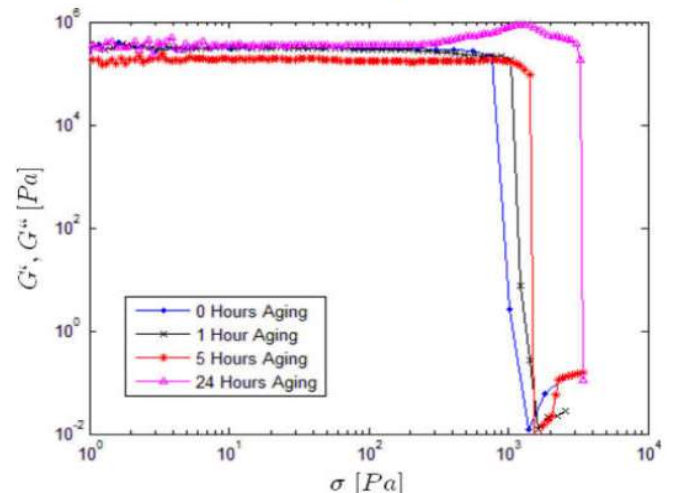


Fig. 56. Stress sweep curve for Oil 4 at 1 Hz for different aging times.

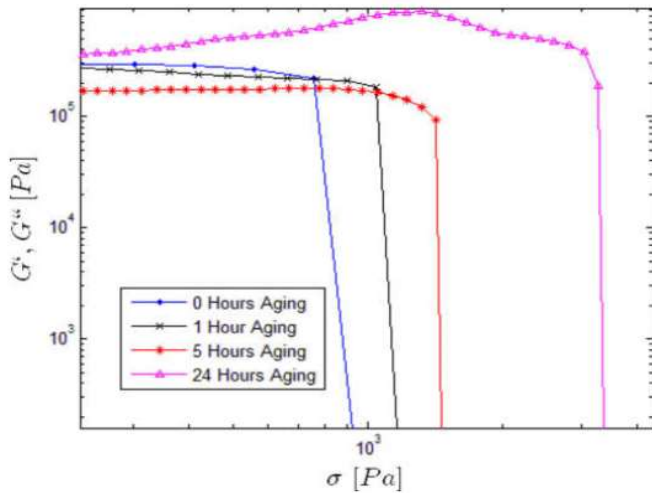


Fig. 57. Zoom of Fig. 56.

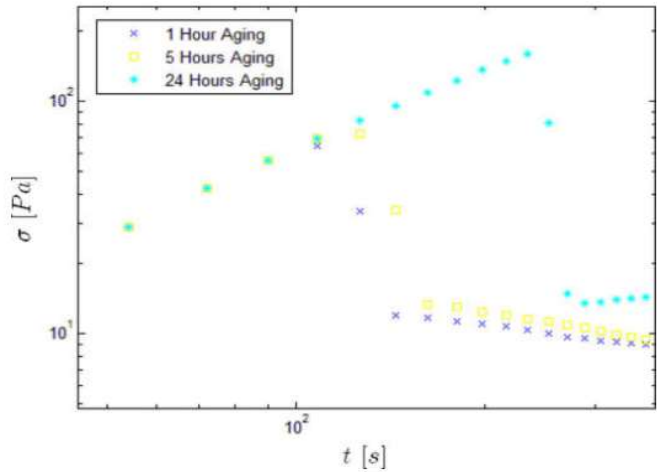
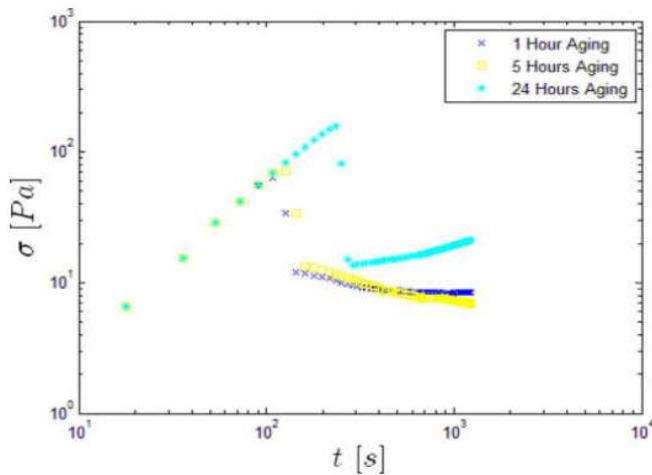
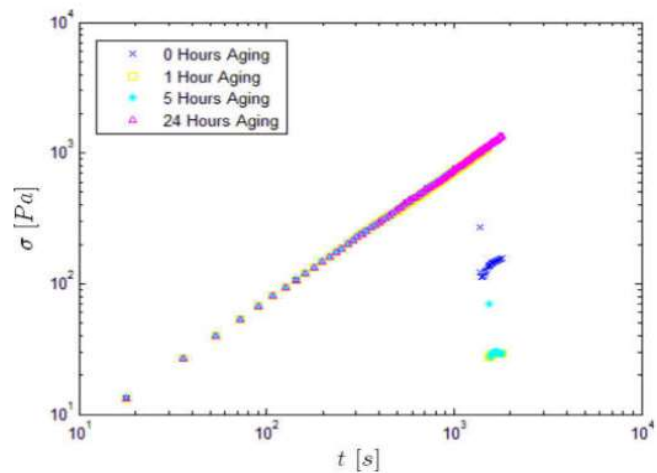


Fig. 59. Zoom of Fig. 58.

Fig. 58. Constant shear rate of $\dot{\gamma} = 0.1 \text{ s}^{-1}$ for Oil 2 for different aging times.Fig. 60. Constant shear rate of $\dot{\gamma} = 0.1 \text{ s}^{-1}$ for Oil 4 for different aging times.

the storage modulus does not change with aging time, but aging influences the point where the structure of the gel breaks down.

This result can be related to what has been discussed previously. We can consider that with aging the gel becomes more ductile, which means it resists a higher plastic deformation, which is why the plateau has the same value, but the deformation is longer before breaking down.

Fig. 57 shows an oscillation of the plateau for Oil 4 when starting the creep region of the stress sweep curve. That behaviour is not what one would expect. It is possible that this phenomenon is not a real rheological behaviour, but since the experiment is done really close to the upper limit of the stress, it is a measurement error. That experiment was done in triplicate, and the plateau was the same in all experiments, but in two of them, the upper limit was reached before the end of the creep regions, and there was no crossover of the storage modulus and the loss modulus. Only in this experiment, we can observe a breakdown in the structure, and the limit was reached only one point after the breakdown.

The results of the influence of aging in transient phenomenon when a constant shear rate is applied are shown from Figs. 58–61. It can be seen for both oils that aging does not influence the

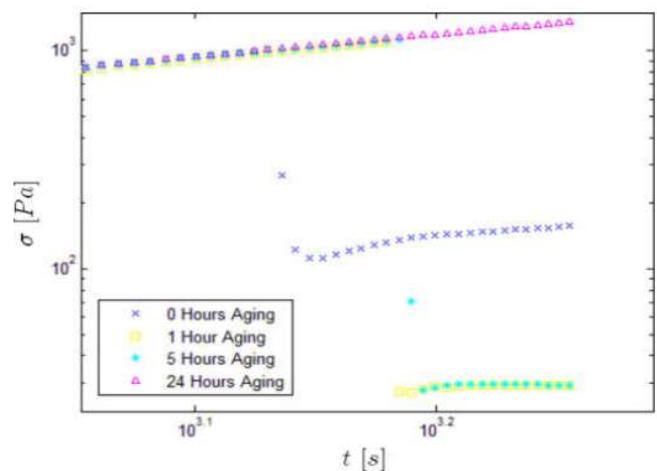


Fig. 61. Zoom of Fig. 60.

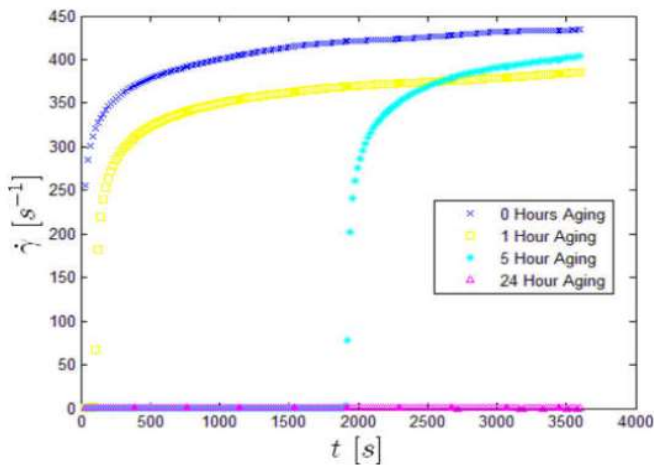


Fig. 62. Constant shear stress tests with 100 Pa and Oil 2 for different aging times.

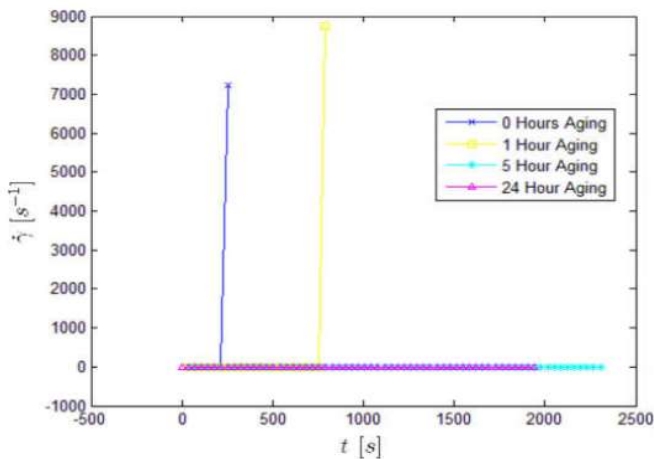


Fig. 63. Constant shear stress tests with 1000 Pa and Oil 4 for different aging times.

slope when under elastic behaviour, while it does influence the overshoot point of the oil. This is interesting, since it is an agreement with the results of the oscillatory test. A material with the same elastic strength but that could deform more plastically would show a higher overshoot, which can be seen for both oils.

The final results of this manuscript shown in Figs. 62 and 63, are the influences of aging time on a transient flow constant shear stress. The results are interesting, because as the aging time rises, the time necessary for breakdown also rises. It is important to distinguish the time necessary for breakdown from the apparent yield stress.

In one of the experiments where we measured apparent yield stress, using the flow curve, we applied each controlled stress for 30 min and waited until the steady state was reached, and then we increased the stress and waited again. If we had an infinite amount of time, maybe we would have found an apparent yield stress lower than what we measured.

In the results shown in Figs. 62 and 63, there is no flow when the oil aged for 24 h, which does not mean that the apparent yield stress increased above the stress applied $\sigma = 100$ Pa., rather it is possible that the time was not long enough to destroy the structure.

All the results shown in Fig. 63 are from experiments that reached the upper security stress limit of the rheometer. In other words, the rheometer stopped the experiment because it could not reach higher stresses.

5. Final remarks

Steady state experiments can present oscillation that does not represent any physical meaning. This can occur when one thinks the flow has reached equilibrium, but it has not. In our experiments, we show that if you apply 5 min for each point of the flow curve it is not enough to reach the steady state, rather when we waited for 30 min at each point, the equilibrium was reached, and the oscillation disappeared.

For highly paraffinic oils, the gel at 5 °C is strong. In steady state experiments, once you reach the apparent yield stress, the breakdown was fast and the rheometer could not measure points in between the apparent yield stress and the dynamic yield stress, even though the rheometer applied a stress for 30 min before raising the shear rate again.

The experimental data for all six oils have the same tendency in steady state. The equation proposed by de Souza Mendes and Thompson [38] for steady state was able to predict the experimental data with accuracy. In dimensionless form, the steady state for the six oils can be predicted with only one set of parameters, also with small errors. This was a surprising result, since we have up to three orders of magnitude of differences in the stress response for some of the oils.

Oscillatory tests for the six oils had a stable linear region with the storage modulus and the loss modulus crossing over and stabilizing when the shear stress amplitude rose enough. The point where the storage modulus starts to decrease abruptly was considered to be the apparent yield stress and had a good accuracy with the value obtained in the steady state experiment.

Transient experiments under constant shear rate were also performed and the result followed the same tendency as shown in the literature. The overshoot could be seen for the highly paraffinic oils and could not be seen for the oils with low percentage of wax. The model proposed by de Souza Mendes and Thompson [38] when using the storage modulus obtained from the constant shear rate experiment could predict the behaviour with good accuracy.

Constant shear stress experiments have shown the behaviour expected. For the six oils we could see that for a stress smaller than the apparent yield stress there was no flow during the experimental time. For stress bigger than the apparent yield stress there would be a transient flow and then the oil would reach steady state. The simulation, however, could predict the behaviour, but without good accuracy. Both the time when the breakdown occurred and the final value under steady state yielded a high number of errors.

Aging time influences the behaviour of the Oils 2 and 4, however, not as reported in the literature. There is no influence when elastic behaviour is dominant in the gel, when it is in the linear region of the oscillatory test. The difference can be noticed only on the edge of the linear region, where the deformations are high. We analyzed it as if the aging makes the material more ductile, and therefore, the material would be able to deform more while the elastic response would remain constant.

Another influence of aging time is the time necessary for the structure breakdown under a constant stress. The time clearly increases with aging. If this relationship could be extrapolated to infinity we would have the yield stress, but because that is not an engineering reality, what we see is for the times we did the experiment we have reached a limit for both oils.

2. PAPER 2: Experimental study of the necessary pressure to start-up the flow of a gelled waxy crude oil

OMAE2017-62438

EXPERIMENTAL STUDY OF THE NECESSARY PRESSURE TO START-UP THE FLOW OF A GELLED WAXY CRUDE OIL

Charlie Van Der Geest

School of Mechanical Engineering
 Campinas, Sao Paulo, Brazil
 charlievander@gmail.com

Vanessa C. Bizotto Guersonit

Center for Petroleum Studies
 Campinas, Sao Paulo, Brazil
 vanessa@cepetro.unicamp.br

Luiz Antônio Simões Salomão Junior

Repsol Sinopec
 Rio de Janeiro, Rio de Janeiro, Brazil
 la.simoes@repsolsinopec.com

Antonio C. Bannwart

School of Mechanical Engineering
 Campinas, Sao Paulo, Brazil
 bannwart@fem.unicamp.br

ABSTRACT

The current study regards a recurrent problem in the oil industry when dealing with waxy crude oils in offshore fields. When a waxy crude stays static in the seabed for any reason, it will cool down below the pour point and form a crystalline structure. The strength of a crystalline structure rises with time and as temperature decreases, which is why the minimum pressure necessary to restart a flow rises when an oil stays static for longer time. When designing subsea structures, the assumption is when the pressure is enough to overcome a threshold stress the flow restart occurs. This threshold stress is related to what the literature calls apparent yield stress. However, there is considerable evidence that a simplified relation of this rheological parameter and the necessary pressure will provide overestimated value, and therefore, a better understanding of the phenomenon involved in this process is required. To understand the phenomenon, we build an experimental apparatus that allow us to represent condition of temperature close to bottom of the sea, and a pressurization system that allow us to control the inlet pressure with precision. The apparatus is composed of a one-inch pipeline that is submerged in a water bath (5°C) and a nitrogen system with controlled valves to pressurize the inlet of the pipeline. When studding the restart of a flow of a gelled waxy crude, there is a lot of discussion in the literature, many studies suggests that the rheological behaviour, the compressibility and the shrinkage of the oils are the most important phenomena involved. We obtained some interesting results that can help in that discussion. Experiments with an oil with a high percentage of wax that build up a strong crystalline structure shows that the oil have an interesting behaviour in the pipeline when comparing

to the rheological behaviour. To be able to provide to the industry a reliable prediction of the gelled waxy restart pressure, a lot of experimentation and improvement in the models are necessary. We compare the experimental data with the prediction of a model comprising a weakly compressible fluid with an elasto-viscoplastic thixotropic behaviour in order to be able to improve the knowledge and the get closer to the results expected from the industry.

INTRODUCTION

The problem of a blocked pipeline filled with gelled waxy crudes may occur when the production is interrupted. At the bottom of the sea, at 4 °C, the heat loss leads to the precipitation of wax crystals in the oil. The oil passes through two critic temperatures before it start behaving like a solid. First, the Wax Appearance Temperature (WAT), which is when dispersed crystals of wax starts to appear in the fluid. Second, the pour point, which is when the crystalline structure's strength is enough for the elastic behaviour overcome the viscous behaviour. When the temperature of the crude decreases more than the pour point's temperature, the rheological behaviour change abruptly, which can block the pipeline. (Fung *et al.*, 2006; Thomason, 2000; Venkatesan, *et al.*, 2003; Wardhaugh, & Boger, 1987.).

When designing subsea systems that will produce waxy crudes, a simple way to do is a simplified linear momentum balance. The assumption is that when the pressure is enough to overcome the yield stress, the restart occurs. The crystalline structure's breakdown, hence the flow restart, demands pressures higher than the operational pressure to flow the oil without precipitated wax. Therefore, an accurate prediction of start-up

pressures is essential for designing pipelines and pumps of subsea facilities. The problem is that there is evidence that this simplified linear momentum balance calculation overestimates the necessary pressure. (Geest, *et al.*, 2015; Chang *et al.*, 1998; Fleming *et al.*, (2013)).

Many have studied the problem of restart of a pipeline blocked with gelled waxy crude (Chang *et al.*, 1999; Davidson *et al.*, 2004; Lee, 2008; Wachs *et al.*, 2009; de Souza Mendes *et al.*, 2012; de Oliveira & Negrao 2015; Van Der Geest *et al.*, 2015). In those studies, there are different ways to approach the problem. When dealing with the conservation equations, there are mathematical models that consider a gelled crude displaced by a non-gelled crude and some that uses 1.5 D models to simulate the problem. When discussing the rheological behaviour, the complexity rises from simple constitutive equations all the way to complex elasto-viscoplastic thixotropic models.

EXPERIMENTAL APPARATUS

Restart Apparatus

Figure 1 shows the experimental apparatus built in CEPETRO to study flow assurance problems related to wax. The rig allow us to do two sets of experiments, study the wax deposition, and, the subject of this manuscript, study the restart of gelled waxy crude oils.

There is a water bath, which is connected to a heat exchanger and a chiller, allowing the water's temperature control from 90 °C to 5 °C. The pipeline inside the water bath is common for the wax deposition and restart experiments. Inside this pipeline in the water bath that the phenomena occur.

As can be seen, we have three tanks, two to do restart experiments and one to do deposition test. Only with a set of valves is possible to modify the experiment, choosing between restart experiment, single-phase wax deposition and multiphase wax deposition. The pipeline used for the restart experiment is highlighted in red and blue, the red is the pipeline connecting the tanks with the water bath, blue is the pipeline inside the water bath.

A pressure gauge (Rosemount 2088) in the inlet, two differential pressure gauge (Rosemount 3051) distributed in the pipeline and temperature sensors (PT100 4 wires) to measure both the oil's temperature and water's temperature compose the instrumentation for the restart experiment.

With this experimental apparatus is possible to do a few interesting measurements and study most of the effects that can influence the restart experiment. It is possible to study the influence of water's temperature, initial oil's temperature, shear rate history, aging time, time necessary to the start-up when a constant pressure is applied and the restart pressure in a continuously increasing inlet's pressure.

We built algorithms to control every variable using PID controller in order to our apparatus be as accurate as possible. Algorithms controls oil mass flow rate and temperatures of oil and water during the deposition tests. Inlet pressure and water's temperature in restart experiments.

The nitrogen generator is used in two of three possible experiments, restart and deposition under multiphase flow. In restart, we apply pressure to the waxy crude placed in the external tank (Green Line), and there is an electric pneumatic valve BR240S, that connects the nitrogen line to the external tank, allowing the control of the inlet pressure.

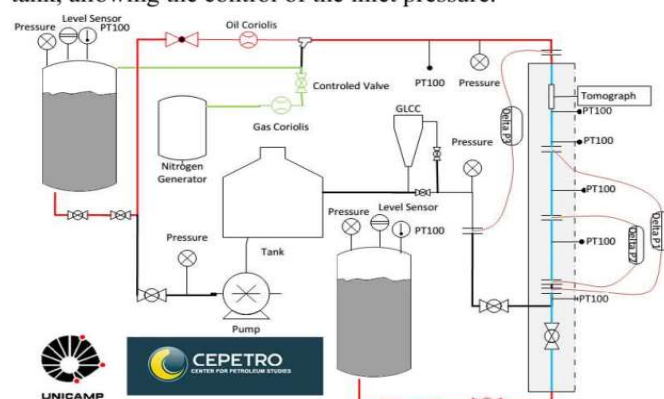


Figure 1. Layout of the experimental apparatus used for the restart test.

Rheometer

We executed the experiments using a controlled-stress rheometer MARS III from HAAKE GmbH with a cone and plate geometry. Diameter of 35 mm and 2 degree of angle with a gap of 0.105 mm. Crystal size of wax was more than 25 times smaller than the gap size, which guarantees that the measurement were not erroneous due to crystal's influence.

We activated the Peltier plate of the rheometer to control temperature and cooling rate. We also controlled the gap with the thermo-gap option. The gap option is necessary to prevent the oil to lose contact with the surface once it shrinks, guaranteeing that there are no mistakes due to slipping on the surface.

TEST PROTOCOLS

Restart Experiments

In this manuscript, we will not show the influence of all the boundary conditions that we discussed in last section. We will only show the influence of aging in the restart experiment with a real gelled waxy crude.

Before any testing the oil samples stood in the inner tank for 2 hours at 60 °C under stirring in order to ensure a good homogenization and the effective dissolution of all paraffin content in the crude oil. Meanwhile, the algorithm controlled the temperature of the water bath at 60 °C.

To start the procedure, all valves that connect the inner tank, test section and external tank were opened, hence, the horizontal pipeline was filled with the waxy crude oil until achieve the same level in the both tanks. The tanks were open to atmosphere during the filling procedure.

Once the pipeline was filled with oil, the temperature of the water bath was decreased to 5 °C. When the oil temperature in the test section reached approximately 5 °C. The gelled waxy

crude oil was aged for 1, 5 or 24 hours to check if the time necessary to restart the flow at constant pressure increases with aging time. After aging the gel, the pressurization system was switched-on, initiating the restart test.

During the cooling down, we monitored the differential pressure sensors to see whether the differential pressure would increase. That could happen for two reasons, one is the shrink due to temperature decrease at the same state, the molecules at liquid state would vibrate slower, and therefore the pressure would be smaller. Secondly, due to the crystallization of wax, some sort of vacuum appears in the middle of the pipeline (Phillips et al., 2011), which would also provoke a decrease on pressure inside the pipeline.

Initially, the tanks are at atmospheric pressure, then the pressure was increased using a nitrogen cylinder coupled to the external tank, we increased the pressure from atmospheric to the wanted pressure in approximately 15 seconds, and then, we waited to verify the necessary time to flow start-up.

During the experiment, we monitored eleven variables. Pipelines' inlet pressure, two differential pressures in the water bath, pressure in both tanks, level of the oil in both tanks, three temperatures and mass flow rate.

Rheometer Experiments

The preparation of the sample follows a procedure in order to erase thermal and shear stress histories. We homogenize the sample by preheating to 70°C and keeping for 2 hours. Once the samples were in the rheometer, the Peltier plate controlled temperature in 70°C and rheometer applied a shear rate of 10 s⁻¹ for 10 minutes to erase thermal history effects. Following, we cooled down to 5°C at the rate of 1°C/min without shear rate and finally we did the experiment. We did the rheological experiments in triplicate. The data of different samples of the same oil have a difference up to 20% of standard deviation.

In the steady state experiment, because it is necessary to pass the transient condition before you obtain the experimental data, every time we raised the shear stress we waited for 30 minutes before collecting the point.

MATHEMATICAL MODEL

De Oliveira and Negrao (2015) proposed the model used here to compare the experimental results with simulations of flow start-up of gelled waxy crude oil. The model uses the characteristic method to solve the conservation of mass and momentum equations, and uses the rheological model proposed by de Souza Mendes and Thompson (2013) to represent the rheological behaviour.

Both the rheological model and the characteristic method used here will be briefly discussed, for further information, consult the literature.

As shown in de Oliveira and Negrao (2015) and discussed in Van Der Geest *et al.*, (2015) the start-up can be characterized as Stokes flow, hence, there are terms of equations (1) e (4) that are two orders of magnitude smaller than others, therefore can be neglected.

Another important consideration is that the fluid is weakly compressible, which is modelled by applying the definition of

compressibility only in the mass conservation equation and maintain the linear momentum conservation as incompressible.

Dimensionless Analysis

The variables of interest are now scaled based on what de Sousa Mendes and Thompson (2013) proposed and de Oliveira and Negrao (2015). Characteristic shear rate is the ratio of sound speed and diameter of the pipeline (c/d). Characteristic shear stress is the dynamic shear stress τ_{yd} . In addition, the characteristic time to be the time until the pressure wave reach the end of the pipeline (l/c).

Using those characteristic variables, we can obtain the following dimensionless parameter:

$$\eta_0^* = \frac{\eta_0 \dot{\gamma}_{yd}}{\tau_{yd}}; \eta_\infty^* = \frac{\eta_\infty \dot{\gamma}_{yd}}{\tau_{yd}}; \tau_y^* = \frac{\tau_y}{\tau_{yd}}; \dot{\gamma}_{yd}^* = \frac{\dot{\gamma}_{yd}}{c/d};$$

$$K^* = \frac{K \tau_{yd}^{n-1}}{\eta_\infty^n}; t_{eq}^* = \frac{t_{eq}}{l/c}; G_0^* = \frac{G_0 l}{\eta_\infty c}$$

Mass Conservation

Equation (1) is the differential equation for mass conservation considering a compressible fluid with compressibility of α .

$$\frac{\partial p}{\partial t} + \frac{1}{\alpha} \frac{\partial V}{\partial z} + V \frac{\partial p}{\partial z} = 0 \quad (1)$$

From Equation (1), disregarding the small inertial term we obtain (2).

$$\frac{\partial p}{\partial t} + \frac{1}{\alpha} \frac{\partial V}{\partial z} = 0 \quad (2)$$

From Equation (2) using the dimensionless numbers we obtain (3).

$$\frac{\partial p^*}{\partial t^*} + \eta_\infty^* \phi \frac{\partial V^*}{\partial z^*} = 0 \quad (3)$$

Momentum Conservation

Equation (4) is the differential equation for linear momentum conservation considering an incompressible fluid.

$$\rho \frac{\partial V}{\partial t} + \rho V \frac{\partial V}{\partial z} + \frac{\partial p}{\partial z} = -\frac{4}{d} \tau_w \quad (4)$$

From Equation (4), disregarding small inertial term we obtain (5).

$$\rho \frac{\partial V}{\partial t} + \frac{\partial p}{\partial z} = -\frac{4}{d} \tau_w \quad (5)$$

From Equation (5) using the dimensionless numbers we obtain (6).

$$\frac{\partial p^*}{\partial z^*} + \eta_\infty^* \phi \frac{\partial V^*}{\partial t^*} + \tau_w^* = 0 \quad (6)$$

Rheological model

Constitutive Equation

The constitutive equation is based in an analogue with two springs and one dampers. The idea is to represent the elastic behaviour with springs and viscous behaviour with damper, allowing the model to predict the elasto-viscoplastic behaviour. Equation (7) is the result proposed by de Sousa Mendes and Thompson (2013).

$$\frac{\theta_2}{\eta_\infty} \left(\frac{\tau}{\theta_1} + \dot{\tau} \right) = (\dot{\gamma} + \theta_2 \ddot{\gamma}) \quad (7)$$

From Equation (7) using the dimensionless numbers we obtain (8).

$$-\frac{\partial v^*}{\partial r^*} + \theta_2^*(\lambda) \frac{\partial}{\partial t^*} \left(\frac{\partial v^*}{\partial r^*} \right) = \frac{2}{\eta_\infty} r^* \theta_2^*(\lambda) \left(\frac{\tau_w^*}{\theta_1^*(\lambda)} + \dot{\tau}_w^* \right) \quad (8)$$

Steady State Equation

The model proposed by de Sousa Mendes and Thompson (2013) uses the Equation (9) as steady state viscosity function. In this equation, there are two yields stresses, the static (τ_y) and dynamic (τ_{yd}); the shear rate of transition between them ($\dot{\gamma}_{yd}$); there are the Herschel Buckley parameters (K, n) and two viscosities, the initial (η_0) and final (η_∞).

$$\eta_{eq}(\dot{\gamma}) = \left(1 - e^{-\frac{\eta_0 \dot{\gamma}}{\tau_y}} \right) \left(\frac{\tau_y - \tau_{yd}}{\dot{\gamma}} e^{-\frac{\dot{\gamma}}{\dot{\gamma}_{yd}}} + \frac{\tau_{yd}}{\dot{\gamma}} + K \dot{\gamma}^{n-1} \right) + \eta_\infty \quad (9)$$

From Equation (9) using the dimensionless numbers we obtain (10).

$$\eta_{eq}^*(\dot{\gamma}) = \left(1 - e^{-\frac{\eta_0^* \dot{\gamma}_{eq}^*}{\tau_y^*}} \right) \left(\frac{(\tau_y^* - 1)}{\dot{\gamma}_{eq}^*} e^{-\frac{\dot{\gamma}_{eq}^*}{\dot{\gamma}_{yd}^*}} + \frac{1}{\dot{\gamma}_{eq}^*} + K^* (\eta_\infty^*)^n \dot{\gamma}_{eq}^{*n-1} \right) + \eta_\infty^* \quad (10)$$

Once we have the value of the viscosity in the equilibrium, it is possible to calculate the value of the shear stress in the equilibrium shown in Equation (11).

$$\tau_{eq}^*(\dot{\gamma}) = \eta_{eq}^* \dot{\gamma}_{eq}^* \quad (11)$$

The structural parameters reaches the equilibrium when the build-up and breakdown rates are the same. Equation (12) show the dimensionless equation.

$$\lambda_{eq} = \ln \left(\frac{\eta_{eq}^*}{\eta_\infty^*} \right) \quad (12)$$

Initial Condition

Equation (13) is used to calculate the structural parameter for the completely structured material.

$$\lambda_0 = \ln \left(\frac{\eta_0^*}{\eta_\infty^*} \right) \quad (13)$$

Characteristic Times

Equation (14) is the dimensionless relaxation time, while Equation (15) is the dimensionless retardation time.

$$\theta_1^* = \frac{1}{G_0^*} (1 - e^\lambda) e^{\lambda - m \left(\frac{1}{\lambda} - \frac{1}{\lambda_0} \right)} \quad (14)$$

$$\theta_2^* = \frac{1}{G_0^*} (1 - e^\lambda) e^{-m \left(\frac{1}{\lambda} - \frac{1}{\lambda_0} \right)} \quad (15)$$

The structural viscosity function

In Equation (16) there is the structural viscosity which is a function of the structure parameter λ and the purely viscous component η_∞ .

$$\eta^*(\lambda) = \eta_\infty^* e^\lambda \quad (16)$$

The Structure parameter

In Equation (17) there is the structural viscosity

$$\frac{d\lambda}{dt^*} = \frac{1}{t_{eq}} \left[\left(\frac{1}{\lambda} - \frac{1}{\lambda_0} \right)^a - \left(\frac{\lambda}{\lambda_{eq}(\tau)} \right)^b \left(\frac{1}{\lambda_{eq}(\tau)} - \frac{1}{\lambda_0} \right)^a \right] \quad (17)$$

Numerical Method

The equations were solved using the characteristic method for the conservation of mass and momentum and using the runge-kutta method for both differential equations of the rheological model. The details on the method and procedure are also in the literature.

Figure 2 and Figure 3 are the validation of the algorithm we developed. The difference in the solution is basically that de Oliveira & Negrao (2015) solve the differential equation using Euler's method and our algorithm uses Runge-Kutta. It is possible to see that the algorithm produces the same results that in the literature.

The simulation shown in Figure 2 and Figure 3 are the restart of a weakly compressible Newtonian fluid. In the literature, they show the analytical solution of this problem, which allow us to validate the algorithm.

We can see in Figure 2 the time evolution of pressure for three different axial position, once a constant pressure was applied as boundary condition. It is possible to see the oscillation due to the compressibility.

It is possible to see in Figure 3 the time evolution of velocity in the middle of the pipeline, the time necessary to the pressure to be felt in this axial position was about 0.4 dimensionless time and the oscillation until the steady state is reached.

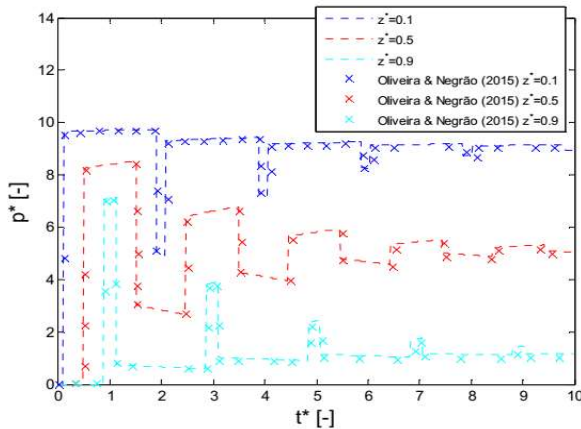


Figure 2. Comparison the algorithm created and the results published by Oliveira & Negrão (2015) for evolution of pressure of a restart of a Newtonian fluid.

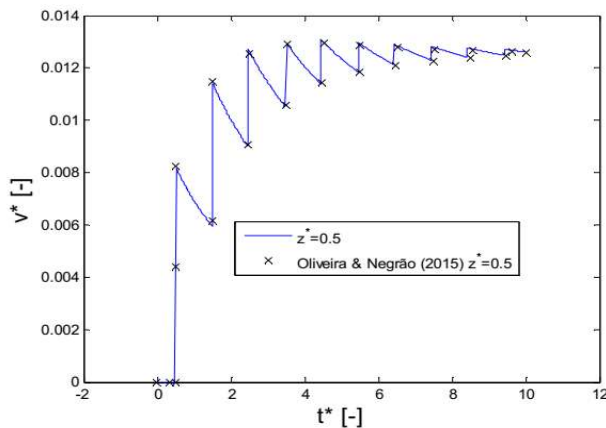


Figure 3. Comparison the algorithm created and the results published by Oliveira & Negrão (2015) for evolution of velocity of a restart of a Newtonian fluid.

RESULTS

We did all the experiments, with exception of the chromatography, in triplicate. The results shown do not provide an accurate statistical analysis, once three experiments are a small number of samples to build a normal curve and to know accurately the standard deviation. Unfortunately, the experiments are complex and take a reasonable amount of time, which makes impossible to repeat more than three times each condition. All the results show the error related to the standard deviation and to the sensor's error. We demonstrate the reproducibility for the restart experiment in Table 6.

Physical Characterization

In order to study the oil composition, we did a gas chromatography measuring the amount of hydrocarbons from C7

to C40. Figure 4 shows that the weight percentage of linear alkanes from C8 to C12 and from C32 up to C40 are lower than from C12 to C32.

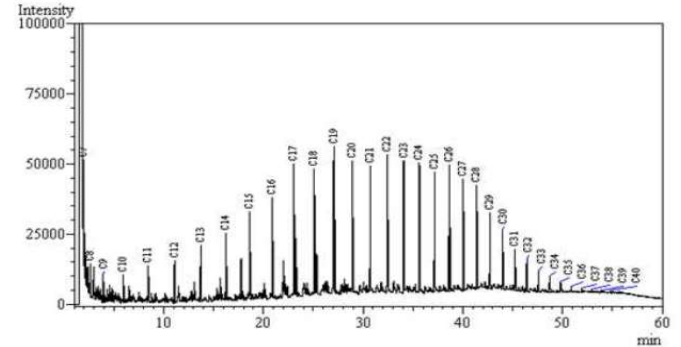


Figure 4. Gas Chromatography of the oil.

The weight percentage of any hydrocarbon can be obtained from the gas chromatography with an integration method. We will not get in detail the method used to obtain the results shown in Table 1.

Table 1. Weight Percentage of n-alkanes from the gas chromatography

Mass Percentage [%]							
C7	0,222	C16	0,470	C25	0,590	C34	0,140
C8	0,069	C17	0,590	C26	0,622	C35	0,071
C9	0,153	C18	0,572	C27	0,570	C36	0,050
C10	0,119	C19	0,600	C28	0,502	C37	0,040
C11	0,168	C20	0,593	C29	0,387	C38	0,031
C12	0,227	C21	0,574	C30	0,329	C39	0,017
C13	0,292	C22	0,602	C31	0,226	C40	0,004
C14	0,333	C23	0,597	C32	0,174		
C15	0,430	C24	0,604	C33	0,116		
Total n-alkanes				11,08 %			

Table 1 shows that for n-alkanes ranging from C8 to C12 and from C32 up to C40 the weight percentage is less than 0,2%. In between there is a plateau from C17 to C26 with approximately 0,6% of weight percentage. This oil has approximately 11% of wax.

Figure 5 shows another important bench experiment to verify the oil's behaviour. We did a differential scanner

calorimetry (DSC) to verify the wax appearance temperature (WAT) and the second event of wax solidification.

As has been discussed in the literature a few times (Ronningsen *et al.*, 1991; Yi & Zhang, 2011; Paso *et al.*, 2009) the second event starts to occurs when the amount of wax crystals in the oil reaches a threshold that changes how the fluid behaves macroscopically. At that temperature, the oil starts behaving like a non-Newtonian fluid, and is when the oil starts to shrink and create a void inside a pipeline (Phillips *et al.*, 2011).

For the oil studied in this manuscript, the WAT, measured in the DSC experiment, is around 47,5 °C and the second event starts to occurs at a temperature around 25°C.

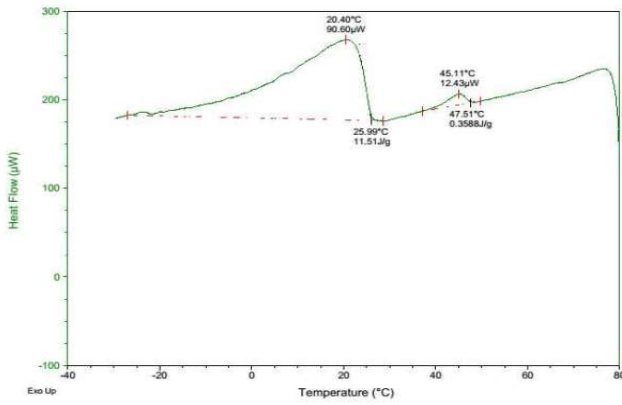


Figure 5. Differential Scanning Calorimetry of the oil

Rheological characterization

Figure 6 shows the experimental data of a steady state experiment for the oil without aging time. It is possible to see the apparent yield stress, which is at the end of the elastic region. It is also possible to see the shear-banding phenomenon, and consequently the dynamic yield stress.

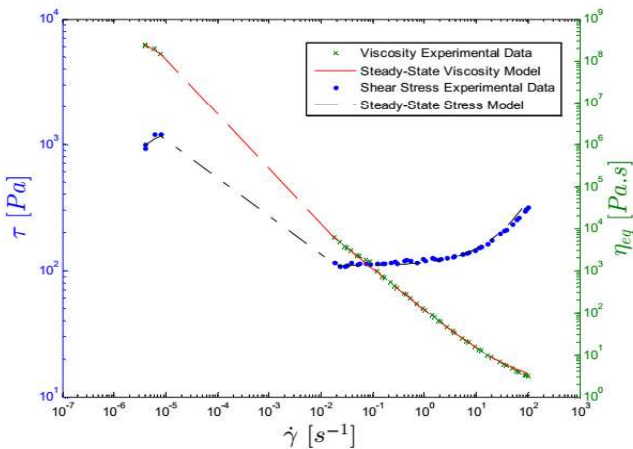


Figure 6. Experimental data and model using Equation (9).

It is also possible to see the behaviour of the viscosity, which is extremely high for small shear rates and it decays continuously to small values at high shear rates.

Also in Figure 6 we can observe the results of the Equation (9) when the values of the physical and empirical parameters shown in Table 2 are used.

Table 2 shows the values obtained from steady state equation for the oil.

Table 2. Parameters obtained from the steady state.

Parameters	Value	Units
K	6 ± 1	$Pa \cdot s^n$
n	0.7 ± 0.1	-
η_0	$5 \cdot 10^8 \pm 0.9$	$Pa \cdot s$
η_∞	1 ± 0.2	$Pa \cdot s$
τ_y	1100 ± 241	Pa
τ_{yd}	118 ± 21	Pa
$\dot{\gamma}_{yd}$	$3 \cdot 10^{-3} \pm 0.5 \cdot 10^{-3}$	s^{-1}

Figure 7 shows the oscillatory tests data. We can see the elastic region, where the material has constant and stable storage and loss moduli. Figure 7 also shows the breakdown of the cristaline structure as the amplitude of the stress rises. When the structure is completely destroyed another plateau where the loss modulus is higher than the storage modulus occurs.

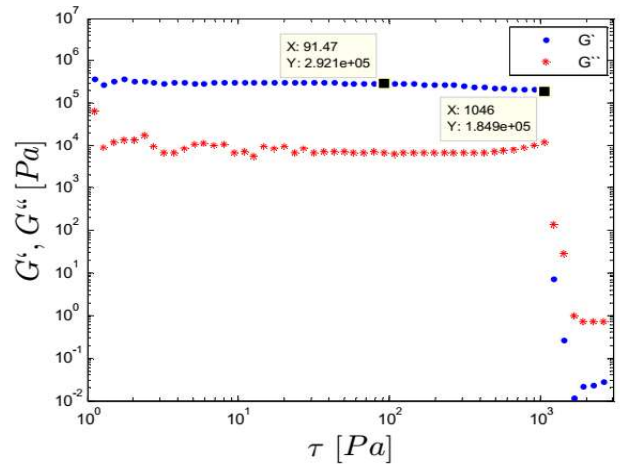


Figure 7. Stress sweep curve for Oil at 1Hz 1 hour of aging time.

Table 3 shows the results of the main physical parameters of the commercial oil. The storage modulus in the elastic regime and the static yield stress, which can be compared to the results from the oscillatory experiments.

Table 3. Parameters obtained from the Oscillatory Test

Parameters	Value	Units
G_0	$2.9 \cdot 10^5 \pm 0.5 \cdot 10^5$	Pa
τ_y	980 ± 196	Pa

In the model, we could use the apparent yield stress obtained from the steady state curve or from the oscillatory test. Table 4 shows a comparison of both values, it is at the same order of magnitude, with 20% error.

Table 4. Comparison of the values obtained from the steady state and oscillatory tests.

τ_y [Pa]		
-	Steady State	Oscillatory
Oil	1100 ± 241	980 ± 196

The empirical parameters of the models, a , b , m and the equilibrium time were obtained from dynamic rheological test, constant shear rate test and constant shear stress test.

Calculating the dimensionless parameters used in the model for the oil, we have the results shown in Figure 5

Table 5. Parameters obtained from the steady state.

Parameters	formula	Value
η_0^*	$\frac{\eta_0 c}{\tau_{yd} d}$	$1.3 \cdot 10^4$
η_∞^*	$\frac{\eta_\infty c}{\tau_{yd} d}$	1
τ_y^*	$\frac{\tau_y}{\tau_{yd}}$	10.2
$\dot{\gamma}_{yd}^*$	$\frac{\dot{\gamma}_{yd}}{c}$	$7.6 \cdot 10^{-8}$
K^*	$\frac{K \tau_{yd}^{n-1}}{\eta_\infty^n}$	1.43
n^*	n	0.7

With this values of apparent yield stress and the experimental apparatus described before, the value of the necessary pressure to restart the flow considering the crude incompressible and time-independent we would need 11.2 bar.

Restart experiments

The wireless differential pressure sensor is incapable of measuring pressure waves when the flow is starting up. The acquisition rate of the differential sensor is 0.25 Hz, which is too small to see the pressure waves. Figure 8 shows differential pressure and temperature during cooling down. Because the time to cool down from 60 to 5 was around 2 hours, we were able to measure with the low frequencies sensors.

It is possible to see in Figure 8 that the differential pressures increases when the temperature of the water reaches around the second event of wax precipitation, shown in Figure 5. The pressure in the inlet was kept constant, just the hydrostatics due to oil in the tanks. That phenomenon was reproducible in all experiments. Phillips *et al.*, (2011) also observed the same phenomenon.

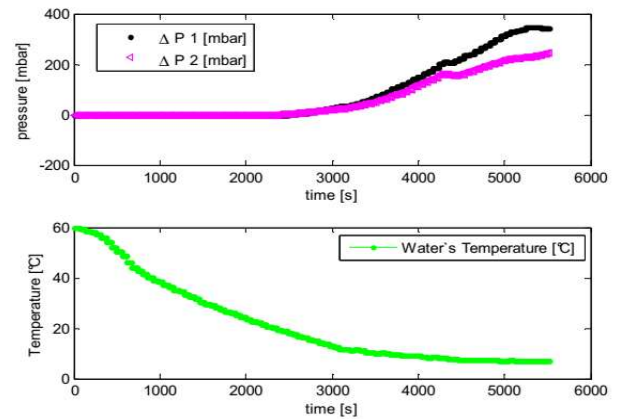


Figure 8. Differential Pressure and Water's Temperature during cooling down.

Figure 8 shows the evidence discussed before. If the shrinkage were due to temperature decrease at liquid state, it would be possible to see a small increase of differential pressure before reaching the temperature of the second event. Because the pressure at the middle of the pipeline just started to decrease at around 20 °C, the shrinkage and creation of voids discussed in a few studies are the best assumption.

Once we have discussed the physical characterization of the oil and the experimental procedure, we can start discussing the results of the restart experiments. Figure 9 shows the results of one experiment, the level of the tank changes abruptly when the restart occurs, the pressure drops and the Coriolis starts to measure the mass flow rate.

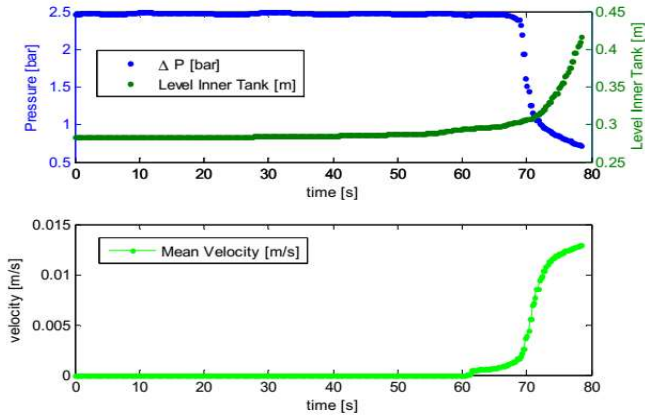


Figure 9. Experimental results of the restart test for 0 hour of aging time.

When doing experiments we did it in triplicate. As can be seen in Figure 10 and Figure 11, the results can be repeated with acceptable accuracy. When measuring the start-up time, we have to decide which of the sensors we will consider. Because the level sensor is more precise in detecting variation than the Coriolis assembled in the pipeline, the necessary time will be when the variation of the inner tank overcomes its systematic error. Figure 10 shows the results of the inner tank in a log scale to facilitate the visualization of the start-up. Figure 11 shows both the results of pressure and velocity for the same experiments.

The experiment stopped when all the oil from the one tank went to the other. It would be interesting to measure all the transient motion until it reached permanent, but because we have a small amount of oil in the system, this is unachievable.

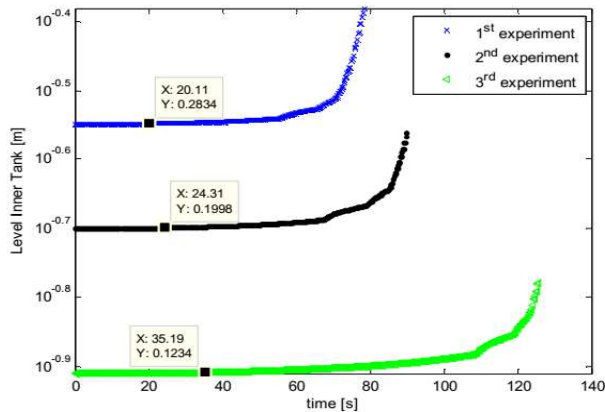


Figure 10. Reproducibility of the level of the inner tank for restart test for 0 hour of aging time.

As can be seen in Figure 10, when we pump the oil from the deposition tank to the start-up tanks, the amount of oil is slightly

different. If we consider the worst case scenario, the difference was 20 cm of oil, which would generate 0.01 bar of hydrostatic pressure, because we are dealing with pressures three orders of magnitude higher in the start-up, we consider that those variations can be disregarded for the time being.

It is possible to see the necessary time to restart the flow has a standard deviation of around 30%. Table 6 shows the calculation of the mean values and the error, we found that for all experiments and aging time, the error is around 30%.

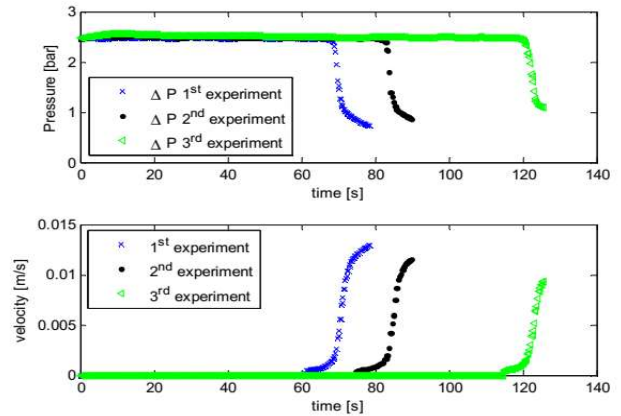


Figure 11. Reproducibility results of the restart test for 0 hour of aging time.

Table 6. Reproducibility of Experiment for 0 hour of aging.

-	ΔP [bar]	Time for restart [s]
1 st	2.475 ± 0.008	20.1 ± 0.1
2 nd	2.49 ± 0.01	24.3 ± 0.1
3 rd	2.51 ± 0.02	35.2 ± 0.1
	ΔP	26.5 ± 7.8

Because the idea of this study is to be able to improve the knowledge and the designing tools for the industry, we will present the results in a dimensionless way.

To study the necessary time to start-up the flow, we show in Figure 12 three results with different differential pressures. It is important to note, that those are one of the experiments, and all of them were done in triplicate. The results of the necessary time to restart along with the standard deviation of that measurement is shown in Table 7 in dimensionless form.

The results will be shown with the dimensionless values on the axis, but the subtitle will show the real boundary condition, that facilitate the comprehension of what is been discussed.

It is possible to observe that, as expected, as the differential pressure rises the time necessary to start-up the flow decreases. The results are shown in semi log x axis, because the time necessary when 2.5 bar were applied is one order of magnitude smaller than when 1.4 was applied, and for 0.6 bar we did not even observe the flow start-up.

It is wrong to assume that we observe the yield stress when applying 0.6 bar. As has been discussed by (de Souza Mendes *et al.*, 2012; de Oliveira & Negrao 2015; Van Der Geest *et al.*, 2015), it is probable that the flow did not start because there was not enough time. Perhaps, if we had an experiment longer than 4000s, we might have observed the start-up.

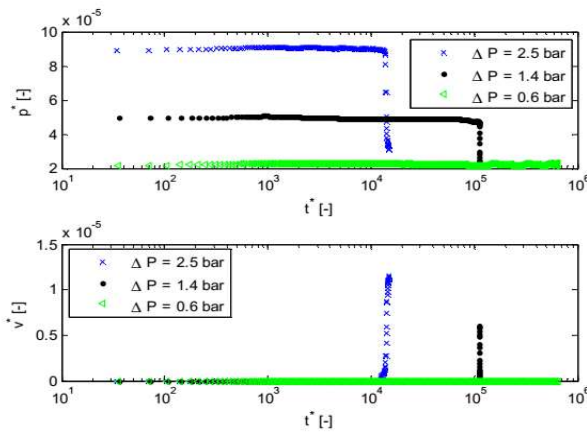


Figure 12. Experiments applying different differential pressures

Table 7 shows the value of the dimensionless time normalized by the necessary time for the pressure wave to reach the end of the pipeline. Because we have an experimental apparatus of 6 meters, we have a high dimensionless time.

Table 7. Dimensionless results for different applied pressures.

ΔP [bar]	ΔP^* [-]	t^* [-]
2.5	$9.10 \cdot 10^{-5}$	$4.3 \cdot 10^3 \pm 1.1 \cdot 10^3$
1.4	$4.98 \cdot 10^{-5}$	$4.810^4 \pm 1.3 \cdot 10^4$
0.6	$2.26 \cdot 10^{-5}$	—

As we mentioned before, in this manuscript we shall not discuss every possible variable that might influence the start-up of gelled waxy crude oils in cold environments. The only other variable we will study is aging time.

The results presented in Figure 13 show that as the aging time rises the necessary time to restart the flow at constant pressure also rises significantly. The results considered to be the start-up time obtained from the level sensor are shown in Table 8.

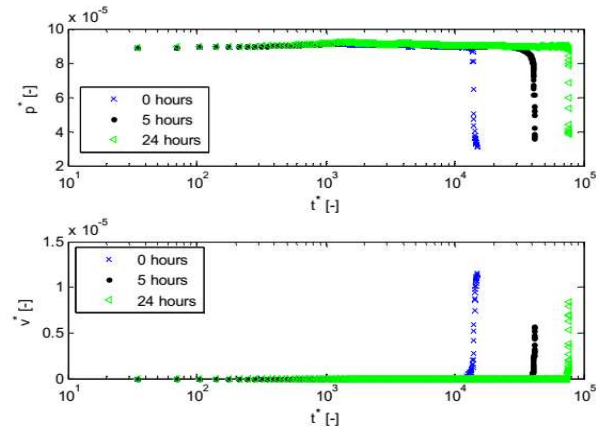


Figure 13. Experimental results of different aging times with 2.5 bar of inlet pressure.

Table 8. Dimensionless results for different aging times.

Aging [hours]	ΔP^* [-]	t^* [-]
0	$9.10 \cdot 10^{-5}$	$4.3 \cdot 10^3 \pm 1.1 \cdot 10^3$
5	$4.98 \cdot 10^{-5}$	$2.5 \cdot 10^3 \pm 1.1 \cdot 10^3$
24	$2.26 \cdot 10^{-5}$	$3.0 \cdot 10^4 \pm 8.4 \cdot 10^3$

Because we want to see if the model is able to predict experimental data, we have to manipulate the measurement of the level of the tank to the velocity in the outlet of the pipeline. The tank and the connection to the water bath is heated, therefore there is no shrinkage. Based on that we used a simplified mass balance to calculate the mean velocity at the end of the pipeline based on the data of the level of the inner tank.

The results presented in Figure 14 show that the transient simulation could predict the start-up with good accuracy for 0 hours of aging. The detailed discussion on the empirical parameters used, the grid sizes and simulation time shall be discussed elsewhere.

As it is possible to see in Figure 14 the velocity at the end of the pipeline rises above the experimental data. The simulation stopped at that point, because the idea in this manuscript is just to verify the necessary time to restart the flow. With that in mind, we can say that the model reaches the goal with good accuracy.

In order to show better what happened in the simulation, Figure 15 shows the pressure propagation in the pipeline at different times. We can observe that the simulation stopped still in the transient part. It is possible to see to that as time goes by the pressure at each point rises. In the beginning of the pipeline, up to $z^* = 0.1$ the pressure is near to reach the permanent flow, while at the end the pressure is starting to rise.

At the beginning of the simulation, there was a lot of oscillation, as Oliveira and Negrao (2015) explained this is due to the highly elastic response of the fluid before it starts to break down and not some problems with the algorithm convergence.

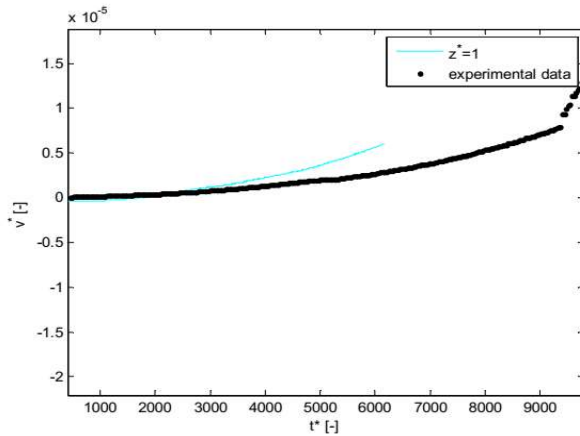


Figure 14. Comparison of the experimental data of start-up and the simulation.

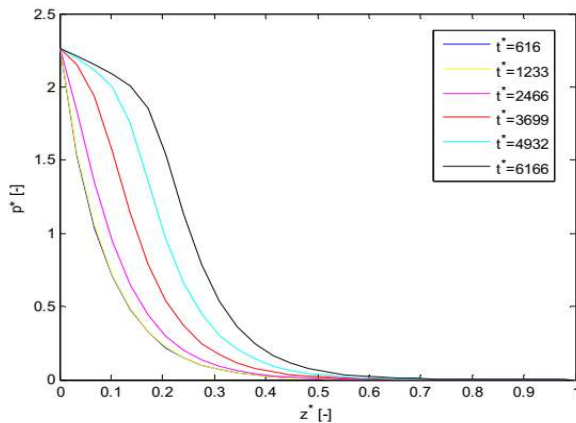


Figure 15. Pressure distribution in the pipeline at different times.

CONCLUSION

The studied oil has a high percentage of wax, with a WAT at around 47 °C and the second event of wax precipitation been around 25°C. This crude has these precipitation events at temperatures higher than the literature usually reports, which can increase the flow assurance problems in the field.

The rheology results show that the apparent yield stress of this oil is around 1000 Pa. If we had used the classic force balance considering the oil incompressible and time independent, we would need 11.2 bar of pressure to restart it. As we have seen, we start it with 1.4 bar. That does not mean that

1.4 is the minimum pressure necessary to restart, just that we did not get enough time for lower pressure to restart.

After the upgrade on the control system of the experimental apparatus, it is able to measure the restart phenomenon with accuracy and reproducibility. There is a clear influence of the inlet pressure, as expected. As the inlet pressure rises the time necessary to restart decreases. The second clear influence is the aging time. As the aging time rises, the time necessary to restart the flow also rises.

Finally, the model proposed by Oliveira and Negrao (2015) is able to predict the time necessary to restart the flow in the case tested. A further comparison of the model with more experimental data need to be done to have stronger evidence of the predictability of the model.

NOMENCLATURE

a, b, m	Empirical Parameters
c	Velocity Pressure Wave
l	Pipeline's Length
d	Pipeline's Diameter
t_{eq}	Equilibrium Time
n	Herschel Buckley exponential term
k	Herschel Buckley apparent viscosity
G_0	Storage Modulus fully structured
τ_y	Apparent Yield Stress
τ_{yd}	Dynamic Yield Stress
η_0	Viscosity of fully structured
η_∞	Viscosity of fully destroyed
G'	Storage Modulus
G''	Loss Modulus
λ	Structure parameter
λ_0	Initial Structure parameter
λ_{eq}	Structure parameter at equilibrium
α	Compressibility
p	Pressure
ΔP	Differential Pressure
v	Velocity
z^*	Dimensionless Axial Position
t^*	Dimensionless Time
r^*	Dimensionless radius
p^*	Dimensionless Pressure
v^*	Dimensionless Velocity

ACKNOWLEDGMENTS

The authors wish to thank the company Repsol-Sinopec Brazil for the financial and technical support in this study. Also would like to thank ANP (National Agency of Petroleum, Natural Gas and Biofuels) and CAPES (Brazilian Federal Agency for Support and Evaluation of Graduate Education within the Ministry of Education of Brazil) for the financial support.

REFERENCES

- Andrade, D. E., da Cruz, A. C., Franco, A. T., & Negrao, C. O. (2015). Influence of the initial cooling temperature on the gelation and yield stress of waxy crude oils. *Rheologica Acta*, 54(2), 149-157.

- Callaghan, P. T. (2008). Rheo NMR and shear banding. *Rheologica Acta*, 47(3), 243-255.
- Chang, C., Nguyen, Q. D., & Rønningsen, H. P. (1999). Isothermal start-up of pipeline transporting waxy crude oil. *Journal of non-newtonian fluid mechanics*, 87(2), 127-154.
- Chang, C., Boger, D. V., & Nguyen, Q. D. (1998). The yielding of waxy crude oils. *Industrial & engineering chemistry research*, 37(4), 1551-1559.
- Chang, C., Boger, D. V., & Nguyen, Q. D. (2000). Influence of thermal history on the waxy structure of statically cooled waxy crude oil. *SPE Journal*, 5(02), 148-157.
- Cheng, D. C. (1986). Yield stress: a time-dependent property and how to measure it. *Rheologica Acta*, 25(5), 542-554.
- Davidson, M. R., Nguyen, Q. D., Chang, C., & Rønningsen, H. P. (2004). A model for restart of a pipeline with compressible gelled waxy crude oil. *Journal of non-newtonian fluid mechanics*, 123(2), 269-280.
- de Oliveira, G. M., & Negrao, C. O. (2015). The effect of compressibility on flow start-up of waxy crude oils. *Journal of Non-Newtonian Fluid Mechanics*, 220, 137-147.
- de Souza Mendes, P. R., de Abreu Soares, F. S. M., Ziglio, C. M., & Gonçalves, M. (2012). Startup flow of gelled crudes in pipelines. *Journal of Non-Newtonian Fluid Mechanics*, 179, 23-31.
- Phillips, D. A., Forsdyke, I. N., McCracken, I. R., & Ravenscroft, P. D. (2011). Novel approaches to waxy crude restart: Part 1: Thermal shrinkage of waxy crude oil and the impact for pipeline restart. *Journal of Petroleum Science and Engineering*, 77(3), 237-253.
- Helgeson, M. E., Vasquez, P. A., Kaler, E. W., & Wagner, N. J. (2009). Rheology and spatially resolved structure of cetyltrimethylammonium bromide wormlike micelles through the shear banding transition. *Journal of Rheology (1978-present)*, 53(3), 727-756.
- Lee, H. S. (2008). Computational and rheological study of wax deposition and gelation in subsea pipelines. ProQuest.
- Lin, M., Li, C., Yang, F., & Ma, Y. (2011). Isothermal structure development of Qinghai waxy crude oil after static and dynamic cooling. *Journal of Petroleum Science and Engineering*, 77(3), 351-358.
- Lopes-da-Silva, J. A., & Coutinho, J. A. (2007). Analysis of the isothermal structure development in waxy crude oils under quiescent conditions. *Energy & Fuels*, 21(6), 3612-3617.
- Morrison, F. A. (2001). Understanding rheology. Oxford University Press, USA.
- Ovarlez, G., Rodts, S., Chateau, X., & Coussot, P. (2009). Phenomenology and physical origin of shear localization and shear banding in complex fluids. *Rheologica acta*, 48(8), 831-844.
- Paso, K., Kompalla, T., Oschmann, H. J., & Sjöblom, J. (2009). Rheological degradation of model wax-oil gels. *Journal of Dispersion Science and Technology*, 30(4), 472-480.
- Ritter, R. A., & Batycky, J. P. (1967). Numerical prediction of the pipeline flow characteristics of thixotropic liquids. *Society of Petroleum Engineers Journal*, 7(04), 369-376.
- Rønningsen, H. P. (2012). Rheology of petroleum fluids. *Ann. Trans. Nord. Rheo. Soc.*, 20, 11-18.
- Rønningsen, H. P., Bjoerndal, B., Baltzer Hansen, A., & Batsberg Pedersen, W. (1991). Wax precipitation from North Sea crude oils: 1. Crystallization and dissolution temperatures, and Newtonian and non-Newtonian flow properties. *Energy & Fuels*, 5(6), 895-908.
- Tarcha, B. A., Forte, B. P., Soares, E. J., & Thompson, R. L. (2015). Critical quantities on the yielding process of waxy crude oils. *Rheologica Acta*, 54(6), 479-499.
- Thomason, W. H. (2000). Start-up and shut-in issues for subsea production of high paraffinic crudes. In Offshore Technology Conference. Offshore Technology Conference.
- Wachs, A., Vinay, G., & Frigaard, I. (2009). A 1.5 D numerical model for the start up of weakly compressible flow of a viscoplastic and thixotropic fluid in pipelines. *Journal of Non-Newtonian Fluid Mechanics*, 159(1), 81-94.
- Van Der Geest, C., Bizotto Guersoni, V. C., Merino-Garcia, D., & Bannwart, A. C. (2015). The Influence of Compressibility and Shrinkage in the Start-up of a Flow of Gelled Waxy Crudes in Pipelines. In OTC Brasil. Offshore Technology Conference.
- Venkatesan, R., Östlund, J. A., Chawla, H., Wattana, P., Nydén, M., & Fogler, H. S. (2003). The effect of asphaltenes on the gelation of waxy oils. *Energy & fuels*, 17(6), 1630-1640.
- Visintin, R. F., Lapasin, R., Vignati, E., D'Antona, P., & Lockhart, T. P. (2005). Rheological behaviour and structural interpretation of waxy crude oil gels. *Langmuir*, 21(14), 6240-6249.
- Wardhaugh, L. T., & Boger, D. V. (1987). Measurement of the unique flow properties of waxy crude oils. *Chemical engineering research & design*, 65(1), 74-83.
- Wardhaugh, L. T., & Boger, D. V. (1991). The measurement and description of the yielding behaviour of waxy crude oil. *Journal of Rheology (1978-present)*, 35(6), 1121-1156.
- Yi, S., & Zhang, J. (2011). Relationship between waxy crude oil composition and change in the morphology and structure of wax crystals induced by pour-point-depressant beneficiation. *Energy & Fuels*, 25(4), 1686-1696.

**3. PAPER 3: Wax Deposition Experiment with Highly Paraffinic
Crude Oil in Laminar Single-Phase Flow Unpredictable by
Molecular Diffusion Mechanism**

Wax Deposition Experiment with Highly Paraffinic Crude Oil in Laminar Single-Phase Flow Unpredictable by Molecular Diffusion Mechanism

Charlie Van Der Geest,^{*,†,§} Vanessa C. Bizotto Guersoni,[‡] Daniel Merino-Garcia,[§] and Antonio Carlos Bannwart[†]

[†]Department of Mechanical Engineering and [‡]Center for Petroleum Studies, University of Campinas, Campinas, São Paulo 13083-970, Brazil

[§]Repsol Technology Center, 28933 Mostoles, Madrid, Spain

ABSTRACT: Wax deposition data for a Brazilian crude oil was investigated using a facility designed to study flow assurance problems related to waxy crude oils. This work reports the preliminary efforts behind validating the pressure drop methods in place for identifying deposition, i.e., isothermal and nonisothermal flows were evaluated, to confirm whether it was possible to differentiate between temperature gradient effects, and wax deposition. Additionally, deposition experiments show a phenomenon that is not commonly reported in the literature. Once the oil's temperature was below the wax appearance temperature and the water temperature at 5 °C, the deposit did not start to build up immediately; it only began after a period of time. Under some conditions the pressure drop only began increasing after 1 day. These results show that, at least for highly paraffinic crudes, models based on molecular diffusion alone cannot predict when and where the deposit will form, which is a major concern in the industry. We believe that other mechanisms such as shear dispersion, Brownian diffusion, and the non-Newtonian behavior of waxy crudes at low temperatures should be considered. In this experimental setup two different ways were used to measure deposit thickness: (1) pressure drop and (2) weight of the deposit.

INTRODUCTION

In the petroleum industry, there are a number of problems that occur when crude oil/gas flows from the reservoir to the production unit. To address all those issues and guarantee a smooth operation, the petroleum industry developed a technical discipline called “flow assurance”. The most common flow assurance concerns are wax deposition, restart of gelled waxy crudes, emulsion/foam formation, hydrate blockages, asphaltene precipitation, and inorganic scaling.

Crude oil is a complex mixture of nonpolar and polar organic compounds, where high molecular weight nonpolar molecules lead to solid deposits upon temperature reduction. This phenomenon is critical in areas with low ambient temperatures, such as the seabed in deep waters.

Wax deposition is a problem that has been known for decades, and there is vast literature regarding this phenomenon. The oldest references deal with onshore problems,^{1,2} and as operations expanded in the industry, offshore ones had to be dealt with.^{3–7} In the literature there are also a few reviews on this issue, discussing the mechanisms which cause deposition, the influence of other phases (gas and water), technologies for inhibiting wax growth, and methods for measuring the performance of said technologies.^{8–11}

Over the past couple of decades, a huge effort has been expended to explain and predict wax deposition. There are several independent experimental rigs from a number of research teams performing measurements on different kinds of fluids.^{6,12–18} Modeling has also undergone extensive development with both mechanistic and compositional approaches.^{4,7,19–22}

Most models consider molecular diffusion as the driving force behind deposition.^{4,6,19} Basically, the pipeline is in contact with the cold environment and the bulk is at high temperature, leading to a radial temperature gradient. At some point the oil reaches the wax appearance temperature (WAT). At that point the paraffin molecules start to precipitate near the pipe's wall, creating a radial concentration gradient and creating a gel (thin layer) at the cold surface.⁴ After this initial porous layer has been created, the concentration gradient both in the bulk (diffusion) and in the deposit (counterdiffusion) is what drives the molecular diffusion mechanism.^{8,10,23}

Once this thin layer is formed, we can discuss the phenomenon inside the deposit, how it grows and ages. The model proposed by Singh et al.⁴ has been used by most studies with good predictability. The model proposes that the deposit is a porous media where counterdiffusion is constantly acting, increasing both the wax fraction and the wax deposit thickness. Hence the percentage of molecules with high molecular weight increases while the percentage of light hydrocarbon molecules decreases over time; gas chromatographic results have repeatedly shown this phenomenon.^{4,6,12,15}

Even though most studies consider molecular diffusion as the most relevant mechanism in the bulk, there is experimental evidence which supports the need to further explore other mechanisms.^{8,10,22} Also, we show evidence of the necessity to study the initial incipient gel formation kinetics, once the

Received: January 22, 2018

Revised: February 28, 2018

Published: February 28, 2018

models disregard the time to form it, which is why the models predict the deposit to start to build up immediately. That assumption has been corroborated by most experimental data in the literature,^{4,6–8} which is why the study of the kinetics of the formation of the incipient gel has not been done in wax deposition facilities. These phenomena are important to improve the models; otherwise we may be unable to completely quantify the wax deposition.^{8,10,22}

There are recent studies investigating the influence of supersaturation upon the molecular diffusion mechanism.^{7,16–19,24} They discuss what the effect is when the heat transfer rate is faster than the precipitation rate. It is also known that some degree of supersaturation will always occur before the precipitation, due to entropy.²⁴ The issue is to tackle the degree of supersaturation impact on the increase in the deposit thickness, and the degree of supersaturation impact on the gelation process to form the initial incipient gel layer.^{23,25}

One experimental study which aids that discussion is Hoffmann and Amundsen.⁶ They concluded that, even though molecular diffusion is the driving force behind wax deposition, a different type of deposit structure that was rough and irregular could not be described by a molecular diffusion based model; thus new mechanisms should be considered.

Another interesting experiment was done by Cabanillas et al.²⁶ They studied the influence of precipitated molecules on the deposition at temperatures below the WAT. The results show that, when there is precipitated wax in the bulk, the deposit thickness doubles in comparison with when the bulk temperature is above the WAT. The observation of crystal motion did not reveal lateral displacement toward the wall; rather it showed crystal moving with the flow, decelerating, and eventually stopping,²⁶ indicating an influence from non-Newtonian behavior (gelation).

Paso and Fogler²³ have also studied the gelation enhancing deposition effect and have shown the existence of a critical carbon number (CCN). Wax molecules with carbon numbers higher than the CCN diffuse from the bulk to the deposit, while smaller molecules counterdiffuse from the deposit to the bulk. They observed the effects of temperature in depletion of the components of the crude.

Zheng et al.²⁸ has investigated the influence of non-Newtonian behavior on highly waxy crude oils. They did simulations solving conservation of momentum equations for non-Newtonian time-independent constitutive equations and used those solutions to calculate heat and mass transfer diffusivity, improving the accuracy of simulation compared with field scale data. A next step for this kind of simulation would be to solve mass, momentum, and energy equations simultaneously with a time-dependent constitutive equation.²⁹

Another interesting experimental study dealing with wax deposition was obtained by Veiga et al.,¹⁷ where they measured the deposit's thermal conductivity and showed that what most models consider is accurate. There is no radial variation in the deposit's thermal conductivity.

In this paper, deposition rates that cannot be solely explained by the molecular diffusion mechanism will be shown. The current paper is an experimental study of wax deposition in single phase flow. The main difference from other experimental studies discussed in the literature is the characteristics of the oil we used. We used a real, highly waxy crude oil which we will characterize later. This oil is highly viscous and becomes non-Newtonian around 30 °C, one of the reasons for which it was the subject of a study.

This paper shows experiments for verifying the influences of flow rate and temperature, all in laminar flow. Wax deposition experiments have been done with a similar oil¹⁸ with behavior similar to the one reported, i.e., deposition rate profiles which cannot be described by the molecular diffusion mechanism alone.

■ EXPERIMENTAL APPARATUS AND PROTOCOLS

Gas Chromatography. The best way to verify the molecular content of the deposit would be to do high temperature gas chromatography (HTGC), but we do not have that capability in the laboratory yet; thus we did gas chromatography that could measure up to C40. We understand that this is not the best option, because the influence of molecules in the range C40–C60 is crucial to understanding the phenomenon of deposition. Unfortunately, that is all we are capable of doing up to date.

To determine the composition of the deposit, we used the methodology for integration of peaks based on ASTM D5917-15 and ASTM D7360-11. The instrument we used was a GC 2010 Plus from Shimadzu. With this instrument and method, we were able to measure weight percentages from C7 to C40.

We injected 1 μ L of the sample at a temperature of 250 °C. To start we set the temperature at 50 °C for 2 min. Afterward, the temperature rose at a rate of 10 °C/min up to 320 °C and remained at that temperature for 15 min.

Differential Scanning Calorimeter. In the literature there is a vast analysis as to the best method for determining the WAT/ WDT.^{24–30} It is important to point out that the best way to experimentally approach phase equilibrium in mixtures is to use the dissolution temperature (WDT), instead of the precipitation temperature (WAT), because of the supersaturation necessary before precipitating the first molecule.²⁴ Both methods do not reach equilibrium because the experiments are kinetic; thus they do not reach steady state. However, the WDT approaches equilibrium because the entropy of the dissolved wax is lower than that of the crystallized wax.

We agree that the DSC and measurements in a rheometer are not the best at defining the first molecule precipitation, which would be microscopy. The reason is because a large amount of wax needs to precipitate in order to release a measurable amount of heat or change the rheological behavior; thus they are not very accurate.²⁷ However, since that is not the focus of this paper, we will consider the beginning of the exothermic phenomenon in the DSC as the WAT.

The equipment used to perform the DSC was a TA Instruments Q2000. All measurements were done following ASTM D4419-90. The first procedure was to homogenize the samples, so we preheated the samples to 60 °C for 2 h. Afterward we inserted the samples into the calorimeter; the calorimeter was at 80 °C and held at that temperature for 10 min before the experiment was started. After that the temperature decreased from 80 to –30 °C at a rate of –1 °C/min.

Rheometer. We performed the rheological measurements in a controlled-stress rheometer, MARS III from HAAKE GmbH, in a cone-and-plate geometry with a diameter of 60 mm and 1° of angle with a truncation of 0.054 mm. We activated the Peltier plate on the rheometer to control the temperature and cooling rate. We also controlled the truncation using the thermo-gap option.³¹

The first procedure was to erase the oil's thermal and shear history. We homogenized the sample by preheating to 70 °C and maintaining for 2 h. Once the samples were in the rheometer, the Peltier plate controlled the temperature at 70 °C and the rheometer applied a shear rate of 10 s^{–1} for 10 min to erase thermal history effects.

After the homogenization process we started the experiments. We cooled the sample by 2.5 °C with a constant shear rate at a rate of 5 °C/min and waited at that temperature for 30 min for steady state before doing the measurement. The time needed to reach steady state is based on a previous study.³¹ This means that the time for each measurement was 30.5 min: 0.5 min between the previous temperature and the new and 30 min at that temperature to reach steady state. We

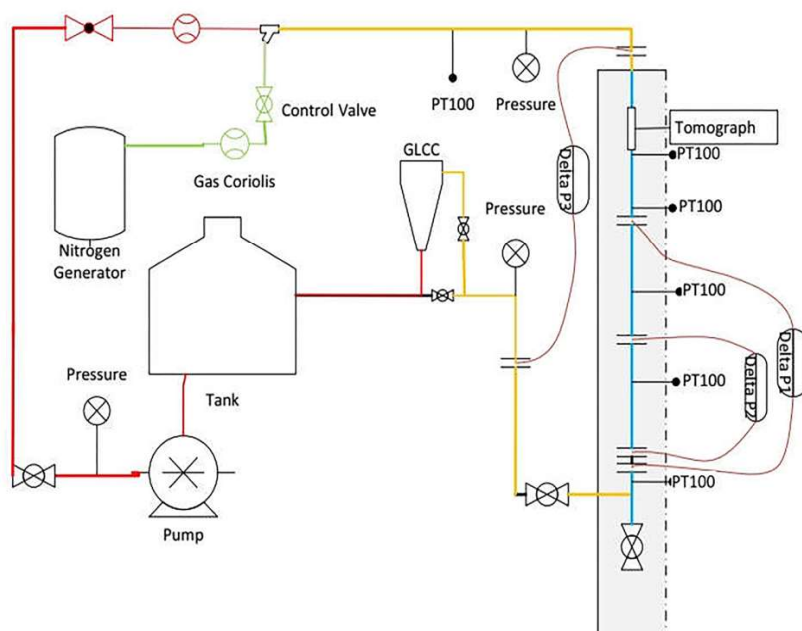


Figure 1. Layout of the experimental apparatus.

did the rheological experiments in triplicate, and the data from different samples of the same oil had up to 10% margin of error.

Deposition Rig. Figure 1 shows part of the experimental apparatus built in CEPETRO to study flow assurance problems related to wax. The apparatus enables two kinds of experiments: (1) study of start-up of gelled waxy crudes³² and (2) wax deposition.

First, there is a water bath, shown in [Figure 1](#) as the box outside the blue pipeline. We can control the water's temperature in a range 90–5 °C, done with a heat exchanger and a chiller; the system for controlling the water temperature is not shown in [Figure 1](#).

We have one heated tank for controlling the oil temperature. In this experiment both single-phase and multiphase wax deposition experiments can take place. The pipeline in red is the single-phase flow. The injection point for the nitrogen is after we measure the oil mass flow rate. The yellow pipeline is where there is two-phase flow before and after the water bath. In addition, as mentioned previously, the blue pipeline is inside the water bath, where the deposition occurs.

There is a pressure gauge (Rosemount 2088 with accuracy = ± 0.05 bar) in the water bath inlet, and three differential pressure gauges (Rosemount 3051 with accuracy = ± 2.5 mbar) distributed in the pipeline along with temperature sensors (four-wire PT100 sensors with accuracy = ± 1 °C). We measure the oil's temperature in the water bath inlet and in the outlet and also the water's temperature.

Four-wire PT100 sensors are the most accurate sensors we could find. The manufacturers argue that the accuracy of this sensor at 0 °C is within 0.05 °C. In our experimental apparatus, however, due to a few difficulties, we could not measure the temperature with a random error margin lower than 1 °C. Even though we believe that it is possible to improve this measurement, this error is similar to other studies in the literature.⁴²

The most important sensor in the apparatus is the ΔP_1 , which was installed in order to measure the differential pressure after both the hydrodynamic boundary layer and the heat transfer boundary layer were developed. There is nothing between the beginning and the end of the measurement.

Another important issue that needs to be addressed is the pipeline wall temperature. In the literature, there are a few studies that measure the temperature at the wall, and then control that temperature.^{4,26} In our apparatus, we can only measure the water temperature. To find out the wall temperature, we calculate it using heat transfer equations. Because we cannot control the temperature in the pipeline wall, we

always run the water with the maximum volumetric flow rate and control the temperature of the water. The lab is working to install an optical fiber as a temperature sensor, to actually measure the wall temperature.

The pipeline inside the water bath is made of copper. The issue of the material's influence on the wax deposition has been raised, but there are a few studies in the literature that show that copper does not alter deposition.⁴⁴ We decided to use copper because it has a higher thermal conductivity.

With this experimental apparatus, most of the effects that can influence deposition may be studied. The influence of water temperature, initial oil temperature, and temperature gradient, among other things, can all be evaluated. We control every variable using a PID controller in order for our apparatus to be as accurate as possible. We control the oil mass flow rate, nitrogen mass flow rate, water volumetric flow rate, and oil and water temperatures during the deposition tests. The nitrogen line is shown in green in [Figure 1](#).

Before starting any test, the oil samples stood in the inner tank for 2 h at 60 °C while being stirred, in order to ensure a good homogenization and an effective dissolution of all paraffin content into the crude oil. Meanwhile, we also kept the temperature of the water bath at 60 °C. After 2 h, we started the oil pump and circulated the oil under isothermal conditions at 60 °C with the bath for another hour.

After 3 h of stabilization, we set the oil flow rate and then started the cool down procedure. The water and oil temperature decreased to the desired oil inlet temperature. After the oil and the water reached the final oil inlet temperature, we cooled the water to 5 °C. After the test, the cleaning process between tests was the following: heat the water and the oil to 60 °C and leave it for 2 h, until the oil pressure drop reached the value measured for a clean pipeline.

Once all the temperatures reached the final desired temperatures, we controlled all the variables during the next 4–5 days and measured the buildup process. The main method to infer the wax deposition thickness was the differential pressure method; in one experiment, the line was pigged to scrap the deposit off the wall and the mass of the deposit was measured to compare and verify whether the indirect method with pressure drop was adequate.^{4,6–8,13}

OIL PROPERTIES

This waxy crude oil is a dead oil that was produced in a Brazilian offshore field; the composition of the oil is not the same as that of the oil produced, due to loss of light hydrocarbons in experimental procedures. The oil we used for the experiment has 12 wt % heavy weight paraffin. The WAT and WDT determined with the DSC method are 34 and 46 °C,⁴³ respectively.

It is important to highlight that we did DSC experiments before and after the end of all the experiments in order to guarantee that the composition of the oil did not change during the experiments. The modification in the composition occurred before the experiments started and was constant during the whole experimental campaign.

Solubility. The DSC curve for this oil is shown in the bottom of Figure 2. With these results we can integrate and

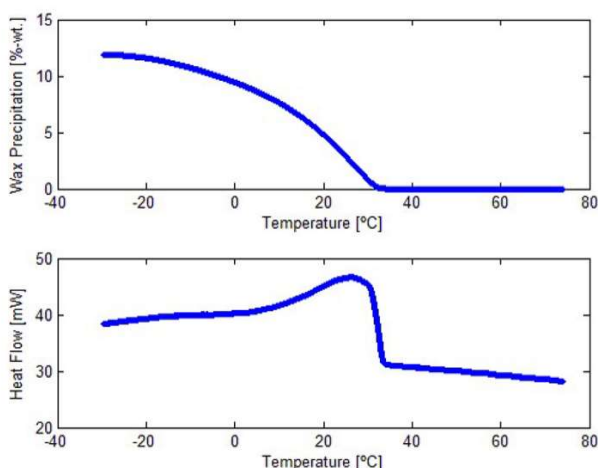


Figure 2. DSC and precipitation curves of the oil.

obtain the precipitation curve for this oil. It is possible to observe one exothermic event. The beginning of the exothermic process is what will be considered as the WAT, which is where the rate of precipitation drastically increases.^{27,43} It is important to highlight that this crude has its composition modified considerably from that of the real waxy crude that was produced. Normally waxy crudes have two exothermic peaks: the first is where the WAT is obtained and the second is near the pour point (PP). For the crude used, there is only one peak due to modifications on its composition that occurred in transportation, storage, and previous experimental procedures.

The precipitation curve is used to quantify the oil's solubility. To calculate the solubility, we use the standard thermal effect for wax precipitation.^{27,33–35} In this paper we will use the model proposed by Singh et al.⁴ to compare with the experimental data. The model considers the thermodynamic equilibrium condition radially, which means that the molecular diffusion equation is solved without considering supersaturation.^{7,16} The solubility curve shown in Figure 3 is an input of the model.⁴

Figure 3 shows the precipitation peak of the DSC in the solubility curve, around 34 °C. The best fit was done using the least-squares method, and we used a polynomial equation to fit the data.

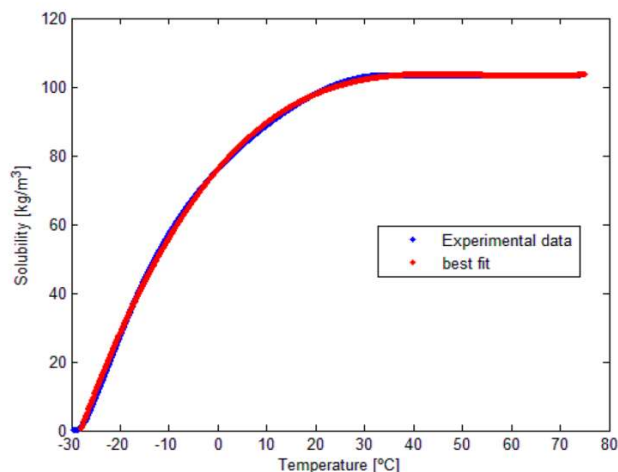


Figure 3. Solubility curve and the best fit to use in the model.

The model proposed by Singh et al.⁴ has an input of the solubility with temperature and a derivative of the solubility with temperature. Both can be obtained from the experimental data shown in Figure 3.

Viscosity. In the literature there are few studies on wax deposition with highly viscous crude. The oil we studied has a higher viscosity than most studies.^{4,6,7,9} There is a study by Venkatesan and Creek¹⁸ using a crude oil with features along the same order of magnitude as the oil studied here, with considerable viscosity variation from 30 cP at 60 °C to 10⁵ cP at 5 °C.

Some oils have a strong influence of both temperature and shear rate once the wax starts to precipitate and the oil becomes non-Newtonian.^{6,17,18} It is important to emphasize that before we model the viscosity we need to discuss the method of measurement. The shearing forces influence the formation and destruction of conglomerates of molecules, which obviously influences viscosity; thus we need to wait to reach equilibrium between buildup and breakdown of conglomerates before doing measurements. Because this oil is highly paraffinic, it takes a long time to reach steady state; thus the effect of shear rate and temperature can be wrongly measured if one is not careful.

As can be seen in Figure 4, we need to wait for 30 min at every point before measuring the viscosity. This discussion also appears in Van Der Geest et al.³¹ and is important because if you do not wait to reach steady state the viscosity will always be overpredicted.

Because we are not interested in merging the phenomenon related to pressure loss due to rheological effects or due to diameter reduction, we will only do experiments with the bulk temperature above 40 °C. Obviously, the temperature near the pipeline will be below that temperature, but this will be simplified the same way Hoffmann and Amundsen⁶ did; we will consider a friction factor for nonisothermal flow.

The viscosity behavior in the Newtonian region is usually modeled with an exponential Arrhenius type equation, shown in eq 1, where viscosity (η) is calculated using a constant related to the entropy for activation of flow (A), activation energy of viscous flow (E_a), gas universal constant (R), and absolute temperature (T).²⁷

$$\eta(T) = Ae^{E_a/RT} \quad (1)$$

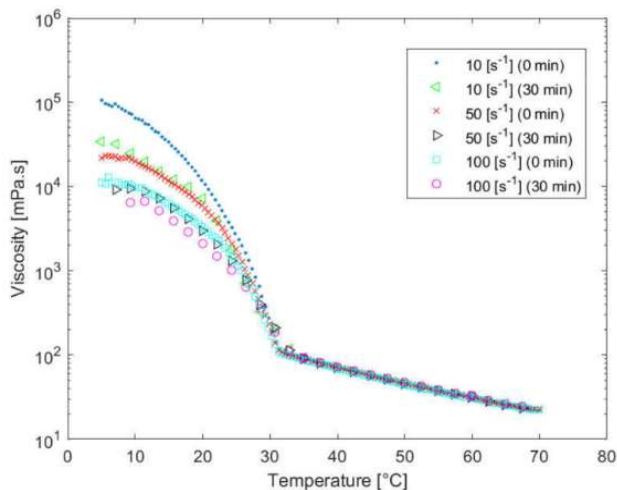


Figure 4. Viscosity of the oil for different shear rates.

Once there are many precipitated molecules within the oil, the oil becomes non-Newtonian and the Arrhenius curve can no longer predict behavior.²⁷ In order to model the behavior, we separated the non-Newtonian region in two and did a least-squares method to verify the best equation for predicting it. The reason for this is that for the crude oil studied we cannot see the influence of shear rate above 26 °C. At temperatures lower than 26 °C the influence of shear rate became strong, and thus a model that is dependent on both temperature and shear rate is necessary. For the non-Newtonian region below 26 °C we used a type of logarithmic equation shown in eq 2. The results for the viscosity fit with temperature are shown in Figure 5.

$$\eta(T, \dot{\gamma}) = B(\dot{\gamma}) + C(\dot{\gamma}) \ln(T) \quad (2)$$

Most studies in the literature do not model viscosity dependent on both the shear rate and temperature, but because this oil changes viscosity drastically, we had to consider it in order to verify the influence. When studying deposition experiments, we actually have a nonisothermal flow, thus a radially nonisoviscous flow.⁶

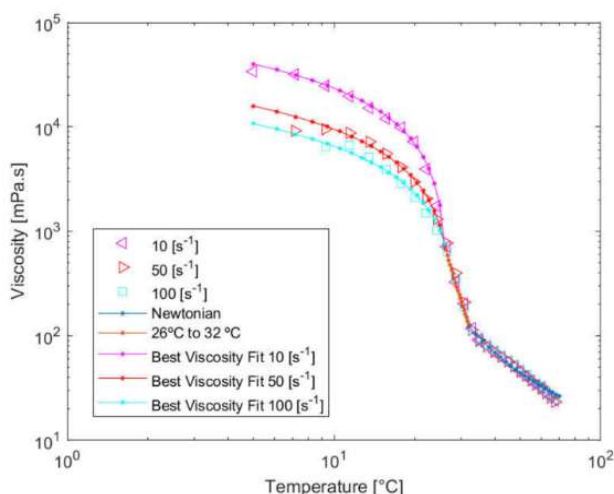


Figure 5. Viscosity of the oil from 70 to 5 °C.

Density. One final property that also varies with temperature is the oil density. Figure 6 shows the variation of the oil's

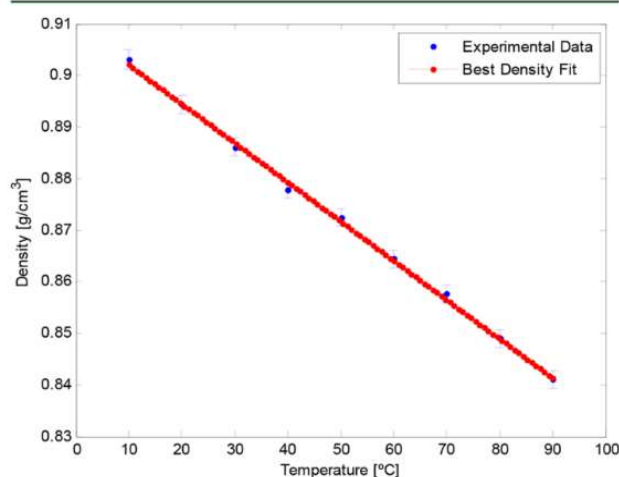


Figure 6. Density of the oil varying with temperature.

density with temperature. As can be seen, the variation is linear, as expected; at 90 °C we have approximately 0.84 g cm⁻³ and at 5 °C approximately 0.91 g cm⁻³. The equation obtained by the least-squares method has also been used in the model dependent on temperature.

RESULTS AND DISCUSSION

Preliminary Study. Isothermal Flow. When dealing with developed incompressible laminar flow inside horizontal pipelines without diameter change, energy conservation can be simplified to obtain eq 3.³⁶

$$\frac{\Delta P}{\rho g} = \left(f \frac{L}{D_w} + \sum K_i \right) \frac{V^2}{2g} \quad (3)$$

For the two sensors in the water bath, ΔP_1 and ΔP_2 , there is no local loss, because there is no sensor in the way and no elbows. From eq 3 we can progress to eq 4 by considering the classical analytical solution for the friction factor of laminar flow inside pipelines.³⁶

$$f = \Delta P_{\text{exp}} \frac{D_w^5 \pi^2}{8L\rho Q^2} = \frac{64}{Re} \quad (4)$$

The results of this experimental apparatus comparing the friction factor with the Reynolds number can be seen in Figure 7. As expected, the friction factor follows the analytical solution for laminar flow with good accuracy.

For the turbulent flow we used two classic equations to calculate the friction factor, Blassius and Colebrook for smooth pipelines, shown in eqs 5 and 6, respectively. As can be seen in Figure 7, both can predict the data with good accuracy.

$$f = \Delta P_{\text{exp}} \frac{D_w^5 \pi^2}{8L\rho Q^2} = 0.316 Re^{-1/4} \quad (5)$$

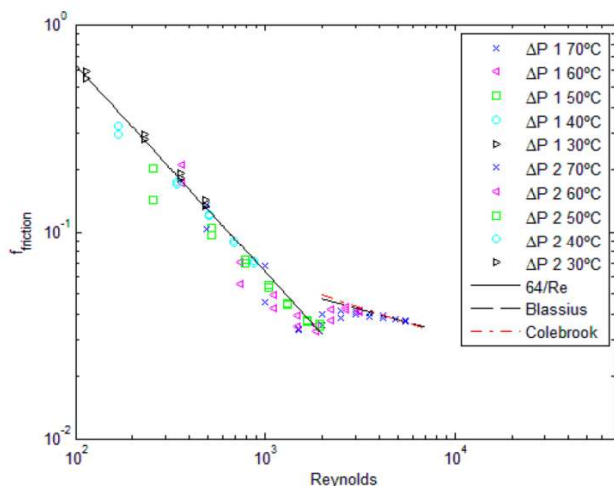


Figure 7. Friction factor variation with Reynolds for the two sensors ΔP_1 and ΔP_2 inside the water bath.

$$f = \Delta P_{\text{exp}} \frac{D_w^5 \pi^2}{8L\rho Q^2} = \left(-1.8 \log_{10} \left(6.9 \frac{D_w \pi \eta}{4Q\rho} + \left(\frac{\epsilon}{3.7D_w} \right)^{1.1} \right) \right)^{-2} \quad (6)$$

For the sensor ΔP_3 , there are two PT100 sensors and two elbows and a tomograph. In order to solve that issue, we used the friction factor obtained in ΔP_1 and ΔP_2 , shown in Figure 7, and calculated a general local loss coefficient using eq 3. The value for our system's loss coefficient is 25.02.

Figure 8 shows the laminar flow and turbulent flow data as well as the calculated friction factor. The data was predicted with good accuracy for the sensor ΔP_3 .

It can be seen that the transition from laminar flow to turbulent flow in our experimental apparatus with this crude oil starts to occur at approximately $Re = 2000$ and the transition goes up to $Re = 3000$. With the results shown above, we

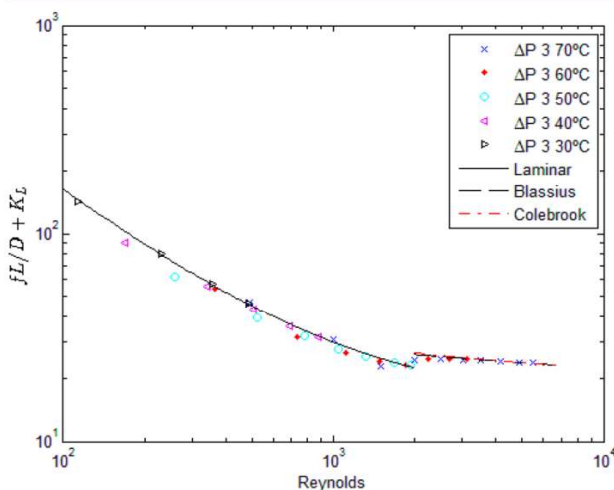


Figure 8. Friction factor and minor losses for the sensor ΔP_3 for isothermal flow.

concluded that we can use the Blasius equation to calculate the friction factor of isothermal flow in turbulent flow at low Reynolds numbers.

Our preliminary fluid dynamic experiments could only be done up to $Re = 6000$, as greater velocities would lead to a temperature rise above 70°C due to friction. We decided not to do experiments above 70°C , both for security reasons and because at that temperature no deposition occurs. The matrix of experiments for studying deposition was only for laminar flow.

Another important piece of information is that we used sensor ΔP_2 for the calibration process and verification of measurements, but for the deposition experiments shown later in this paper we did not use the results. The reason is that the margin of error for the measurements was too high compared to ΔP_1 . In the case of ΔP_3 , there is no way to guarantee that the local pressure drop increases along with the wax buildup; hence, the pressure drop methodology could not be used for this sensor.

Friction factor is a powerful tool for designing systems. The issue is that it was developed for isothermal flow. The classical solution, described above, is only valid for constant viscosity. In cases where heat transfer occurs, the alternative would be to consider a nonisoviscous flow; thus the solution is no longer valid.⁶

We will next discuss Heat Transfer and then the non-isothermal friction factor in the section Nonisothermal Flow. We have to consider the nonisothermal friction factor in this experiment because this oil's viscosity significantly changes radially.

Heat Transfer. A radial heat transfer from a hot fluid flowing inside a pipeline to a cold fluid flowing outside the pipeline is an undergraduate problem of heat transfer. The thermal circuit involves three resistances: convection of the hot fluid, conduction of the pipeline, and convection of the cold fluid.³⁷ However, when dealing with real situations, investigation of the heat transfer within waxy crude oil flowing in the seabed can get complicated.

In our experiment, there is a hot waxy crude flowing inside a copper pipeline and cold water flowing on the outside. In this paper, the goal is to estimate the temperature of the inner wall of the pipeline, in order to predict the viscosity in the wall and therefore predict the friction factor.⁶ Equation 7 shows the general equation for heat transfer.⁴⁵

$$q = U_{\text{tot}} A (T_{\infty \text{ oil}} - T_{\infty \text{ water}}) \quad (7)$$

When the pipeline is clean, without the wax layer, there are only three thermal resistances: the oil, the pipeline wall, and the water. But once the wax deposit forms, there is a fourth thermal resistance: the deposit works as an insulation. For the simplified analysis that we will show below, we are disregarding the fourth resistance. Our aim is to calculate the temperature at the wall in the beginning of the experiment. Equation 8 shows the equation for the total heat transfer coefficient (U_{tot}).

$$\frac{1}{U_{\text{tot}}} = \frac{1}{h_{\text{oil}}} + \frac{D_w \ln\left(\frac{D_o}{D_w}\right)}{2k_{\text{pipe}}} + \frac{1}{h_{\text{water}}} \quad (8)$$

The Nusselt number for internal flow can be seen in eq 9.³⁷ All the dimensionless parameters are calculated based on the values in the bulk, with the exception of the viscosity at the wall.

$$Nu_{niso} = \begin{cases} 1.86 \left(\frac{Re Pr D_w}{L} \right)^{1/3} \left(\frac{\eta_b}{\eta_w} \right)^{0.14}, & Re < 2000, Pr \geq 5 \\ \frac{\frac{f_{niso}}{8} (Re - 1000) Pr}{1.07 + 12.7 \left(\frac{f_{niso}}{8} \right)^{0.5} (Pr^{2/3} - 1)}, & 2000 < Re < 5 \times 10^6 \end{cases} \quad (9)$$

The water flows in a rectangular channel with the pipeline parallel to the flow, and we used the correlation of hydraulic diameter to calculate the heat transfer. We also measure the water volumetric flow rate and maintained at turbulent flow; this way we can use eq 10.³⁷

$$Nu_{water} = 0.023 Re^{4/5} Pr^{1/3} \quad (10)$$

With those equations it is possible to obtain the amount of heat transfer and calculate the temperature at the pipeline wall.

$$T_w = T_{\infty oil} + \frac{U_{tot}}{h_{oil}} (T_{\infty oil} - T_{\infty water}) \quad (11)$$

Nonisothermal Flow. To measure the friction factor for nonisothermal flow under our experimental conditions, we considered that the wax deposition in 3 min is irrelevant, which means that it does not alter the pressure drop even if the temperature of the inner pipeline is below the WAT. During that time, we measured the pressure drop and calculated the nonisothermal friction factor.⁶

Because we consider that the friction factor solution is an important tool, we try to calculate the friction factor with the solution proposed by Sieder and Tate³⁸ and used by Hoffmann and Amundsen.⁶

$$f_{niso} = f_{iso} \left(\frac{\eta_b}{\eta_w} \right)^k \quad (12)$$

The last important parameter is the shear rate at the wall. Because the viscosity is dependent on shear rate, we have to calculate the shear rate to calculate the viscosity. Equation 13 is the shear rate value at the wall.³⁶

$$\dot{\gamma}_w = \frac{1}{8} f \frac{\rho_{oil}}{\eta_{oil}} V^2 \quad (13)$$

Basically, the problem is to calculate the friction factor we need to calculate the viscosity at the wall, but the viscosity is dependent on the shear rate and on the temperature and the shear rate and temperature calculation are dependent on the viscosity at the wall.

In order to resolve all the issues, we did an iterative solution, where we gave an initial estimation to the viscosity at the wall, calculated the friction factor, the shear rate, and the temperature at the wall, and recalculated the viscosity; once the algorithm converged, the algorithm ended. Figure 9 shows the flowchart of the algorithm.

Once we have the algorithm we can do measurements to adjust the empirical value of the nonisothermal friction factor (k). Hoffmann and Amundsen⁶ show the calculation for a turbulent flow and found the value of k of 0.07 and verified that it did not change considerably. Bern et al.³⁹ confirm this by saying that the nonisothermal friction factor only needs to be used for low Reynolds numbers. We show our measurements in Figure 10; the best fit we obtained was when $k = -0.07$, which means a strong increase in the friction factor.

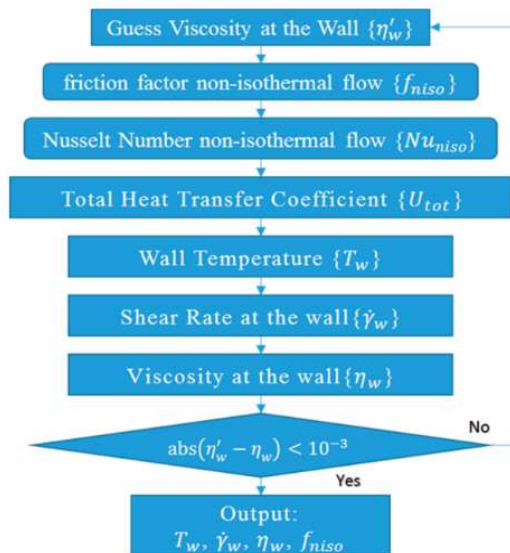


Figure 9. Flowchart calculation of nonisothermal friction factor.

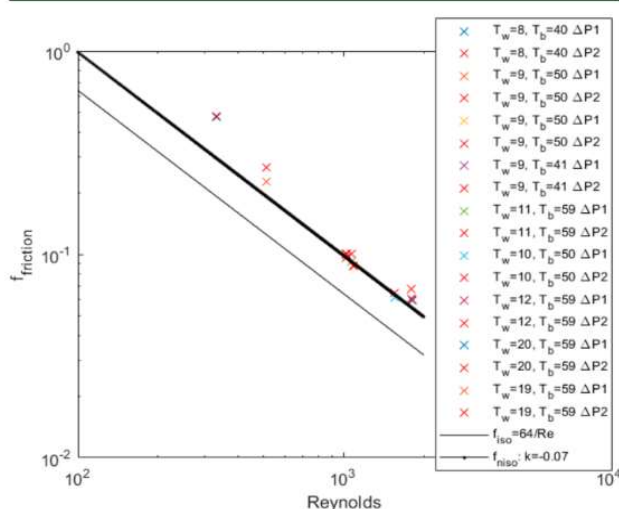


Figure 10. Friction factor for nonisothermal flow varying the wall temperature (T_w) and the bulk temperature (T_b).

It is important to observe that even with the best fit the errors are big, which means that considering the rheological behavior in such cases might be interesting. To do numerical simulations of conservation of momentum, the variation in the rheological behavior due to the nonisoviscous flow would need to be considered.

Calculation of the Wax Thickness. The method we used to calculate the friction factor is based on the pressure drop data^{6,9,13} and has been modified by the solution shown above. First, we calculate the nonisothermal friction factor shown in the section **Nonisothermal Flow**, and second we consider the pressure drop and the friction factor in the beginning of the experiment as the parameters for normalization.^{13,40} The formula is shown in eq 14

$$F(\delta) = \left(\frac{dP}{dL} \right)_t - \left(\frac{f_{\text{niso}} V^2}{D_w} \right)_t \sim 0 \quad (14)$$

The pressure drop and the diameter in the beginning of the experiment are known, and the pressure drop is measured throughout the experiment. Equation 14 becomes dependent only on the diameter. Basically, the velocity depends on the diameter and the friction factor depends on the diameter. We solved eq 14 with the Newton–Raphson method and compared the results with the solution using the algorithm for the nonisothermal friction factor.

Because we use the experimental pressure drop in the beginning of the experiment to define the pressure drop, we considered that any variation is due to diameter variation. In the beginning of the experiment the flow is already non-isothermal; thus the variation in pressure drop is really only due to diameter variation.

The issue with this method is that, as the wax builds up, the temperature in the oil and deposit interface increases, so the viscosity would also decrease, which would decrease the friction factor and therefore the pressure drop. If we disregard this phenomenon, we would underpredict the wax deposit. The only way to verify whether the calculations are correct is to measure the deposit with a different technique, which is the reason we scraped off the deposit with a “pig” operation, as shown in the section [Reproducibility and Measurement Verification](#).

Reproducibility and Measurement Verification. The first thing we verified was the reproducibility of the experiments. We did at least two experiments under each condition; the experiments were reproducible as can be seen in Figure 11. All the data shown in this paper were calculated with the raw data from the pressure gauge sensor; there is no average or filtering process.

As can be seen in Figure 11, the data dispersion decreases as the temperature of the bulk decreases. This can be explained by the increase in viscosity and hence a higher pressure drop; the accuracy of the sensor increases with the increase in the differential pressure.

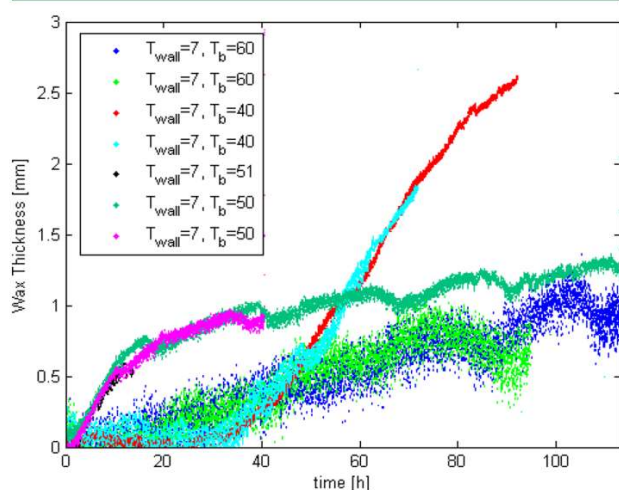


Figure 11. Single-phase wax deposition reproducibility.

It is important to note that the wall temperatures are the same because the Reynolds number is not constant. In these results we simply want to show the reproducibility of the experiments. The influences of temperatures and mass flow rate will be discussed later in the paper. In Figure 11 the main focus of this paper can already be seen: the time necessary for the deposit to start. To our knowledge, the only study which has shown something similar is Venkatesan and Creek.¹⁸ This is interesting because molecular diffusion cannot explain the delay and the industry has serious issues predicting where the deposit will occur.

To verify the wax thickness calculation using the pressure drop we did a pigging process, and weighed the deposit mass.⁸ Before we show the comparison, it is important to highlight that because of the way the experimental apparatus was built, it is impossible to do the pig operation in the whole pipeline: we can only remove wax from the first half of the pipeline. As can be seen in Figure 1, the measurement of ΔP_1 is at the halfway end of the pipeline. We decided to measure the differential pressure at that point in order to have a developed heat and hydrodynamic condition.

It is also important to mention that the pig procedure is time-consuming in this experimental facility, so we could not do it in every experiment. We agree that to better understand the deposition phenomena the composition of the deposit needs to be studied under each condition. As Soedarmo et al.¹⁵ show, there are a variety of diverging physical hypotheses for wax deposition. To better understand them, it is necessary to visualize the deposit and study the composition. We intend to modify the experimental apparatus in order to be able to do that in a next experimental matrix. We show an example of removed wax deposit in Figure 12.



Figure 12. Wax deposit removed in the pig operation.

Based on our experimental facility there would be another possibility, which is to calculate the wax thickness using the ΔP_3 sensor, as it measures the differential pressure in the whole water bath. The problem is that there are curves and temperature sensors inside the water bath; hence the pressure drop increase due to wax deposit could not be inferred by the pressure drop method.

Comparison of both methods is shown in Figure 13. There is a discrepancy in the results. The mass measurements show a smaller deposit than the pressure drop method, a difference of 20%. But they do follow the same tendency. We believe that that discrepancy is due to the different areas of measurement. As Singh et al.⁴ point out, the deposition at the beginning of the

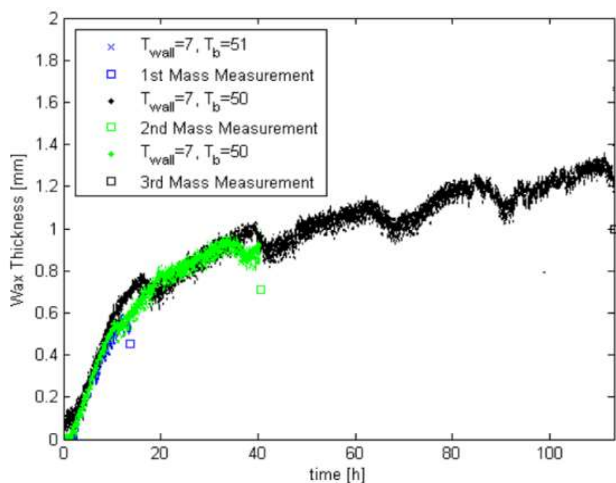


Figure 13. Comparison of pressure drop method and mass of the deposit to calculate wax thickness.

pipeline tends to be smaller than the deposition at the end of the pipeline as time increases.

The only experiments where we did the pig procedure were the ones shown in Figure 13. With those results we concluded that the pressure drop methodology is accurate enough to investigate the wax deposition, even with an error of 20%, as discussed above. We did the gas chromatography of the deposit that we removed; the results are in Figure 14. As we can see, the general trend is similar to the literature.^{4,6,7,13}

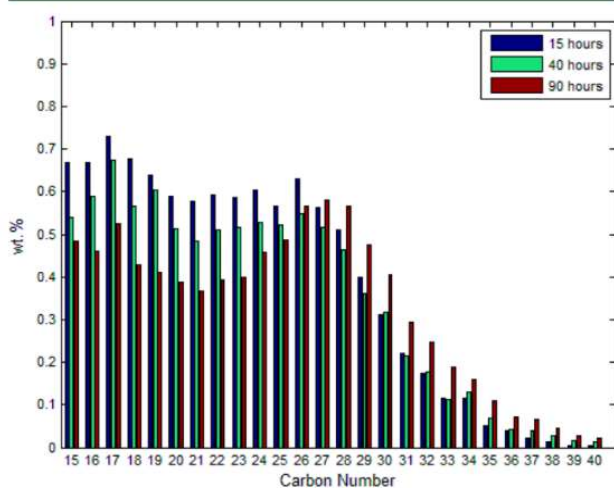


Figure 14. Chromatography of deposit on the verification process.

As discussed before, HTGC would be the best way to study the wax content of the deposit. Unfortunately that is not possible; thus we measured only up to C40. We can observe that the weights of hydrocarbons from C15 to C26 decrease over the time of deposition, while the weights of hydrocarbons with C30–C40 increase over time. This is explained by molecular diffusion in a porous media.¹⁹

Erosion Velocity Limit Verification. The API 14E⁴¹ is a recommendation practice for petroleum industries to design pipelines. The recommendation is that there is a threshold velocity above which erosion becomes a concern. There is a

vast literature showing that the value obtain by the proposed empirical formulation is highly conservative. We used that value to guarantee that in our experiments we eliminate that possibility. The erosion velocity limit in our experiment is 4.2 m/s; thus we only did experiments of deposition with mean velocities up to 3.5 m/s.

Main Results. We will start by discussing things that are well-known in the literature, such as the influence of flow rate and the influence of temperature. Both are well-established by experimental data. After that we will show the results that deserve this paper, which are the delay in the beginning of the deposit.

Flow Rate Influence. To study the influence of flow rate, we did experiments at three bulk temperatures: 60, 50, and 40 °C. The influence of flow rate under laminar flow is well-established in the literature;^{4,26} i.e., as the flow rate rises the wax deposit thickness decreases. Singh et al.⁴ were able to model this behavior using only molecular diffusion with good accuracy for a model oil.

Experiments under laminar conditions with precipitated wax crystals done by Cabanillas et al.²⁶ have also shown the influence of shear rate. They have observed that the deposit decreases as the flow rate rises both for precipitated wax in the bulk and for the oil above the WAT. Their results were also obtained with model oil.

We show the results for the oil at 60 °C in Figure 15. The first obvious thing is the temperature increase in the wall as the

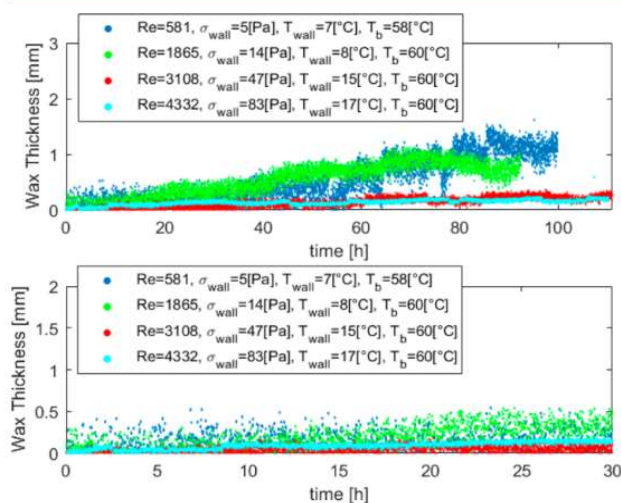


Figure 15. Comparison of wax deposition thickness buildup by varying oil flow rate with $T_b = 60$ °C.

oil flow rate rises. To reemphasize, we do not measure the temperature in the pipeline wall: the PID system controls the water temperature.

The decrease in wax deposition with the increase of Reynolds number in this experiment can be due to both factors, increase of flow rate and increase of the temperature at the wall, each shown in the literature.⁴ As the wall temperature rises, the deposit thickness decreases, and as the flow rate rises the deposit thickness also decreases. To better study the influence of each variable, we need to isolate them. We decided to not do that at 60 °C because the measurement margin of error was large due to the small viscosity. Thus, we isolate the variables for lower temperatures.

To decide whether we were measuring the deposit decrease due to increase in the pipeline's temperature or due to rise in flow rate, we did the experiment with the bulk at 50 °C controlling the temperature of the water. This way we can be sure that the influence is only because of the shear rate caused by different flow rates.

Figure 16 shows the result of wax deposition for constant bulk temperature and wall temperature and changing the oil

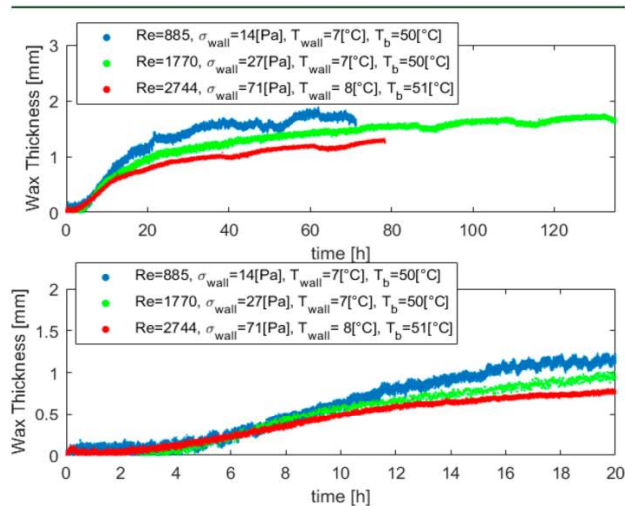


Figure 16. Comparison of wax deposition thickness buildup by varying oil flow rate with $T_b = 50$ °C and $T_w = 7$ °C.

flow rate. It can be seen that as the shear rate rises the wax deposit thickness decreases. The pipeline temperature result within experimental error and, as already discussed, the temperature measurement are not as accurate as one would like.

When addressing deposition rate, once the deposition starts, we have the normal profile shown in the literature.^{4,6,9} The deposition rate is initially high and decreases as the deposit builds up. The explanation for such behavior is that the deposit acts as an insulator, hence the temperature at the oil and the deposit interface increases, leading to a lower precipitation rate and thus a lower and lower thickness increase.

Before the deposition starts, however, we have a long period without deposition, around 5 h for this setup; i.e., there is no increase in the pressure drop for the first 5 h. Even with all the error margin in the temperature measurements, there is no possible justification for this phenomenon in molecular diffusion. Under these conditions the bulk is above the WAT, which means that there is no precipitated wax, which also means that Brownian diffusion and shear dispersion cannot be deposition mechanisms. This only leads to one final explanation: the influence of non-Newtonian behavior.

The last experiment at constant temperature is at 40 °C. At this temperature the oil is closer to the WAT; hence the WAT is reached radially closer to the center of the pipeline. This means that there are precipitated molecules closer to the bulk, but not a high amount. Figure 17 shows the results, and this is where the problem with molecular diffusion being the most relevant mechanism is most evident.

The beginning of the deposit buildup for the oil at 40 °C and low Reynolds is around 25 h after all the experiments reached all the desired conditions. These results cannot be explained by

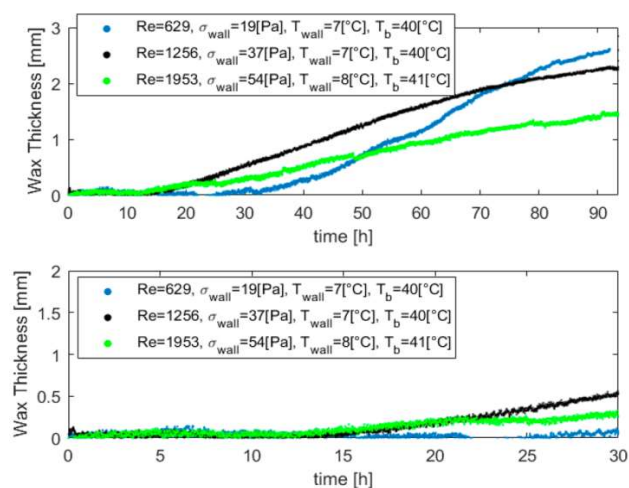


Figure 17. Comparison of wax deposition thickness buildup by varying oil flow rate with $T_b = 40$ °C and $T_w = 8$ °C.

molecular diffusion. Once the deposition starts, the deposition rate approaches the profile extensively shown in the literature.^{4,6,13}

The mechanism which could possibly explain the delay in the deposit buildup would be shear dispersion. This phenomenon dictates that the precipitated particles move in the cross section in the direction of the lower shear rate.¹⁰ This means that all the particles would gather in the bulk and flow in the core; thus there is no particle in the wall to start the deposit.

Because the Brownian diffusion mechanism tends to send the precipitated molecules in the bulk in the direction of the wall, there is a competition between Brownian diffusion and shear dispersion. Once some of the particles are deposited in the wall, the deposition starts to grow as expected. This might be the most plausible explanation for the delay in the start of the deposit.

As the flow rate rises, the shear rate rises as well as the Brownian diffusion coefficient, and thus the Brownian mechanism is more relevant. This is a possible explanation as to why the deposit began earlier for higher flow rates. This is also the case for experiments at 50 °C shown in Figure 16. As the flow rate increases the deposit starts earlier, but in those experiments, the times are different by 1 h, while for 40 °C there is around 10 h of difference.

Another possible explanation for this phenomenon is the influence of rheology in initiation of the wax deposit for oils with high viscosity and high paraffin percentage: the gelation process. If we consider a conglomerate of molecules flowing in the oil with both shear dispersion and Brownian diffusion acting on them, as the temperature decreases, and the oil becomes non-Newtonian, the apparent yield stress of this fluid might be reached, and this would be the beginning of the deposit.

Besides all the discussion made so far, there is a possibility that has not been discussed, which is the influence of surface chemistry in the deposit. It is possible that the copper surface is influencing the gelation process, influencing the strength of the conglomerates of molecules and thus the initialization of the deposition.

Once this deposit is formed another mechanism becomes important, which is the shear stripping mechanism, i.e., removal of wax molecules from the deposit due to shear stress. The

thing is this effect is much more intense for turbulent flows than for laminar flows. In the experiments shown in this paper, there are only laminar flow and transition from laminar to turbulent flow. But because we are dealing with high viscosity oil, the shear stress at the wall is high even at laminar flow; therefore, we believe that this might be the reason for the delay of the deposit.

Influence of Temperature. In our experiments, we definitely need to improve the temperature measurements. Soedarmo et al.⁷ showed that, with an error of ± 1.1 °C, the error of the calculation using the equilibrium model goes up to 50% due to the steep variation in the solubility with temperature. However, in this paper we do not intend to discuss the advances in the molecular diffusion based models, but rather to show evidence that for highly paraffinic oils other mechanisms are at least as important as diffusion.

The results shown below are a comparison of the influence of temperature. The issue is that in our experimental apparatus we control the oil flow rate and its temperature, not the Reynolds number. As the temperature changes, the viscosity changes, and thus the Reynolds number changes. We considered that for the analysis done in this paper this variation can be overlooked. In order to compare the results more accurately in future experiments, the control will be done based on the Reynolds number instead of the flow rate.

All the results shown in Figure 18 have been shown before. We present them again in order to compare the results. As can

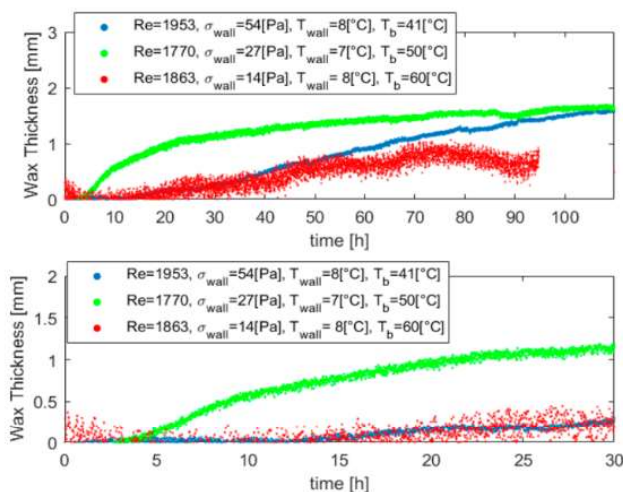


Figure 18. Comparison of wax deposition thickness buildup by varying oil temperature with $Re \approx 1850$ and $T_w = 8$ °C.

be seen, the main issue which is the start of the deposition is again highlighted when we compare bulk temperatures. For the oil at 60 °C the pressure drop is smaller because the viscosity is smaller; hence the error on the sensor is near the variation in pressure drop due to the diameter reduction. As such, we cannot verify the deposition rate or the time necessary for deposition to begin.

For the oil at 50 and 40 °C we can show a considerable difference. Again, for the oil at 50 °C there are no precipitated molecules in the bulk; the particles must precipitate near the wall. If we consider that the first molecule deposits are due to diffusion and rheological behavior, this may explain why

deposition at higher temperatures starts to occur faster than at lower temperatures.

The last comparison is shown in Figure 19. We compare temperature variation results for a lower Reynolds number and

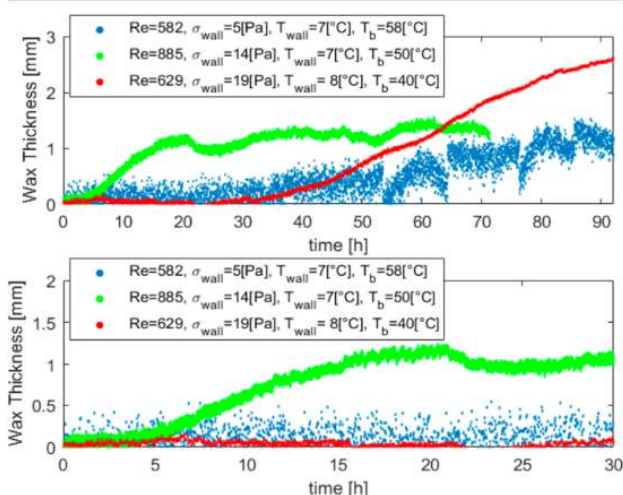


Figure 19. Comparison of wax deposition thickness buildup by varying oil temperature with $Re \approx 650$ and $T_w = 7$ °C.

the results show the same tendency as for a higher Reynolds number, but still laminar flow, as shown in Figure 18. First, at 60 °C both the deposition rate and the time before the deposition starts are within the sensor margin of error. For 50 °C the deposition started way before 40 °C. The same explanation discussed before could be applied in this case.

Even though this paper shows evidence of an effect that molecular diffusion cannot explain, we do not have enough data to confirm whether shear dispersion¹⁰ and Brownian diffusion are the mechanisms that govern the beginning of deposition for highly paraffinic crude oil.

Another important point to make is that in the literature most results do not present this delay in the deposition start. The only experimental data known by this group was published by Venkatesan and Creek.³¹ The crude oil that they use has some similarity to the oil studied in this paper.

Simulation. Using the model based on the equilibrium model proposed by Singh et al.,⁴ for the deposit and the all the oil properties discussed above we obtained the results shown in Figure 20. We used the aspect ratio of 3 as measured by Soedarmo et al.,¹⁶ and we calculated the molecular diffusivity according to the method proposed by Hayduk and Minhas.⁴⁶ The value for the molecular diffusivity used was $D_{wo} = 2 \times 10^{-10}$ [m²/s], which is the near the value used by Singh et al.⁴ The diffusivity should be further studied.

The heat transfer calculations were done using all the equations for mass conservation proposed by Singh et al.⁴ with the heat transfer equations shown in eqs 15 and 16. Equation 15 is the global heat transfer equation with the deposit and the latent heat of solidification.

$$q = U_{tot}A(T_{oil} - T_{water}) - 2\pi k_{wax}[C_{wb} - C_{ws}(T_i)]\Delta H \quad (15)$$

The only difference between eqs 16 and 8 is the conduction between the wax deposits. In the simulation we used the value for the deposit's thermal conductivity obtained by Veiga et al.¹⁷

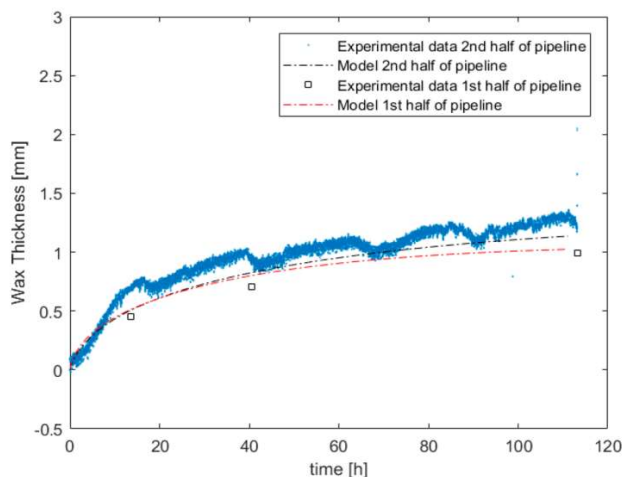


Figure 20. Simulation of results using Singh et al.⁴

The results show that constant thermal conductivity over time is a proper assumption.

$$\frac{1}{U_{\text{tot}}} = \frac{1}{h_{\text{oil}}} + \frac{D_i \ln\left(\frac{D_o}{D_i}\right)}{2k_{\text{wax}}} + \frac{D_w \ln\left(\frac{D_o}{D_w}\right)}{2k_{\text{pipe}}} + \frac{1}{h_{\text{water}}} \quad (16)$$

We only simulate the experiment where we have both pressure drop data and mass data from the pig operation. We decided to simulate this experiment because the deposit's profile is similar to the ones that molecular diffusion is able to model, as has been discussed before. As can be seen in Figure 20, the molecular diffusivity model can predict the deposit's final thickness both at the beginning of the pipeline and at the end, but the rate of buildup in the beginning is considerably wrong.

To better predict the behavior of this oil, the non-Newtonian behavior should be considered. A momentum equation considering two dimensions or at least 1.5 dimensions³² to properly calculate the shear rate and shear stress, and thus rheological properties at the interface between the deposit and the bulk, is necessary to more accurately predict the behavior.

CONCLUSION

An experimental apparatus was built in the interest of studying wax deposition of commercial crude oils from Brazil. This facility was remodeled from a previous facility that existed in the laboratory. This setup makes it possible to study the two main problems with flow assurance related to waxy crude oils: (1) flow start-up of gelled waxy crude oils and (2) wax deposition under two-phase flow. In this paper we show wax deposition experimental results for a highly paraffinic commercial crude oil obtained under single-phase laminar flow.

To check all the instrumentation of our apparatus, we did preliminary flow studies under isothermal conditions and nonisothermal conditions without wax deposition. The idea was to confirm instrument accuracy and determine whether we could model these kinds of flows. We applied a simple algorithm to compensate for the nonisoviscous flow that takes place in wax deposition experiments.

We have experimental evidence that, for highly paraffinic oils, molecular diffusion alone cannot predict when the deposition will start. This is usually not a problem because in most

experimental data in the literature the buildup starts as soon as the temperature at the wall reaches the WAT. But that was not the case for the oil studied in this paper. After the oil was at the desired temperature and the water was at 5 °C, wax took some time to start building up: around 5 h for the oil at 50 °C and around 24 h in the worst-case scenario.

This time delay before the deposit starts to build up was shown for a shorter period of time in the literature for a similar oil under different conditions.¹⁸ The problem is there are many more experimental studies with condensates and model oils than with real high paraffin content crude, which is the reason we decided to publish this study.

In experiments where the oil was above the WAT, after the pressure drop starts to increase caused by the wax deposit buildup, the wax deposition rate follows the same profile as in most of the literature. Molecular diffusion is perfectly capable of predicting this behavior; thus we believe that after there is a thin layer of deposit the main mechanism of buildup and aging is indeed molecular diffusion.

When we did experiments with oil temperature in the bulk near the WAT, the time before the deposition begins was longer. We believed that this could be explained as effects of shear dispersion, Brownian diffusion, and non-Newtonian behavior. That would increase the difficulty in predicting where the deposition occurs and when, since these mechanisms are harder to model.

Finally, we used the model proposed by Singh et al.⁴ to predict the experimental data using this apparatus. After molecular diffusivity and aspect ratio were defined, the model was able to predict the final wax thickness. The deposition rate however is not well predicted: it overestimates the buildup because it cannot predict the delay in the deposition. We believe that with a momentum equation considering non-Newtonian behavior we could considerably improve those results.

AUTHOR INFORMATION

Corresponding Author

*E-mail: charlievander@gmail.com.

ORCID

Charlie Van Der Geest: 0000-0003-3469-2140

Notes

The authors declare no competing financial interest.

ACKNOWLEDGMENTS

The authors wish to thank the company Repsol–Sinopec Brazil for their financial and technical support in this study. Also we would like to thank ANP (National Agency of Petroleum, Natural Gas and Biofuels) (254/2014) and CAPES (Brazilian Federal Agency for Support and Evaluation of Graduate Education within the Ministry of Education of Brazil) (33003017) for their financial support. We would also like to thank the ALFA research group for their support.

NOMENCLATURE

Acronyms

WAT = wax appearance temperature
WDT = wax dissolution temperature
DSC = differential scanning calorimeter
PID = proportional integral derivative
EM = equilibrium model
PP = pour point

Variables

- ΔP = differential pressure
 T = temperature
 g = gravity
 A = constant related to entropy of the activation
 E_a = activation energy of viscous flow
 B = empirical constant
 C = empirical constant
 R = gas universal constant
 h = heat transfer coefficient
 k = thermal conductivity
 K = local head loss
 L = length
 D = pipeline diameter
 d = diameter without deposit
 f = friction factor
 V = velocity
 Q = volumetric flow rate
 U = heat transfer coefficient

Dimensionless Variables

- Re = Reynolds number
 Pr = Prandtl number
 Nu = Nusselt number

Greek Symbols

- η = viscosity
 $\dot{\gamma}$ = shear rate
 ρ = density
 ϵ = roughness
 σ = shear stress

Subscripts

- l = local
 m = mean
 w = inner wall
 wax = wax deposit
 o = outer
 i = interface
 iso = isothermal
 $niso$ = nonisothermal
 exp = experimental
 tot = total
 $ooil$ = bulk of the oil
 $owater$ = water away from the wall

REFERENCES

- (1) Reistle, C. E., Jr. *Methods of Dealing with Paraffin Troubles Encountered in Producing Crude Oil*; No. BM-TP-414; Bureau of Mines: Washington, DC, 1928.
- (2) Bilderback, C. A.; McDougall, L. A. Complete paraffin control in petroleum production. *JPT, J. Pet. Technol.* **1969**, 21 (09), 1151–1156.
- (3) Asperger, R. G.; Sattler, R. E.; Tolonen, W. J.; Pitchford, A. C. *Prediction of Wax Buildup in 24 in. Cold, Deep Sea Oil Loading Line*; SPE-10363-MS; Society of Petroleum Engineers: 1981.
- (4) Singh, P.; Venkatesan, R.; Fogler, H. S.; Nagarajan, N. Formation and aging of incipient thin film wax-oil gels. *AIChE J.* **2000**, 46 (5), 1059–1074.
- (5) Paso, K. G.; Fogler, H. S. Influence of n-paraffin composition on the aging of wax-oil gel deposits. *AIChE J.* **2003**, 49 (12), 3241–3252.
- (6) Hoffmann, R.; Amundsen, L. Single-phase wax deposition experiments. *Energy Fuels* **2010**, 24 (2), 1069–1080.
- (7) Soedarmo, A. A.; Daraboina, N.; Sarica, C. Validation of wax deposition models with recent laboratory scale flow loop experimental data. *J. Pet. Sci. Eng.* **2017**, 149, 351–366.
- (8) Aiyejina, A.; Chakrabarti, D. P.; Pilgrim, A.; Sastry, M. K. S. Wax formation in oil pipelines: A critical review. *Int. J. Multiphase Flow* **2011**, 37 (7), 671–694.
- (9) Sarica, C.; Panacharoensawad, E. Review of paraffin deposition research under multiphase flow conditions. *Energy Fuels* **2012**, 26 (7), 3968–3978.
- (10) Azevedo, L. F. A.; Teixeira, A. M. A critical review of the modeling of wax deposition mechanisms. *Pet. Sci. Technol.* **2003**, 21 (3–4), 393–408.
- (11) Merino-Garcia, D.; Corraera, S. Cold flow: A review of a technology to avoid wax deposition. *Pet. Sci. Technol.* **2008**, 26 (4), 446–459.
- (12) Huang, Z.; Lu, Y.; Hoffmann, R.; Amundsen, L.; Fogler, H. S. The effect of operating temperatures on wax deposition. *Energy Fuels* **2011**, 25 (11), 5180–5188.
- (13) Panacharoensawad, E.; Sarica, C. Experimental study of single-phase and two-phase water-in-crude-oil dispersed flow wax deposition in a mini pilot-scale flow loop. *Energy Fuels* **2013**, 27 (9), 5036–5053.
- (14) Valinejad, R.; Nazar, A. R. S. An experimental design approach for investigating the effects of operating factors on the wax deposition in pipelines. *Fuel* **2013**, 106, 843–850.
- (15) Soedarmo, A. A.; Daraboina, N.; Lee, H. S.; Sarica, C. Microscopic Study of Wax Precipitation - Static Conditions. *Energy Fuels* **2016**, 30 (2), 954–961.
- (16) Soedarmo, A. A.; Daraboina, N.; Sarica, C. Microscopic study of wax deposition: mass transfer boundary layer and deposit morphology. *Energy Fuels* **2016**, 30 (4), 2674–2686.
- (17) Veiga, H.; Fleming, F. P.; Azevedo, L. F. A. Wax deposit thermal conductivity measurements under flowing conditions. *Energy Fuels* **2017**, 31, 11532–11547.
- (18) Venkatesan, R.; Creek, J. Wax deposition and rheology: Progress and problems from an operator's view. In *Offshore Technology Conference, Houston, TX, USA*; Offshore Technology Conference: 2010; pp 3–6.
- (19) Huang, Z.; Lee, H. S.; Senra, M.; Scott Fogler, H. A fundamental model of wax deposition in subsea oil pipelines. *AIChE J.* **2011**, 57 (11), 2955–2964.
- (20) Svendsen, J. A. Mathematical modeling of wax deposition in oil pipeline systems. *AIChE J.* **1993**, 39 (8), 1377–1388.
- (21) Ramirez-Jaramillo, E.; Lira-Galeana, C.; Manero, O. Modeling wax deposition in pipelines. *Pet. Sci. Technol.* **2004**, 22 (7–8), 821–861.
- (22) Merino-Garcia, D.; Margarone, M.; Corraera, S. Kinetics of waxy gel formation from batch experiments. *Energy Fuels* **2007**, 21 (3), 1287–1295.
- (23) Paso, K. G.; Fogler, H. S. Bulk stabilization in wax deposition systems. *Energy Fuels* **2004**, 18 (4), 1005–1013.
- (24) Andrade, D. E.; Neto, M. A. M.; Negrão, C. O. The importance of supersaturation on determining the solid-liquid equilibrium temperature of waxy oils. *Fuel* **2017**, 206, 516–523.
- (25) Paso, K.; Senra, M.; Yi, Y.; Sastry, A. M.; Fogler, H. S. Paraffin polydispersity facilitates mechanical gelation. *Ind. Eng. Chem. Res.* **2005**, 44 (18), 7242–7254.
- (26) Cabanillas, J. P.; Leiroz, A. T.; Azevedo, L. F. Wax Deposition in the Presence of Suspended Crystals. *Energy Fuels* **2016**, 30 (1), 1–11.
- (27) Roenningsen, H. P.; Bjoerndal, B.; Baltzer Hansen, A.; Batsberg Pedersen, W. Wax precipitation from North Sea crude oils: 1. Crystallization and dissolution temperatures, and Newtonian and non-Newtonian flow properties. *Energy Fuels* **1991**, 5 (6), 895–908.
- (28) Zheng, S.; Saidoun, M.; Palermo, T.; Mateen, K.; Fogler, H. S. Wax Deposition Modeling with Considerations of Non-Newtonian Characteristics: Application on Field-Scale Pipeline. *Energy Fuels* **2017**, 31, 5011–5023.
- (29) Frigaard, I. A.; Paso, K. G.; de Souza Mendes, P. R. Bingham's model in the oil and gas industry. *Rheol. Acta* **2017**, 56 (3), 259–282.
- (30) Bhat, N. V.; Mehrotra, A. K. Measurement and prediction of the phase behavior of wax-solvent mixtures: Significance of the wax disappearance temperature. *Ind. Eng. Chem. Res.* **2004**, 43 (13), 3451–3461.

- (31) Van Der Geest, C.; Guersoni, V. C. B.; Merino-Garcia, D.; Bannwart, A. C. Rheological study under simple shear of six gelled waxy crude oils. *J. Non-Newtonian Fluid Mech.* **2017**, *247*, 188–206.
- (32) Van Der Geest, C.; Guersoni, V. C. B.; Salomão, L. A. S., Jr.; Bannwart, A. C. Experimental Study of the Necessary Pressure to Start-Up the Flow of a Gelled Waxy Crude Oil. In *ASME 2017 36th International Conference on Ocean, Offshore and Arctic Engineering*; American Society of Mechanical Engineers: 2017.
- (33) Chen, J.; Zhang, J.; Li, H. Determining the wax content of crude oils by using differential scanning calorimetry. *Thermochim. Acta* **2004**, *410* (1), 23–26.
- (34) Yi, S.; Zhang, J. Relationship between waxy crude oil composition and change in the morphology and structure of wax crystals induced by pour-point-depressant beneficiation. *Energy Fuels* **2011**, *25* (4), 1686–1696.
- (35) Coto, B.; Coutinho, J. A. P.; Martos, C.; Robustillo, M. D.; Espada, J. J.; Pena, J. L. Assessment and improvement of n-paraffin distribution obtained by HTGC to predict accurately crude oil cold properties. *Energy Fuels* **2011**, *25* (3), 1153–1160.
- (36) White, F. M. *Fluid Mechanics, in SI Units*; McGraw-Hill: 2011.
- (37) Cengel, Y. A. *Heat Transfer, a Practical Approach*; McGraw-Hill: 2003.
- (38) Sieder, E. N.; Tate, G. E. Heat transfer and pressure drop of liquids in tubes. *Ind. Eng. Chem.* **1936**, *28* (12), 1429–1435.
- (39) Bern, P. A.; Withers, V. R.; Cairns, R. J. Wax deposition in crude oil pipelines. In *European Offshore Technology Conference and Exhibition*; Society of Petroleum Engineers: 1980.
- (40) Chen, X. T.; Butler, T.; Volk, M.; Brill, J. P. Techniques for measuring wax thickness during single and multiphase flow. In *SPE Annual Technical Conference and Exhibition*; Society of Petroleum Engineers: 1997.
- (41) American Petroleum Institute. *Recommended Practice for Design and Installation of Offshore Production Platform Piping Systems*; American Petroleum Institute: 1991.
- (42) Todi, S. *Experimental and Modeling Studies of Wax Deposition in Crude-Oil-Carrying Pipelines*. Ph.D. Thesis, University of Utah, Salt Lake City, UT, 2005.
- (43) Anaya, Y. K.; Guersoni, V. C.; Perles, C. E.; Bannwart, A. C. Flow Assurance of Waxy Crude Oils: Physicochemical Characterization and Critical Temperatures. Presented at the Rio Oil & Gas Expo and Conference, Rio de Janeiro, Oct 24–27, 2016.
- (44) Paso, K.; Kompalla, T.; Aske, N.; Rønningsen, H. P.; Øye, G.; Sjöblom, J. Novel surfaces with applicability for preventing wax deposition: a review. *J. Dispersion Sci. Technol.* **2009**, *30* (6), 757–781.
- (45) Davenport, T. C.; Conti, V. J. Heat transfer problems encountered in the handling of waxy crude oils in large pipelines. *J. Inst. Pet.* **1971**, *57* (555), 147.
- (46) Hayduk, W.; Minhas, B. S. Correlations for prediction of molecular diffusivities in liquids. *Can. J. Chem. Eng.* **1982**, *60* (2), 295–299.

4. PAPER 4: A modified elasto-viscoplastic thixotropic model for two commercial gelled waxy crude oils

A modified elasto-viscoplastic thixotropic model for two commercial gelled waxy crude oils

Charlie Van Der Geest¹ · Vanessa C. Bizotto Guersoni² · Daniel Merino-Garcia³ · Antonio C. Bannwart¹

Received: 4 September 2014 / Revised: 23 February 2015 / Accepted: 11 March 2015 / Published online: 18 April 2015
 © Springer-Verlag Berlin Heidelberg 2015

Abstract A severe problem to flow assurance occurs when subsea flowlines become blocked with gelled waxy crudes. To design proper surface pump facilities, it is essential to know the minimum pressure required to restart the flow. Simulating and predicting this minimum pressure require the understanding of several physical phenomena, including compressibility, shrinkage, and rheological behavior. This study aims to characterize and simulate the rheological behavior of two commercial waxy crude oils. Based on its survey of the literature, we select the de Souza Mendes and Thompson (2013) model to fit the oil's behavior and then conduct, using a rheometer, a considerable number of experiments with the selected oils. To verify the solution of our algorithm, we compared our theoretical solutions with some results of the literature. When comparing the simulation with experiments, the model was unable to predict the data perfectly; hence, we propose a modified version without changing the physical meaning of the equations, to improve its predictions. Once any of the empirical parameters were able to influence the elastic behavior in such a way that the shear stress

decreased with time, the structural elastic modulus function was modified, which means that the relation of the structure parameter and the storage modulus was modified. One of the interesting results of the analysis is when relating the storage modulus and a new parameter added in the modification, a value was found to be, regardless of the aging time or the oil used, constant.

Keywords Waxy crude oil · Rheological model · Yield stress

Nomenclature: Roman symbols

a, b, m	Empirical parameters
C	Atom of carbon
H	Atom of hydrogen
t_{eq}	Equilibrium time (s)
n	Herschel-Bulkley exponential term
k	Herschel-Bulkley apparent viscosity (Pa.s)
G_0	Storage modulus of the completely structured material (Pa)
G_s	Structural elastic modulus (Pa)
G'	Storage modulus (Pa)
G''	Loss modulus (Pa)

Greek symbols

λ	Structure parameter
λ_0	Initial value of the structure parameter
λ_{eq}	Structure parameter at equilibrium
γ	Strain (m)
γ_e	Elastic strain (m)
γ_v	Viscous strain (m)
τ	Shear stress (Pa)
τ_y	Static limit of the shear stress (Pa)
τ_{yd}	Dynamic shear stress (Pa)
$\dot{\gamma}$	Shear rate (s^{-1})
$\dot{\gamma}_1$	Transition shear rate from static to viscous (s^{-1})

✉ Charlie Van Der Geest
 charlievander@gmail.com
 Vanessa C. Bizotto Guersoni
 vanessa@cepetro.unicamp.br
 Daniel Merino-Garcia
 dmerinog@repsolsinopec.com
 Antonio C. Bannwart
 bannwart@fem.unicamp.br

¹ School of Mechanical Engineering, University of Campinas, Campinas 13083-860, Brazil

² Center for Petroleum Studies, University of Campinas, UNICAMP, Campinas 13083-970, Brazil

³ Repsol Sinopec Brazil, Rio de Janeiro 22250-040, Brazil

η	Apparent viscosity (Pa.s)
η_{∞}	Purely viscous (Pa.s)
η_s	Structural viscosity (Pa.s)
η_v	Addition of η_{∞} and η_s (Pa.s)
η_0	Initial viscosity (Pa.s)
η_{eq}	Viscosity at equilibrium (Pa.s)
θ_1	Relaxation time (s)
θ_2	Retardation time (s)

Introduction

Crude oils are a complex mixture of hydrocarbons in which the majorities are saturated alkanes. In some cases, the concentration of high molecular linear alkanes is very high, leading to the appearance of solids when fluids are cooled below a threshold temperature, termed wax appearance temperature (WAT); in these cases, the fluids are typically called waxy oils. The wax fraction of the oil comprises the molecules that are expected to solidify upon temperature decrease and typically contain molecules with alkyl chain length greater than 18 units. The percentage of such hydrocarbons in oils worldwide usually ranges from 1 to 50 % (Ajienka and Ikoku 1991).

Oil production in the next decades will have a greater contribution from subsea environments, where ambient temperature is as low as 3–4 °C. Consequently, problems associated to solid appearance at low temperatures (such as waxes and hydrates) are becoming more significant. Flow assurance problems associated to waxes range from increased pressure drop, mainly because of diameter reduction, and line blockages. As

remediation costs are quite high, there is a trend in the last decades to develop predictive methods for wax deposition and gelation of the crude oil (Srivastava et al. 1993; Chang et al. 1998, 1999; da Silva and Coutinho 2004; Lee 2008; Luthi 2013).

While wax deposition during flow has advanced to the degree of developing predictive models, the restart of the flow in a pipe full of gelled waxy crude still lacks a commercial tool that is capable of describing the phenomena in its full complexity. When prolonged shutdowns (planned or unplanned) occur, the resultant loss of heat leads to the gelation of the oil when temperature drops below its pour point. The literature has several examples of attempts of generating models to predict the restart of the flow in these conditions (Davidson et al. 2004; Vinay et al. 2009; Phillips et al. 2011a, b).

When designing the pipelines and the pump facilities, engineers usually do a simplified force balance. The assumption is that when the pressure is enough to overcome the yield stress, the restart occurs. The problem is that there is evidence that this calculation is overestimated; therefore, a better rheological modeling of these oils is necessary once they present an “elasto-viscoplastic thixotropic” behavior, which is a complex mixture of plasticity, elasticity, and thixotropy.

For a number of years, researchers have discussed the concept of yield stress, with Barnes and Walters (1985) going so far as to call its definition a myth. For engineering concerns, however, the notion of yield stress is quite useful, capable, as de Souza Mendes and Thompson (2013) pointed out, of predicting the behavior of real fluids. On the other hand,

Fig. 1 Steady-state curve for oil 1 after 1 h of aging

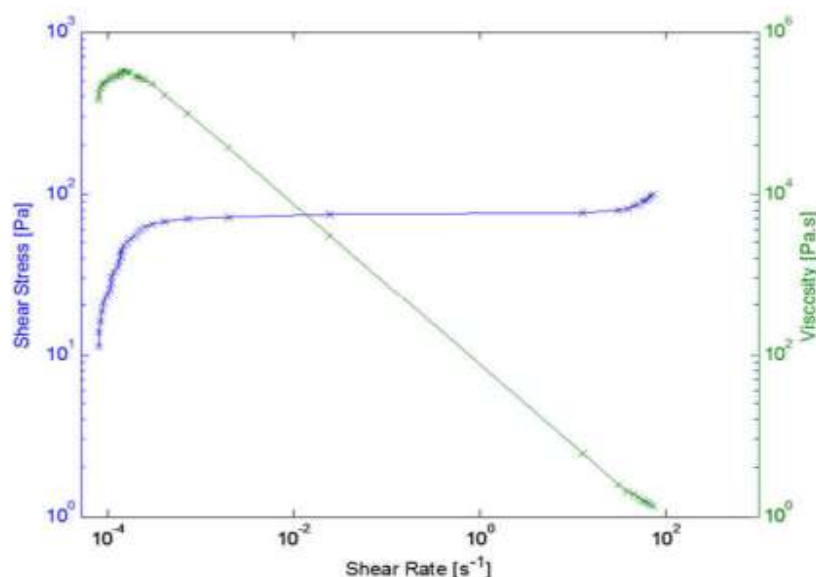
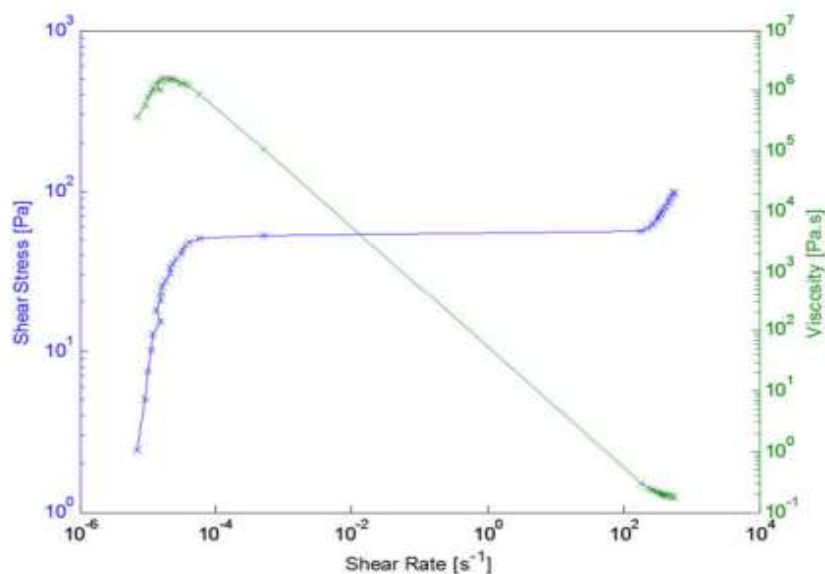


Fig. 2 Steady-state curve for oil 2 after 1 h of aging



thixotropic behavior has received varied definitions along history. For instance, *The Oxford Encyclopedic Dictionary of Physics* (Thewlis 1962) says:

Certain materials behave as solids under very small applied stresses but under greater stresses become liquids. When the stresses are removed the material settles back into its original consistency. This property is particularly associated with certain colloids which form gels when

left to stand but which become sols when stirred or shaken, due to a redistribution of the solid phase.

In this manuscript, we present a study on the rheological behavior and the attempt on modeling two commercial gelled waxy crudes. First, there is a full rheological characterization of the oils. Second, we show an attempt to predict the data with an elasto-viscoplastic thixotropic model proposed by de Souza Mendes and Thompson (2013), and finally, as the

Fig. 3 Stress sweep curve for oil 1 at 1 Hz without aging time

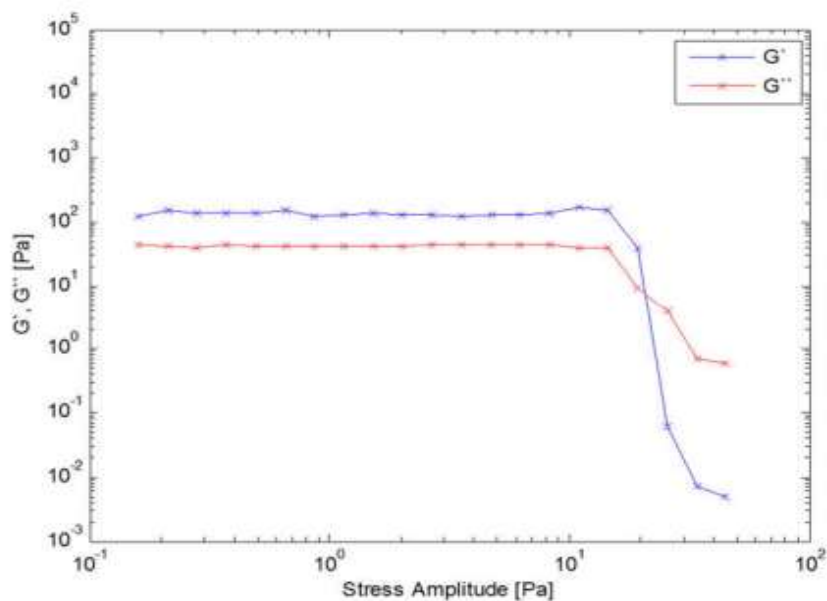
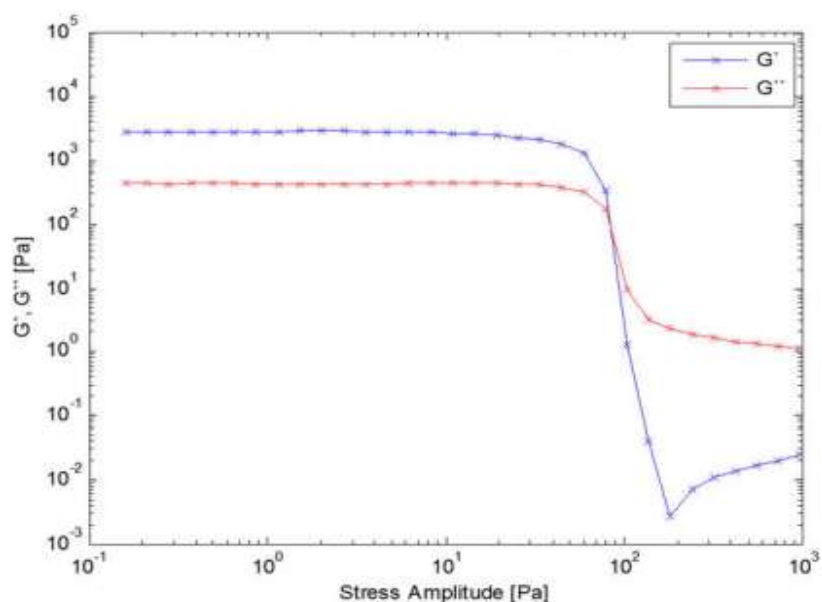


Fig. 4 Stress sweep curve for oil 2 at 1 Hz without aging time



model could not predict the data, we modified one equation, which produced satisfactory results.

Rheological characterization

Two waxy crude oil samples were used in this study (oil 1 and 2). They are oil samples that have been stabilized to eliminate, from the results, the impact of light ends. The difference between them is the weight percentages of high molecular

weight n-paraffins, approximately 5 and 10 %, for oil 1 and oil 2, respectively.

Test procedure

All experiments were performed in a controlled-stress rheometer (MARS III from HAAKE GmbH), using a cone and plate geometry with a diameter of 60 mm and a cone angle of 1°. Luthi (2013) showed that this geometry could be used because the size of paraffin crystals are reasonably smaller (2 μm) than

Fig. 5 Constant shear rate flow for oil 1 and 1 h of aging time

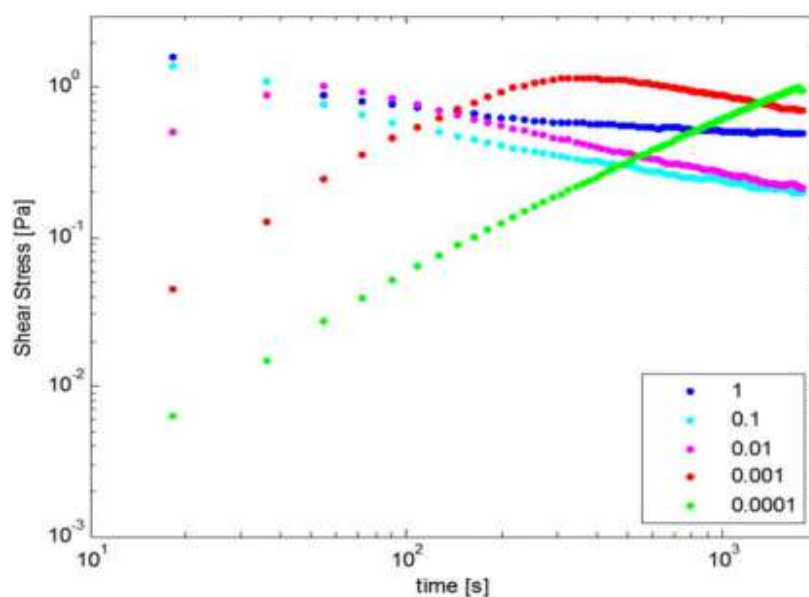
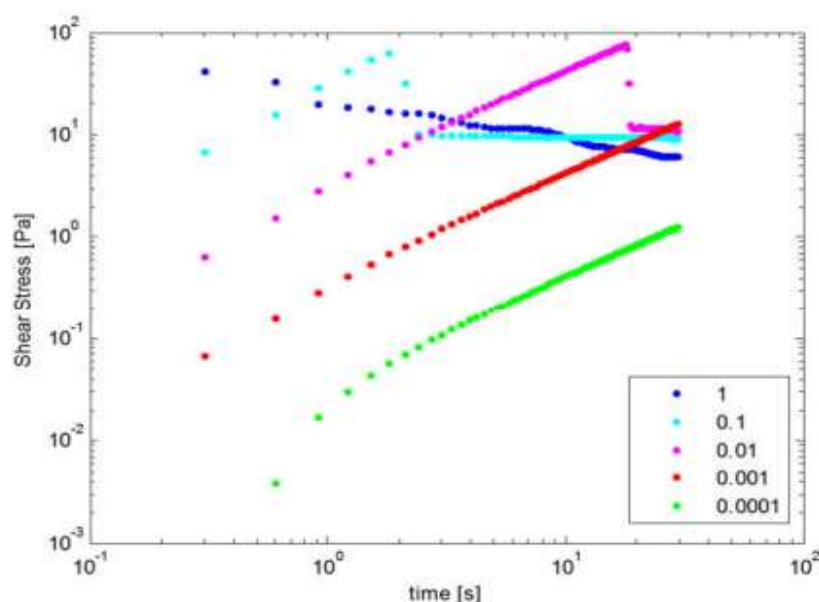


Fig. 6 Constant shear rate flow for oil 2 and 1 h of aging time



the gap (0.052 mm); thus, the results are independent from crystal size. Sample's temperature and cooling rate were controlled using the rheometer Peltier plate. The gap was adjusted with the thermogap option, which means that as the fluid shrinks, the rheometer would decrease the size of the gap to keep in touch with the fluid surfaces.

The initial procedure was adopted for all rheological analysis: We preheated the samples in a closed bottle to 70 °C and maintained at that temperature for 2 h. This

step ensured a stable chemical composition and achieved, therefore, reproducibility of the data. At 70 °C, the oil temperature is above of wax appearance temperature (WAT), determined by differential scanning calorimetry (DSC). Samples were then put in the rheometer, kept at 70 °C and at a shear rate of 10 s⁻¹ for 10 min to erase thermal history effects. Finally, the samples were cooled statically to 5 °C at a rate of 1 °C/min and left at rest for aging times of 1, 5, and 24 h.

Fig. 7 Thixotropic loop for oil 1

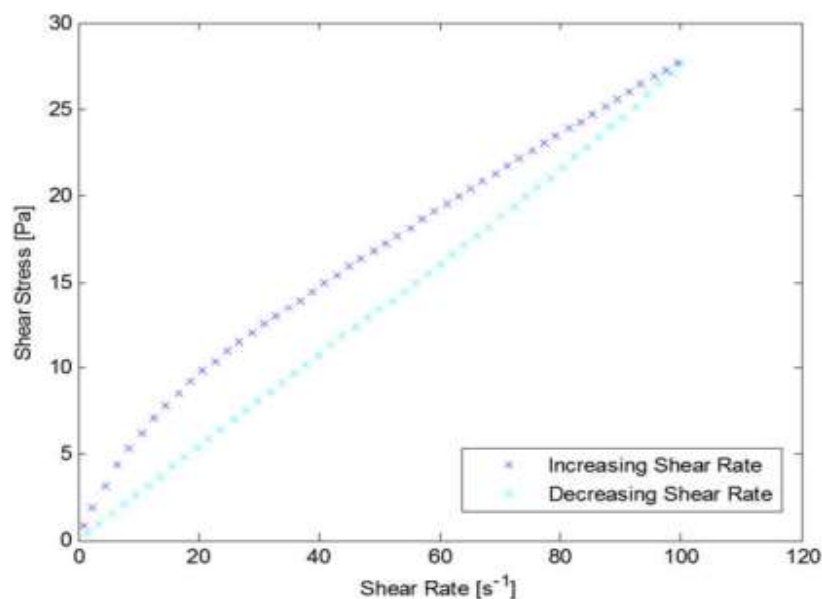
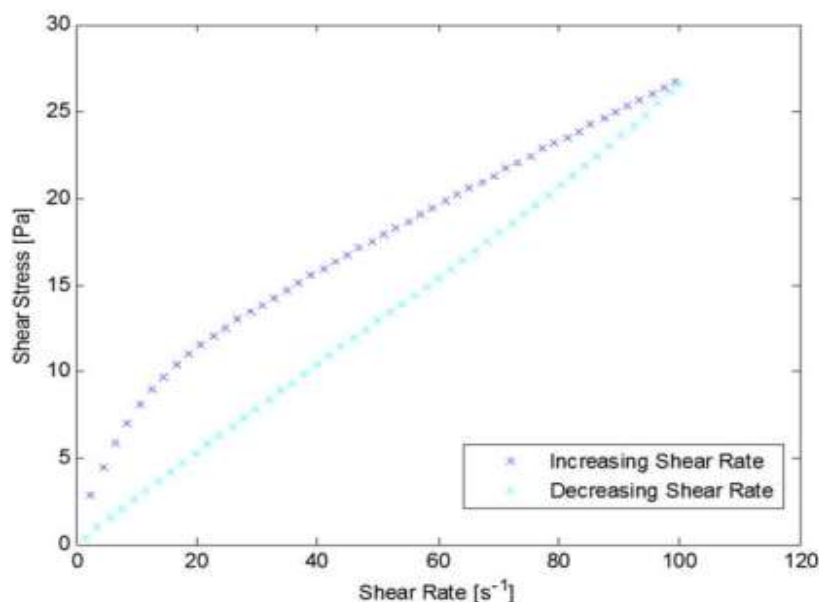


Fig. 8 Thixotropic loop for oil 2

Flow curve

This result represents the steady-state shear stress and viscosity as a function of the shear rate. Figures 1 and 2 display the experimental data after 1 h of aging for oil 1 and oil 2, respectively. The data was obtained in triplicate, with accuracy.

In both experiments, it is possible to see what looks like an elastic behavior before the yield stress. Barnes and Walters (1985) argued that a material that appears to have a yield stress, if you have the technology or the time to apply the stress for long enough time, you will actually see a deformation of the material. After the apparent yield stress is reached, it is possible to verify the viscoplastic behavior of Herschel-Bulkley for both the oils.

Oscillatory flow

The oscillatory test is a classic way to quantifying the behavior of viscoelastic materials, by verifying the elastic (linear region) response of the material.

After samples had reached 5 °C, oscillation stress sweep was performed at 1 Hz, applying stress values ranging from 0.01 to 1000 Pa. Figures 3 and 4 show the results of oil 1 and oil 2, respectively.

This test allows verifying the storage modulus, the loss modulus during the elastic region. The elastic shear stress and the static shear stress in the yielding region (Chang et al. 1998).

Constant shear rate flow

Applying a constant shear rate will result in an overshoot stress followed by decay towards the steady-state value. This decay can be abrupt or gradual, depending on the amount of wax and the kind of failure that is happening. For higher aging time, the stress overshoot is greater because the gel is more structured and rigid and a delay time is observed to break up the gel in comparison with aging the time 1 h.

Both crudes behave similarly. Figures 5 and 6 show the result for oil 1 and oil 2, respectively. The higher stress required by oil 2 can be explained by the fact that this crude has higher paraffin content than oil 1. A time-independent fluid would exhibit constant shear stress for every shear rate.

Before the overshoot, the fluid behaves elastically. The overshoot is usually caused by the thixotropic behavior, because the microstructure starts to break down and a fluid with massive viscosity starts to flow.

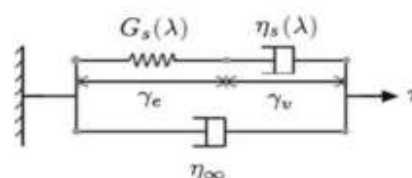
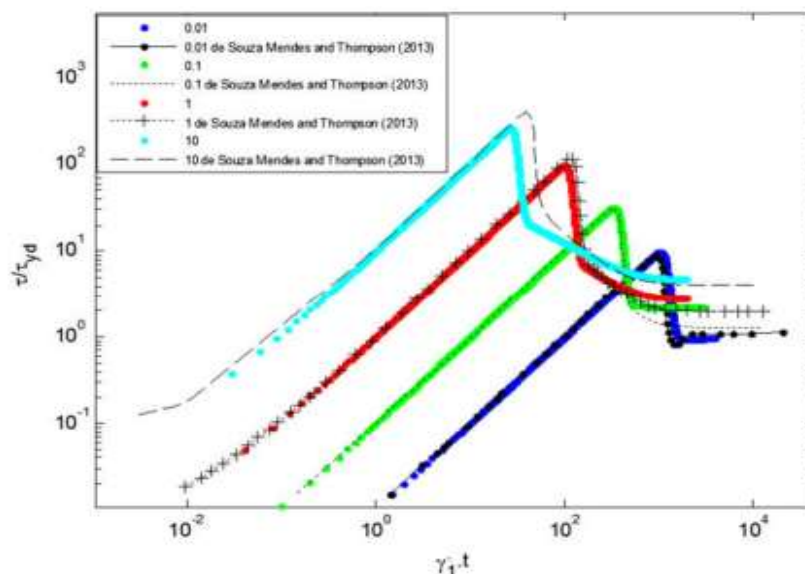
**Fig. 9** Physical analogy of de Souza Mendes and Thompson's (2013) model

Fig. 10 Time evolution of stress for constant shear-rate flows; comparing results of de Souza Mendes and Thompson (2013) with the Euler's method used in this manuscript



Thixotropic loop

One way to quantify the thixotropy is to verify the hysteresis of the material. A thixotropic loop is an experiment that measures the stress while the shear rate rises and decreases.

After the samples reached 5 °C in the rheometer, a shear rate of 1 s⁻¹ was applied for 60 s and then increased to 100 s⁻¹ and immediately decreased to 1 s⁻¹.

The result of this experiment is similar to the flow curve; the difference is that the structure was destroyed by applying 1 min of shear rate before starting to measure. That is why there is no yield stress in the beginning of the experiment.

The existence of hysteresis for both oils is clear as indicated in Figs. 7 and 8, which represents a thixotropic behavior. One of the ways to quantify the thixotropy is to calculate the area inside the loop.

Fig. 11 Steady-state shear stress curves and Herschel-Bulkley simulation for oil 1

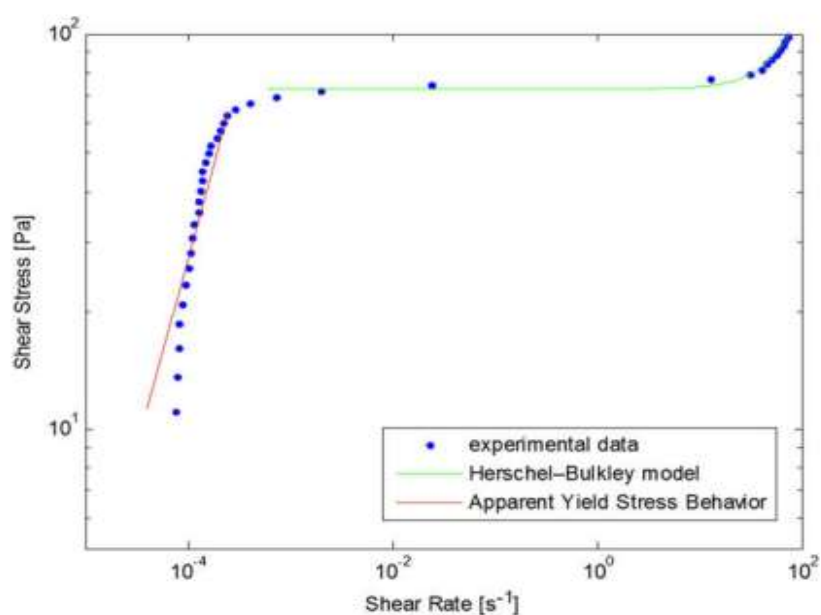
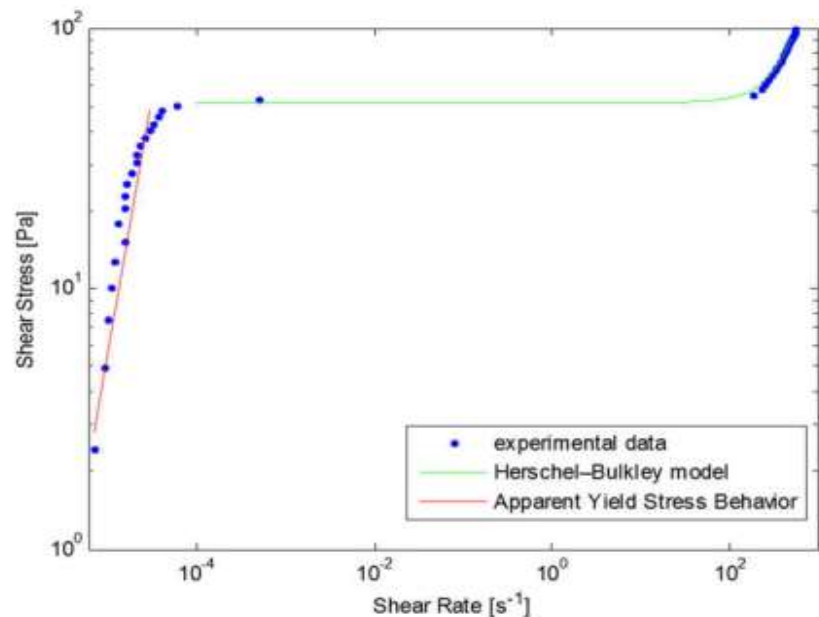


Fig. 12 Steady-state shear stress curves and Herschel-Bulkley simulation for oil 2



Rheological models

With the results presented in the last section, it is possible to verify that gelled crudes have complex rheological behavior. The flow curves show an apparent yield stress. Oscillatory test shows a change on the behavior from solid-like to liquid-like. The dynamic curves with constant shear rate show an overshoot of the stress. Finally, the thixotropic loop shows a change on the viscosity with time.

Many models in the literature try to predict complex behavior including thixotropy, elasticity, and plasticity (Slibar and Paslay 1963; Tiu and Boger 1974; Toorman 1997; Chang et al. 1999; Dullaert and Mewis 2005; Dullaert and Mewis 2006; Mewis and Wagner 2009; de Souza Mendes 2011; de Souza Mendes and Thompson 2013). There are a few reviews on those models (Mewis 1979; Barnes 1997, 1999; Mujumdar et al. 2002; de Souza Mendes and Thompson 2012). The Dullaert and Mewis (2005) and de Souza Mendes and Thompson

(2013) are among the most common ones. We used the model of de Souza Mendes and Thompson (2013) in this study because it has a plausible physical explanation based on a mechanical analog and possesses an equation for the structure parameter dependent on shear stress, while the structure parameter equation of Dullaert and Mewis (2005) is dependent only on the shear rate.

In fact, the structure should mainly depend on shear stress. This argument can be illustrated through the following example: If a small stress is applied to a structured oil, it will undergo a strain. If it stays within the elastic behavior, then once the stress stops, the oil should restructure. If, on the other hand, the applied stress stays long enough, the structure could reach a point where it starts to break down, and the yield stress itself decreases. Then, and only then, a fluid-like behavior is observed, giving rise to shear rate. That is why the model of Dullaert and Mewis cannot predict constant shear stress experiments.

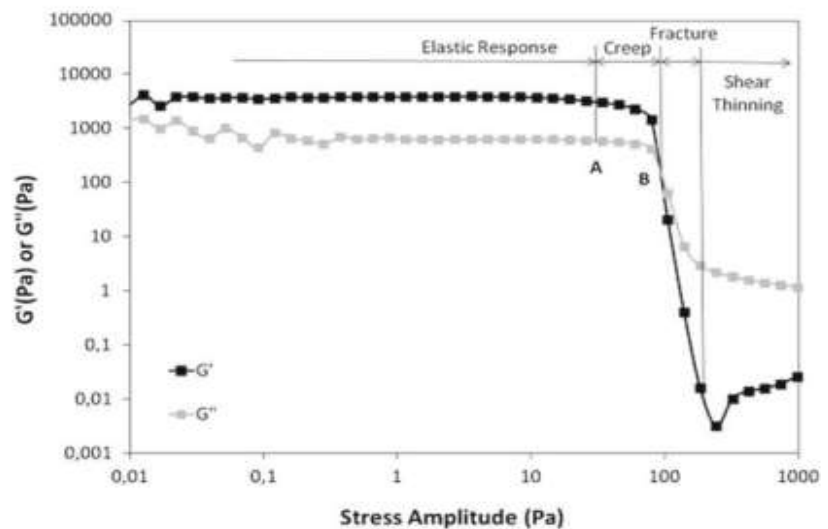
Table 1 Parameters obtained from steady-state test, oil 1

Parameters	Values	Units
K (Herschel-Bulkley)	2.110^{-2}	Pa. s ⁿ
n (Herschel-Bulkley)	1.7	—
η_0	10^5	Pa. s
τ_{yd}	0.2	Pa
$\dot{\gamma}_{yd}$	6.10^{-4}	s ⁻¹

Table 2 Parameters obtained from steady state test, oil 2

Parameters	Values	Units
K (Herschel-Bulkley)	0.3210^{-3}	Pa. s ⁿ
n (Herschel-Bulkley)	1.89	—
η_0	10^6	Pa. s
τ_{yd}	10	Pa
$\dot{\gamma}_{yd}$	10^{-4}	s ⁻¹

Fig. 13 Stress sweep curve for oil 2 at 1 Hz without aging time



The de Souza Mendes and Thompson (2013) model

Given that a full discussion of the generalization of classical rheological models is available elsewhere (de Souza Mendes and Thompson 2012), we only briefly describe here the physical understanding of this complex rheological model. The model is based on an analogy between the viscoelastic behavior and a mechanical analog with springs and dampers, as illustrated in Fig. 9. The solid-like behavior can be compared to a spring and the liquid-like behavior to dampers. When viscosity is at its highest point (oil fully structured), the rheological behavior is dominated by the spring-like component. When viscosity is low (no structure), the rheological behavior is dominated by the damper-like component, creating resistance to flow.

Parameter λ represents the structure of the gel network that the fluid generates below the pour point. This dimensionless parameter is common to all models that are considered as “indirect micro-structural approaches” (Mujumdar et al. 2002).

Typically, when a gel is fully structured, λ is equal to 1 and, as the gel loses structure and behaves more liquid-like, this value approaches zero. The model proposed by de Souza Mendes and Thompson, however, uses a different approach. They considered the fully structured fluid (λ_0) to depend on the initial and final viscosity. This is further described below.

Table 3 Parameters obtained from the oscillatory tests for oil 1

Parameters	Values	Units
η_{∞}	0.1	Pa. s
τ_y	8	Pa
G_0	100	Pa

With this structural dimensionless parameter, the model is able to account for the thixotropy, elasticity, plasticity, and viscous behavior of waxy oil. The next section lays out the main components of the model.

The constitutive equation comes from the description of the stress and strain in the system, as shown in Eq. (1).

$$\frac{\theta_2}{\eta_{\infty}} \left(\frac{\tau}{\theta_1} + \dot{\tau} \right) = (\dot{\gamma} + \theta_2 \ddot{\gamma}) \quad (1)$$

Equation (1) relates the stress τ , the derivative of stress versus time $\dot{\tau}$, with the shear rate $\dot{\gamma}$ and the derivative of shear rate versus time $\ddot{\gamma}$. There are two new terms relaxation time (θ_1) and retardation time (θ_2). Equations (2) and (3) are their respective mathematical definitions (de Souza Mendes 2011).

$$\theta_1 = \left(1 - \frac{\eta_{\infty}}{\eta_v(\lambda)} \right) \frac{\eta_v(\lambda)}{G_s(\lambda)} \quad (2)$$

$$\theta_2 = \left(1 - \frac{\eta_{\infty}}{\eta_v(\lambda)} \right) \frac{\eta_{\infty}}{G_s(\lambda)} \quad (3)$$

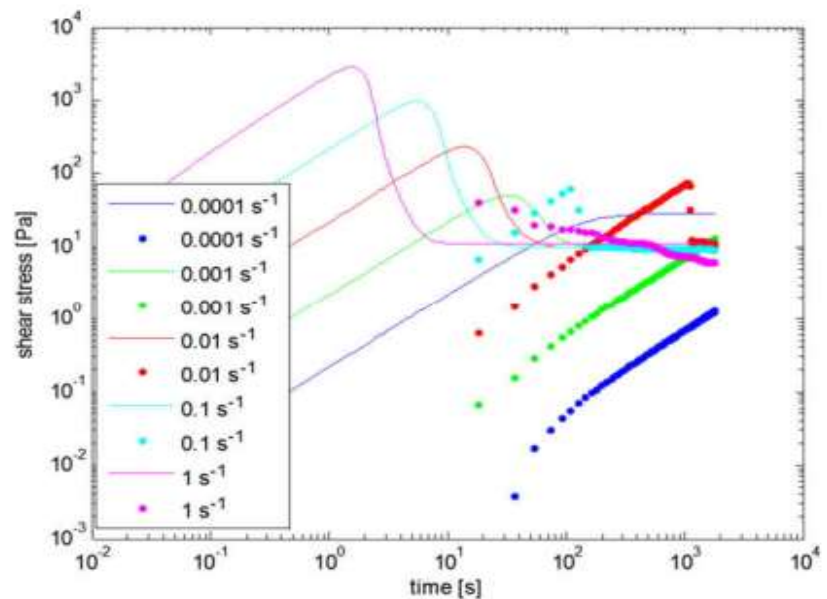
1) The structural elastic modulus function

Parameter $G_s(\lambda)$ is defined as the shear modulus. It is related to the storage modulus (G_0), and it represents the

Table 4 Parameters obtained from the oscillatory tests for oil 2

Parameters	Values	Units
η_{∞}	1.05	Pa. s
τ_y	122	Pa
G_0	2200	Pa

Fig. 14 Experimental and simulation of oil 2 using the empirical parameters by de Souza Mendes and Thompson (2013)



“variation of the elastic constant factor” of the spring. m is an empirical parameter.

$$G_s = G_0 e^{m \left(\frac{1}{\lambda} - \frac{1}{\lambda_0} \right)} \quad (4)$$

2) The structural viscosity function

The η_s is the structural viscosity, represented by a function of the viscous response of the microstructure. The last physical term in Fig. 9 is η_∞ , representing purely viscous behavior (i.e., $\lambda=0$). It is necessary to represent the fact that when $G_s \rightarrow \infty$, a purely viscous behavior has been attained. At such conditions, viscosity is calculated as $\eta_v = \eta_s + \eta_\infty$.

In Eq. (5), there is a correlation of structural viscosity function with the structure parameter λ and the purely viscous component η_∞ . A full discussion of the physical meaning can be found elsewhere (de Souza Mendes and Thompson 2013).

$$\eta_v(\lambda) = \eta_\infty e^\lambda \quad (5)$$

The next phenomenon to be described is the equilibrium state, also known as steady state. Such a state arises when buildup and breakdown rates are equal. The flow curve is the result of achieving this point for each shear rate. Equation (6) shows the equilibrium structure parameter.

$$\lambda_{eq} = \ln \left(\frac{\eta_{eq}}{\eta_\infty} \right) \quad (6)$$

The domain of the viscosity $\eta_v(\lambda) \rightarrow [\eta_\infty, \eta_0]$ is directly proportional to the structure parameter $\lambda \rightarrow [0, \lambda_0]$. Hence, it

is possible to define the initial structure parameter that has been discussed earlier, shown in Eq. (7).

$$\lambda_0 = \ln \left(\frac{\eta_0}{\eta_\infty} \right) \quad (7)$$

Finally, Eq. (8) describes the variation of the viscosity in steady state. This equation is used later to match experimental data.

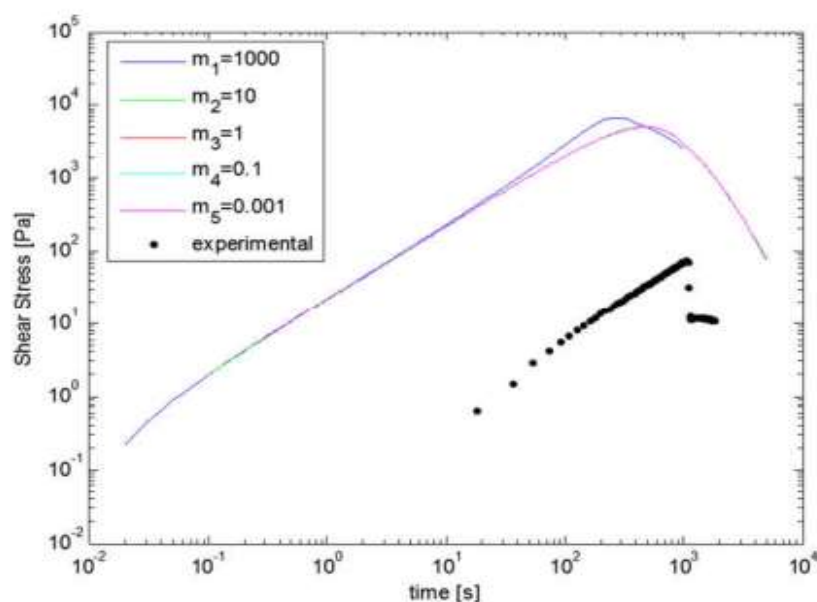
$$\eta_{eq}(\dot{\gamma}) = \left(1 - e^{-\frac{\tau_y}{\dot{\gamma}}} \right) \left(\frac{\tau_y - \tau_{yd}}{\dot{\gamma}} e^{-\frac{\tau_y}{\dot{\gamma}}} + \frac{\tau_{yd}}{\dot{\gamma}} + K \dot{\gamma}^{n-1} \right) + \eta_\infty \quad (8)$$

There are a number of variables in this equation yet to be explained. They are related to the steady state. The τ_y is the static limit of the stress. That is to say, it is the point at which the fluid will stop behaving like a solid and start behaving like a liquid. The second parameter is τ_{yd} , the dynamic stress, which is the shear stress caused by the flow after the structure has been totally degraded. The point of transition from τ_y to τ_{yd} is $\dot{\gamma}_{yd}$, which is the shear rate that represents the change from the solid-like behavior to the liquid-like behavior,

Table 5 Empirical parameters reported in de Souza Mendes and Thompson (2013)

Parameters	Values	Units
m	1	—
a	1	—
b	1	—
t_{eq}	100	s

Fig. 15 Analysis of the influence of the empirical parameter m for the shear rate of 0.01 s^{-1}



where the viscous behavior is dominant. That does not mean that the structure is completely destroyed, only that the viscous flow becomes predominant.

The last two parameters k and n are related to the classical viscoplastic model of Herschel-Bulkley (Herschel and Bulkley 1926). k represents the apparent viscosity and n the power-law term of the rheological behavior.

3) The structure parameter

Equation (10) represents the approach to the structure parameter, where t_{eq} is the characteristic time. The first term on the right-hand side is the structure buildup and the second term the break-down. Equation (11) is the final equation presented by de Souza Mendes and Thompson (2013).

Fig. 16 Analysis of the influence of the empirical parameter a for the shear rate of 0.01 s^{-1}

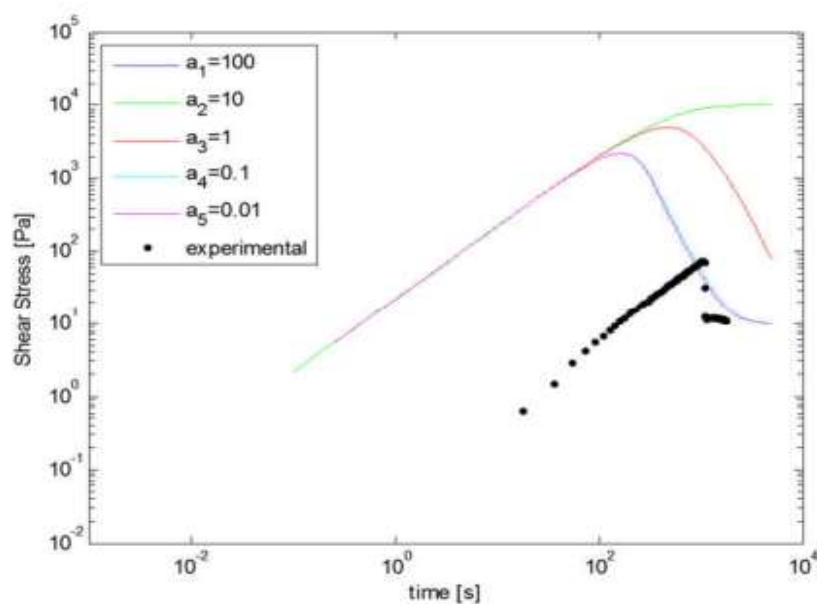
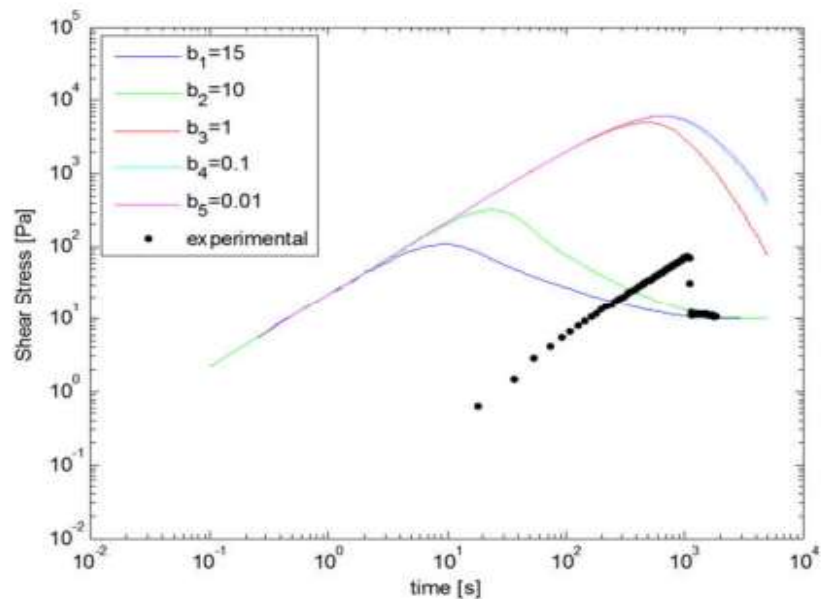


Fig. 17 Analysis of the influence of the empirical parameter b for the shear rate of 0.01 s^{-1}



$$\frac{d\lambda}{dt} = \frac{1}{t_{eq}} \left(\left(\frac{1}{\lambda} - \frac{1}{\lambda_0} \right)^a - f(\tau) \lambda^b \right) \quad (9)$$

$$\frac{d\lambda}{dt} = \frac{1}{t_{eq}} \left[\left(\frac{1}{\lambda} - \frac{1}{\lambda_0} \right)^a - \left(\frac{\lambda}{\lambda_{eq}(\tau)} \right)^b \left(\frac{1}{\lambda_{eq}(\tau)} - \frac{1}{\lambda_0} \right)^a \right] \quad (10)$$

Numerical solution

Euler's numerical method was used to solve the differential equations. First, to validate the algorithm, the simulation was made with the parameter values described in de Souza Mendes and Thompson (2013). Figure 10 shows a dimensionless curve that represents the time evolution of stress for

Fig. 18 Analysis of the influence of the empirical parameter t_{eq} for the shear rate of 0.01 s^{-1}

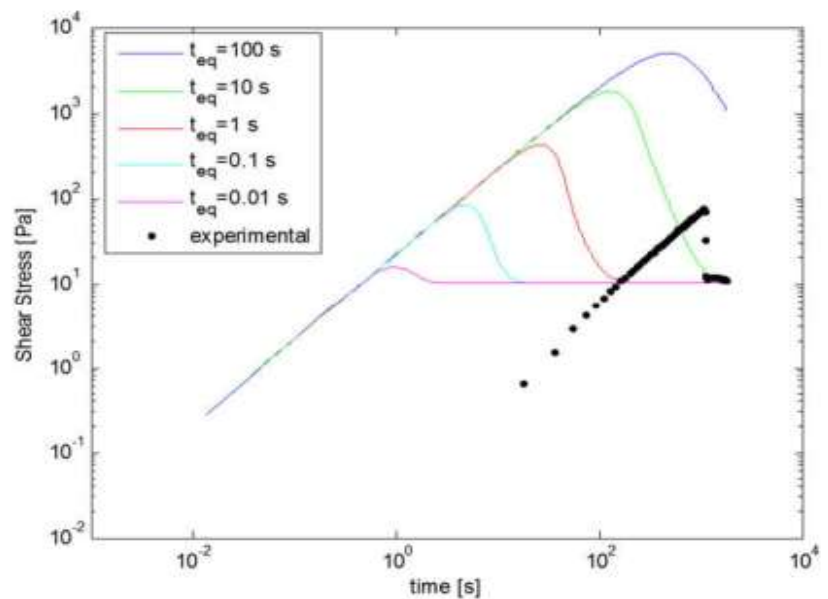
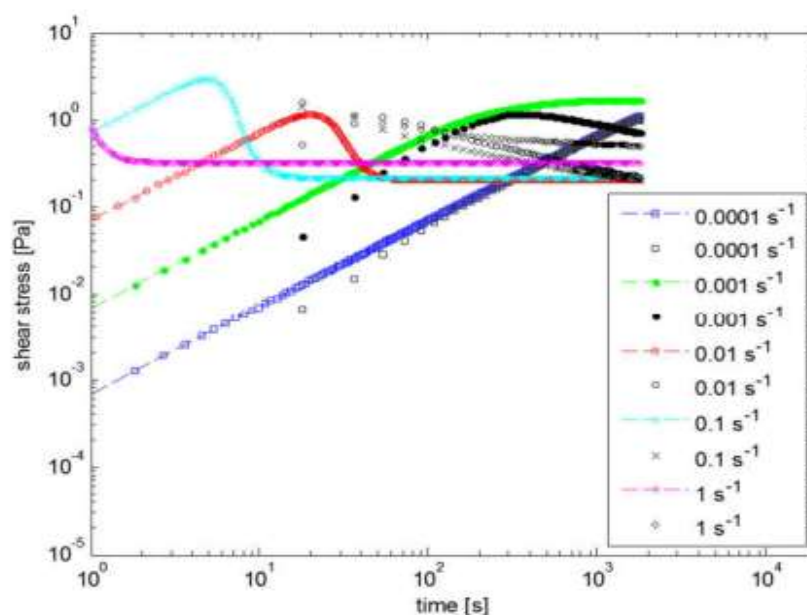


Fig. 19 Stress evolution for oil 1 and 1 h of aging time, for breakdown experiments



constant shear rates. The dimensionless time has a specific shear rate defined by de Souza Mendes (2009) which represents the beginning of the power law region in a steady-state curve. The difference for small shear rate is almost none. Thus, the algorithm was considered to be coherent and subsequently applied during the analysis described in the sections that follow.

Rheological parameters

Figures 11 and 12 show the experimental results and Herschel-Bulkley fit. Finally, the curves show the simulation of a Newtonian fluid with very high viscosity, which is a feature of an apparent yield stress material. Tables 1 and 2 report the parameters obtained. All the parameters were obtained with the least square method.

At this point, it is worth pointing out that the steady-state curve is not a stable curve. It has been discussed in other studies (Chang et al. 1998; de Souza Mendes 2009) and been experimentally proven for these oils on Luthi (2013) that is why the rest of the parameters are not obtained using this approach. Oscillatory tests are more reliable (see Fig. 13),

and they were carried out to obtain the parameters of the model, as discussed by Chang et al. (1998), de Souza Mendes (2009), and Luthi (2013).

A and B are the transition points. Point B is the static limit, defined as τ_y . Storage modulus is the plateau value for G' in Fig. 13, which is mathematically defined in Eq. (12). Final viscosity η_{∞} can be obtained from Eq. (13) by the classic loss modulus.

$$\lim_{\lambda \rightarrow \lambda_0} G' = G_0 \quad (11)$$

$$\lim_{\lambda \rightarrow \lambda_0} G'' = \omega \eta_{\infty} \quad (12)$$

These tests were carried out for both oil samples for several aging times. The results for oil 1 and oil 2 for 1 h of aging are shown in Tables 3 and 4, respectively.

Comparison model versus experiments

After the parameters with physical meaning have been obtained, it is necessary to obtain the empirical ones. The least

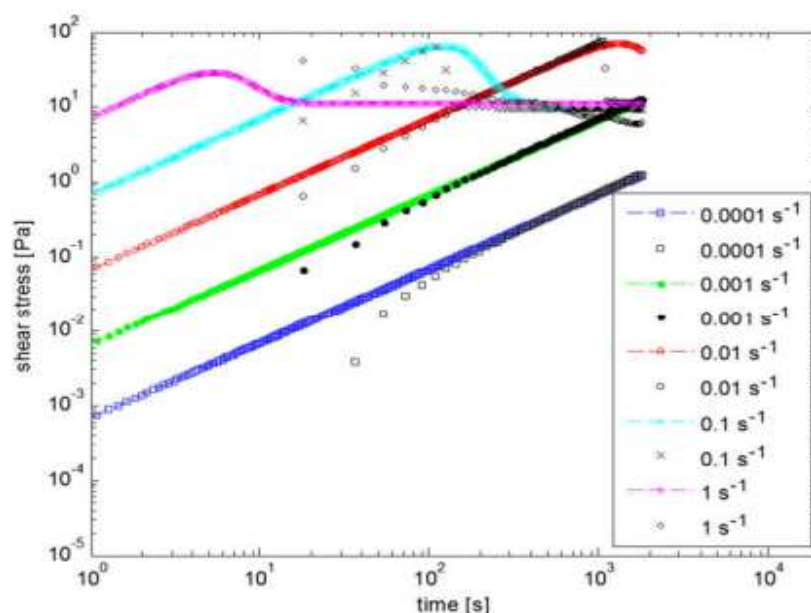
Table 6 Empirical parameters from the transient experiments for oil 1 and 1 h of aging time

Parameters	Values	Units
m	14.29	—
a	1.2	—
b	1.2	—
t_{eq}	0.41	s

Table 7 Empirical parameters from the transient experiments for oil 2 and 1 h of aging time

Parameters	Values	Units
m	314.19	—
a	3	—
b	3	—
t_{eq}	0.41	s

Fig. 20 Stress evolution for oil 2 and 1 h of aging time, for breakdown experiments



square method was applied to the transient experiments. The main problem is that the model cannot reproduce the experimental data with accuracy. As shown in Fig. 14, in the test of constant shear rate, the variation of the shear stress with time has—regardless of the range of the empirical parameters—a delay from the data to the model.

Figure 14 compares the experimental results with the simulation ones, for empirical parameters equal to the ones reported in the literature by de Souza Mendes and Thompson (2013). The values of the empirical parameters are shown in Table 5.

Empirical parameters

A sensitivity analysis was performed covering a large domain of each parameter to show that the empirical parameters could

Table 8 Stress overshoot error comparing the simulation with the experimental data for oil 2

Stress overshoot				
Shear rate (s^{-1})	Experimental (Pa)	Model (Pa)	Error (Pa)	Error %
1	42.11	28.50	13.62	47
0.1	63.55	65.40	1.85	2.8
0.01	77.13	69.93	7.20	10.3
0.001	13.08	12.49	0 ^a	0 ^a
0.0001	1.29	1.25	0 ^a	0 ^a

^a For shear rates of 0.001 and 0.0001 the stress overshoot was not reached, neither in the experiment nor in the model, that is why there is no error

not reproduce the experimental data. Figures 15, 16, 17, and 18 show the impact of each parameter on the results for a shear rate of $0.01 s^{-1}$. The other parameters were kept constant at the values displayed in Table 5.

None of the empirical parameters delays the whole curve to fit the experimental data. This occurs because none of them directly influences the elastic behavior.

Modification of the model

We propose to modify the model by adding another empirical parameter in the elastic term; in this way, the trend would be maintained, and the shear stress slope could change with time.

This generalization does not disrupt the physical meaning of the equation for the following reason: Although it is no longer the only parameter, the elastic behavior is still directly

Table 9 The error of the time to reach the overshoot of the simulation with the experimental data for oil 2

Time to reach the overshoot				
Shear rate (s^{-1})	Experimental (s)	Model (s)	Error (s)	Error %
1	18	15.31	2.69	14.9
0.1	108	130.15	22.15	20.5
0.01	1062	1,334.3	272.35	25.6
0.001	1782	1782	0 ^a	0 ^a
0.0001	1782	1782	0 ^a	0 ^a

^a For shear rates of 0.001 and 0.0001 the stress overshoot was not reached, neither in the experiment nor in the model, that is why there is no error

Table 10 Empirical parameters from the transient experiments for oil 2 and 5 h of aging time

Parameters	Values	Units
m	619	–
a	3	–
b	3	–
t_{eq}	0.41	s

proportional to the storage modulus, but the relation between the variation of the structure parameter and the variation of the elastic response is not representable by the initial formulation. In other words, the spring constant has decreased, and the elastic response to stress is not as strong as proposed by de Souza Mendes and Thompson (2013).

The most generic solution would be to add one parameter, resulting in Eq. (14).

$$G_s = \left(\frac{G_0}{m_{new}} \right) e^{m_{old} \left(\frac{1}{\lambda} - \frac{1}{\lambda_0} \right)} \quad (13)$$

In our case, the influence of parameter m_{old} can be held by parameters a and b , as can be seen in Figs. 15, 16, and 17 and we simply reformulate Eq. (13), removing parameter m_{old} . The result can be seen in Eq. (14). This has been done because one of the main comparisons about all the models is how many empirical parameters they have. One of the best aspects about the model proposed by de Souza Mendes and Thompson (2013) is the reduced number.

$$G_s = \left(\frac{G_0}{m} \right) e^{\left(\frac{1}{\lambda} - \frac{1}{\lambda_0} \right)} \quad (14)$$

All the equations of the modified Souza Mendes and Thompson model are summarized here for better visualization.

$$\frac{\theta_2}{\eta_{\infty}} \left(\frac{\tau}{\theta_1} + \dot{\tau} \right) = (\dot{\gamma} + \theta_2 \cdot \ddot{\gamma}) \quad (1)$$

$$\theta_1 = \left(1 - \frac{\eta_{\infty}}{\eta_v(\lambda)} \right) \frac{\eta_v(\lambda)}{G_s(\lambda)} \quad (2)$$

$$\theta_2 = \left(1 - \frac{\eta_{\infty}}{\eta_v(\lambda)} \right) \frac{\eta_{\infty}}{G_s(\lambda)} \quad (3)$$

$$G_s = \left(\frac{G_0}{m} \right) e^{\left(\frac{1}{\lambda} - \frac{1}{\lambda_0} \right)} \quad (14)$$

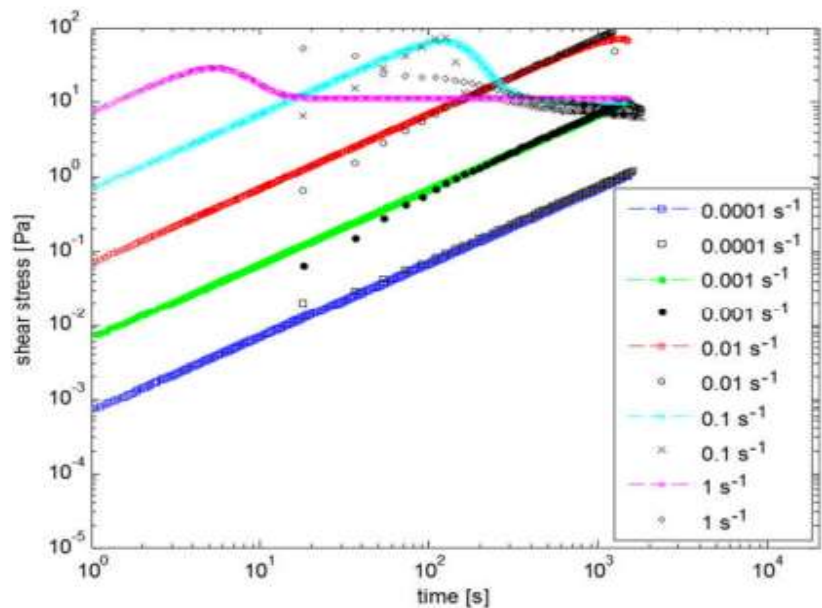
$$\eta_v(\lambda) = \eta_{\infty} e^{\lambda} \quad (5)$$

$$\lambda_{eq} = \ln \left(\frac{\eta_{eq}}{\eta_{\infty}} \right) \quad (6)$$

$$\lambda_0 = \ln \left(\frac{\eta_0}{\eta_{\infty}} \right) \quad (7)$$

$$\eta_{eq}(\dot{\gamma}) = \left(1 - e^{-\frac{\tau_0}{\dot{\gamma}}} \right) \left(\frac{\tau_y - \tau_{yd}}{\dot{\gamma}} e^{-\frac{\tau_y}{\dot{\gamma}}} + \frac{\tau_{yd}}{\dot{\gamma}} + K \dot{\gamma}^{n-1} \right) + \eta_{\infty} \quad (9)$$

$$\frac{d\lambda}{dt} = \frac{1}{t_{eq}} \left[\left(\frac{1}{\lambda} - \frac{1}{\lambda_0} \right)^a - \left(\frac{\lambda}{\lambda_{eq}(\tau)} \right)^b \left(\frac{1}{\lambda_{eq}(\tau)} - \frac{1}{\lambda_0} \right)^a \right] \quad (11)$$

Fig. 21 Stress evolution for oil 2 and 5 h of aging time, for breakdown experiments

Results and discussion

After the algorithm with the new equation is developed, the results are more coherent with the experimental data. Figure 19 shows that all the elastic behavior is better predicted by the modeling. The final shear stress is also predicted. The main point is the prediction of the overshoot.

The values of the empirical parameters were calculated by the least square method with the data of the experiment with shear rate of 0.01 s^{-1} ; once the parameters were calculated, we simulated the results with the other shear rates. The final results can be seen in Table 6 and Fig. 19 for oil 1 and Table 7 and Fig. 20 for oil 2.

After the elastic and the dynamic shear stress are calculated with good accuracy, the next goal is to see how accurate the model can predict the overshoot point. Table 8 shows the error for oil 2. Table 9 shows the error of the time necessary to reach the maximum stress, where the solid-like behavior turns liquid-like.

The error goes up as the shear rate rises. This happens because the empirical parameters were calculated with a shear rate of 0.01 s^{-1} and used in the simulation of all the other shear rates. To decrease the error, we should calculate the empirical parameters for each curve of constant shear rate.

The idea is a procedure for the industry; we want to verify if it is possible to do only one kinetic test and be able to predict the behavior of the gelled crude. The error rises as the difference between the actual shear rate and the one used to calculate the empirical parameter rises. For the industry, when trying to simulate the restart, the results we obtained are reasonable, since the shear rate's domain of the problem is up to 0.1 s^{-1} .

The model's idea is to simulate the oil's behavior independently of aging time. Hence, once the empirical parameters were calculated (a , b , t_{eq}), they were not modified, even if that generated a high error. The only one that could not be kept constant was m . But the ratio $\frac{G_0}{m}$ remained constant. In Table 10 and Fig. 21, we show the results for oil 2 for 5 h of aging time. The mean of the oscillatory test results is $G_0=4333 \text{ Pa}$.

We observed that independently of the oil and of the aging time, the result of the ratio of the storage modulus by the empirical parameter m is $\frac{G_0}{m} \approx 7$.

The same procedure was done for both oil samples for all the aging times, and the ratio was always the same. This is an unusual result, probably a coincidence, but it could also be evidence of constant for all waxy crudes. To ascertain that possibility, many more tests with different oil samples and other materials are needed.

Final remarks

Rheological studies with two commercial waxy crude oil samples were performed to verify and define their rheological behavior under yielding at low temperature. This subject is very important to restart of blocked subsea flowlines with gelled waxy crudes.

There are available physical models to represent and explain the rheology during yielding. The model applied in this paper is a modification of de Souza Mendes and Thompson (2013). The alterations proposed do not affect the physical meaning of the parameters, but fit better our experimental results.

The comparison of the proposed model versus experimental data shows an acceptable error when predicting the elastic phase of the flow and the final viscous flow (up to 15 % error for both oil samples, independent of aging time). The highest error occurred when simulating the value of the shear stress and the time dependence (35 % for oil 1 with 5 h of aging time).

The ratio of the storage modulus to the parameter m obtained is the same for both oil samples at all aging times. A possible explanation is that there might be a constant related to the paraffins that relates the “spring constant” with the variation of the structure parameter. To generalize this conclusion, more tests are needed using different oil samples, and aging times.

For practical use, this model can be implemented in a generic simulator to address restart conditions, as long as sufficient experimental information is available to quantify the parameters that are not universal.

Acknowledgments The authors would like to thank PRH-ANP and Repsol-Sinopec-Brazil, for the financial support to this work.

References

- Ajienka JA, Ikoku CU (1991) The effect of temperature on the rheology of waxy crude oils
- Barnes HA (1997) Thixotropy—a review. *J Non-Newtonian Fluid Mech* 70(1):1–33
- Barnes HA (1999) The yield stress—a review or ‘παντα ρει’—everything flows? *J Non-Newtonian Fluid Mech* 81(1):133–178
- Barnes HA, Walters K (1985) The yield stress myth? *Rheol Acta* 24(4):323–326
- Chang C, Boger DV, Nguyen QD (1998) The yielding of waxy crude oils. *Ind Eng Chem Res* 37(4):1551–1559
- Chang C, Nguyen QD, Rønningsen HP (1999) Isothermal start-up of pipeline transporting waxy crude oil. *J Non-Newtonian Fluid Mech* 87(2):127–154
- da Silva JAL, Coutinho JA (2004) Dynamic rheological analysis of the gelation behaviour of waxy crude oils. *Rheol Acta* 43(5):433–441
- Davidson MR, Dzuy Nguyen Q, Chang C, Rønningsen HP (2004) A model for restart of a pipeline with compressible gelled waxy crude oil. *J Non-Newtonian Fluid Mech* 123(2):269–280
- de Souza Mendes PR (2009) Modeling the thixotropic behavior of structured fluids. *J Non-Newtonian Fluid Mech* 164(1):66–75

- de Souza Mendes PR (2011) Thixotropic elasto-viscoplastic model for structured fluids. *Soft Matter* 7(6):2471–2483
- de Souza Mendes PR, Thompson RL (2012) A critical overview of elasto-viscoplastic thixotropic modeling. *J Non-Newtonian Fluid Mech* 187:8–15
- de Souza Mendes PR, Thompson RL (2013) A unified approach to model elasto-viscoplastic thixotropic yield-stress materials and apparent yield-stress fluids. *Rheol Acta* 52(7):673–694
- Dullaert K, Mewis J (2005) A model system for thixotropy studies. *Rheol Acta* 45(1):23–32
- Dullaert K, Mewis J (2006) A structural kinetics model for thixotropy. *J Non-Newtonian Fluid Mech* 139(1):21–30
- Herschel WH, Bulkley R (1926) Konsistenzmessungen von Gummi-Benzollösungen. *Kolloid Z* 39:291–300
- Lee HS (2008). Computational and rheological study of wax deposition and gelation in subsea pipelines. ProQuest
- Luthi IF (2013). Rheological characterization of a waxy crude oil and experimental study of the restart of a line blocked with gelled waxy crude. Campinas: Faculty of Mechanical Engineering, State University of Campinas, 124 p. Master Thesis
- Mewis J (1979) Thixotropy—a general review. *J Non-Newtonian Fluid Mech* 6(1):1–20
- Mewis J, Wagner NJ (2009) Thixotropy. *Adv Colloid Interf Sci* 147:214–227
- Mujumdar A, Beris AN, Metzner AB (2002) Transient phenomena in thixotropic systems. *J Non-Newtonian Fluid Mech* 102(2):157–178
- Phillips DA, Forsdyke IN, McCracken IR, Ravenscroft PD (2011a) Novel approaches to waxy crude restart: part 1: thermal shrinkage of waxy crude oil and the impact for pipeline restart. *J Pet Sci Eng* 77(3):237–253
- Phillips DA, Forsdyke IN, McCracken IR, Ravenscroft PD (2011b) Novel approaches to waxy crude restart: part 2: an investigation of flow events following shut down. *J Pet Sci Eng* 77(3):286–304
- Slibar A, Paslay PR (1963) Steady-state flow of a gelling material between rotating concentric cylinders. *J Appl Mech* 30(3):453–460
- Srivastava SP, Handoo J, Agrawal KM, Joshi GC (1993) Phase-transition studies in alkanes and petroleum-related waxes—a review. *J Phys Chem Solids* 54(6):639–670
- Thewlis J (1962) Oxford encyclopedia dictionary of physics
- Tiu C, Boger DV (1974) Complete rheological characterization of time-dependent food products. *J Texture Stud* 5(3):329–338
- Toorman EA (1997) Modelling the thixotropic behaviour of dense cohesive sediment suspensions. *Rheol Acta* 36(1):56–65
- Vinay G, Wachs A, Frigaard I (2009) Start-up of gelled waxy crude oil pipelines: a new analytical relation to predict the restart pressure. In: Asia Pacific Oil and Gas Conference & Exhibition. Society of Petroleum Engineers

**5. PAPER 5: INFLUENCE OF AGING IN EQUILIBRIUM TIME
OF GELLED WAXY CRUDE OIL IN RHEOMETER AND
PIPELINE**

INFLUENCE OF AGING IN THE EQUILIBRIUM TIME OF A GELLED WAXY CRUDE OIL IN RHEOMETER AND PIPELINE

Charlie Van Der Geest^{a)} Vanessa C. Bizotto Guersoni^{b)} Antonio Carlos Bannwart^{a)}

^{a)} *Department of Mechanical Engineering - University of Campinas. Campinas, São Paulo, Brazil.*

^{b)} *Center for Petroleum Studies - University of Campinas. Campinas, São Paulo, Brazil.*

Abstract

For this study, an experimental apparatus was built to investigate the phenomenon of flow start-up of gelled waxy crudes. The apparatus is composed of a cold-water bath and a pipeline inside it connected to two tanks. These tanks can be pressurized, which enabled us to study the pressure start-up and the transient flow during start-up. In this paper, we study the influence of aging on the flow start-up, both in a rheometer and in the experimental apparatus; we model the rheological behaviour with an elasto-viscoplastic thixotropic model and the restart of the pipeline with a weakly compressible fluid. Our experimental procedure diverges from those of most experiments in the literature. In these, the inlet pressure increases continuously until the flow starts, at which point, so the argument goes, the apparent yield stress has been reached. With that type of procedure, however, it is impossible to distinguish whether there was an overshoot due to the elastic response of the material. Thus, we propose a different type of procedure wherein a constant pressure is applied and the time until the flow restart is measured. The idea of the study is to isolate the influence of aging on the equilibrium time, an important variable that has yet to receive in the literature the attention it warrants. The comparison between model and experimental data sheds light on the phenomena involved in the restart of gelled waxy crudes.

1 INTRODUCTION

When producing waxy crude oils in offshore fields, oil producers deal with some severe and costly problems [1][2][3]. One of the worst of these occurs when there is a shutdown, for whatever reason, and the crude must remain at seabed. As the heat of the crude is transferred to the cold environment, the seabed temperature is 4°C, the crude lying in the pipeline cools. If the shutdown persists, the temperature of the oil can drop to the gelation temperature. This is the point at which severe financial problems can be incurred ([4]-[5]). Producers have in fact abandoned pipelines owing to their being blocked by gelled waxy crude. For safety reasons, the decision was to not restart the flow [6].

In the process of it cooling down, the crude oil passes through two critical temperature. First, it reaches the Wax Appearance Temperature (WAT), at which point wax molecules start to precipitate in the oil [7]. Second, it reaches the gelation point, also called the pour-point. This is when more molecules precipitate and aggregate and ultimately form crystalline structures ([8]-[11]). At the gelation temperature and below, the aggregation of wax crystals modifies the behavior of the oil, sometimes precluding it from flowing. This aggregation of

molecules is usually called a molecular matrix, and their characteristics are deeply influenced by the initial and boundary conditions that prevail during their formation [12].

Besides the starting and ending temperatures, the way that the oil cools down deeply affects the final molecular matrix within the gel. The final crystalline structure is shaped by a number of variables that impact the nucleation process, that is, the process by which crystals grow and interlock. When other variables are kept constant, the gel strength is directly proportional to the final temperature ([12]-[13]). The shear rate during cooling tends to decrease the strength of the structure [14]; also, the final molecular structure has been shown to also be influenced by the initial temperature [14]. Finally, one of the most studied variables is the cooling rate, both at quiescent condition or under shear rate, and this rate heavily influences the growth and gel matrix development, with the literature providing discrepant results ([15]-[16]).

As Mendes et al., (2016)[17] have pointed out, to understand and predict the restart pressure of the pipeline, we would have to simulate the condition of the pipeline during the shut-down and cooling. The structure with-in the gelled crude oil is completely heterogeneous both axially and radially due to the variables discussed before. In this study, however, we considered a homogeneous elasto-viscoplastic fluid throughout the pipeline, which might help explain the discrepancy in results shown further on.

The main goal of this study is concerned with another variable that influences the molecular structure, aging time. There are studies that have found that aging had no influence on the rheological properties [18]. Other studies have argued that the aging increases the storage modulus (G') ([10], [16]). In our previous study [28], we observed no influence on the storage modulus, but we did observe an influence on the equilibrium time. To further explore that observation, we decided to apply stresses higher than the yield stress and study the time necessary for the shear rate to rise. That method allowed us to validate the transient prediction of the rheological model.

Below the gelation temperature the oil has a time-dependent behavior and shows elastic, plastic, and viscous behaviors [19]. The rheological behavior of gelled waxy crudes has in fact been the subject of many studies ([16]-[29]). All the methods and procedures to study the rheological behavior are important, but when discussing start-up phenomenon there is one rheological property that is arguably the most important and that property is apparent yield stress ([1], [8]-[10]). Most studies use the apparent yield stress to study the influence of all the boundary and initial conditions discussed above.

Within the scientific community, debate continues regarding the definition and measurability of the yield stress ([30]-[38]). It is not our intention to discuss it, as more methods have been proposed to measure it than to measure any other rheological property [37]. We introduce it here because most experimental studies related to the flow start-up of gelled crudes have used the procedure of increasing the inlet pressure either constantly or in steps until restart occurs ([11], [12], [39], [40]). With few exceptions, like the study of Magda et al., (2013) [41].

The problem with a constant or step-wise increase is that it precludes the opportunity to verify whether the oil would have restarted with a lower inlet pressure. On the other hand, it is impossible to apply a small pressure and wait interminably to verify if the flow will restart. This is the same problem when trying to measure the yield stress in a rheometer. We thus decided to apply a high enough stress and to keep the boundary conditions constant in the rheometer (constant stress/ creep experiment) and in the pipeline (constant inlet and outlet pressure). We would then study the transient phenomena of the restart.

In this paper, we use the rheological parameters obtained and discussed in [28] to isolate a variable directly related to the transient response of the material; that variable is the equilibrium time. Equilibrium time can be thought of as the time necessary for the material to reach a steady state once submitted to a stress. In other words, the time necessary for the break down rate and the build-up rate to equalize.

When the crude cools down in a pipeline, the oil shrinks. Once it has, the voids created in the shrinking process does not necessarily fill, because the oil contains some crystals or crystalline matrix that preclude the flow [42]. Thus, it is also essential that we understand the volumetric phenomenon involved in the cooling down process, for that phenomenon causes the gelled crude to have a compressibility that cannot be disregarded when dealing with restart. Thus, recent attempts in modelling and simulating the restart consider the fluid to be weakly compressible [42], [43]. The mathematical solution we use in this paper is 1.5 dimensional, which was proposed by Oliveira and Negrao (2015) [43].

The ALFA research group has built algorithms to investigate flow assurance problems related to paraffin. Rheological behavior of gelled waxy crudes, start-up of a pipeline with gelled waxy crude and wax deposition under single phase. We will, from now on, call the predictions of these algorithms the ALFAWAX predictions.

In this manuscript, we compare the predictions of the ALFAWAX for start-up of a pipeline with gelled waxy crudes with experimental data. To do that and to compare with results from the literature we did a preliminary experiment. We increased the pressure continuously until the flow restarted. The idea was to verify whether we would observe an overshoot in the inlet pressure and, if so, by how much.

After we finished the preliminary study, in the final experiments we applied a step pressure almost instantly (0.2 s) and waited until the flow restarted. This was done because we would like to compare the simulation results with the experimental data, and a more reliable way to carry out the experiments is to apply a constant boundary condition. The idea of the procedure is to isolate the influence of the rheological behaviour, studying the transient behaviour of the material, instead of the transient momentum due to increasing pressure.

The contribution of this experiment is to validate the model and thereby help the industry in security issues by predicting the time necessary for constant pressure to restart the flow. It is possible to predict that time with a model that can consider the transient rheological behaviour and the conservation of momentum. With this experimental procedure, we are able to study not only whether the flow restarts but when it restarts and to then adjust the model to predict the time delay between applying pressure and the restart being initiated.

Let's suppose that an emergency occurs. Oil lies in the pipeline for a long time and the conditions generate a strong molecular matrix. The company concludes that they cannot, for security reasons, apply the necessary pressure to start the flow immediately. Without knowing the transient rheological behaviour, there is no way to know if the flow will restart when a lower pressure is applied. For the oil and the apparatus study in this paper, a pressure of approximately $P_{inlet} = 12 \cdot 10^5 \text{ Pa}$ was calculated as the pressure necessary to immediately restart the flow. Using a simplified momentum conservation, we did all the experiments with $P_{inlet} = 2.5 \cdot 10^5 \text{ Pa}$ and the flow, after some time, restarted in all of them.

2 EXPERIMENTAL PROCEDURE

To investigate gelled waxy crude oil's behaviour with reproducibility, it is necessary to erase both the thermal and shear history ([11]-[15]), or as Andrade *et al.*, [14] shows, create a new thermal and shear history by setting the initial temperature [14]. The next step is to control the cooling rate with accuracy once it has influenced the final structure to a great extent ([11], [15]). While this procedure limits the capacity of the experiment to represent a real case, it allows us to better understand the phenomenon.

2.1 Properties of the Oil

The first thing we present are the main results of the full characterization of the oil studied. The density was measured using an Anton Paar DMA 4500 Density Meter. The water content was measured by the Karl-Fischer method, using a Mettler Toledo T50 Titrator. The wax appearance temperature (WAT) was obtained by Differential Scanning Calorimetry (DSC) with a Q2000 TA Instruments calorimeter. The composition in saturates, aromatics, resins and asphaltenes were obtained using a SARA analysis. The quantification of wax was made by centrifugation of crude oil, using a Rotanta 460R centrifuge, at 4000 rpm (3756 G) below the pour point at 5°C. The properties are summarized in Table 1.

2.2 Rheological Tests

We used a controlled-stress rheometer MARS III from HAAKE GmbH with a cone and plate geometry having a diameter of 60 mm, 1 degree of angle, and truncation of 0.052 mm. The rheometer used the Peltier plate to control the temperature and cooling rate.

The pre-experimental procedure was to homogenize the sample by preheating it to 65°C and maintaining it at that temperature for 2 hours. Once the samples were in the rheometer, the Peltier plate controlled the temperature at 60°C and the rheometer applied a shear rate of 10 s^{-1} for 10 minutes to erase thermal history effects. Next, we cooled the sample down to 5°C at a rate of 1°C/min without shear rate and, finally, applied aging times of 1, 5, and 24 hours [28].

It is important to point out that we modified the experimental procedure of the rheometer when compared to the values obtained in the previous study. In the process of erasing the thermal and stress history, we had to follow different procedures. In the pipeline during the start-up procedure, we increased the temperature only up to 60°C out of security concerns for the facility. In our previous study, we used an initial temperature of 70°C; in this study, we took the rheological measurements at 60°C to better compare the results from the rheometer with the facility. In the simulation, however, we used the values obtained from that previous work for steady state. This approach is not ideal, but as shown by Andrade *et al.*, [14], if the temperature is above the critical temperature, then the final molecular structure is similar and so too is the rheological behaviour.

2.3 Start-Up Facility

An apparatus, shown in Figure 1, was built to study the restart of the flow of gelled waxy crudes. With this apparatus, it is possible to apply pressure at the inlet with nitrogen (green line). The apparatus is composed of two tanks connected through a pipeline. The experimental section (blue line) is fully instrumented and there is a water bath around it.

Before the water bath, the pipeline is covered in a resistance that controls its temperature (red line).

The phenomenon of gelation occurs inside the part of the pipeline (blue line) that is inside the water bath. With the water, we can control the temperature from 60°C to 5°C. This allows us to clean the pipeline once the experiment is finished and to repeat experiments by changing the water temperature.

With this setup, we eliminate one possible phenomenon that can interfere or influence the restart, the penetration of pressurized fluid into the gelled waxy crude. When dealing with restarts, the less viscous fluid tends to generate a plug and flow within the fluid it is pushing. In this case, we avoid that by pressurizing the tank, which has oil in the bottom. It is possible that the hot oil will generate the plug, but because the viscosity of the oil is high, that phenomenon has been disregarded.

The pipeline between the tanks is instrumented with the following: differential pressure gauges (Rosemount 3051) along the water bath, a pressure gauge in the inlet (Rosemount 2088), a temperature sensor along the pipeline (PT100 4 wires), and a Coriolis to measure the oil flow rate.

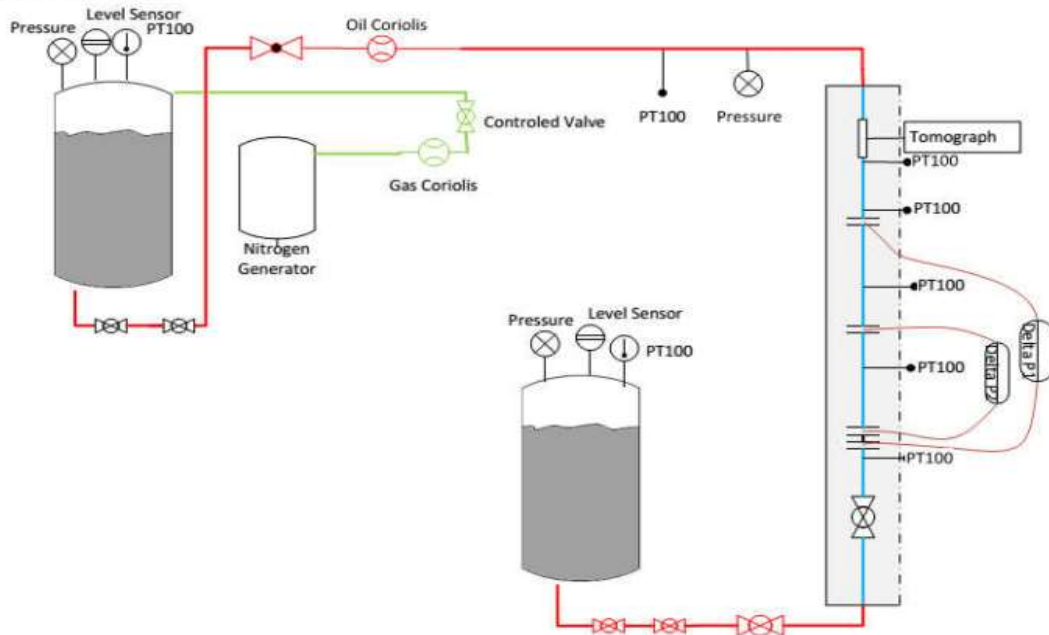


Figure 1. Layout of the experimental apparatus.

To erase the thermal and shear history, we kept the oil in a tank for two hours while stirring it at 60°C. With this procedure we could ensure good homogenization and dissolution of the crystals. The Wax Dissolution Temperature (WDT) of this oil is 46°C; some discussion of this can be found in Van Der Geest *et al.*, (2018) [44]. While we resolubilized the wax crystals in the oil we also kept the entire pipeline and the water at 60°.

Before discussing the experimental protocol, it is important to highlight one important point of all the experiments shown in this paper. They were all done with the tank that was not connected to the nitrogen system opened to the atmosphere. This means that as the pipeline was filled and during the aging, the system was under atmospheric pressure. This is

important because the influence of pressure during the cooling process can decrease the voids inside the crystalline matrix, thus changing the final compressibility of the gel. That influence of pressure was disregarded in these experiments, as the cooling down took place at atmospheric pressure.

Once the pre-procedure was done, we commenced the start-up test protocol. First, we filled the pipeline and waited until the level in both tanks was equalized. We then began decreasing the water temperature. Once the final temperature of 5°C was reached, the oil aged for the desired time. Finally, we applied the pressure and measured the time necessary until the restart.

At this point, another important point of discussion is necessary. The crystalline matrix that will form is completely dependent on the cooling rate that the oil is submitted to, as has been shown many times in the literature ([45]-[48]). Despite its potential interest, we did not investigate the influence of the cooling rate in the restart. Anyway, to ensure that we could compare the results from the rheometer to the results of the pipeline, we cooled the water down at 1 °C/min [49]. That cooling rate is faster than what happens in real fields. However, due to the time-consuming nature of the experiments and the time we had available in which to do them, that was the slowest rate we could afford.

When dealing with waxy crude oils, according to the literature, the reproducibility in the rheometer ranges from 15 to 30%, while in start-up experiments it ranges from 20% and 35% ([11], [14]-[15]). All of those errors are related to the pressure/stress and not to the time, which is even harder to reproduce due to the stochastic characteristic of the molecular matrix formation. For all experiments we have a time-to-restart error of 50%.

3 MATHEMATICAL MODEL

3.1 Rheological Model

The rheological model used in this manuscript was that proposed by Souza Mendes, and Thompson (2013) [38]. As a number of manuscripts have extensively described this model, we present it just briefly in the next section.

3.1.1 Steady State Equation

This equation is composed of the following: two yield stresses, the apparent (σ_y) and dynamic (σ_{yd}); the shear rate of transition between them ($\dot{\gamma}_{yd}$), the Herschel Bulkley parameters (K, n); and two viscosities, the viscosity of the fully structured fluid (η_0) and the viscosity when the crystalline structure is completely destroyed (η_∞). As discussed in Van Der Geest et al., (2017) [28], Equation (1) predicted the data with good accuracy.

$$\eta_{eq}(\dot{\gamma}) = \left(1 - e^{-\frac{\eta_0 \dot{\gamma}}{\sigma_y}}\right) \left(\frac{\sigma_y - \sigma_{yd}}{\dot{\gamma}} e^{-\frac{\dot{\gamma}}{\dot{\gamma}_{yd}}} + \frac{\sigma_{yd}}{\dot{\gamma}} + K \dot{\gamma}^{n-1}\right) + \eta_\infty \quad (1)$$

It is possible to calculate the value of the shear stress (σ_{eq}) in the equilibrium with Equation (2).

$$\sigma_{eq}(\dot{\gamma}) = \eta_{eq} \dot{\gamma}_{eq} \quad (2)$$

This model uses a tool common to rheological models—a dimensionless parameter that has a maximum value when the crystalline matrix is completely formed and has a value of zero when the oil is devoid of crystals. The fluid is Newtonian. The steady state occurs when the build-up of crystals occurs at the same rate as their breakdown. It can be quantified based on Equation (3).

$$\lambda_{eq} = \ln\left(\frac{\eta_{eq}}{\eta_{\infty}}\right) \quad (3)$$

3.1.2 Completely Structured Condition

The structure parameter for when the crystalline matrix is completely formed can be obtained with the ratio of the viscosities of the fully structured fluid and the completely destroyed fluid. As shown in Equation (4).

$$\lambda_0 = \ln\left(\frac{\eta_0}{\eta_{\infty}}\right) \quad (4)$$

3.1.3 Characteristic Times

Equation (5) is the relaxation time and Equation (6) is the retardation time; both are the material time responses. One is the response once the stress stops and the second is the response after the stress is applied.

$$\theta_1 = \left(1 - \frac{\eta_{\infty}}{\eta_v(\lambda)}\right) \frac{\eta_v(\lambda)}{G_s(\lambda)} \quad (5)$$

$$\theta_2 = \left(1 - \frac{\eta_{\infty}}{\eta_v(\lambda)}\right) \frac{\eta_{\infty}}{G_s(\lambda)} \quad (6)$$

3.1.4 The structural elastic modulus function

The elastic response of the material is quantified using Equation (7). The only parameter that has not been described yet in Equation (7) is m , which is an empirical parameter.

$$G_s = G_0 e^{m\left(\frac{1}{\lambda} - \frac{1}{\lambda_0}\right)} \quad (7)$$

3.1.5 The structural viscosity function

Equation (8) describes the structural viscosity. It represents a way to quantify the viscosity using the structure parameter λ and the completely destroyed viscosity (η_{∞}).

$$\eta_v(\lambda) = \eta_{\infty} e^{\lambda} \quad (8)$$

3.1.6 The Structure Parameter

Equation (9) is the differential equation that describes the time dependence of the structural parameter. It is dependent on the material equilibrium time (t_{eq}) and some empirical parameters, parameter (a) influences the build-up rate and parameter (b) the breakdown rate of the structure.

$$\frac{d\lambda}{dt} = \frac{1}{t_{eq}} \left[\left(\frac{1}{\lambda} - \frac{1}{\lambda_0}\right)^a - \left(\frac{\lambda}{\lambda_{eq}(\sigma)}\right)^b \left(\frac{1}{\lambda_{eq}(\sigma)} - \frac{1}{\lambda_0}\right)^a \right] \quad (9)$$

3.1.7 Constitutive Equation

Equation (10) is the constitutive equation proposed by Souza Mendes and Thompson (2013) [38]. It is a differential equation that is composed of both relaxation (θ_1) and retardation (θ_2) times.

$$\frac{\theta_2}{\eta_\infty} \left(\frac{\sigma}{\theta_1} + \frac{\partial \sigma}{\partial t} \right) = \left(\dot{\gamma} + \theta_2 \frac{\partial \dot{\gamma}}{\partial t} \right) \quad (10)$$

3.2 Governing Equations

The literature provides a few ways to solve the governing equations when dealing with the start-up of gelled waxy crudes. There are solutions that consider the replacement of the oil with a hot oil that has Newtonian behaviour, assuming the fluid to be compressible [50]. Solutions that consider a 2D momentum conservation equation considering compressible fluid [51] and there are efforts to solve the problem considering a 1.5 D momentum conservation without losing valuable information but gaining considerable computational time [42][43].

We used the solution proposed by De Oliveira and Negrao (2015) [43]. This one uses a 1.5D momentum conservation. They solved the axial mass and momentum conservation using the method of Characteristics (MOC) and considered the rheological behaviour in the radial direction. We implemented an algorithm in the ALFAWAX with their proposed solution that we will briefly discuss in the next section.

3.2.1 Axial Mass Conservation

Equation (11) is the axial direction (z) mass conservation. The weakly compressible solution considers the compressibility (α) only in the mass conservation [43]. Here pressure (p) and mean velocity (V) are the variables that have not been described yet.

$$\frac{\partial p}{\partial t} + \frac{1}{\alpha} \frac{\partial V}{\partial z} + V \frac{\partial p}{\partial z} = 0 \quad (11)$$

3.2.2 Axial Momentum Conservation

Equation (12) is the axial linear momentum conservation considering an incompressible fluid. The variables in this equation are shear stress in the pipeline wall (σ_w), the density (ρ), and the diameter (d).

$$\rho \frac{\partial V}{\partial t} + \rho V \frac{\partial V}{\partial z} + \frac{\partial p}{\partial z} = -\frac{4}{d} \sigma_w \quad (12)$$

3.2.3 Dimensionless Equations

Solving the equations using dimensionless numbers allows us to extrapolate similar solutions to field scales, which is the final goal of studies like this. With that in mind and using similar dimensionless numbers based on previous works ([38], [43]), we transform all the equations shown above into dimensionless equations.

The characteristic shear rate is the ratio of the pressure wave speed (c) by the diameter (d) of the pipeline (c/d), the characteristic stress is the dynamic yield stress (σ_{yd}), and the

characteristic time is the time of propagation of the pressure wave through the whole pipeline (l/c). With those characteristic parameters, we can obtain the dimensionless numbers.

$$\eta_0^* = \frac{\eta_0 c}{\sigma_{yd} d}; \eta_\infty^* = \frac{\eta_\infty c}{\sigma_{yd} d}; \sigma_y^* = \frac{\sigma_y}{\sigma_{yd}}; \dot{\gamma}_{yd}^* = \frac{\dot{\gamma}_{yd}}{\frac{c}{d}}; \dot{\gamma}_{eq}^* = \frac{\dot{\gamma}_{eq}}{\frac{c}{d}}; K^* = \frac{K \sigma_{yd}^{n-1}}{\eta_\infty^n};$$

$$G_0^* = \frac{G_0 l}{\eta_\infty c}; p^* = \frac{pd}{4\sigma_{yd} l}; V^* = \frac{V}{c}; t^* = \frac{tc}{l}; z^* = \frac{z}{l}.$$

In Equations (15) and (16) the inverse of isothermal compressibility appears as the multiplication of the dimensionless viscosity (η_∞^*) and a new term, (ϕ). This term can be interpreted as a relationship of the viscous dissipations and the inertia of the pressure wave [43].

We will show only the dimensionless form of the two most complicated equations in the rheological model. Equation (13) is the dimensionless steady state viscosity and Equation (14) is the dimensionless constitutive equation. It is possible to obtain Equations (15) and (16) from Equations (11) and (12), using the dimensionless numbers and disregarding the inertial terms, which are two orders of magnitude smaller when dealing with the restart problem [43].

$$\eta_{eq}^*(\dot{\gamma}) = \left(1 - e^{-\frac{\eta_0^* \dot{\gamma}_{eq}^*}{\tau_y^*}}\right) \left(\frac{(\tau_y^* - 1)}{\dot{\gamma}_{eq}^*} e^{\frac{\dot{\gamma}_{eq}^*}{\dot{\gamma}_{yd}^*}} + \frac{1}{\dot{\gamma}_{eq}^*} + K^* (\eta_\infty^*)^n \dot{\gamma}_{eq}^{*n-1} \right) + \eta_\infty^* \quad (13)$$

$$-\frac{\partial v^*}{\partial r^*} + \theta_2^* \frac{\partial}{\partial t^*} \left(-\frac{\partial v^*}{\partial r^*} \right) = \frac{2}{\eta_\infty^*} r^* \theta_2^* \left(\frac{\sigma_w^*}{\theta_1^*} + \frac{\partial \sigma_w^*}{\partial t^*} \right) \quad (14)$$

$$\frac{\partial p^*}{\partial t^*} + \eta_\infty^* \phi \frac{\partial V^*}{\partial z^*} = 0 \quad (15)$$

$$\frac{\partial p^*}{\partial z^*} + \eta_\infty^* \phi \frac{\partial V^*}{\partial t^*} + \sigma_w^* = 0 \quad (16)$$

3.2.4 Solution of Equations

The method of characteristic (MOC) was used to transform the two partial differential equations (PDE)—conservation of mass and linear momentum, that is, Equations (15) and (16)—into four ordinary differential equations (ODE). The final equations of the axial solution proposed by De Oliveira and Negrao (2015) [43] are shown in Equations (17) and (18).

$$\left. \begin{aligned} \frac{dp^*}{dt^*} + \eta_\infty^* \phi \frac{dV^*}{dt^*} + \sigma_w^* &= 0 \\ \frac{dz^*}{dt^*} &= +1 \end{aligned} \right\} C^+ \quad (17)$$

$$\left. \begin{aligned} -\frac{dp^*}{dt^*} + \eta_\infty^* \phi \frac{dV^*}{dt^*} + \sigma_w^* &= 0 \\ \frac{dz^*}{dt^*} &= -1 \end{aligned} \right\} C^- \quad (18)$$

To solve the differential equations of the rheological model, we used the Runge-Kutta method. To validate the ALFAWAX algorithm, we compared our results with those obtained by de Oliveira and Negrao (2015) [43]. The simulations shown in Figure 2 and Figure 3 is the restart of a weakly compressible Newtonian fluid. The only difference in the numerical solution is that we used the 4th order Runge-Kutta method while de Oliveira and Negrao (2015) used the Euler method.

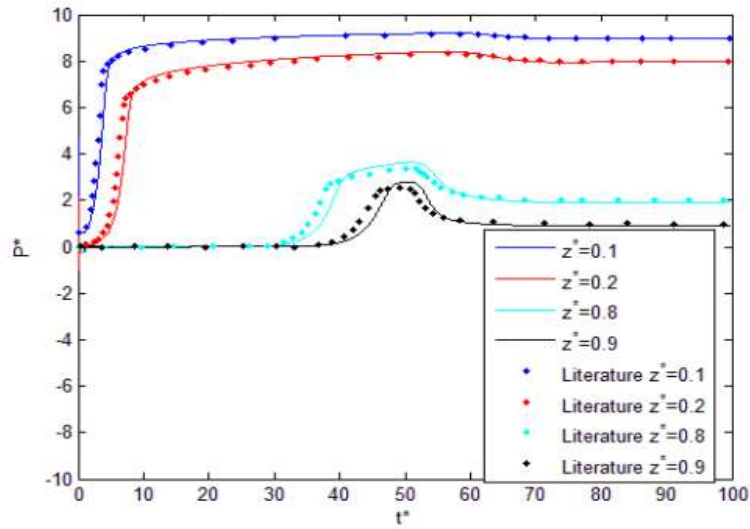


Figure 2. Comparison of pressure propagation during a start-up of ALFAWAX and that of Oliveira and Negrao (2015)

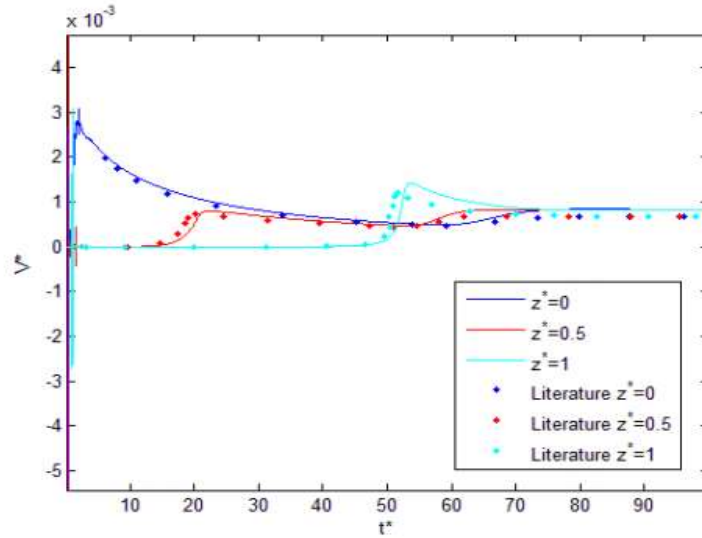


Figure 3. Comparison of Velocity during a start-up of ALFAWAX and that of de Oliveira and Negrao (2015)

Both solutions presented in the figures above have the same axial, radial, and temporal discretization. With 20 points in the radial direction and 100 points in the axial direction, we were able to obtain satisfactory results. Thus in all the simulations shown in this paper, that was the mesh used.

4 PRELIMINARY STUDY

All the results presented in this preliminary section are part of a larger rheological characterization published in [28]. We show some results again and some new results of the models related to aging time to shed light on the start-up phenomenon and the influence of rheological behaviour.

4.1 Properties of the Oils

Table 1 shows some properties of the oil.

Table 1. General Properties of the oil.

Parameters	oil	Units
$\rho @ 20^\circ\text{C}$	865 ± 1	kg/m^3
$^\circ\text{API}$	30.9 ± 0.1	-
H_2O	0.13 ± 0.01	%
WAT	34 ± 4	$^\circ\text{C}$
WDT	46 ± 4	$^\circ\text{C}$
Saturates	81.4 ± 0.1	%
Aromatics	2.1 ± 0.1	%
Resins	14.8 ± 0.1	%
Asphaltenes	1.7 ± 0.1	%

Table 2 shows the rheological properties this oil in steady state. These results and the full rheological characterization have been presented in Van Der Geest *et al.*, (2017) [28].

Table 2. Parameters obtained from the steady state.

Parameters	Value	Units
K	6 ± 1	$\text{Pa} \cdot \text{s}^n$

N	0.7 ± 0.1	-
η_0	$5 \cdot 10^8 \pm 0.9$	<i>Pa.s</i>
η_∞	1 ± 0.2	<i>Pa.s</i>
σ_y	1203 ± 241	<i>Pa</i>
σ_{yd}	118 ± 21	<i>Pa</i>
$\dot{\gamma}_{yd}$	$3 \cdot 10^{-3} \pm 0.5 \cdot 10^{-3}$	s^{-1}

Table 3 shows the rheological properties obtained in the oscillatory experiment. The storage modulus is the rheological property that we use to model the elastic response.

Table 3. Parameters obtained from the Oscillatory Test

Parameters	Oil 4	Units
G_0	$2.9 \cdot 10^5 \pm 2 \cdot 10^4$	<i>Pa</i>

There are another 4 parameters (a , b , m , t_{eq}) that are in the model and cannot be obtained in either steady state or oscillatory experiments. We usually obtained them based on the transient experiments of constant shear rate [28]. In this paper, we will use all constant empirical parameters and will study the physical parameters that are directly related to the transient behaviour—the equilibrium time—of the material.

Table 4. Values of the empirical Parameters used in the simulation

Parameters	Oil 4	Units
a	1	-
b	1	-
m	1	-

4.2 Cooling down Process

It has been shown by Magda et al., (2013) [41] that during the cooling down process the pressure profile of the oil inside the pipeline changes. They hypothesise that due to the gelation and the contact with the wall, the gelled crude responds elastically to the differential pressure and does not flow. We wanted to see if we could reproduce that behaviour in the experimental apparatus described before. The results are shown in Figure 4.

In Magda et al., (2013) they apply a pressure in one side of the pipeline and leave the other side closed and observe a decrease in the absolute pressure throughout the pipeline. In the procedure described here, all the valves were open, so the inlet and outlet of the pipeline were under the hydrostatic pressure of the column of oil. The differential pressure increase

means that the absolute pressure in the middle of the pipeline decreased, the same phenomenon reported by Magda et al., (2013).

The second phenomenon that they observe, however, is an increase in the pressure sometime after the coolant reached the desired temperature. They point out that this might mean that the structure somehow has yield, but when they restart the flow, they observe that the structure has not yield. In our experiment we do not see that event. Once the coolant has reached the desired temperature, the differential pressure stays constant until we apply the pressure to restart the flow.

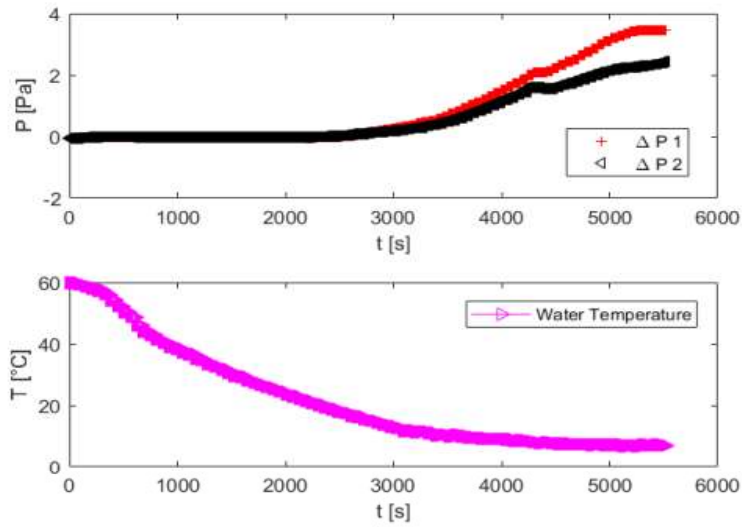


Figure 4. Differential pressure in the pipeline during cooling down process as shown in [52].

4.3 Influence of Pressure Ramp

Experiments were carried out to verify the influence of the pressure ramp in the restart without any aging time. The fastest ramp experiment was performed with a positive displacement pump, while the second was performed with the nitrogen pressurization system. The idea was to confirm the results presented in [15] and study the influence of pressure ramp in our system.

As the literature has shown already, our experiments demonstrate the time dependence of the material's response. The results shown in Table 5 are of interest. With the higher pressure ramp, the flow restarted at a higher pressure, demonstrating the material's transient behaviour. This can be explained by the elastic behaviour of the gelled crude. With the second ramp, the longer time allowed for the oil structure to break down and it started to flow at lower pressures.

Table 5. Time and Pressure to restart the flow at different pressure ramps for no aging time.

Pressure Ramp [Pa/s]	ΔP_s [Pa]	σ_s [Pa]	Time for restart [s]
212	$1.4 \cdot 10^5 \pm 0.3 \cdot 10^5$	154 ± 11	$6.6 \cdot 10^2 \pm 1 \cdot 10^2$

6	$0.48 \cdot 10^5 \pm 0.03 \cdot 10^5$	56.1 ± 0.3	$8.5 \cdot 10^3 \pm 0.5 \cdot 10^3$
---	---------------------------------------	----------------	-------------------------------------

4.4 General Simulation Results

We first discuss the general results of the simulation using all the parameters shown above and applying a small equilibrium time. This allows us to investigate all the phenomena involved in the restart—from the pressure wave propagation to the entire flow starting and reaching steady state. Those results are shown in Figure 5, Figure 6, Figure 7, and Figure 8 for the case of inlet pressure of $P_{inlet} = 2.5 \cdot 10^5 \text{ Pa}$ and equilibrium time of $t_{eq} = 10\text{s}$.

This section of the general results of the simulation are provided here because, when compared with the experimental data shown below, the point of interest is in the time necessary to restart. Hence, the simulation stops before the entire flows reaches steady state. Even if we wanted to study the transient flow of the entire pipeline after the restart occurred, we have no experimental data for that. Indeed, once the flow started we did not manage to control the inlet pressure at a constant; the pressure dropped faster than we could control it.

When we apply pressure (step or ramp) as a boundary condition, we obtain an oscillation response of the material due to its compressibility and elasticity. The oscillation is the pressure-wave propagation and reflection in the gelled crude oil crystalline structure, which possesses a strong elastic response. Due to viscous dissipation, that pressure-wave propagation dissipates completely after running throughout the pipeline a few times. When the structure matrix has an equilibrium time (t_{eq}) orders of magnitude higher than the dissipation time of the oscillation, that propagation is negligible in the restart time.

The pressure step inlet is a boundary condition, not applicable in real cases, where there is a pressure ramp before the final pressure is reached. For these experimental results, however, the time scale of the pressure dissipations is orders of magnitude faster than the time for restart. We thus use it as a boundary condition. In Figure 5, we show the pressure propagation in the entire simulation. In this case the flow restarted at around $t^* = 800$, but the velocities reached the same value at around $t^* = 1200$ due to compressibility (Figure 8), which is when the pressure at every axial point stopped varying, and thus, differential pressure throughout the pipeline was constant.

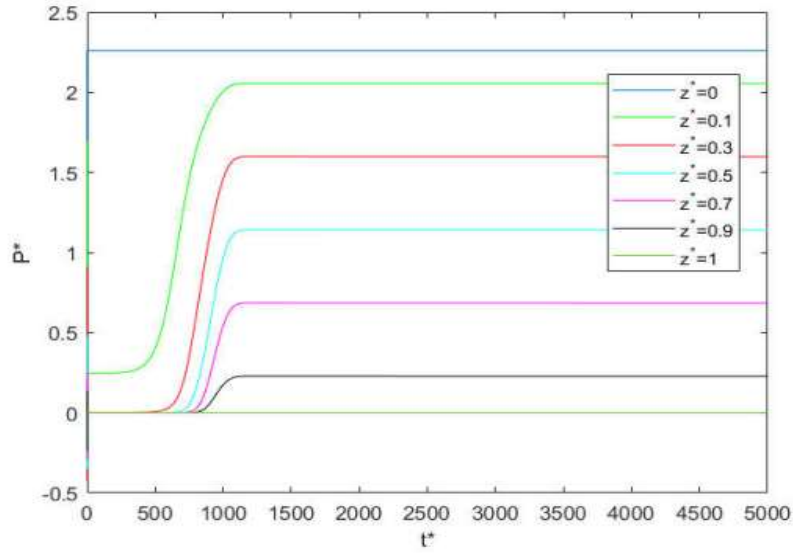


Figure 5. Pressure profile for restart $t_{eq} = 10 \text{ s}$; $P_{inlet} = 2.5 \cdot 10^5 \text{ Pa}$.

Figure 6 illustrates a zoom during an early moment of the simulation that is shown in its entirety in Figure 5. Every time the pressure wave passes through an axial position, the material has an elastic response. It is for this reason the oscillation continues for some time before stabilizing. What dissipates the energy of the pressure wave, eventually stopping it, is the high viscosity of the gelled crude. The relationship between the pressure-wave inertia and the viscous dissipation (ϕ) is low, which means that for this gelled crude oil the dissipation occurs quickly.

At $t^* = 1$ the pressure wave reaches the end of the pipeline and starts to move back. Therefore, the point $z^* = 0.9$ oscillates two times in a row—first when the pressure wave reaches the end of the pipeline and second when the pressure wave is returning. As can be seen in Figure 6, the pressure wave passes through all points three times before dissipating. This means that, before the pressure-wave energy was dissipated, it travelled to the end of the pipeline, back, and to the end once more. After that point, the whole pipeline is under stress, but due to the high crystalline matrix, the flow did not start for a considerably longer time.

When the goal is to determine the start-up time, the influence of the pressure wave in this simulation is negligible. To have significant influence, the dimensionless time necessary for the dissipation ($t^* = 3$) should be the same order of magnitude as the equilibrium time of the material ($t_{eq}^* = 1667$).

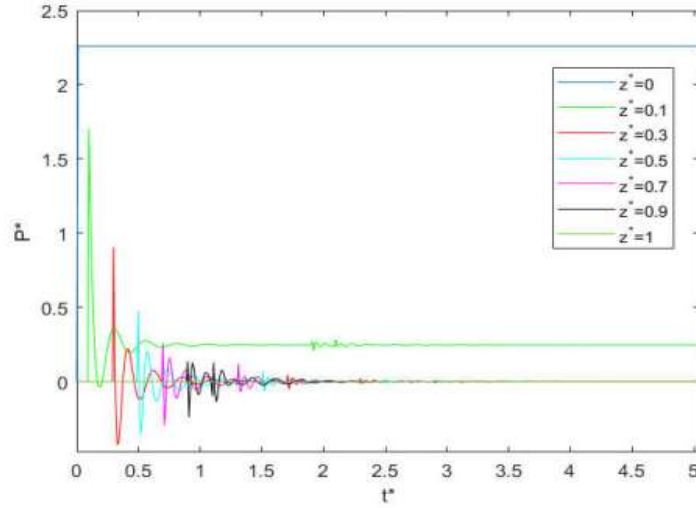


Figure 6. Pressure wave propagation after a step of pressure at different axial positions $t_{eq} = 10 \text{ s}$; $P_{inlet} = 2.5 \cdot 10^5 \text{ Pa}$.

Figure 7 shows the velocity profile at a different axial position. When plotted this way, the velocity at all the axial positions would appear to have the same profile, though is not the case. Thus, we show a zoom in Figure 8. As can be seen, after the flow starts, there is transient flow until steady state is reached. The transient flow is composed of the acceleration of the flow and by the transient rheological properties of the fluid.

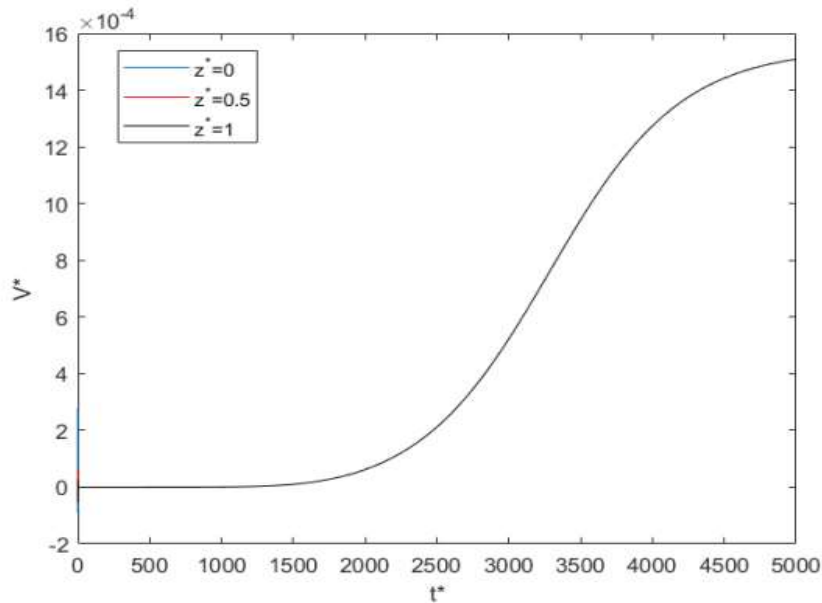


Figure 7. Mean velocity at different axial positions $t_{eq} = 10 \text{ s}$; $P_{inlet} = 2.5 \cdot 10^5 \text{ Pa}$.

When we do a zoom of the velocity at different axial positions, we can observe that the velocity starts to increase at the beginning of the pipeline before it does so at the end. This

occurs because the oil at the beginning of the pipeline is under a higher stress at the wall, due to higher differential pressure. Hence, the crystalline structure is destroyed more quickly there than at the end. Once the flow starts at the beginning of the pipeline, the stress increases at the end until eventually the entire pipeline starts to flow. At that point, the flow can be considered to have restarted.

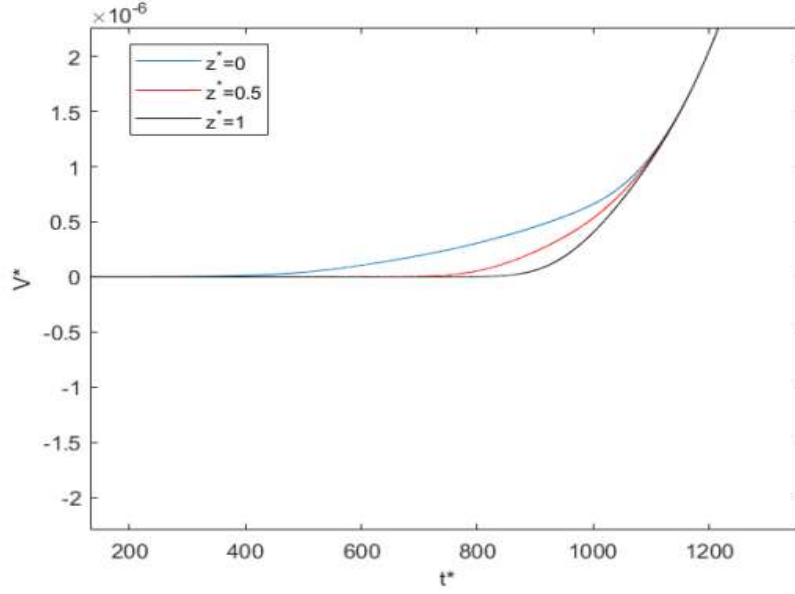


Figure 8. Zoom on the restart for mean velocity at different axial positions $t_{eq} = 10$ s; $P_{inlet} = 2.5 \cdot 10^5$ Pa.

5 RESULTS AND DISCUSSION

The objective of this paper is to study the influence of aging time on the equilibrium time of gelled waxy crude oils and to examine how this time period is influenced by scale and geometry. This is accomplished by comparing results from the rheometer and the pipeline. In pursuing this objective, we have done experiments at constant shear stress in the rheometer, which is the closest simulation of the restart in the pipeline that we can perform in a rheometer.

All the experiments done in the rheometer are at a stress just above the apparent yield stress. The idea is not to investigate the influence of the applied stress. Such an investigation has been carried out elsewhere [25].

5.1 Aging in the Rheometer

The general results obtained in the rheometer are shown in Figure 9. After doing the entire procedure described above, we applied a stress of $\sigma = 1300$ Pa and measured the time that elapsed before the flow started. It is important to highlight the fact that the experiment stopped at shear rate of $\dot{\gamma} = 2500$ s⁻¹ out of regard for the limits of the rheometer, but the data is no longer valid for shear rate higher than $\dot{\gamma} = 1000$ s⁻¹ because secondary flows start to appear, and inertial effects are not neglectable at high velocities.

Because the gelled waxy crude studied forms a strong crystalline matrix, the gel breaks down quite abruptly, as can be seen in Figure 9. Once the cone started to move, the shear rate increased so quickly that secondary flows began to appear before steady state was reached. This means that the last points of the experimental data shown below are not a real measurement of the rheological behavior.

As the aging time increases, as can be seen from the figure and as was expected, the equilibrium time of the gelled waxy crude also increases. This means that the crystalline structure is indeed fortifying, for there is more time for the paraffin crystals to interlock and reduce the empty spaces. In no experiment was the steady state reached. Even at low aging times, where the equilibrium time was small, the limit of the sensor was reached before equilibrium.

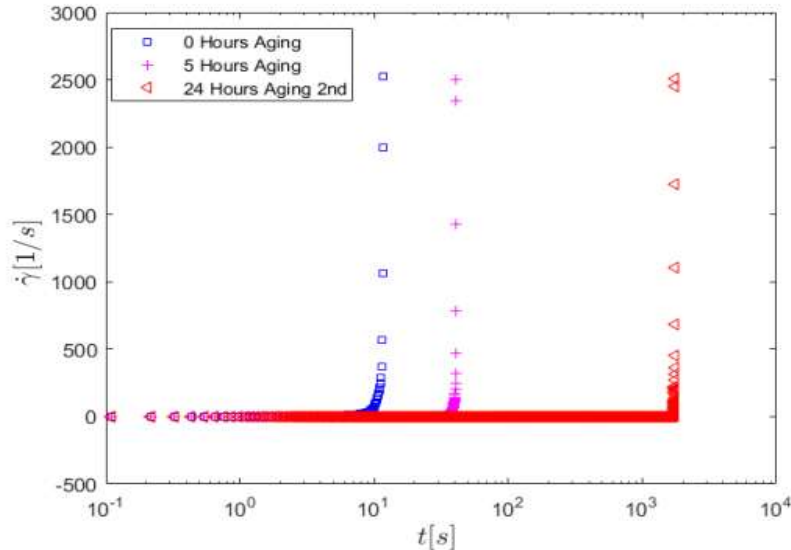


Figure 9. Constant Shear Stress Tests with 1300 Pa and Oil for different Aging Times.

When dealing with complex fluids, reproducibility is hard. Even when doing experiments in a rheometer with every possible variable under control, the structure matrix can vary widely. To reiterate, the experimental error of the time necessary for the start-up was 50%.

5.2 Aging in the Pipeline

Figure 10 shows the data of restart experiments. The experiment stops when the pressure drops, and the Coriolis starts to measure the mass flow rate. A discussion of the procedure can be found in Van Der Geest *et al.*, (2017) [52]. We observe here the same problem found with the rheometer; we do not reach steady state. Here, however, it is for a different reason. Once the flow started, we could not manage to keep the inlet pressure constant, so the pressure would drop as soon as the flow started. But as our aim was to study the time necessary for the restart to occur, these results are good enough.

As can be seen in Figure 10 the time necessary to start the flow increases as the aging time increases, which is the same tendency shown in the rheometer. Again, with more time

for paraffin crystals to grow and to increase the interlocking matrix, the strength of the gel rises, making more time necessary for it to be destroyed.

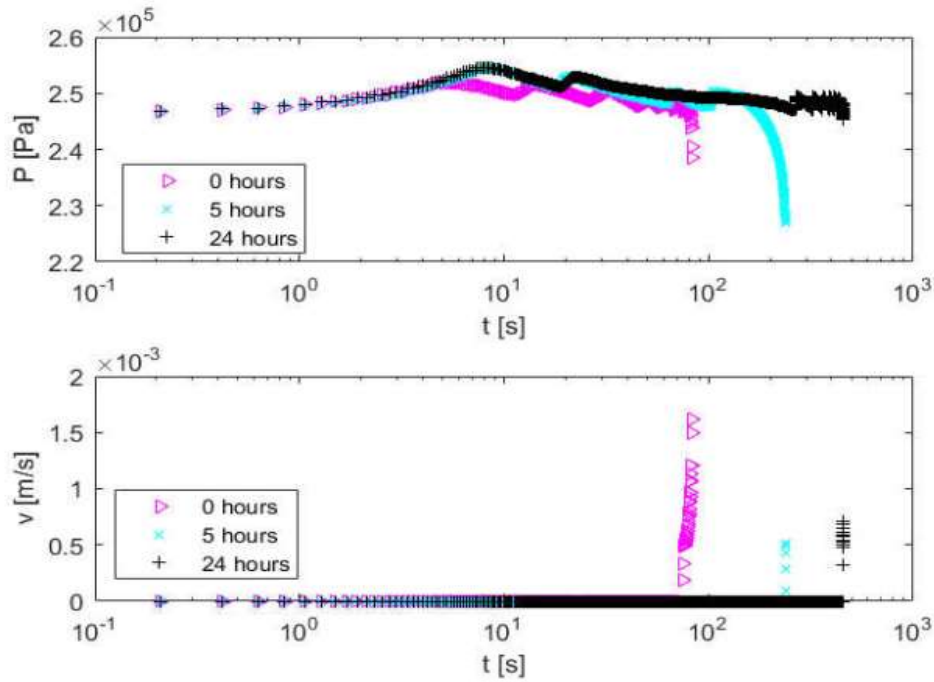


Figure 10. Experimental results of the restart test for different aging times at constant pressure.

Once the results of both experiments—those done in the rheometer and in the pipeline—have been discussed and the general results of the model have also been discussed, a comparison can be made of the experimental data and the simulation results. This is provided in the next section.

5.3 Comparison of Simulation and Experimental data

Figure 11 shows a comparison of the rheological model [26] and the experimental data shown in Figure 9. As noted above, we did not reach steady state. Thus, the experimental data at high shear rates is not the rheological behavior of the gelled waxy crude.

The model hypothesizes that the final steady state shear rate is equal to $\dot{\gamma} = \sigma/\eta_{eq}(\sigma)$, which is the plateau shown in Figure 11. That value cannot be compared with experimental data for this oil. In Van Der Geest *et al.*, (2017) [28], however, we verified that, for oils with weaker crystalline structures, such a hypothesis was correct.

Even though that discussion is important, it does not interfere with the goal of this paper, which is to predict the time necessary for the flow to start up once the sample was under stress. We show those results in Figure 12. We obtained the equilibrium time using the experimental data as calibration.

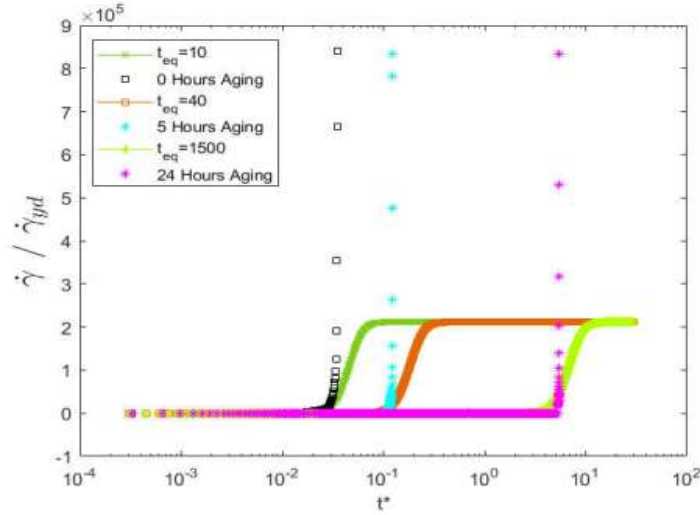


Figure 11. Comparison of experimental data and simulation of the rheological behavior at constant shear stress of the gelled waxy crude.

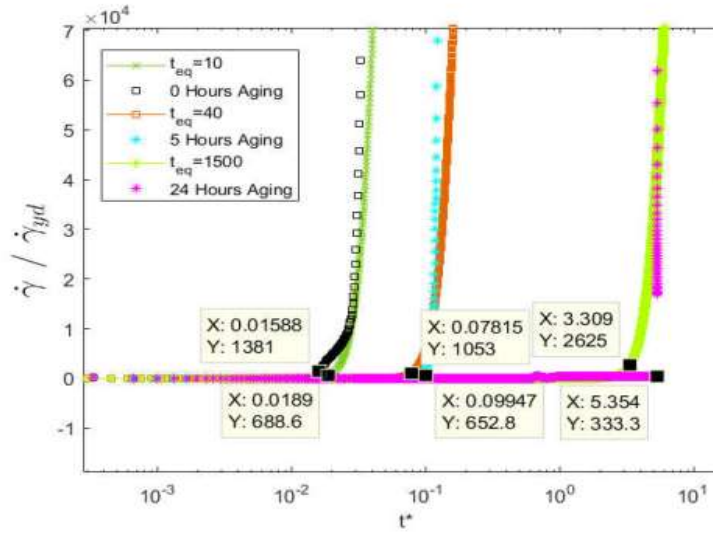


Figure 12. Zoom of the comparison of experimental data and simulation of the rheological behavior at constant shear stress of the gelled waxy crude.

In Table 6, we compare the results of the experimental time to increase the shear rate and the simulation results. The equilibrium time used in each simulation is also shown. That value was adjusted to fit the data. It demonstrates that as the crystalline structure becomes more interlocked, more time is necessary to destroy it under a constant stress. As can be seen, for no aging time is the equilibrium time small. Neither does it increase linearly with aging, at least not in the rheometer.

Table 6. Comparison of the experimental time and the simulation results for the rheometer

Aging [hours]	σ [Pa]	t_{eq} [s]	t_{exp}^*	$t_{sim}^* [-]$
0	1300	10	$1.6 \cdot 10^{-2} \pm 1 \cdot 10^{-2}$	$1.8 \cdot 10^{-2}$
5	1300	40	$9.9 \cdot 10^{-2} \pm 4 \cdot 10^{-2}$	$7.8 \cdot 10^{-2}$
24	1300	1500	5.3 ± 2	3.3

The results of the simulation of the pipeline are shown in Figure 13 through Figure 15. The idea is again to simulate the necessary time to restart the flow. In this simulation, we also have the pressure wave propagation that is discussed above. However, because the equilibrium time is orders of magnitude higher than the time necessary for the pressure wave to reach the end of the pipeline, the pressure wave influences the overall phenomenon only slightly.

In Figure 13, it is possible to see that the flow starts at around $t^* = 8000$ and due to the compressibility of the fluid, the restart at the end of the pipeline starts only at $t^* = 12000$. Which is approximately the value we obtained experimentally, to obtain that result the equilibrium time was $t_{eq} = 200$ s. As pointed out above, in this manuscript we do not intend to study the flow after it restarts. This is because at that point we could not keep the boundary condition constant.

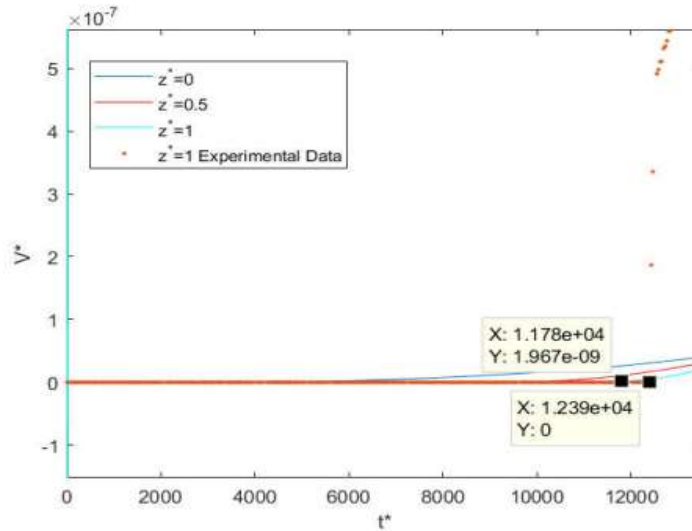


Figure 13. Comparison of simulation and experimental start-up time for 0 hours of aging. $t_{eq} = 200$ s; $P_{inlet} = 2.5 \cdot 10^5$ Pa

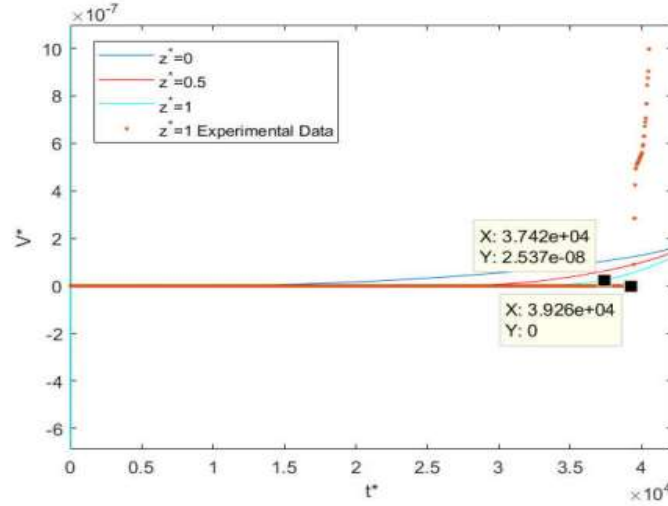


Figure 14. Comparison of simulation and experimental start-up time for 5 hours of aging. $t_{eq} = 700 \text{ s}$; $P_{inlet} = 2.5 \cdot 10^5 \text{ Pa}$

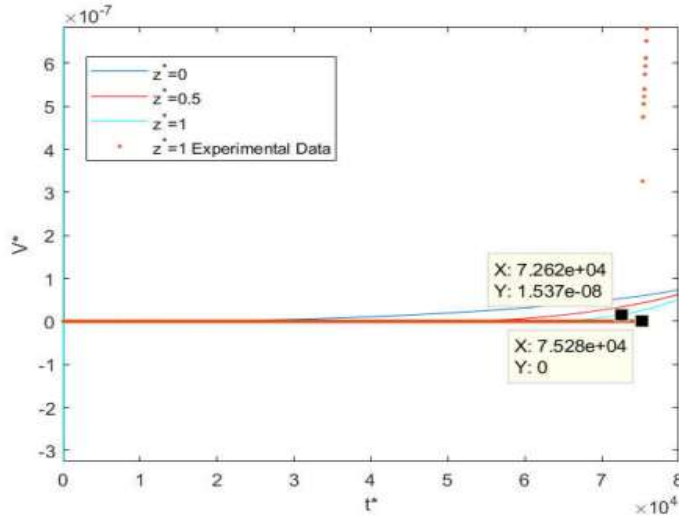


Figure 15. Comparison of simulation and experimental start-up time for 24 hours of aging. $t_{eq} = 1500 \text{ s}$; $P_{inlet} = 2.5 \cdot 10^5 \text{ Pa}$

The results of the equilibrium time in the pipeline, when keeping all other variables constant, can be seen in Table 7. In this case the equilibrium time apparently rises nearly linearly with aging time.

Table 7. Dimensionless results for different aging times for inlet pressure of $\Delta P^* = 9.10 \cdot 10^{-5}$.

Aging [hours]	ΔP [Pa]	t_{eq} [s]	t_{exp}^*	$t_{sim}^* [-]$
0	$2.5 \cdot 10^5$	200	$1.2 \cdot 10^4 \pm 0.8 \cdot 10^4$	$1.2 \cdot 10^4$

5	$2.5 \cdot 10^5$	700	$3.9 \cdot 10^4 \pm 1.3 \cdot 10^4$	$3.7 \cdot 10^4$
24	$2.5 \cdot 10^5$	1500	$7.5 \cdot 10^4 \pm 8.4 \cdot 10^3$	$7.3 \cdot 10^4$

For small aging times, as can be seen in Table 8, the equilibrium time of the pipeline and the rheometer are considerably different. During the cooling process, the crude in the pipeline is submitted to a different heat flow profile than is the rheometer. This has been shown many times to influence the final molecular structure and thus the time necessary to start the flow. This might explain why the times are so different from the rheometer and the pipeline.

Apparently, after some time of aging the equilibrium time tends to be the same in both the rheometer and pipeline. That might mean that for long times the structure might become equally strong regardless the thermal and shear histories. That possibility needs to be further explored, both in the rheometer and in the pipeline.

The cooling down of the crude oil in the pipeline apparently generates a gel with a longer equilibrium time than does the cooling down period in the rheometer. In the rheometer, the cooling process is better controlled and more homogeneous, while in the pipeline there is a higher radial temperature gradient. A conflicting behaviour was hypothesized by Venkatesan *et al.* (2005) [9]; the free space favours wax crystal aggregation and growth while at the same time the shearing breaks down the formed crystals.

Because of the temperature profile, the oil in the centre of the pipeline would cool down more slowly under a static condition, which generates a stronger crystalline structure. Similarly, the gel formed near the pipeline wall would provide more space in which the crystals could grow, thus generating a stronger gel. Both situations tend to increase the gel strength, possibly explaining why the equilibrium time in the pipeline is higher.

Table 8. Comparison of equilibrium time in the rheometer and in the pipeline for the same aging time.

Rheometer		Pipeline
Aging [h]	t_{eq} [s]	t_{eq} [s]
0	10	200
5	40	700
24	1500	1500

6 FINAL REMARKS

Both in the rheometer and in the pipeline, the time necessary for the flow to start up again increased with aging. If we consider that all other rheological properties remain constant and the equilibrium time of the gelled waxy crude oil increases with aging, then the hypothesis ought to be that the paraffin crystals grow, becoming more interlocked.

The solution proposed by De Oliveira and Negrão (2015), using the rheological model proposed by de Sousa Mendez and Thompson (2013), can predict the time necessary to start up a pipeline by adjusting only the equilibrium time. This result generates a valuable tool for the industry. Once this variable is measured in a pipeline, it is possible to apply it to a real-

scale field. To better verify that, it is necessary to conduct more experiments of restart in a larger diameter. Nevertheless, this first step is important.

For short aging times, there is a divergence in the equilibrium times obtained in the rheometer and in the pipeline. This divergence may be due to the different temperature profiles of the pipeline and the rheometer during the cooling process. It is likely that the paraffin crystals that precipitated in the pipeline wall can grow radially, increasing the strength of the fluid in general. As discussed by [17] there are heterogeneity both axially and radially in the pipeline that can lead to these results.

The aging process influences differently the strength of the gel in the rheometer and in the pipeline. In the pipeline, apparently, the equilibrium time increases linearly with aging time. For up to 5 hours in the rheometer, however, the aging time influenced little the overall response of the gelled waxy crude oil.

After a period of aging, the equilibrium time of the gel apparently reaches a constant value. After 24 hours of aging, we obtained the same equilibrium time both in the rheometer and in the pipeline. This could mean that eventually the structure reaches an interlocking format that no longer changes. This calls for further experimental analysis, which is being planned for the next experimental matrix.

7 ACKNOWLEDGEMENT

The authors wish to thank the company Repsol–Sinopec Brazil for their financial and technical support in this study. Also, we would like to thank ANP (National Agency of Petroleum, Natural Gas and Biofuels) (254/2014) and CAPES (Brazilian Federal Agency for Support and Evaluation of Graduate Education within the Ministry of Education of Brazil) (33003017) for their financial support. We would also like to thank the ALFA research group for their support.

8 BIBLIOGRAPHY

- [1] Chang, C., Nguyen, Q. D., & Rønningsen, H. P. (1999). Isothermal start-up of pipeline transporting waxy crude oil. *Journal of non-newtonian fluid mechanics*, 87(2), 127-154.
- [2] Chi, Y., Daraboina, N., & Sarica, C. (2017). Effect of the flow field on the wax deposition and performance of wax inhibitors: Cold finger and flow loop testing. *Energy & Fuels*, 31(5), 4915-4924.
- [3] Chi, Y., Daraboina, N., & Sarica, C. (2016). Investigation of inhibitors efficacy in wax deposition mitigation using a laboratory scale flow loop. *AIChE Journal*, 62(11), 4131-4139.
- [4] Davenport, T. C., & Conti, V. J. (1971). Heat transfer problems encountered in the handling of waxy crude oils in large pipelines. *Journal of the Institute of Petroleum*, 5.
- [5] Venkatesan, R., Singh, P., & Fogler, H. S. (2002). Delineating the pour point and gelation temperature of waxy crude oils. *SPE journal*, 7(04), 349-352.
- [6] Singh, P., Venkatesan, R., Fogler, H. S., & Nagarajan, N. (2000). Formation and aging of incipient thin film wax-oil gels. *AIChE Journal*, 46(5), 1059-1074.
- [7] Kok, M. V., Létoffé, J. M., Claudy, P., Martin, D., Garcin, M., & Volle, J. L. (1996). Comparison of wax appearance temperatures of crude oils by differential scanning calorimetry, thermomicroscopy and viscometry. *Fuel*, 75(7), 787-790.

- [8] da Silva, J. A. L., & Coutinho, J. A. (2004). Dynamic rheological analysis of the gelation behaviour of waxy crude oils. *Rheologica Acta*, 43(5), 433-441.
- [9] Venkatesan, R., Nagarajan, N. R., Paso, K., Yi, Y. B., Sastry, A. M., & Fogler, H. S. (2005). The strength of paraffin gels formed under static and flow conditions. *Chemical Engineering Science*, 60(13), 3587-3598.
- [10] Lopes-da-Silva, J. A., & Coutinho, J. A. (2007). Analysis of the isothermal structure development in waxy crude oils under quiescent conditions. *Energy & Fuels*, 21(6), 3612-3617.
- [11] Lee, H. S. (2008). Computational and rheological study of wax deposition and gelation in subsea pipelines.
- [12] Jemmett, M. R., Magda, J. J., & Deo, M. D. (2012). Heterogeneous organic gels: rheology and restart. *Energy & Fuels*, 27(4), 1762-1771.
- [13] Chang, C., Boger, D. V., & Nguyen, Q. D. (1998). The yielding of waxy crude oils. *Industrial & engineering chemistry research*, 37(4), 1551-1559.
- [14] Andrade, D. E., da Cruz, A. C., Franco, A. T., & Negrão, C. O. (2015). Influence of the initial cooling temperature on the gelation and yield stress of waxy crude oils. *Rheologica Acta*, 54(2), 149-157.
- [15] Rønningsen, H. P. (1992). Rheological behaviour of gelled, waxy North Sea crude oils. *Journal of Petroleum Science and Engineering*, 7(3-4), 177-213.
- [16] Lin, M., Li, C., Yang, F., & Ma, Y. (2011). Isothermal structure development of Qinghai waxy crude oil after static and dynamic cooling. *Journal of Petroleum Science and Engineering*, 77(3), 351-358.
- [17] Mendes, R., Vinay, G., & Coussot, P. (2016). Yield stress and minimum pressure for simulating the flow restart of a waxy crude oil pipeline. *Energy & Fuels*, 31(1), 395-407.
- [18] Chang, C., Boger, D. V., & Nguyen, Q. D. (2000). Influence of thermal history on the waxy structure of statically cooled waxy crude oil. *SPE Journal*, 5(02), 148-157.
- [19] de Souza Mendes, P. R., de Abreu Soares, F. S. M., Ziglio, C. M., & Gonçalves, M. (2012). Startup flow of gelled crudes in pipelines. *Journal of Non-Newtonian Fluid Mechanics*, 179, 23-31.
- [20] Kane, M., Djabourov, M., & Volle, J. L. (2004). Rheology and structure of waxy crude oils in quiescent and under shearing conditions. *Fuel*, 83(11), 1591-1605.
- [21] Visintin, R. F., Lapasin, R., Vignati, E., D'Antona, P., & Lockhart, T. P. (2005). Rheological behavior and structural interpretation of waxy crude oil gels. *Langmuir*, 21(14), 6240-6249.
- [22] Tinsley, J. F., Jahnke, J. P., Dettman, H. D., & Prud'home, R. K. (2009). Waxy gels with asphaltenes 1: characterization of precipitation, gelation, yield stress, and morphology. *Energy & Fuels*, 23(4), 2056-2064.
- [23] Magda, J. J., El-Gendy, H., Oh, K., Deo, M. D., Montesi, A., & Venkatesan, R. (2008). Time-dependent rheology of a model waxy crude oil with relevance to gelled pipeline restart. *Energy & Fuels*, 23(3), 1311-1315.
- [24] Wardhaugh, L. T., & Boger, D. V. (1991). The measurement and description of the yielding behavior of waxy crude oil. *Journal of Rheology* (1978-present), 35(6), 1121-1156.
- [25] El-Gamal, I. M., & Gad, E. A. M. (1997). Low temperature rheological behavior of Umbarka waxy crude and influence of flow improver. *Revue de l'Institut Français du Pétrole*, 52(3), 369-379.
- [26] Hou, L., & Zhang, J. (2010). A study on creep behavior of gelled Daqing crude oil. *Petroleum Science and Technology*, 28(7), 690-699.
- [27] Dimitriou, C. J., McKinley, G. H., & Venkatesan, R. (2011). Rheo-PIV analysis of the yielding and flow of model waxy crude oils. *Energy & Fuels*, 25(7), 3040-3052.
- [28] Van Der Geest, C., Guersoni, V. C. B., Merino-Garcia, D., & Bannwart, A. C. (2017). Rheological study under simple shear of six gelled waxy crude oils. *Journal of Non-Newtonian Fluid Mechanics*, 247, 188-206.

- [29] Mendes, R., Vinay, G., Ovarlez, G., & Coussot, P. (2015). Modeling the rheological behavior of waxy crude oils as a function of flow and temperature history. *Journal of Rheology*, 59(3), 703-732.
- [30] Barnes, H. A., Walters, K. (1985). The yield stress myth?. *Rheologica Acta*, 24(4), 323-326.
- [31] Schurz, J. (1992). Letter to the editor: A yield value in a true solution. *J. Rheol.*, 36(7), 1319-1321.
- [32] Evans, I. D. (1992). On the nature of the yield stress. *Journal of Rheology*, 36, 1313-1318.
- [33] Barnes, H. A. (1999). The yield stress—a review or ‘ $\pi\alpha\nu\tau\alpha \rho\epsilon\iota$ ’—everything flows?. *Journal of Non-Newtonian Fluid Mechanics*, 81(1), 133-178.
- [34] Møller, P. C., Mewis, J., & Bonn, D. (2006). Yield stress and thixotropy: on the difficulty of measuring yield stresses in practice. *Soft matter*, 2(4), 274-283.
- [35] Balmforth, N. J., Frigaard, I. A., & Ovarlez, G. (2014). Yielding to stress: recent developments in viscoplastic fluid mechanics. *Annual Review of Fluid Mechanics*, 46, 121-146.
- [36] Tarcha, B. A., Forte, B. P., Soares, E. J., & Thompson, R. L. (2015). Critical quantities on the yielding process of waxy crude oils. *Rheologica Acta*, 54(6), 479-499.
- [37] Coussot, P., Nguyen, Q. D., Huynh, H. T., & Bonn, D. (2002). Viscosity bifurcation in thixotropic, yielding fluids. *Journal of rheology*, 46(3), 573-589.
- [38] de Souza Mendes PR, Thompson RL (2013) A unified approach to model elasto-viscoplastic thixotropic yield-stress materials and apparent yield-stress fluids. *Rheol Acta* 52(7):673–694.
- [39] Fossen, M., Øyangen, T., & Velle, O. J. (2013). Effect of the pipe diameter on the restart pressure of a gelled waxy crude oil. *Energy & Fuels*, 27(7), 3685-3691.
- [40] Frigaard, I. A., Paso, K. G., & de Souza Mendes, P. R. (2017). Bingham’s model in the oil and gas industry. *Rheologica Acta*, 56(3), 259-282.
- [41] Magda, J. J., Elmadhoun, A., Wall, P., Jemmett, M., Deo, M. D., Greenhill, K. L., & Venkatesan, R. (2013). Evolution of the pressure profile during the gelation and restart of a model waxy crude oil. *Energy & Fuels*, 27(4), 1909-1913.
- [42] Wachs, A., Vinay, G., & Frigaard, I. (2009). A 1.5 D numerical model for the start up of weakly compressible flow of a viscoplastic and thixotropic fluid in pipelines. *Journal of Non-Newtonian Fluid Mechanics*, 159(1), 81-94.
- [43] de Oliveira, G. M., & Negrao, C. O. (2015). The effect of compressibility on flow start-up of waxy crude oils. *Journal of Non-Newtonian Fluid Mechanics*, 220, 137-147.
- [44] Van Der Geest, C., Guersoni, V. C. B., Merino-Garcia, D., & Bannwart, A. C. (2018). Wax Deposition Experiment with Highly Paraffinic Crude Oil in Laminar Single-Phase Flow Unpredictable by Molecular Diffusion Mechanism. *Energy & Fuels*, 32(3), 3406-3419.
- [45] Paso, K., Senra, M., Yi, Y., Sastry, A. M., & Fogler, H. S. (2005). Paraffin polydispersity facilitates mechanical gelation. *Industrial & engineering chemistry research*, 44(18), 7242-7254.
- [46] Roenningsen, H. P., Bjoerndal, B., Baltzer Hansen, A., & Batsberg Pedersen, W. (1991). Wax precipitation from North Sea crude oils: 1. Crystallization and dissolution temperatures, and Newtonian and non-Newtonian flow properties. *Energy & Fuels*, 5(6), 895-908.
- [47] Chang, C., Boger, D. V., & Nguyen, Q. D. (1998). The yielding of waxy crude oils. *Industrial & engineering chemistry research*, 37(4), 1551-1559.
- [48] Andrade, D. E., da Cruz, A. C., Franco, A. T., & Negrão, C. O. (2015). Influence of the initial cooling temperature on the gelation and yield stress of waxy crude oils. *Rheologica Acta*, 54(2), 149-157.
- [49] Paso, K., Kompalla, T., Oschmann, H. J., & Sjöblom, J. (2009). Rheological degradation of model wax-oil gels. *Journal of Dispersion Science and Technology*, 30(4), 472-480.
- [50] Davidson, M. R., Nguyen, Q. D., Chang, C., & Rønningsen, H. P. (2004). A model for restart of a pipeline with compressible gelled waxy crude oil. *Journal of non-newtonian fluid mechanics*, 123(2), 269-280.

- [51] Vinay, G., Wachs, A., & Agassant, J. F. (2005). Numerical simulation of non-isothermal viscoplastic waxy crude oil flows. *Journal of Non-Newtonian Fluid Mechanics*, 128(2-3), 144-162.
- [52] Van Der Geest, C., Guersoni, V. C. B., Junior, L. A. S. S., & Bannwart, A. C. (2017, June). Experimental Study of the Necessary Pressure to Start-Up the Flow of a Gelled Waxy Crude Oil. In *ASME 2017 36th International Conference on Ocean, Offshore and Arctic Engineering* (pp. V008T11A050-V008T11A050). American Society of Mechanical Engineers.
- [53] Wardhaugh, L. T., & Boger, D. V. (1991). Flow characteristics of waxy crude oils: application to pipeline design. *AIChE Journal*, 37(6), 871-885.
- [54] Morrison, F. A. (2001). *Understanding rheology*. Oxford University Press, USA.
- [55] Callaghan, P. T. (2008). Rheo NMR and shear banding. *Rheologica Acta*, 47(3), 243-255.
- [56] Ovarlez, G., Rodts, S., Chateau, X., & Coussot, P. (2009). Phenomenology and physical origin of shear localization and shear banding in complex fluids. *Rheologica acta*, 48(8), 831-844.
- [57] Van Der Geest, C., Guersoni, V. C. B., Merino-Garcia, D., & Bannwart, A. C. (2015). A modified elastoviscoplastic thixotropic model for two commercial gelled waxy crude oils. *Rheologica Acta*, 54(6), 545-561.
- [58] Divoux, T., Barentin, C., & Manneville, S. (2011). Stress overshoot in a simple yield stress fluid: An extensive study combining rheology and velocimetry. *Soft Matter*, 7(19), 9335-9349.
- [59] Helgeson, M. E., Vasquez, P. A., Kaler, E. W., & Wagner, N. J. (2009). Rheology and spatially resolved structure of cetyltrimethylammonium bromide wormlike micelles through the shear banding transition. *Journal of Rheology* (1978-present), 53(3), 727-756.
- [60] Cho, K. S., Hyun, K., Ahn, K. H., & Lee, S. J. (2005). A geometrical interpretation of large amplitude oscillatory shear response. *Journal of rheology*, 49(3), 747-758.
- [61] Ewoldt, R. H., Hosoi, A. E., & McKinley, G. H. (2008). New measures for characterizing nonlinear viscoelasticity in large amplitude oscillatory shear. *Journal of Rheology*, 52(6), 1427-1458..

6. CONCLUSIONS

Steady state experiments can present oscillation that does not represent any physical meaning. This can occur when one thinks the flow has reached equilibrium, but it has not. In our experiments, we show that if you apply 5 minutes for each point of the flow curve it is not enough to reach the steady state, rather when we waited for 30 minutes at each point, the equilibrium was reached, and the oscillation disappeared.

For highly paraffinic oils, the gel at 5 °C is strong. In steady state experiments, once you reach the apparent yield stress, the breakdown was fast and the rheometer could not measure points in between the apparent yield stress and the dynamic yield stress, even though the rheometer applied a stress for 30 minutes before raising the shear rate again.

The experimental data for all six oils have the same tendency in steady state. The equation proposed by de Sousa Mendes & Thompson (2013) for steady state was able to predict the experimental data with accuracy. In dimensionless form, the steady state for the six oils can be predicted with only one set of parameters, also with small errors. This was a surprising result, since we have up to three orders of magnitude of differences in the stress response for some of the oils.

Oscillatory tests for the six oils had a stable linear region with the storage modulus and the loss modulus crossing over and stabilizing when the shear stress amplitude rose enough. The point where the storage modulus starts to decrease abruptly was considered to be the apparent yield stress and had a good accuracy with the value obtained in the steady state experiment.

Transient experiments under constant shear rate were also performed and the result followed the same tendency as shown in the literature. The overshoot could be seen for the highly paraffinic oils and could not be seen for the oils with low percentage of wax. The model proposed by de Sousa Mendes & Thompson (2013) when using the storage modulus obtained from the constant shear rate experiment could predict the behavior with good accuracy.

Constant shear stress experiments have shown the behavior expected. For the six oils we could see that for a stress smaller than the apparent yield stress there was no flow during the experimental time. For stress bigger than the apparent yield stress there would be a transient flow and then the oil would reach steady state. The simulation, however, could predict the behavior, but without good accuracy. Both the time when the breakdown occurred and the final value under steady state yielded a high number of errors.

Aging time influences the behavior of the oils 2 and 4, however, not as reported in the literature. There is no influence when elastic behavior is dominant in the gel, when it is in the linear region of the oscillatory test. The difference can be noticed only on the edge of the linear region, where the deformations are high. We analyzed it as if the aging makes the material more ductile, and therefore, the material would be able to deform more while the elastic response would remain constant.

Another influence of aging time is the time necessary for the structure breakdown under a constant stress. The time clearly increases with aging. If this relationship could be extrapolated to infinity we would have the yield stress, but because that is not an engineering reality, what we see is for the times we did the experiment we have reached a limit for both oils.

An experimental apparatus was built in the interest of studying wax deposition of commercial crude oils from Brazil. This facility was remodeled from a previous facility that existed in the laboratory. This setup makes it possible to study the two main problems with flow assurance related to waxy crude oils; 1) flow start-up of gelled waxy crude oils and 2) wax deposition under two-phase flow.

The rheological behaviour study shows that the apparent yield stress of the oil used in the restart experiment is around 1000 Pa. Had we used the classic force balance taking the oil to be incompressible and time independent, we would have needed 11.2 bar of pressure to restart it. As we have shown, we were able to start the flow with 1.4 bar. And this does not mean that 1.4 bar is the minimum pressure necessary to restart, it is likely that lower pressures would have restarted after longer periods of time.

There was, as expected, a clear influence of the inlet pressure on the time needed to re-start the flow. As the inlet pressure increases, the time necessary to restart decreases. The second clear influence is the aging time. As the aging time rises, the time necessary to restart the flow also rises.

Finally, the model proposed by Oliveira and Negrão (2015) can predict the time necessary to restart the flow in the case tested. A further comparison of the model with more experimental data needs to be done to have stronger evidence of the predictability of the model.

To check all the instrumentation of our apparatus we did preliminary flow studies under isothermal conditions and non-isothermal conditions without wax deposition. The idea was to confirm instrument accuracy and determine whether we could model these kinds of flows. We applied a simple algorithm to compensate for the non-isoviscous flow that takes place in wax deposition experiments.

We have experimental evidence that for highly paraffinic oils, molecular diffusion alone cannot predict when the deposition will start. This is usually not a problem because in most experimental data in the literature the buildup starts as soon as the temperature at the wall reaches the WAT. But that was not the case for the oil studied in this manuscript. After the oil was at the desired temperature and the water was at 5°C wax took some time to start building up; around 5 hours for the oil at 50°C and around 24 hours in the worst-case scenario.

This time delay before the deposit starts to build up was shown for a shorter period of time in the literature for similar oil under different conditions (Venkatesan & Creek, 2010). The problem is there are many more experimental studies with condensates and model oils than with real high paraffin content crude, which is the reason we decided to publish this study.

In experiments where the oil was above the WAT, after the pressure drop starts to increase caused by the wax deposit build up, the wax deposition rate follows the same profile as in most the literature. Molecular diffusion is perfectly capable of predicting this behavior, thus we believe that after there is a thin layer of deposit the main mechanism of buildup and aging is indeed molecular diffusion.

When we did experiments with oil temperature in the bulk near the WAT, the time before the deposition begins was longer. We believed that this could be explained as effects of shear dispersion, Brownian diffusion and non-Newtonian behavior. That would increase difficulty in predicting where the deposition occurs and when, since these mechanisms are harder to model.

Finally, we used the model proposed by Singh *et al.*, (2000) to predict the experimental data using this apparatus. After molecular diffusivity and aspect ratio were defined, the model is able to predict final wax thickness. The deposition rate however is not well predicted, it overestimates the buildup because it cannot predict the delay in the deposition. We believe that with a momentum equation considering non-Newtonian behavior we could considerably improve those results.

7. FUTURE WORK

Rheology

All the rheological studies performed in this dissertation were in simple shear flow. In order to better understand the rheological behavior, it is important to obtain the normal stress for the yield stress point and for all the other experimental procedures. Such a study would be interesting for commercial oil and model oil. Once we have all that data it would be possible to use the results to test new models proposed in the literature.

Another important issue that remains nearly unexplored in the literature is the influence of pressure in the rheological behavior. Thus, I recommend doing rheological experiments at higher pressures to verify the importance of compressibility when gas is dissolved into the oil phase.

An important field of study is to better understand the properties of waxy crude oils and their influence in the rheological behavior. It seems relevant to know the format and geometrical properties of paraffin molecules. It would be interesting to run experiments in a particle accelerator (such as the recently constructed SIRIUS) to verify the aspect ratio of the paraffin molecules.

Flow Restart

To better understand how the boundary conditions influence the behavior of the oil in the pipeline, it would be interesting to run an extensive experimental matrix with different oils and initial conditions. We only did a relatively small set of experiments due to time limitation.

Build a new apparatus to study the influence of diameter and pipeline materials, which are two incredibly important variables for the restart for which no experimental investigation was found in the literature.

The weakly compressible model we use can be improved by implementing the compressibility in the momentum conservation. That would not increase the computational time significantly and would allow to remove a simplification hypothesis that might influence considerable the simulation results.

Wax Deposition

Verify the non-isothermal model against data of wax deposition under turbulent flow. The wax deposition experiments we did were under laminar phase, the non-isothermal consideration helped improving the predictions of the model, it is important to extend that

analysis. The wax deposition model we use does not consider the supersaturation. Implement it by considering the effect of the second law of thermodynamics may be interesting.

The same relevant parameters for the restart problem are relevant for the wax deposition. Thus, to build a new apparatus to study the influence of diameter and materials could be relevant to better understand the influence of such parameters in structure of the deposit and its kinetics.

8. BIBLIOGRAPHY

- 1 Aiyejina, A., Chakrabarti, D. P., Pilgrim, A., & Sastry, M. K. S. (2011). Wax formation in oil pipelines: A critical review. *International Journal of Multiphase Flow*, 37(7), 671-694.
- 2 Ajienka JA, Ikoku CU (1991) The effect of temperature on the rheology of waxy crude oils
- 3 American Petroleum Institute. Production Dept. (1991). Recommended practice for design and installation of offshore production platform piping systems. American Petroleum Institute.
- 4 ANAYA JAIMES, Yurley Karina. Flow assurance of waxy crude oil: physical and chemical characterization, critical temperatures and rheological behavior for the restart problem -experimental study University of Campinas, Faculty of Mechanical Engineering.
- 5 Anaya, Y. K., Guersoni, V. C., Perles, C. E., & Bannwart, A. C. (2016). Physicochemical Characterization and Critical Temperatures.
- 6 Andrade, D. E., da Cruz, A. C., Franco, A. T., & Negrao, C. O. (2015). Influence of the initial cooling temperature on the gelation and yield stress of waxy crude oils. *Rheologica Acta*, 54(2), 149-157.
- 7 Andrade, D. E., Neto, M. A. M., & Negrão, C. O. (2017). The importance of supersaturation on determining the solid-liquid equilibrium temperature of waxy oils. *Fuel*, 206, 516-523.
- 8 Asperger, R. G., Sattler, R. E., Tolonen, W. J., & Pitchford, A. C. (1981). Prediction of wax buildup in 24 inch cold, deep sea oil loading line.
- 9 Azevedo, L. F. A., & Teixeira, A. M. (2003). A critical review of the modeling of wax deposition mechanisms. *Petroleum Science and Technology*, 21(3-4), 393-408.
- 10 Balmforth, N. J., Frigaard, I. A., & Ovarlez, G. (2014). Yielding to stress: recent developments in viscoplastic fluid mechanics. *Annual Review of Fluid Mechanics*, 46, 121-146.
- 11 Barnes, H. A. (1997). Thixotropy a review. *Journal of Non-Newtonian Fluid Mechanics*, 70(1), 1-33.
- 12 Barnes, H. A. (1999). The yield stress—a review or ‘*παντα ρει*’—everything flows?. *Journal of Non-Newtonian Fluid Mechanics*, 81(1), 133-178.
- 13 Barnes, H. A., Walters, K. (1985). The yield stress myth?. *Rheologica Acta*, 24(4), 323-326.
- 14 Bauer, W. H., Collins, E. A. (1967). Thixotropy and dilatancy. *Rheology: Theory and applications*, 4, 423-459.
- 15 Bern, P. A., Withers, V. R., & Cairns, R. J. (1980, January). Wax deposition in crude oil pipelines. In *European offshore technology conference and exhibition*. Society of Petroleum Engineers.
- 16 Bhat, N. V., & Mehrotra, A. K. (2004). Measurement and prediction of the phase behavior of wax-solvent mixtures: Significance of the wax dis appearance temperature. *Industrial & engineering chemistry research*, 43(13), 3451-3461.
- 17 Bilderback, C. A., & McDougall, L. A. (1969). Complete paraffin control in petroleum production. *Journal of Petroleum Technology*, 21(09), 1-151.
- 18 Cabanillas, J. P., Leiroz, A. T., & Azevedo, L. F. (2015). Wax Deposition in the Presence of Suspended Crystals. *Energy & Fuels*, 30(1), 1-11.
- 19 Callaghan, P. T. (2008). Rheo NMR and shear banding. *Rheologica Acta*, 47(3), 243-255.
- 20 Cengel, Y. A. (2003). Heat transfer a practical approach. McGraw-Hill.
- 21 Chang, C., Boger, D. V., & Nguyen, Q. D. (1998). The yielding of waxy crude oils. *Industrial & engineering chemistry research*, 37(4), 1551-1559.
- 22 Chang, C., Boger, D. V., & Nguyen, Q. D. (2000). Influence of thermal history on the waxy structure of statically cooled waxy crude oil. *SPE Journal*, 5(02), 148-157.
- 23 Chang, C., Nguyen, Q. D., & Rønningsen, H. P. (1999). Isothermal start-up of pipeline transporting waxy crude oil. *Journal of non-newtonian fluid mechanics*, 87(2), 127-154.

- 24 Chen, J., Zhang, J., & Li, H. (2004). Determining the wax content of crude oils by using differential scanning calorimetry. *Thermochimica Acta*, 410(1), 23-26.
- 25 Chen, X. T., Butler, T., Volk, M., & Brill, J. P. (1997, January). Techniques for measuring wax thickness during single and multiphase flow. In SPE Annual Technical Conference and Exhibition. Society of Petroleum Engineers.
- 26 Cheng, D. C. (1986). Yield stress: a time-dependent property and how to measure it. *Rheologica Acta*, 25(5), 542-554.
- 27 Cho, K. S., Hyun, K., Ahn, K. H., & Lee, S. J. (2005). A geometrical interpretation of large amplitude oscillatory shear response. *Journal of rheology*, 49(3), 747-758.
- 28 Coto, B., Coutinho, J. A. P., Martos, C., Robustillo, M. D., Espada, J. J., & Pena, J. L. (2011). Assessment and improvement of n-paraffin distribution obtained by HTGC to predict accurately crude oil cold properties. *Energy & Fuels*, 25(3), 1153-1160.
- 29 da Silva, J. A. L., & Coutinho, J. A. (2004). Dynamic rheological analysis of the gelation behaviour of waxy crude oils. *Rheologica Acta*, 43(5), 433-441.
- 30 Davenport, T. C., & Conti, V. J. (1971). Heat transfer problems encountered in the handling of waxy crude oils in large pipelines. *Journal of the Institute of Petroleum*, 5.
- 31 Davidson, M. R., Nguyen, Q. D., Chang, C., & Rønningsen, H. P. (2004). A model for restart of a pipeline with compressible gelled waxy crude oil. *Journal of non-newtonian fluid mechanics*, 123(2), 269-280.
- 32 de Oliveira, G. M., & Negrao, C. O. (2015). The effect of compressibility on flow start-up of waxy crude oils. *Journal of Non-Newtonian Fluid Mechanics*, 220, 137-147.
- 33 de Souza Mendes, P. R., (2009) Modeling the thixotropic behavior of structured fluids. *J Non-Newtonian Fluid Mech* 164(1):66–75
- 34 de Souza Mendes, P. R., (2011) Thixotropic elasto-viscoplastic model for structured fluids. *Soft Matter* 7(6):2471–2483
- 35 de Souza Mendes, P. R., Thompson, R. L., (2012) A critical overview of elasto-viscoplastic thixotropic modeling. *J Non-Newtonian Fluid Mech* 187:8–15
- 36 de Souza Mendes, P. R., Thompson, R. L., (2013) A unified approach to model elasto-viscoplastic thixotropic yield-stress materials and apparent yield-stress fluids. *Rheol Acta* 52(7):673–694
- 37 de Souza Mendes, P. R., de Abreu Soares, F. S. M., Ziglio, C. M., & Gonçalves, M. (2012). Startup flow of gelled crudes in pipelines. *Journal of Non-Newtonian Fluid Mechanics*, 179, 23-31.
- 38 de Souza Mendes, P. R., Thompson, R. L., Alicke, A. A., & Leite, R. T. (2014). The quasilinear large-amplitude viscoelastic regime and its significance in the rheological characterization of soft matter. *Journal of Rheology*, 58(2), 537-561.
- 39 Dimitriou, C. J., McKinley, G. H., & Venkatesan, R. (2011). Rheo-PIV analysis of the yielding and flow of model waxy crude oils. *Energy & Fuels*, 25(7), 3040-3052.
- 40 Divoux, T., Barentin, C., & Manneville, S. (2011). Stress overshoot in a simple yield stress fluid: An extensive study combining rheology and velocimetry. *Soft Matter*, 7(19), 9335-9349.
- 41 Dullaert K., Mewis J. (2005) A model system for thixotropy studies. *Rheol Acta* 45(1):23–32
- 42 Dullaert K., Mewis J. (2006) A structural kinetics model for thixotropy. *J Non-Newtonian Fluid Mech* 139(1):21–30
- 43 El-Gamal, I. M., & Gad, E. A. M. (1997). Low temperature rheological behavior of Umbarka waxy crude and influence of flow improver. *Revue de l'Institut Français du Pétrole*, 52(3), 369-379.
- 44 Evans, I. D. (1992). On the nature of the yield stress. *Journal of Rheology*, 36, 1313-1318.
- 45 Ewoldt, R. H., Hosoi, A. E., & McKinley, G. H. (2008). New measures for characterizing nonlinear viscoelasticity in large amplitude oscillatory shear. *Journal of Rheology*, 52(6), 1427-1458.
- 46 Frigaard, I. A., Paso, K. G., & de Souza Mendes, P. R. (2017). Bingham's model in the oil and gas industry. *Rheologica Acta*, 56(3), 259-282.

- 47 Hayduk, W., & Minhas, B. S. (1982). Correlations for prediction of molecular diffusivities in liquids. *The Canadian Journal of Chemical Engineering*, 60(2), 295-299.
- 48 Helgeson, M. E., Vasquez, P. A., Kaler, E. W., & Wagner, N. J. (2009). Rheology and spatially resolved structure of cetyltrimethylammonium bromide wormlike micelles through the shear banding transition. *Journal of Rheology* (1978-present), 53(3), 727-756.
- 49 Herschel W. H, Bulkley R. (1926) Konsistenzmessungen von Gummi-Benzollösungen. *Kolloid Z* 39:291–300
- 50 Hoffmann, R., & Amundsen, L. (2009). Single-phase wax deposition experiments. *Energy & Fuels*, 24(2), 1069-1080.
- 51 Hou, L., & Zhang, J. (2010). A study on creep behavior of gelled Daqing crude oil. *Petroleum Science and Technology*, 28(7), 690-699.
- 52 Huang, Z., Lee, H. S., Senra, M., & Scott Fogler, H. (2011). A fundamental model of wax deposition in subsea oil pipelines. *AIChE Journal*, 57(11), 2955-2964.
- 53 Huang, Z., Lu, Y., Hoffmann, R., Amundsen, L., & Fogler, H. S. (2011). The effect of operating temperatures on wax deposition. *Energy & Fuels*, 25(11), 5180-5188.
- 54 Kane, M., Djabourov, M., & Volle, J. L. (2004). Rheology and structure of waxy crude oils in quiescent and under shearing conditions. *Fuel*, 83(11), 1591-1605.
- 55 Kok, M. V., Létoffé, J. M., Claudy, P., Martin, D., Garcin, M., & Volle, J. L. (1996). Comparison of wax appearance temperatures of crude oils by differential scanning calorimetry, thermomicroscopy and viscometry. *Fuel*, 75(7), 787-790.
- 56 Larson, R. G. (2015). Constitutive equations for thixotropic fluids. *Journal of Rheology*, 59(3), 595-611.
- 57 Lee, H. S. (2008). Computational and rheological study of wax deposition and gelation in subsea pipelines.
- 58 Lin, M., Li, C., Yang, F., & Ma, Y. (2011). Isothermal structure development of Qinghai waxy crude oil after static and dynamic cooling. *Journal of Petroleum Science and Engineering*, 77(3), 351-358.
- 59 Lopes-da-Silva, J. A., & Coutinho, J. A. (2007). Analysis of the isothermal structure development in waxy crude oils under quiescent conditions. *Energy & Fuels*, 21(6), 3612-3617.
- 60 Luthi, I. F (2013). Rheological characterization of a waxy crude oil and experimental study of the restart of a line blocked with gelled waxy crude. Campinas: Faculty of Mechanical Engineering, State University of Campinas, 124 p. Master Thesis.
- 61 Magda, J. J., El-Gendy, H., Oh, K., Deo, M. D., Montesi, A., & Venkatesan, R. (2008). Time-dependent rheology of a model waxy crude oil with relevance to gelled pipeline restart. *Energy & Fuels*, 23(3), 1311-1315.
- 62 Merino-Garcia, D., & Correra, S. (2008). Cold flow: A review of a technology to avoid wax deposition. *Petroleum Science and Technology*, 26(4), 446-459.
- 63 Merino-Garcia, D., Margarone, M., & Correra, S. (2007). Kinetics of waxy gel formation from batch experiments. *Energy & fuels*, 21(3), 1287-1295.
- 64 Mewis J., Wagner N. J. (2009) Thixotropy. *Adv Colloid Interf Sci* 147:214–227
- 65 Mewis, J. (1979). Thixotropy-a general review. *Journal of Non-Newtonian Fluid Mechanics*, 6(1), 1-20.
- 66 Møller, P. C., Mewis, J., & Bonn, D. (2006). Yield stress and thixotropy: on the difficulty of measuring yield stresses in practice. *Soft matter*, 2(4), 274-283.
- 67 Morrison, F. A. (2001). Understanding rheology. Oxford University Press, USA.
- 68 Mujumdar, A., Beris, A. N., & Metzner, A. B. (2002). Transient phenomena in thixotropic systems. *Journal of Non-Newtonian Fluid Mechanics*, 102(2), 157-178.
- 69 Ovarlez, G., Rodts, S., Chateau, X., & Coussot, P. (2009). Phenomenology and physical origin of shear localization and shear banding in complex fluids. *Rheologica acta*, 48(8), 831-844.

- 70 Panacharoensawad, E., & Sarica, C. (2013). Experimental study of single-phase and two-phase water-in-crude-oil dispersed flow wax deposition in a mini pilot-scale flow loop. *Energy & Fuels*, 27(9), 5036-5053.
- 71 Paso, K. G., & Fogler, H. S. (2003). Influence of n-paraffin composition on the aging of wax-oil gel deposits. *AIChE journal*, 49(12), 3241-3252.
- 72 Paso, K., Kompalla, T., Aske, N., Ronningsen, H. P., Øye, G., & Sjöblom, J. (2009). Novel surfaces with applicability for preventing wax deposition: a review. *Journal of Dispersion Science and Technology*, 30(6), 757-781.
- 73 Paso, K., Kompalla, T., Oschmann, H. J., & Sjöblom, J. (2009). Rheological degradation of model wax-oil gels. *Journal of Dispersion Science and Technology*, 30(4), 472-480.
- 74 Phillips, D. A., Forsdyke, I. N., McCracken, I. R., & Ravenscroft, P. D. (2011). Novel approaches to waxy crude restart: Part 1: Thermal shrinkage of waxy crude oil and the impact for pipeline restart. *Journal of Petroleum Science and Engineering*, 77(3), 237-253.
- 75 Ramirez-Jaramillo, E., Lira-Galeana, C., & Manero, O. (2004). Modeling wax deposition in pipelines. *Petroleum science and technology*, 22(7-8), 821-861.
- 76 Reistle Jr, C. E. (1928). Methods of dealing with paraffin troubles encountered in producing crude oil (No. BM-TP-414). Bureau of Mines, Washington, DC (USA).
- 77 Ritter, R. A., & Batycky, J. P. (1967). Numerical prediction of the pipeline flow characteristics of thixotropic liquids. *Society of Petroleum Engineers Journal*, 7(04), 369-376.
- 78 Roenningsen, H. P., Bjoerndal, B., Baltzer Hansen, A., & Batsberg Pedersen, W. (1991). Wax precipitation from North Sea crude oils: 1. Crystallization and dissolution temperatures, and Newtonian and non-Newtonian flow properties. *Energy & Fuels*, 5(6), 895-908.
- 79 Rønningsen, H. P. (2012). Rheology of petroleum fluids. *Ann. Trans. Nord. Rheo. Soc*, 20, 11-18.
- 80 Sarica, C., & Panacharoensawad, E. (2012). Review of paraffin deposition research under multiphase flow conditions. *Energy & Fuels*, 26(7), 3968-3978.
- 81 Schurz, J. (1992). Letter to the editor: A yield value in a true solution. *J. Rheol*, 36(7), 1319-1321.
- 82 Sieder, E. N., & Tate, G. E. (1936). Heat transfer and pressure drop of liquids in tubes. *Industrial & Engineering Chemistry*, 28(12), 1429-1435.
- 83 Singh, P., Venkatesan, R., Fogler, H. S., & Nagarajan, N. (2000). Formation and aging of incipient thin film wax-oil gels. *AIChE Journal*, 46(5), 1059-1074.
- 84 Slibar A., Paslay PR (1963) Steady-state flow of a gelling material between rotating concentric cylinders. *J Appl Mech* 30(3):453-460
- 85 Soedarmo, A. A., Daraboina, N., & Sarica, C. (2016). Microscopic study of wax deposition: mass transfer boundary layer and deposit morphology. *Energy & Fuels*, 30(4), 2674-2686.
- 86 Soedarmo, A. A., Daraboina, N., & Sarica, C. (2017). Validation of wax deposition models with recent laboratory scale flow loop experimental data. *Journal of Petroleum Science and Engineering*, 149, 351-366.
- 87 Soedarmo, A. A., Daraboina, N., Lee, H. S., & Sarica, C. (2016). Microscopic Study of Wax Precipitation - Static Conditions. *Energy & Fuels*, 30(2), 954-961.
- 88 Srivastava SP, Handoo J, Agrawal KM, Joshi GC (1993) Phase-transition studies in alkanes and petroleum-related waxes—a review. *J Phys Chem Solids* 54(6):639-670
- 89 Svendsen, J. A. (1993). Mathematical modeling of wax deposition in oil pipeline systems. *AIChE Journal*, 39(8), 1377-1388.
- 90 Tarcha, B. A., Forte, B. P., Soares, E. J., & Thompson, R. L. (2015). Critical quantities on the yielding process of waxy crude oils. *Rheologica Acta*, 54(6), 479-499.
- 91 Thewlis J (1962) Oxford encyclopedia dictionary of physics
- 92 Thomason, W. H. (2000). Start-up and shut-in issues for subsea production of high paraffinic crudes. In *Offshore Technology Conference*. Offshore Technology Conference.

- 93 Tinsley, J. F., Jahnke, J. P., Dettman, H. D., & Prud'home, R. K. (2009). Waxy gels with asphaltenes 1: characterization of precipitation, gelation, yield stress, and morphology. *Energy & Fuels*, 23(4), 2056-2064.
- 94 Tiu C, Boger DV (1974) Complete rheological characterization of time-dependent food products. *J Texture Stud* 5(3):329–338
- 95 Todi, S. Experimental and Modeling Studies of Wax Deposition in Crude-Oil-Carrying Pipelines. Ph.D. Thesis, University of Utah, Salt Lake City, UT, 2005
- 96 Toorman E. A. (1997) Modelling the thixotropic behaviour of dense cohesive sediment suspensions. *Rheol Acta* 36(1):56–65
- 97 Valinejad, R., & Nazar, A. R. S. (2013). An experimental design approach for investigating the effects of operating factors on the wax deposition in pipelines. *Fuel*, 106, 843-850.
- 98 Van Der Geest, C., Guersoni, V. C. B., Junior, L. A. S. S., & Bannwart, A. C. (2017, June). Experimental Study of the Necessary Pressure to Start-Up the Flow of a Gelled Waxy Crude Oil. In ASME 2017 36th International Conference on Ocean, Offshore and Arctic Engineering. American Society of Mechanical Engineers.
- 99 Van Der Geest, C., Guersoni, V. C. B., Merino-Garcia, D., & Bannwart, A. C. (2017). Rheological study under simple shear of six gelled waxy crude oils. *Journal of Non-Newtonian Fluid Mechanics*, 247, 188-206.
- 100 Van Der Geest, C., Guersoni, V. C. B., Merino-Garcia, D., & Bannwart, A. C. (2015). The Influence of Compressibility and Shrinkage in the Start-up of a Flow of Gelled Waxy Crudes in Pipelines. In OTC Brasil. Offshore Technology Conference.
- 101 Van Der Geest, C., Guersoni, V. C. B., Merino-Garcia, D., & Bannwart, A. C. (2015). A modified elasto-viscoplastic thixotropic model for two commercial gelled waxy crude oils. *Rheologica Acta*, 54(6), 545-561.
- 102 Veiga, H., Fleming, F. P., & Azevedo, L. F. A. (2017). Wax deposit thermal conductivity measurements under flowing conditions. *Energy & Fuels*.
- 103 Venkatesan, R., & Creek, J. (2010, May). Wax deposition and rheology: Progress and problems from an operator's view. In Offshore Technology Conference, Houston-Texas, USA (pp. 3-6).
- 104 Venkatesan, R., Nagarajan, N. R., Paso, K., Yi, Y. B., Sastry, A. M., & Fogler, H. S. (2005). The strength of paraffin gels formed under static and flow conditions. *Chemical Engineering Science*, 60(13), 3587-3598.
- 105 Venkatesan, R., Östlund, J. A., Chawla, H., Wattana, P., Nydén, M., & Fogler, H. S. (2003). The effect of asphaltenes on the gelation of waxy oils. *Energy & fuels*, 17(6), 1630-1640.
- 106 Venkatesan, R., Singh, P., & Fogler, H. S. (2002). Delineating the pour point and gelation temperature of waxy crude oils. *SPE journal*, 7(04), 349-352.
- 107 Vinay G, Wachs A, Frigaard I (2009) Start-up of gelled waxy crude oil pipelines: a new analytical relation to predict the restart pressure. In: Asia Pacific Oil and Gas Conference & Exhibition. Society of Petroleum Engineers
- 108 Visintin, R. F., Lapasin, R., Vignati, E., D'Antona, P., & Lockhart, T. P. (2005). Rheological behavior and structural interpretation of waxy crude oil gels. *Langmuir*, 21(14), 6240-6249.
- 109 Wachs, A., Vinay, G., & Frigaard, I. (2009). A 1.5 D numerical model for the start up of weakly compressible flow of a viscoplastic and thixotropic fluid in pipelines. *Journal of Non-Newtonian Fluid Mechanics*, 159(1), 81-94.
- 110 Wardhaugh, L. T., & Boger, D. V. (1987). Measurement of the unique flow properties of waxy crude oils. *Chemical engineering research & design*, 65(1), 74-83.
- 111 Wardhaugh, L. T., & Boger, D. V. (1991). Flow characteristics of waxy crude oils: application to pipeline design. *AIChE Journal*, 37(6), 871-885.
- 112 Wardhaugh, L. T., & Boger, D. V. (1991). The measurement and description of the yielding behaviour of waxy crude oil. *Journal of Rheology*, 35(6), 1121-1156.
- 113 White, F. M. (2011). Fluid mechanics, in SI units.

- 114 Yi, S., & Zhang, J. (2011). Relationship between waxy crude oil composition and change in the morphology and structure of wax crystals induced by pour-point-depressant beneficiation. *Energy & Fuels*, 25(4), 1686-1696.
- 115 Zheng, S., Saidoun, M., Palermo, T., Mateen, K., & Fogler, H. S. (2017). Wax Deposition Modeling with Considerations of Non-Newtonian Characteristics: Application on Field-Scale Pipeline. *Energy & Fuels*.

APPENDIX A: COPYRIGHT LICENSE AGREEMENTS

Paper 1



RightsLink®

[Home](#)
[Account Info](#)
[Help](#)


Title: Rheological study under simple shear of six gelled waxy crude oils

Author: Charlie Van Der Geest, Vanessa C. Bizotto Guersoni, Daniel Merino-Garcia, Antonio Carlos Bannwart

Publication: Journal of Non-Newtonian Fluid Mechanics

Publisher: Elsevier

Date: September 2017

© 2017 Elsevier B.V. All rights reserved.

Logged in as:

Charlie Van Der Geest
UNICAMP

Account #:
3000542281

[LOGOUT](#)

Please note that, as the author of this Elsevier article, you retain the right to include it in a thesis or dissertation, provided it is not published commercially. Permission is not required, but please ensure that you reference the journal as the original source. For more information on this and on your other retained rights, please visit: <https://www.elsevier.com/about/our-business/policies/copyright#Author-rights>

[BACK](#)
[CLOSE WINDOW](#)

Copyright © 2018 [Copyright Clearance Center, Inc.](#) All Rights Reserved. [Privacy statement](#). [Terms and Conditions](#).
Comments? We would like to hear from you. E-mail us at customercare@copyright.com

Paper 2

Copyright Permission for PhD dissertation Publication

Beth Darchi <DarchiB@asme.org>

30 January 2018 at 13:50

To: Charlie Van Der Geest <charlievander@gmail.com>

Dear Prof. Van Der Geest,

It is our pleasure to grant you permission to use **all or any part of** the ASME paper "Experimental Study of the Necessary Pressure to Start-Up the Flow of a Gelled Waxy Crude Oil," by Charlie Van Der Geest, Vanessa C. Bizotto Guersoni, Luiz Antônio Simões Salomão Junior and Antonio C. Bannwart, Paper No. OMAE2017-62438, cited in your letter for inclusion in a PhD. dissertation entitled FLOW ASSURANCE STUDY OF WAXY CRUDE OILS: RHEOLOGICAL BEHAVIOUR AND FLOW START-UP OF GELLED WAXY CRUDES AND WAX DEPOSITION to be published by University of Campinas.

Permission is granted for the specific use as stated herein and does not permit further use of the materials without proper authorization. Proper attribution must be made to the author(s) of the materials. **Please note:** if any or all of the figures and/or Tables are of another source, permission should be granted from that outside source or include the reference of the original source. ASME does not grant permission for outside source material that may be referenced in the ASME works.

As is customary, we request that you ensure full acknowledgment of this material, the author(s), source and ASME as original publisher. Acknowledgment must be retained on all pages where figure is printed and distributed.

Many thanks for your interest in ASME publications.

Sincerely,

Beth Darchi

Publishing Administrator

ASME


[2 Park Avenue](#)


[New York, NY 10016-5990](#)


darchib@asme.org

Paper 3

Rightslink® by Copyright Clearance Center

<https://s100.copyright.com/AppDispatchServlet>


[Home](#)
[Account Info](#)
[Help](#)




Title: Wax Deposition experiment with highly paraffinic crude oil in laminar single-phase flow unpredictable by molecular diffusion mechanism

Author: Charlie Van Der Geest, Vanessa C. Bizotto Guersoni, Daniel Merino-Garcia, et al

Publication: Energy & Fuels

Publisher: American Chemical Society

Date: Feb 1, 2018

Copyright © 2018, American Chemical Society

Logged in as:
Charlie Van Der Geest
UNICAMP

Account #:
3000542281

[LOGOUT](#)

PERMISSION/LICENSE IS GRANTED FOR YOUR ORDER AT NO CHARGE

This type of permission/license, instead of the standard Terms & Conditions, is sent to you because no fee is being charged for your order. Please note the following:

- Permission is granted for your request in both print and electronic formats, and translations.
- If figures and/or tables were requested, they may be adapted or used in part.
- Please print this page for your records and send a copy of it to your publisher/graduate school.
- Appropriate credit for the requested material should be given as follows: "Reprinted (adapted) with permission from (COMPLETE REFERENCE CITATION). Copyright (YEAR) American Chemical Society." Insert appropriate information in place of the capitalized words.
- One-time permission is granted only for the use specified in your request. No additional uses are granted (such as derivative works or other editions). For any other uses, please submit a new request.

[BACK](#)[CLOSE WINDOW](#)

Copyright © 2018 [Copyright Clearance Center, Inc.](#) All Rights Reserved. [Privacy statement](#). [Terms and Conditions](#).
Comments? We would like to hear from you. E-mail us at customer@copyright.com

Paper 4

RightsLink Printable License

<https://s100.copyright.com/CustomerAdmin/PLF.jsp?ref=a78c4ee1-8c28...>**SPRINGER NATURE LICENSE
TERMS AND CONDITIONS**

Jan 25, 2018

This Agreement between UNICAMP -- Charlie Van Der Geest ("You") and Springer Nature ("Springer Nature") consists of your license details and the terms and conditions provided by Springer Nature and Copyright Clearance Center.

License Number	4275991367092
License date	Jan 25, 2018
Licensed Content Publisher	Springer Nature
Licensed Content Publication	Rheologica Acta
Licensed Content Title	A modified elasto-viscoplastic thixotropic model for two commercial gelled waxy crude oils
Licensed Content Author	Charlie Van Der Geest, Vanessa C. Bizotto Guersoni, Daniel Merino-Garcia et al
Licensed Content Date	Jan 1, 2015
Licensed Content Volume	54
Licensed Content Issue	6
Type of Use	Thesis/Dissertation
Requestor type	academic/university or research institute
Format	print and electronic
Portion	full article/chapter
Will you be translating?	no
Circulation/distribution	>50,000
Author of this Springer Nature content	yes
Title	FLOW ASSURANCE STUDY OF WAXY CRUDE OILS: RHEOLOGICAL BEHAVIOUR AND FLOW START-UP OF GELLED WAXY CRUDES AND WAX DEPOSITION
Instructor name	ANTONIO CARLOS BANNWART
Institution name	UNIVERSITY OF CAMPINAS
Expected presentation date	Jul 2018
Portions	Full article
Requestor Location	UNICAMP Rua Luverci Pereira de Souza, 609. Campinas, 13083725 Brazil Attn: Charlie Van Der Geest
Billing Type	Invoice

Billing Address UNICAMP
Rua Luverci Pereira de Souza, 609.

Campinas, Brazil 13083725
Attn: Charlie Van Der Geest

Total 0.00 USD

Terms and Conditions

Springer Nature Terms and Conditions for RightsLink Permissions

Springer Customer Service Centre GmbH (the Licensor) hereby grants you a non-exclusive, world-wide licence to reproduce the material and for the purpose and requirements specified in the attached copy of your order form, and for no other use, subject to the conditions below:

1. The Licensor warrants that it has, to the best of its knowledge, the rights to license reuse of this material. However, you should ensure that the material you are requesting is original to the Licensor and does not carry the copyright of another entity (as credited in the published version).

If the credit line on any part of the material you have requested indicates that it was reprinted or adapted with permission from another source, then you should also seek permission from that source to reuse the material.

2. Where **print only** permission has been granted for a fee, separate permission must be obtained for any additional electronic re-use.
3. Permission granted **free of charge** for material in print is also usually granted for any electronic version of that work, provided that the material is incidental to your work as a whole and that the electronic version is essentially equivalent to, or substitutes for, the print version.
4. A licence for 'post on a website' is valid for 12 months from the licence date. This licence does not cover use of full text articles on websites.
5. Where '**reuse in a dissertation/thesis**' has been selected the following terms apply: Print rights for up to 100 copies, electronic rights for use only on a personal website or institutional repository as defined by the Sherpa guideline (www.sherpa.ac.uk/romeo/).
6. Permission granted for books and journals is granted for the lifetime of the first edition and does not apply to second and subsequent editions (except where the first edition permission was granted free of charge or for signatories to the STM Permissions Guidelines <http://www.stm-assoc.org/copyright-legal-affairs/permissions/permissions-guidelines/>), and does not apply for editions in other languages unless additional translation rights have been granted separately in the licence.
7. Rights for additional components such as custom editions and derivatives require additional permission and may be subject to an additional fee. Please apply to Journalpermissions@springernature.com/bookpermissions@springernature.com for these rights.
8. The Licensor's permission must be acknowledged next to the licensed material in print. In electronic form, this acknowledgement must be visible at the same time as the figures/tables/illustrations or abstract, and must be hyperlinked to the journal/book's homepage. Our required acknowledgement format is in the Appendix below.
9. Use of the material for incidental promotional use, minor editing privileges (this does not include cropping, adapting, omitting material or any other changes that affect the meaning, intention or moral rights of the author) and copies for the disabled are permitted under this licence.

10. Minor adaptations of single figures (changes of format, colour and style) do not require the Licensor's approval. However, the adaptation should be credited as shown in Appendix below.

Appendix — Acknowledgements:

For Journal Content:

Reprinted by permission from [the Licensor]: [Journal Publisher (e.g. Nature/Springer/Palgrave)] [JOURNAL NAME] [REFERENCE CITATION (Article name, Author(s) Name), [COPYRIGHT] (year of publication)]

For Advance Online Publication papers:

Reprinted by permission from [the Licensor]: [Journal Publisher (e.g. Nature/Springer/Palgrave)] [JOURNAL NAME] [REFERENCE CITATION (Article name, Author(s) Name), [COPYRIGHT] (year of publication), advance online publication, day month year (doi: 10.1038/sj.[JOURNAL ACRONYM].)]

For Adaptations/Translations:

Adapted/Translated by permission from [the Licensor]: [Journal Publisher (e.g. Nature/Springer/Palgrave)] [JOURNAL NAME] [REFERENCE CITATION (Article name, Author(s) Name), [COPYRIGHT] (year of publication)]

Note: For any republication from the British Journal of Cancer, the following credit line style applies:

Reprinted/adapted/translated by permission from [the Licensor]: on behalf of Cancer Research UK: : [Journal Publisher (e.g. Nature/Springer/Palgrave)] [JOURNAL NAME] [REFERENCE CITATION (Article name, Author(s) Name), [COPYRIGHT] (year of publication)]

For Advance Online Publication papers:

Reprinted by permission from The [the Licensor]: on behalf of Cancer Research UK: [Journal Publisher (e.g. Nature/Springer/Palgrave)] [JOURNAL NAME] [REFERENCE CITATION (Article name, Author(s) Name), [COPYRIGHT] (year of publication), advance online publication, day month year (doi: 10.1038/sj.[JOURNAL ACRONYM].)]

For Book content:

Reprinted/adapted by permission from [the Licensor]: [Book Publisher (e.g. Palgrave Macmillan, Springer etc)] [Book Title] by [Book author(s)] [COPYRIGHT] (year of publication)

Other Conditions:

Version 1.0

Questions? customercare@copyright.com or +1-855-239-3415 (toll free in the US) or +1-978-646-2777.